



HAL
open science

Generation of 3D brown-like adipocytes derived from human iPSCs: A new tool for in vitro preclinical drug discovery and for cell-based therapy to treat obesity

Xi Yao

► **To cite this version:**

Xi Yao. Generation of 3D brown-like adipocytes derived from human iPSCs: A new tool for in vitro preclinical drug discovery and for cell-based therapy to treat obesity. Molecular biology. COMUE Université Côte d'Azur (2015 - 2019), 2019. English. NNT: 2019AZUR6011 . tel-02971203

HAL Id: tel-02971203

<https://theses.hal.science/tel-02971203>

Submitted on 19 Oct 2020

HAL is a multi-disciplinary open access archive for the deposit and dissemination of scientific research documents, whether they are published or not. The documents may come from teaching and research institutions in France or abroad, or from public or private research centers.

L'archive ouverte pluridisciplinaire **HAL**, est destinée au dépôt et à la diffusion de documents scientifiques de niveau recherche, publiés ou non, émanant des établissements d'enseignement et de recherche français ou étrangers, des laboratoires publics ou privés.

THÈSE DE DOCTORAT

Un modèle en 3D d'adipocytes de type brun
dérivés de cellules pluripotentes
induites humaines pour le criblage in vitro de
médicaments et pour la thérapie cellulaire
contre l'obésité

Xi YAO

iBV - CNRS UMR 7277 - INSERM U 1091 - Institut de Biologie Valrose
Faculté de Médecine - NICE

**Présentée en vue de l'obtention
du grade de docteur en**
Interactions Cellulaires et Moléculaires
d'Université Côte d'Azur
Dirigée par Dr Christian Dani
Soutenue le: Le 17 Octobre 2019

Devant le jury, composé de:
Dr Jean-Sébastien Annicotte, DR, Université de Lille 2
Dr Hélène Boeuf, DR2, Université de Bordeaux
Dr Soazig Le Lay, CR, INSERM U1063, Angers
Dr Christian Dani, DR, Université Côte d'Azur

Titre et Identification du jury

Un modèle en 3D d'adipocytes de type brun dérivés de cellules pluripotentes induites humaines pour le criblage in vitro de médicaments et pour la thérapie cellulaire contre l'obésité

JURY

Président du jury:

Dr. Jean-Sébastien Annicotte

DR CNRS

UMR 8199 (CNRS / Université de Lille 2 / Institut Pasteur de Lille)

Génomique Intégrative et Modélisation des Maladies Métaboliques

Integrative Genomics and Modelling of Metabolic Diseases.

Lille, France

Rapportrices:

Dr. Hélène Boeuf

DR2, CNRS

Université de Bordeaux

Bordeaux, France

Dr. Soazig Le Lay

CR INSERM, HDR

INSERM U1063 - SOPAM

"Stress Oxydant et Pathologies Métaboliques"

Institut de Biologie en Santé – IRIS

Angers, France

Directeur de thèse:

Dr. Christian Dani

DR INSERM

iBV, UMR7277 CNRS - UMR1091 INSERM

Université Côte d'Azur

Nice, France

Résumé

L'obésité est la conséquence d'un déséquilibre entre l'apport de calories et la dépense énergétique. Les thérapies basées sur la réduction de l'apport énergétique sont difficiles à suivre dans notre vie moderne et les médicaments anti obésité présentent d'importants effets secondaires. Des stratégies alternatives sont alors requises pour lutter contre l'obésité et les troubles métaboliques associés comme le diabète de type 2 et les maladies cardiovasculaires. Les adipocytes bruns et de type brun, encore appelés beige ou brite (BA), stockent la graisse, mais contrairement aux adipocytes blancs, les BA sont équipés pour brûler les lipides et consommer le glucose afin de dissiper l'énergie stockée. Les BA sécrètent également des adipokines qui vont cibler d'autres organes et pour participer à la régulation des paramètres métaboliques. Ainsi, les BA représentent des cibles cellulaires prometteuses pour lutter contre l'obésité en favorisant la dépense énergétique. Cependant, la rareté des BA chez l'homme adulte, qui est accentuée chez les patients obèses, est une limitation majeure pour un traitement de l'obésité basé sur le BA. La notion d'augmenter la masse de BA en greffant des progéniteurs de BA (BAP) chez des patients obèses a récemment émergé. La preuve de concept a été faite dans des modèles murins. Le prochain défi consiste à identifier une source abondante et fiable de BAP humains. Nous décrivons dans cette thèse la capacité des cellules souches pluripotentes induites humaines (hiPSCs) à générer des BAP et capables de se différencier avec une grande efficacité dans un modèle en 3D en adiposphères.

Les hiPSC- adiposphères ont un profil d'expression de la matrice extracellulaire et des récepteurs couplés à la protéine G (GPCR) similaires aux adiposphères humaines dérivées de progéniteurs adipeux abdominaux sous-cutanés. Ces résultats montrent la pertinence physiologique du modèle hiPSC-adiposphères. De plus, les hiPSC-adiposphères contiennent plus de cellules UCP1 positives que les adiposphères abdominales. L'expression de UCP1 dans les hiPSC-adiposphères est augmentée suite à la stimulation par le 8-CPT-AMPC ou du 8-Br-GMPc de manière aiguë et chronique. Ceci indique que notre modèle 3D présente les caractéristiques métaboliques des adipocytes de type bruns et peut répondre à un criblage de molécules visant à augmenter la dépense énergétique.

Enfin, l'enrichissement du modèle 3D en cellules endothéliales humaines (HDMEC) a été réalisé via une co-culture en suspension. La fonctionnalité des HDMECs intégrées dans les hiPSC-adiposphères a été testée in vitro par la visualisation de l'absorption de LDL. Nous avons aussi montré que les hiPSC-BAs et les HDMEC pouvaient générer des structures de type vascularisées dans le core de la sphère.

En conclusion, le modèle hiPSC-adiposphère représente une source illimitée d'adipocytes d'intérêt thérapeutique qui pourrait, dans un avenir proche constituer un nouvel outil approprié à la fois pour la transplantation chez les patients atteints d'obésité morbide et pour le criblage de médicaments. Le potentiel thérapeutique des hiPSC-adiposphères sera testé prochainement dans un modèle de souris obèses.

Mots Clefs:

adipocytes de type brun, hiPSCs, 3D, co-culture, criblage de médicaments, thérapie cellulaire contre l'obésité

Summary

Obesity results from an imbalance between calorie intake and energy expenditure. Therapies based to reduce energy intake are difficult to follow in our modern life, and drugs can display adverse effects. Alternative strategies are urgently required to fight obesity and associated metabolic disorders. Brown and brown-like adipocytes (BAs) store fat, but in contrast to white adipocytes, BAs are equipped to burn glucose and lipids to dissipate energy stored. BAs also secrete adipokines that signal other organs and regulate metabolism. Therefore, BAs represent promising cell targets to promote energy expenditure and counteract obesity. However, the scarcity of BAs in human adults is a major limitation for a BA-based therapy of obesity, and the notion to increase the BA mass by transplanting BA progenitors (BAPs) in obese patients recently emerged. The proof of concept has been done in murin models. The next challenge is to identify an abundant and reliable source of human BAPs. We recently described the capacity of human induced pluripotent stem cells (hiPSCs) to generate BAPs. During my thesis, we established a procedure to generate hiPSC-BAP spheroids and a method for their differentiation at a high efficiency in hiPSC-brown-like adipospheres. The model was then enriched with Human Dermal Microvascular Endothelial Cells (HDMECs) to better mimic the adipose tissue microenvironment and to improve its therapeutic potential.

BAPs derived from human iPSCs were maintained in suspension to form spheroids able to differentiate into adipospheres. The structure of adipospheres was analysed by confocal microscopy and adipocytes were characterized at the molecular and metabolic levels. We generated adipospheres from two different hiPSC-BAP clones, which are able to fully differentiate from the surface to the core. We compared hiPSC-brown-like adipospheres with the ones generated by hanging drop method, and our model displays comparable pattern regarding to extracellular matrix and adipogenesis, despite the sizes are not defined. We also proved hiPSC-brown-like adipospheres promotes accumulation of brown-like adipocytes that are more biologically active compared to cells maintained in conventional monolayer cell cultures.

In addition, hiPSC-brown-like adipospheres have a similar expression profile of extracellular matrix and G Protein-Coupled Receptors (GPCRs) compared with human adipospheres derived from subcutaneous abdominal adipose progenitors, suggested the physiological relevance of the hiPSC-adiposphere model. Moreover, hiPSC-adipospheres display a more brown-like adipogenic potential than abdominal adipospheres opening the opportunity and advantages for anti-obesity drug testing and cell based therapy to increase the BA mass in patients. Furthermore, hiPSC-adipospheres express UCP1 that can response to the stimulation of 8-CPT-cAMP or 8-Br-cGMP acutely and chronically, which indicated that our 3D model display metabolic characteristics of brown-like adipocytes.

Finally, enrichment with HDMECs was performed via co culture in suspension. HDMECs functionality was tested in vitro by LDL-uptake. We proved that hiPSC-BAPs and HDMECs can co-culture in 3D and differentiate into vascularized hiPSC-brown-like adipospheres with functional tubular-like structure formed inside. Moreover, our co-cultured 3D model can secrete factors like VEGF and FGF2 to support vascularization which mimic in vivo situation.

Altogether, the hiPSC-brown-like adiposphere model represents an unlimited source of human BAPs that in a near future may be a suitable tool for both therapeutic transplantation and for drug screening allowing discovery of novel and safe anti-obesity drugs.

Key words:

brown-like adipocytes, hiPSCs, 3D, co-culture, drug discovery, anti-obesity cell therapy

l'humaine sagesse était tout entière dans ces deux mots :
— *Attendre et espérer!*

Alexandre Dumas

Acknowledgments

First of all, I would like to thank Dr. Hélène Boeuf and Dr. Soazig Le Lay for agreeing to be reporters of my thesis. I also thank Dr. Jean-Sébastien Annicotte for being both an examiner and president of my thesis jury.

I would like to thank the China Scholarship Council for giving me the opportunity to do my four years of thesis. And also thanks to ANRS to fund my project.

A big thank to my doctoral director, Dr. Christian Dani, who accepted and supervised me to do a thesis in his laboratory. I learned a lot from your side. You have brought me a lot at the scientific and methodological level and no doubt that it will serve me in my future. Thank you so much for your patient, your listening and your kindness. I really appreciated the ease of being able to discuss with you about my project. You know that I am getting stressed so easily, and when you say “You are doing very well, don't worry” really helps a lot calm me down. Thank you for always supporting and encouraging me. It was a pleasure to work with you. And the pleasure will continue.

I would like to all the members or ex-members of the team “Stem cells and Differentiations”. Nicole (for your advice and your kindness, and also the cookies from Corsica :)), Claude (for your humor), Phi (for your joy of living), Annie (for your advice and help in the experiments, and nice talking during filling the liquid nitrogen tank :)) and Pascal (for your kindness and humor, and inviting us to your nice mansion to party). Again, I would like to thank all the members in my team for the help you give both in the research and life.

I want to thank the people who help me complete this project. Thanks to the Prism platform and especially to Simon Lachambre. Thank you Simon for your availability, your training and your precious help to set up my experiences, so that I can have nice pictures to show :) . Thanks to the Cytometry platform. Thank you Agnès for your training and your precious help with my experiments, and also nice talking with you during cell sorting :).

Thank you to all members of the team “Cellular and molecular regulation of fat mass ” : Nadine, Didier, Jean-Claude, Nathalie and Zoubir as well as the team “Vessel formation in development and disease” : Béatrice, Kay and Nicole.

Thank you Nicolas, I still remember the acknowledgment part in your thesis telling me and Martin that “be careful the end arrives faster than you think”. And it is my turn now :). Thank you Rayane and Maud, for these moments of fun. Thank you Siyue and Vitali, it is nice to have you in the same floor.

Thank you Claudine, for your kindness and your advice, and especially your help with my settle down in Nice since I don't speak French, you really helped a lot. Don't forget to eat iron and take more sunbathing :) .

Thank you Martina, for your optimism, your joy of life and your humor. You helped me familiar and integrate into the lab and the life in Nice, and I really appreciate that. And talking to you really improved my English a lot :D. Thank you for being friendly, kind and nice to me. Also thank you for inviting Furong and me to Slovakia, and we enjoyed the trip a lot. I hope we can see each other again :).

Thank you Albert, it is nice to have you in our lab for six months. It was a pleasure to work with you, and your lab book helped me a lot since you wrote down all the details :) . Thank you for taking us to try local food in those non tourist places in Barcelona. We enjoyed that night a lot. Thank you very much.

Thank you Christophe, for your friendly and kindness. Thank you for showing me how to do experiments and familiarizing me with the lab when I started my thesis. When I had problems, you were always nice and kind to help me with no doubt. Also, I had a great time hanging out with you and Elena.

Thank you Martin, you helped me a lot after Christophe finished his thesis :). Even though you teased me a lot, I still like talking to you :D. At least, you were nice and kind to me when I was down :). It is great to do the thesis at the same time with you. You brought a lot of laugh to me and kept me company. Thanks for your tips, I didn't struggle a lot during writhing thesis like you :). I hope you are doing well back in Quebec. I miss you.

Thank you Vincent, it is you after Martin. I am the one who always need help, and I am so lucky to have people like you, Martin and Christophe around me to help me all the time. You are patient, thoughtful and kind. You gave me many advices on my project and gave me a lot of confidence. It was nice to take pictures with you together in Valrose. A big thank for helping me fix the wall in my apartment, the moving and everything. I also learned a lot about Nice from you. The sandwich you recommended, that is my favorite :)!

Thanks to the chat group "ChiNice food". I made a lot of friends there. We hang out together to have dinner and beers which is the best moment after a week of work :)! A big thank to the organizer, ZHAO Zhiyan, and also to YUE jiaxing and LI Jing for never be absent :).

Thanks to my longtime friend who has always supported me: ZANG Nan since high school. Even though we do not see each other often, you are always there for me and support me. You know me so well, even more than myself. You are like a psychologist to me, but for free :). I hope you finish writhing your thesis on time, and hang in there!

A big thank to my family and especially my parents, who have always supported and encouraged me in everything I do, even though I don't talk about my work a lot. Thank you for always being there for me.

Furong, I own you a lot. You took good care of me, but I was always lazy to do my part. No wonder you complained about me all the time :). Finally, you can get rid of me after nine years :) . Thank you for nine years of company from undergraduate to PhD. You are a family member to me. I hope you can find a post-doc working on the project you like. I have faith in you, and you will have your own lab and become an excellent PI in the near future :).

The last but not the least, Yuewei. Thank you for appearing in my life. When I think about our relationship, these words “情不知所起，一往而深” comes to my mind. And you remind me of the lyric “You're just too good to be true, I can't take my eyes off you ”. The three months with you in Nice is a beautiful memory to me. The long distance relationship is not easy, and I hope we can get through it. I promise to tell you what I wrote in Casa Batlló when we go there next time :). I love you.

Table of Contents

Titre et Identification du jury	2
Résumé	3
Summary	4
Acknowledgments.....	6
Table of Contents	9
List of Abbreviations.....	11
Bibliographic Introduction	14
I Adipose tissue	15
I.1 Generality.....	15
I.1.1 Distribution.....	16
I.1.1.1 White adipose tissue –WAT.....	16
I.1.1.2 Brown adipose tissue – BAT.....	16
I.1.2 Composition.....	17
I.1.2.1 Mature adipocytes.....	17
I.1.2.2 Stroma vascular fraction (SVF).....	21
I.1.2.2.1 Adipose progenitors (APs).....	21
I.1.2.2.2 Endothelial precursor cells (EPC).....	22
I.1.2.2.3 Extra cellular matrix (ECM)	22
I.1.2.2.4 Immune cells	23
I.1.3 Function.....	23
I.1.3.1 Function of WAT.....	24
I.1.3.1.1 Energy storage in WAT.....	24
I.1.3.1.2 Lipolysis and Its Regulation.....	25
I.1.3.1.3 Endocrine function of WAT.....	26
I.1.3.2 Function of BAT.....	28
I.1.3.2.1 Thermogenesis in BAT.....	28
I.1.3.2.2 Endocrine in BAT.....	31
I.2 Development of adipose tissue.....	35
I.2.1 Adipogenesis	35
I.2.1.1 Commitment.....	35
I.2.1.2 Terminal differentiation.....	37
I.2.2 Developmental origin of adipose progenitors	40
I.2.2.1 Embryonic origin.....	40
I.2.2.2 Origin of the white adipose progenitor.....	40
I.2.2.3 Origin of the brown adipose progenitor.....	41
I.2.2.4 Origin of the beige adipose progenitor.....	42
I.3 Adipose tissue associated pathology	44
I.3.1 Obesity	44
I.3.2 Other diseases associated with obesity.....	46
I.3.2.1 Insulin resistance and type 2 diabetes.....	47
I.3.2.2 Dyslipidemias.....	47
I.3.3 Lipodystrophy	48
II Human “brite”/brown adipocyte cellular models.....	49
II.1 Immortalized cell lines isolated from human BAT	49
II.1.1 Immortalized SVF from human infant BAT	49
II.1.2 Immortalized clonally derived adult human brown adipocytes	50
II.1.3 Immortalized polyclonal brown preadipocyte cell models	51
II.2 Preadipose cell lines and primary preadipocyte culture.....	51

II.2.1 Primary culture of cells isolated from supraclavicular fat in adults.....	52
II.2.2 Primary culture of cells isolated from white adipose tissue.....	53
II.2.3 Human adipose-derived stem cells	53
II.3 Adipocyte progenitors derived from human embryonic stem cells (ESCs)	55
II.4 Adipocyte progenitors derived from induced Pluripotent Stem Cells (hiPSC)	56
II.4.1 iPSC cells.....	57
II.4.1.1 Generation of iPSCs.....	57
II.4.1.2 Applications of iPSCs.....	59
II.4.1.2.1 Cell therapy.....	59
II.4.1.2.2 Disease modeling.....	61
II.4.2 HiPSC-APs as a cell model to study adipogenesis	62
II.4.3 Small Molecules induce hiPSC-BAP brown-like adipogenesis.....	63
II.4.3.1 SB431542.....	64
Mini Review 《Critical Role of TGFβ Pathway in the Differentiation of Human	
Induced Pluripotent Stem Cells into Fat-Burning Adipocytes 》	
II.4.3.2 Ascorbic acid.....	65
II.4.3.3 Epidermal growth factor (EGF).....	65
II.4.3.4 Hydrocortisone.....	66
II.4.4 Perspectives of hiPSCs in the Obesity Field.....	66
Chapter 《Brown-Like Adipocyte Progenitors Derived from Human iPS Cells: A	
New Tool for Anti-obesity Drug Discovery and Cell-Based Therapy? 》	
III Three-dimensional (3D) Cell Culture Systems	68
III.1 3D cell culture technology	69
III.1.1 Aggregate cultures and the formation of spheroids	69
III.1.2 Scaffold-based technologies for 3D cell culture	70
III.1.2.1 Hydrogel technology.....	71
III.1.2.2 Solid scaffold-based technology.....	71
III.2 3D adipocyte culture systems	72
III.2.1 3D adipocyte models	72
III.2.2 Applications of iPSC-brown-like adipospheres in cell therapy	73
Cell models and objectives	75
Results.....	78
I 3D brown-like adipocytes derived from human iPSCs to counteract obesity ..	79
I.1 Establish 3D brown-like adipocyte model derived from human iPSCs to counteract obesity	
.....	79
I.1.1 Article “Generation of 3D brown-like adipocytes derived from human iPSCs: A new tool for in vitro preclinical drug discovery and for cell-based therapy to treat obesity”	79
Conclusion and perspectives	80
Annexes.....	84
References	85

List of Abbreviations

AC	Adenylate cyclase
ACS	Acyl-CoA synthesis
ADSCs	Adipose-derived stem cells
ANGPTL8	Angiopoietin-like 8
ASCs	Adipose stem/stroma cells
AP	Adipose progenitor
ApoB	Apolipoprotein B
β -AR	β -adrenergic receptors
AT	Adipose tissue
ATGL	Adipose triglyceride lipase
BAPs	Brown adipose progenitors
BAT	Brown adipose tissue
BMP	Bone morphogenetic protein
CAC	Citric acid cycle
CAMP	Cyclic AMP
CEBP	CCAAT-Enhancer-Binding Proteins
CETP	Cholesteryl ester transfer protein
CGMP	Cyclic GMP
CM	Chylomicrons
CREB	CAMP response element-binding protein
DAG	Diacylglycerol
EB	Embryoid body
EC	Endothelial cells
ECM	Extracellular matrix
EGF	Epidermal growth factor
EGR1	Early growth response-1
EPC	Endothelial precursor cells
ER	Estrogen receptor
ESC	Embryonic stem cell
FAD	Flavin adenine dinucleotide
FABP	Fatty-acid-binding protein
FFA	Free fatty acid
FGF21	Fibroblast growth factor 21
β -Gal	β -galactosidase
GC	Guanylate cyclase
GHO	Global health observatory

GLUT	Glucose transporter
GPCR	G protein-coupled receptor
GSK3	Glycogen synthasekinase 3
HDL	High density lipoprotein
HGF	Hepatic growth factor
HiPSCs	Human induced pluripotent stem cells
HLA	Human leukocyte antigens
HMADs	Human Multipotent Adipose-Derived Stem Cells
HSL	Hormone-sensitive lipase
IGFBP2	Insulin-like growth factor binding protein 2
IGF1	Insulin-like growth factor 1
IL-6	Interleukin-6
IPSCs	Induced pluripotent stem cells
IRS	Insulin receptor substrate
KCNK3	Potassium channel K3
KLF	Krupple-like factors
LDL	Low density lipoprotein
LPGDS	Lipocalin-Type Prostaglandin D Synthase
LPL	Lipoprotein lipase
MAG	Monoacylglycerol
MAGL	Monoacylglycerol lipase
MAPK	Mitogen-activated protein kinase
MCE	Mitotic clonal expansion
MCP-1	Monocyte chemoattractant protein-1
MEFs	Murine embryonic fibroblasts
Metrn1	Meteorin-like protein
MPC	Mesenchymal progenitor cells
MSC	Mesenchymal stem cells
MTUS1	Mitochondrial tumor suppressor 1
Myf5	Myogenic factor 5
NAD	Nicotinamide adenine dinucleotide
NE	Norepinephrine
NGF	Nerve growth fibre
NO	Nitric oxide
NRG4	Neuregulin 4

Pax7	Paired box 7
PDE-3B	Phosphodiesterase 3B
PDGFR α	Platelet-derived growth factor receptor α
PGC1- α	Peroxisome proliferator-activated receptor gamma coactivator 1-alpha
PI3K	Phosphatidyl inositol 3-kinase
PKA	Protein Kinase A
PKB	Protein B kinase
PKG	Protein Kinase G
PP-1	Phosphatase 1
PPAR γ	Peroxisome Proliferator-Activated Receptor- γ
PRDM16	PRD1-BF-1-RIZ1 homologous domain-containing protein 16
Pref-1	Preadipocyte factor 1
RA	Retinoic acid
RNAi	Interfering RNA
SAT	Subcutaneous WAT
sLR11	Soluble LDL receptor 11
SMA	Spinal muscular atrophy
SREBPs	Sterol regulatory element binding proteins
SVF	Stromal vascular fraction
T3	Triiodothyronine
TAG	Triglycerides
TERT	Telomerase reverse transcriptase
TGF- β	Transforming growth factor β
UCP1	Uncoupling protein 1
VEGFA	Vascular endothelial growth factor A
VLDL	Very low density lipoproteins
VAT	Visceral WAT
WAT	White adipose tissue
WHO	World Health Organization
ZFP	Zinc finger protein

Bibliographic Introduction

I Adipose tissue

Adipose tissue (AT) is a complex organ playing a critical role in physiology and pathophysiology. Until the late 1940s, adipose tissue was only characterized as a tissue containing lipid droplets, which gradually changed after the discovery of leptin, the first adipocyte-derived cytokine (Friedman et al., 1991; Zhang et al., 1994). Leptin release response to changes in nutritional status indicates that AT involved in modulating energy homeostasis, therefore the study about AT had been expanded in aspects of development, function and pathophysiology (Figure. 1) (Rosen and Spiegelman, 2014). Recently, AT even drew more attention due to the increasing of obesity and type II diabetes with 1.7 billion obese people in global (Haslam and James, 2005). Therefore, better understanding about AT in metabolic health and disease is urgently needed.

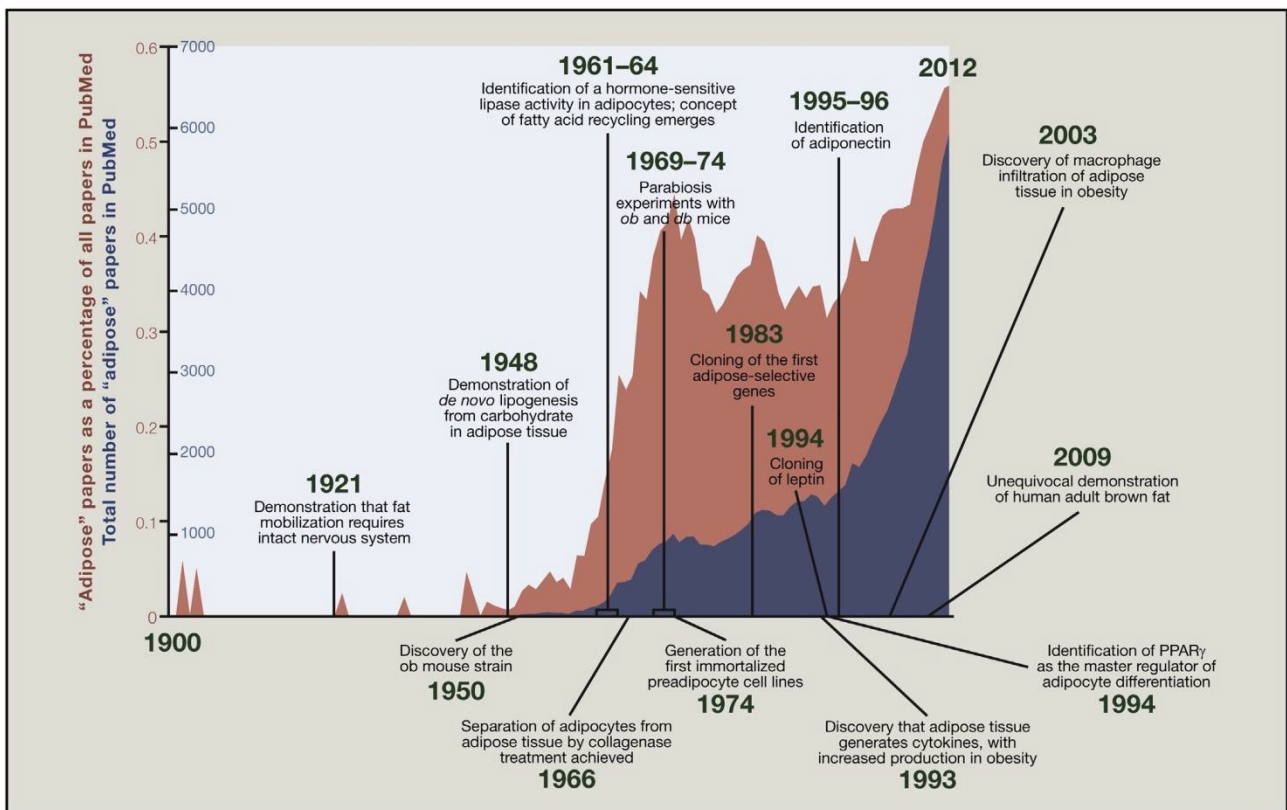


Figure 1. Interest in Adipose Biology Has Risen Over Time (Rosen and Spiegelman, 2014).

I.1 Generality

In humans, AT distributes in many depots through the body, composed with functionally and histologically distinct types of fat: white adipose tissue (WAT) and brown adipose tissue (BAT).

I.1.1 Distribution

I.1.1.1 White adipose tissue -WAT

WAT represents 15 to 20% of body weight in human, which varies depending on age, sex and certain disease like obesity and lipotrophy. The primary purposes of WAT are insulation and energy storage. WAT is distributed throughout the body in two main depots, including subcutaneous WAT (SAT) and visceral WAT (VAT) (Figure. 2) (Gesta et al., 2007; Item and Konrad, 2012). SAT stores >80% of fat in the body, commonly defined as abdominal, gluteal and femoral, whereas VAT comprises mainly depots like perirenal, retroperitoneal, omental and mesenteric. VAT is associated with internal organs, which represent 5–10% in women of total body fat and 10–20% in men, strongly linked with the development of metabolic diseases, like type 2 diabetes and cardiovascular disease. On the other hand, accumulation of subcutaneous fat displays no correlation with these diseases.

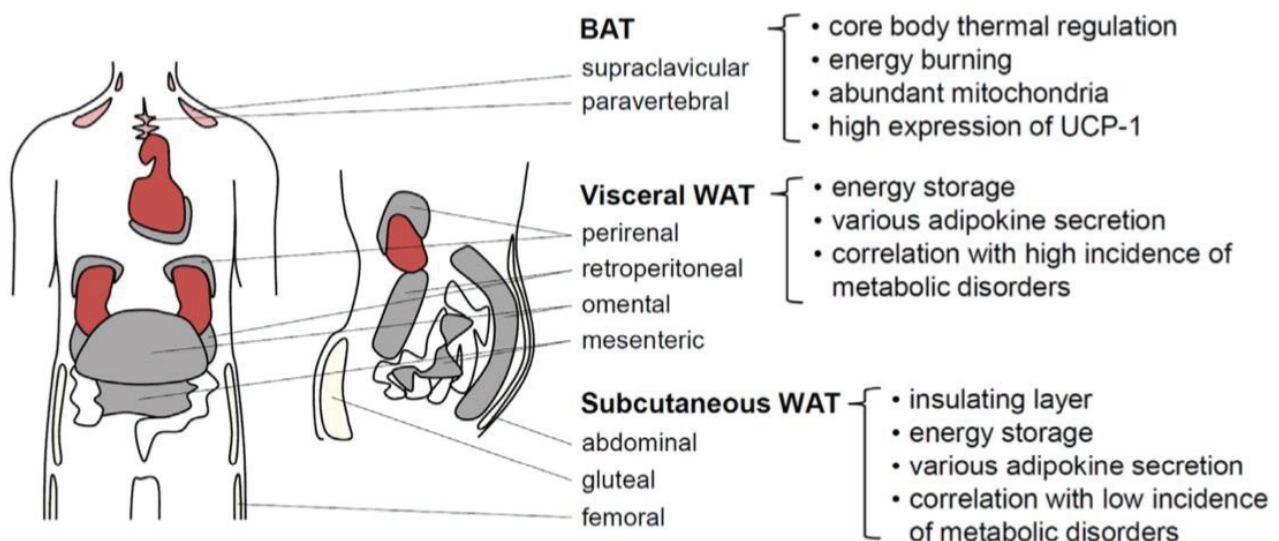


Figure 2. Adipose tissue distribution and functions in energy homeostasis and thermal regulation (Choe et al., 2016).

I.1.1.2 Brown adipose tissue - BAT

In mice, BAT plays an important role in non-shivering thermogenesis to maintain or raise the body core temperature associates with increased energy expenditure and a negative energy balance (Cannon and Nedergaard, 2004). In human, BAT is well known in infant predominantly in the interscapular region. Until 2009, it was the first time to discover functional BAT in adults by cold exposure studies, comprising supraclavicular and paravertebral depots (Figure. 2) (van Marken Lichtenbelt et al., 2009; Virtanen et al., 2009; Saito et al., 2009). BAT was visualized by nuclear medicine imaging technique FDG-PET/CT during cold exposure that showed raised glucose uptake

(Figure. 3) (Nedergaard et al., 2007). The extra heat is produced through mitochondrial uncoupling. The mitochondria in BAT have specific uncoupling protein 1 (UCP1), when activates, the electro-chemical gradient across the inner membrane will be uncoupled which is normally used for ATP synthesis. The respiratory chain activity is stimulated and leading to the generation of heat.

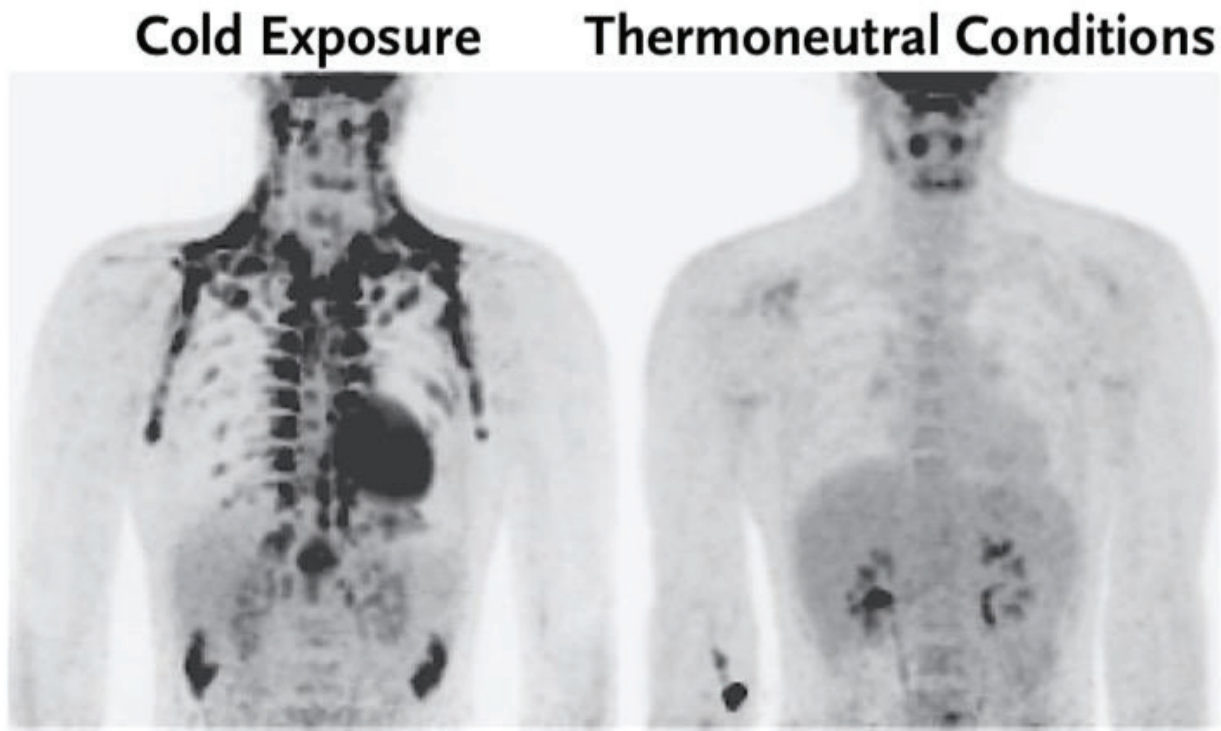


Figure 3. Comparative PET–CT scans reveal the patterns of ¹⁸F-FDG uptake in the same subject from the lean group after exposure to cold and under thermoneutral conditions (van Marken Lichtenbelt et al. 2009).

I.1.2 Composition

Adipose tissue is characterized as cellular heterogeneity, which consists of one third of mature adipocytes, and the remaining are a combination of adipose progenitors (APs), fibroblasts, endothelial cells, immune cells, nerves and multipotent stem cells all embedded in an extracellular matrix (ECM).

I.1.2.1 Mature adipocytes

Mature adipocytes, including white, brown and beige adipocytes, secrete a large amount of adipokines through endocrine, paracrine, and autocrine regulatory processes (Ahima and Flier, 2000; Yudkin et

al., 1999). They play an important role in regulating energy homeostasis, modifying physiological processes, and may mediate pathologies involved in increasing fat mass (Chaldakov et al., 2003; Rajala and Scherer, 2003).

White adipocytes contain one large lipid droplet that occupies over 90% of the cell volume with cytoplasm, nuclei and mitochondria to the periphery of the cell. White adipocytes have low mitochondria density, but can secrete leptin and adiponectin modulating energy homeostasis. Lipids stored in the droplet are primarily triglycerides and cholesteryl esters. Accumulation of lipids determines the size of adipocytes which is 80-90 μm in average and can reach up to 200 μm (Majka et al., 2014) (Figure. 4).

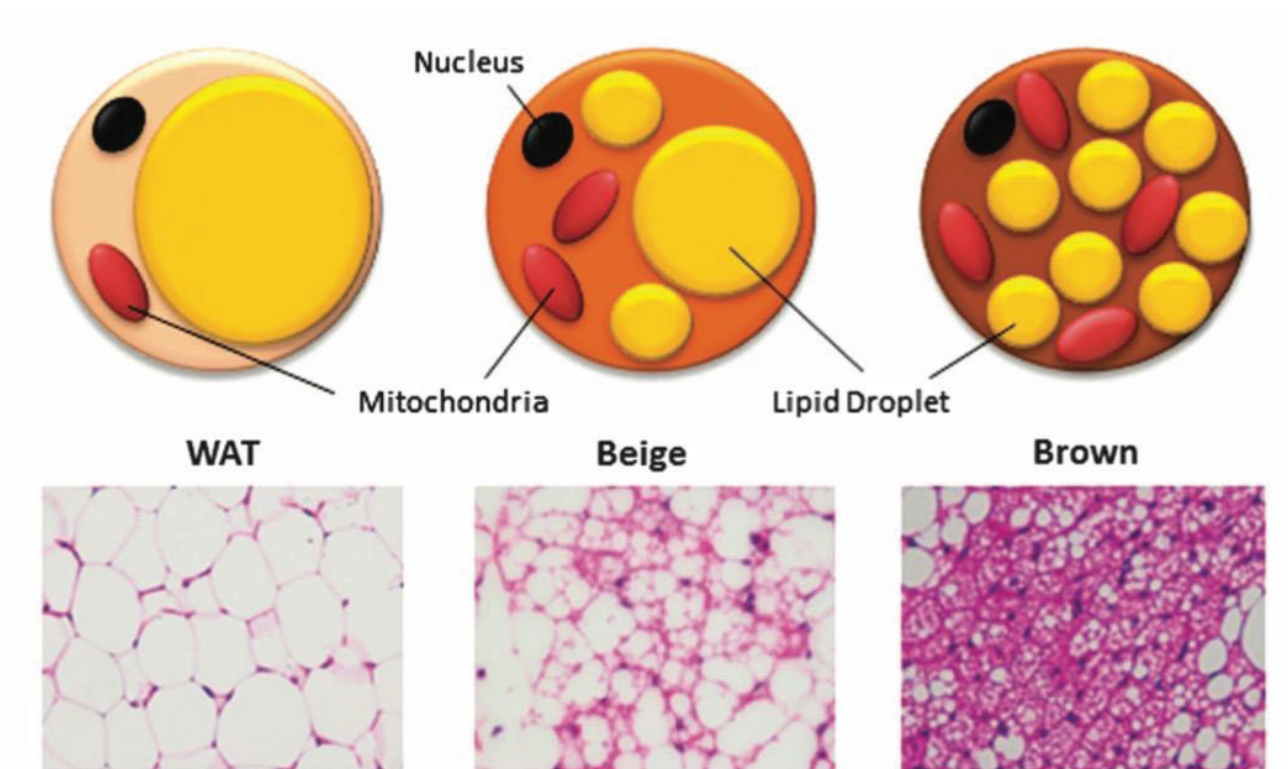


Figure 4. Heterogeneous adipocytes in humans. Morphological differences between WAT, beige and brown adipose tissue (BAT) adipocytes as shown by cartoon and hematoxylin/eosin staining ($\times 40$ magnification) (Kwok et al., 2016).

BATs have different compositions and functions than WATs, with adipocytes having numerous small lipid droplets and high density mitochondria (Figure. 4). In contrast to white adipocytes, brown adipocytes dispersed in BAT are specialized in energy expenditure, consume metabolic substrates and burn fat via the mitochondrial uncoupling protein-1 (UCP-1). Moreover, the ability of brown adipocytes to actively drain circulating glucose and triglycerides to oxidize them can

prevent hyperglycemia and hypertriglyceridemia. Therefore, brown adipocytes represent promising cell targets to counteract obesity in human.

Besides white adipocytes and brown adipocytes, there is another type of adipocytes recently found in the mouse called beige/ brite adipocytes (for brown in white), which express UCP1 with medium density mitochondria and few to many lipid droplets (figure. 4) (Wu et al., 2012). Beige adipocytes mainly exist in subcutaneous WAT in rodents, which can response to external cue, such as cold exposure and chronic treatment of PPAR γ agonist (eg. rosiglitazone) called white “browning” (Shabalina et al., 2013; Kajimura and Saito, 2014; Harms and Seale, 2013; Wu et al., 2013). Upon activation, beige adipocytes express UCP1 protein and exhibits UCP1-dependent thermogenic capacity. In human, UCP1-positive cells appear in dispersed clusters interspersed among white adipocytes resemble the appearance of the beige adipocytes in the subcutaneous white adipose tissue of the mice after cold induction (Wu et al., 2012). The expression of key genes involved in thermogenesis such as *UCP1*, *PRDM16* (*PRD1-BF-1-RIZ1* homologous domain-containing protein 16), *PGC1- α* (*Peroxisome proliferator-activated receptor gamma coactivator 1-alpha*) confirms the thermogenic capacity, but does not make it possible to discriminate between beige or brown. In rodents, many markers have been identified to distinguish different types of adipocytes, and their expressions have been measured in several BAT depots in human adult and infant (Wu et al., 2012; Walden et al., 2012). However, some rodent brown markers express in human WAT, and therefore couldn't be used for identifying human thermogenic adipocytes. Overall, human BAT contains both brown and beige adipocytes. Molecular characterization of infant human inter-scapular BAT compared to adult supraclavicular BAT, indicates that infant human inter-scapular BAT is a truly brown identify and adult human supraclavicular BAT is more likely enriched with markers of rodent beige adipocytes (Lidell et al., 2013; Sharp et al., 2012). A summary of different markers expressing in white, brown and beige adipocytes of mouse and human is present below (Figure. 5) (Peirce et al., 2014).

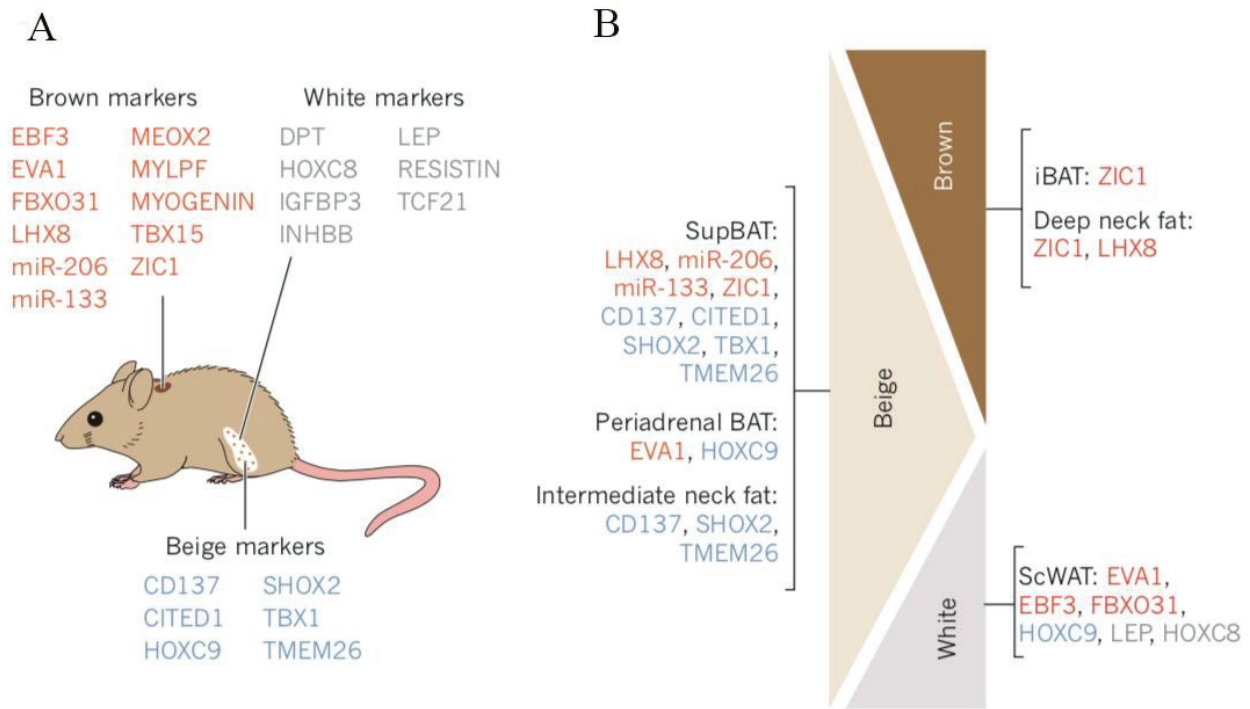


Figure 5. Assessment of rodent brown and beige adipocyte markers in human adipose tissue. A, well-established rodent brown, beige and white markers. Both white and beige markers are found in subcutaneous white adipose tissue (WAT) depots, but beige markers are upregulated after cold exposure. B, A comparison of the rodent brown, beige and white markers that have been found to be enriched in particular human adipose tissue depots (Peirce et al., 2014).

Other studies indicate that brown, beige and white adipocytes are found from superficial to the center of neck fat depot in adult human respectively (Figure. 6) (Cypess et al., 2013). Almost no UCP1 expression under the skin to high UCP1 expression in the deep neck with highest expression of ZIC1, as well as other gene markers expression, indicated the deep net fat is classical brown adipose tissue. The morphology in this adipose tissue consists with classical brown fat (Zingaretti et al., 2009). They also found intermediate *UCP1* expression in the fat depot between the superficial depots and the deepest adipose depots, which looked much like beige/brite depots, but couldn't be determined by the molecular analysis presented. This could be due to the fact that some of the proposed beige markers could not distinguish with few difference in their expression level in beige and white adipose depots, and also variations between individual humans could confound the characterization of beige markers (Wu et al. 2012). However, Lidell *et al.* found that the fat around kidney is probably beige, based on low ZIC1 expression and higher HOXC9 expression which is one of the proposed beige markers (Lidell et al. 2013). Therefore, human brown fat contain both classical brown adipocytes and beige adipocytes just as in mice, and more studies are needed to distinguish brown and beige adipocytes.

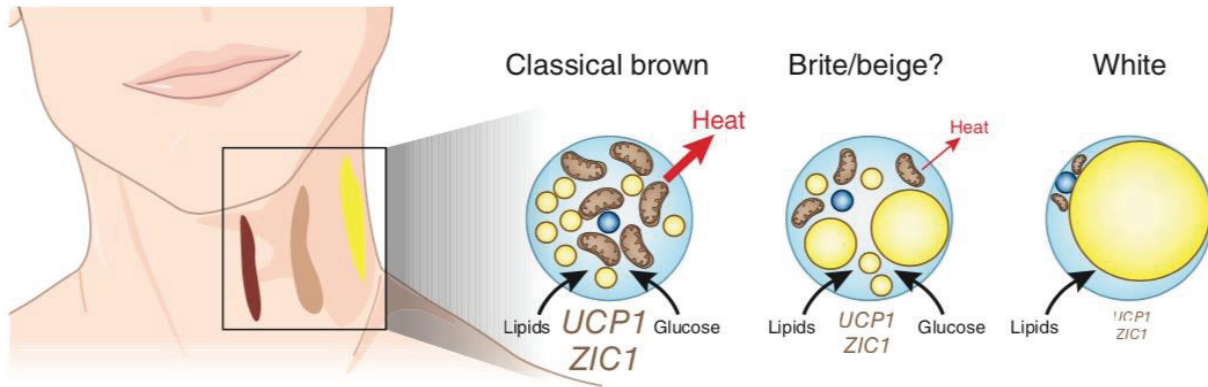


Figure 6. The gradient of brown adipose in the human neck. (Nedergaard and Cannon, 2013)

I.1.2.2 Stroma vascular fraction (SVF)

The adipose SVF, which can easily be isolated from human adipose tissue, is a rich source of adipose-derived stem cells (ADSCs, or ASCs), representing a viable alternative to bone marrow mesenchymal stem cells (BM-MSCs) (Katz et al., 2005; Zuk et al., 2001). Freshly isolated SVF cells are a heterogeneous mixture containing adipose progenitors, preadipocytes, endothelial precursor cells, fibroblasts, and immune cells. Under standard culture conditions after first few passages, these cell populations eventually turn into a relatively homogeneous population of mesenchymal cells.

I.1.2.2.1 Adipose progenitors (APs)

Adipose progenitors (APs), also named preadipocytes, or adipose-derived stem cells (ADSCs) or adipose stem/stroma cells (ASCs), depends on their potential to differentiate into adipocyte only or in additional cell types such as osteoblasts and chondrocytes. Since mature adipocytes do not divide in vivo, proliferation of APs can be recruited to form new fat cells and regeneration of adipocytes (Hauner et al., 1989; Spalding et al., 2008). Therefore, identification of factors regulating APs self-renewal and characterization of the cellular and molecular events involved in the generation of APs could provide a means to better understand development of adipose tissue and the mechanisms of hyperplasia. Furthermore, the cell surface markers have been identified in expanded SVF derived cells, which has similar profile as bone marrow derived MSC, comprising of positive for CD29, CD44, CD71, CD90, CD105/SH2, and SH3 and lacking CD31 and CD45 expression (Zuk et al., 2002). Characterization of fresh CD45 negative, CD34 positive, CD105 positive SVF cells based on CD31 expression demonstrated that CD31 positive cells has poor expansion capacity, whereas CD31 negative cells could expand in vitro and displayed mesenchymal properties (Boquest et al.,

2005). Adipose progenitors may be derived from AT pericytes and tend to be associated with blood vessel (Gupta et al., 2012; Tang et al., 2008; Tran et al., 2012). Since APs can be multipotent cells, they have the capacity to differentiate into adipogenic, chondrogenic and osteogenic lineages (Schulz et al., 2011; Cornelius et al., 1994; Charrière et al., 2003; Rodriguez et al., 2004; Zuk et al., 2002).

I.1.2.2.2 Endothelial precursor cells (EPC)

In addition to APs content, SVF also contains endothelial precursor cells (EPC). In vasculature tissue, damaged endothelial cells can be continually replenished de novo from circulating bone marrow derived EPC. Moreover, a population of cells positive for CD34, CD133 was found in human SVF cells isolated from subcutaneous or visceral adipose tissue, which had the ability to form endothelial colonies in vitro, and could induce angiogenesis in a hindlimb ischemia model in vivo (Miranville et al., 2004). Interestingly, the proportion of cells with the phenotype of angiogenic ability, was positively related to body mass index, which suggests the EPC entrapped in adipose tissue of obese patients may be associated with the regressed angiogenic function in obesity (Urbich and Dimmeler, 2005). Human white AT is highly vascularized, which is necessary for functioning. Each adipocyte has a close contact with the endothelial cells (ECs) nearby, which allows for the blood flow to fetch nutrients, oxygen, growth factors, hormones, cytokines and other cells required for AT homeostasis (Cao, 2013). Because of their perivascular/ endothelial origins, ECs are considered as a niche for adipocyte progenitors (APs) (Han et al., 2011; Tran et al., 2012; Long et al., 2014; Volz et al., 2016). Vascularization is also crucial for white adipocyte browning (Min et al., 2016). More recently it has been proposed a functional interaction between ECs and adipocytes, ECs releasing the natural ligand for PPAR γ (Gogg et al., 2019).

I.1.2.2.3 Extra cellular matrix (ECM)

The ECM has a crucial importance for the functioning of AT. ECM surrounds adipocytes to protect them from disruption by decreasing the mechanical stress through spreading the forces over a larger area of the tissue. Therefore, mature adipocytes spend vast energy to maintain and renew their ECM. It is mediated not only by mechanical forces

but also by insulin, redox status and the supply of oxygen (Mariman and Wang, 2010). In the phase of preadipocytes committed to the storage of triglycerides, synthesis of ECM is increasing and the network of fibrillar collagens surrounding preadipocytes is maintained. The differentiating preadipocytes become embedded in the basal lamina, regulated by a complex set of processing enzymes. The composition of ECM depends on the developmental stage, viability and subtype of the adipocytes, and collagen IV is a major component (Pierleoni et al., 1998). Collagen VI is involved in the pathology of obesity-related disease, which makes it more specific for adipocytes compared to other ECM components (Iyengar et al., 2005; Khan et al., 2009).

I.1.2.2.4 Immune cells

In AT, immune cells comprising almost the full spectrum of known immune cell types, have the physiological in maintaining AT homeostasis, which including angiogenesis, ECM remodelling, activation of inflammatory response, removal of molecular debris and apoptotic cells (Maurizi et al., 2018; Lolmède et al., 2011).

Macrophages are the biggest population of immune cells in AT (Ferrante, 2013). Even though the phenotypes of macrophages are continuous, there is a simplified mean to distinguish two principal phenotypes: M1-like (classically activated) and M2-like (alternatively activated). Recruited M1-like macrophages associate with inflammation and insulin resistance, whereas resident M2-like AT macrophages involve in AT homeostasis. Although the distinction is artificial, macrophages can possess features of both M1 and M2 phenotypes (Martinez and Gordon, 2014).

I.1.3 Function

As mentioned above, WAT is involved in various regulations of energetic homeostasis and endocrine. In energetic homeostasis, WAT stores energy as lipid postprandial use later, which is related to the endocrine function of WAT. BAT is well known for thermogenesis through using the energy of the cell. In order to produce heat and regulate body temperature, it also has endocrine functions that are linked to the thermogenic process and metabolism. These two tissues are important in energy homeostasis.

I.1.3.1 Function of WAT

I.1.3.1.1 Energy storage in WAT

One of the main functions of adipose tissue is to store energy in the form of triglycerides (TAG). This storage can be carried out in two ways: either by the re-uptake of plasma free fatty acids to follow the hydrolysis of TAG from lipoproteins or by de novo lipogenesis. Lipogenesis is a process of fatty acid and TAG synthesis, stimulated by high fat and/or carbohydrate intake. Acetyl-CoA synthesis fatty acids and esterification of free fatty acids to glycerol form TAGs. Most Fatty acids used for TAG synthesis in AT come from the diet. In humans, AT has all the enzymes involved in lipogenesis, but this process is more likely to occur in the liver. (Björntorp and Sjöström, 1978; Sjöström et al., 1973). Glucose, the main substrate for lipogenesis, induces the release of insulin which activates lipogenesis and inhibits pancreatic glucagon releasing. In contrast, lipogenesis will be inhibited during fasting because reduced blood glucose and free fatty acid levels (Kersten, 2001).

AT mainly build up its lipid reserves by the re-uptake of free fatty acid (FFA). After eating, lipogenesis in the liver leads to increase levels of TAG. TAGs are stored in circulating particles, mainly chylomicrons (CM) that are produced from chyle and very low density lipoproteins (VLDL) formed in the liver. Because of their size, they can not pass through the blood capillaries to get close to the adipocytes in order to transfer their lipid content into these cells. TAGs must be dissociated into FFA and released by CM or VLDL via lipoprotein lipase (LPL) (Wong and Schotz, 2002; Wong et al., 1997). LPL is produced and activated by adipocytes under the effect of insulin after postprandial period; otherwise, it decreases in fasting (Sadur and Eckel, 1982). LPL is secreted by the adipocytes and released into the lumen of capillaries where it becomes anchored to ECs. Here, LPL interacts with CMs and VLDL to liberate fatty acids and monoacylglycerol (MAG), facilitating their uptake (Seo et al., 2000) (Figure. 7).

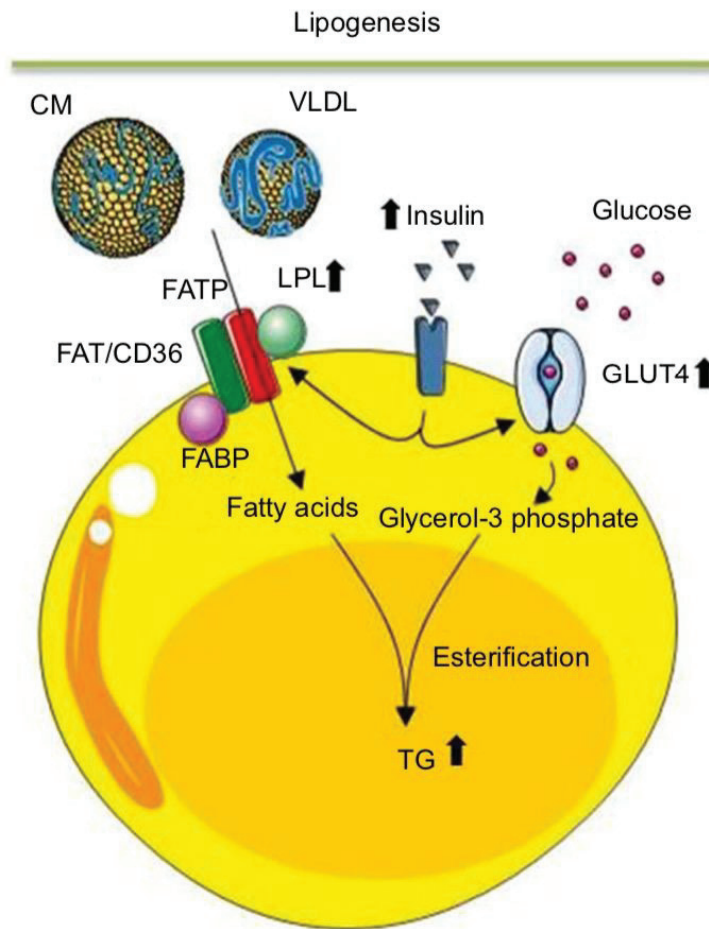


Figure 7. Lipogenesis and triglycerides synthesis (Badimon et al., 2015).

I.1.3.1.2 Lipolysis and Its Regulation

Lipolysis is involved when energy in the body is low and requires the use of TAG reserves. FFAs are the most energy products released by adipose tissue. To release the three FFAs that are linked to glycerol by ester groups, there are mainly three enzymes involved: adipose triglyceride lipase (ATGL), hormone-sensitive lipase (HSL) and monoacylglycerol lipase (MAGL).

This phenomenon makes it possible to provide a large source of energy in the form of ATP to metabolically active tissues such as muscles. Lipolysis is specific for adipocytes and its major regulators in humans are catecholamines, natriuretic peptides and insulin which will act on Protein Kinase A (PKA) or Protein Kinase G (PKG).

Catecholamines, mainly including adrenaline, norepinephrine and dopamine, are organic compounds derived from tyrosine. Norepinephrine released by sympathetic nerves stimulates lipolysis through β -adrenergic receptors consist of three sub types (β_1 -AR, β_2 -AR and β_3 -AR). In white adipocytes, β_1 -AR and β_2 -AR are involved in lipolysis (Barbe et al., 1996). These receptors are coupled to Adenylate Cyclase (AC) by stimulating G proteins (Gs proteins), which leads to activation of PKA in a manner dependent on cyclic AMP. In contrast, neuropeptide Y inhibits lipolysis by coupling inhibitory G proteins (Gi proteins) to AC.

Natriuretic peptides are known for their implications in the cardiovascular and renal systems. In 2000, a study showed that these peptides are powerful lipolytic agents both in vivo and in vitro (Sengenès et al., 2000). Their signaling is different from that of catecholamines. The activation of the peptide A receptor induces the activation of guanylate cyclase (GC), which induces nucleotide cyclization from GTP to cGMP instead of ATP. cGMP activates protein kinase G (PKG) which will phosphorylate HSL to induce lipolysis (Sengenes et al., 2003). This lipolysis is independent of the signaling pathways of β -AR (Galitzky et al., 2001).

Insulin is also involved in inhibiting the lipolytic process, in particular through a cAMP-dependent mechanism. Insulin binds to its receptor and causes phosphorylation of a regulatory subunit of Phosphatidyl inositol 3-kinase (PI3K), which will induce its activation. The activated PI3K will phosphorylate one of its targets: the protein B kinase (PKB) also known as Akt. PKB phosphorylates and activates phosphodiesterase 3B (PDE-3B), which will degrade cAMP to AMP and prevent stimulation of PKA (Langin, 2006). However, PDE-3B is unable to interact with cGMP (Moro et al., 2004). Phosphatase 1 (PP-1) is a cAMP-independent mechanism of insulin involved protein. Insulin activates PP-1 by phosphorylation, which induces rapid dephosphorylation and deactivation of HSL, thus inhibits lipolysis (Olsson and Belfrage, 1987; Ragolia and Begum, 1998; Strålfors and Honnor, 1989).

I.1.3.1.3 Endocrine function of WAT

In recent years, WAT has been considered as an endocrine organ because the discovery of leptin. Thus, WAT is not only known for its capacity for energy storage but also fundamental for systemic metabolism. The number of adipokines has expanded rapidly including leptin, adiponectin, resistin, serpin, lipocalin-2, Pai-1, RBP4, Zn a-2 glycoprotein, vaspin, visfatin, omentin, apelin, and chemerin involved in systemic effects and also TNF- α , IL-6, and MCP-1 that exert inflammatory response or cell migration (MacDougald and Burant, 2007). Figure 8 showed some adipokines and

their function in the control of energy balance (Vázquez-Vela et al., 2008). Because issue of adipokines exceeds the scope of this thesis, only selected adipokines will be mentioned in more detail.

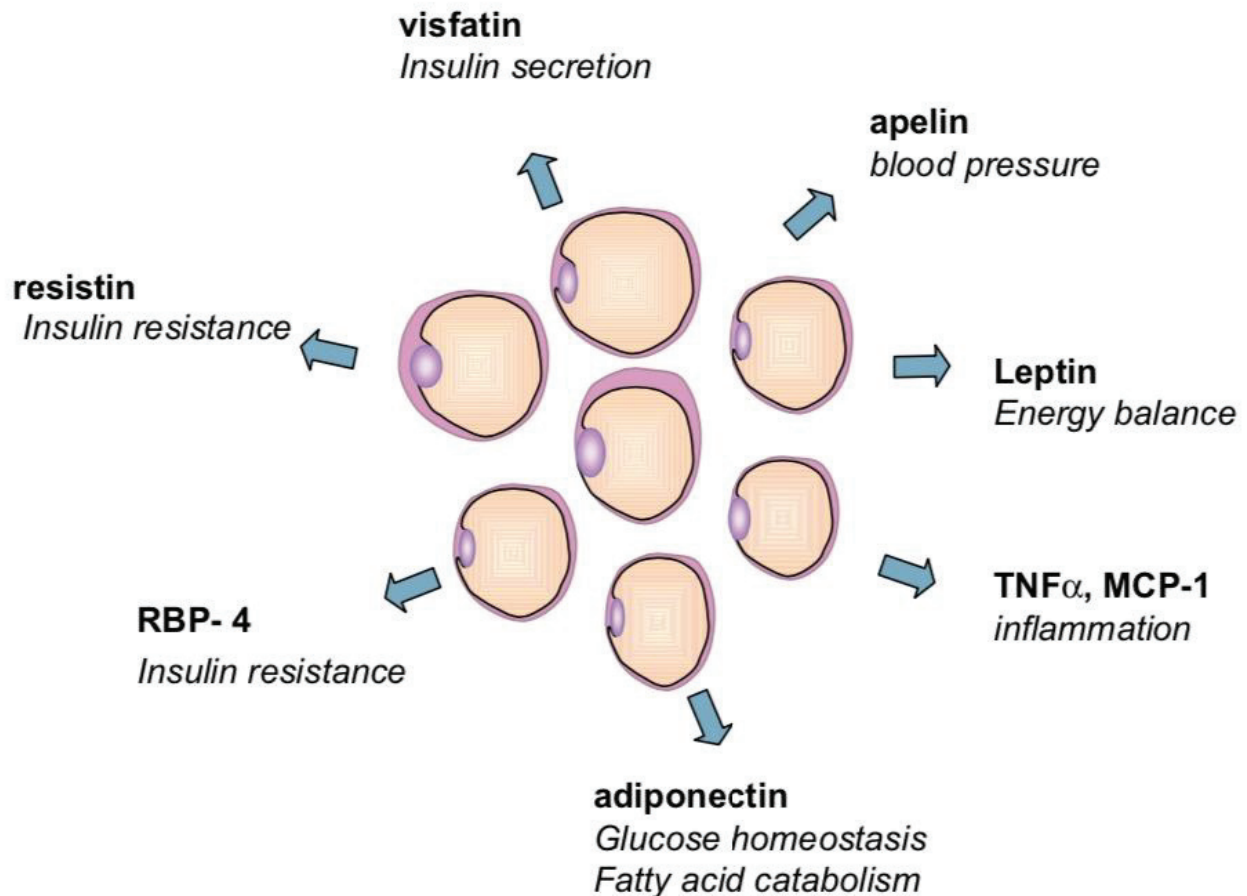


Figure 8. Adipose tissue as endocrine organ. Adipocytes secrete several proteins with endocrine functions designated as adipokines that regulate glucose and fatty metabolism in peripheral tissues, energy expenditure homeostasis, inflammatory response, and blood pressure, among others. Imbalanced secretion of some of these adipokines is associated with obesity and metabolic syndrome (Vázquez-Vela et al., 2008).

Adiponectin

Adiponectin is present at high levels in blood (3-30 $\mu\text{g/ml}$), which particularly produced by adipocytes (Ouchi et al., 2003). Plasma levels of adiponectin, IL6 and C-reactive protein (CRP) are negatively correlated with the accumulation of body fat, especially visceral fat (Ryo et al., 2004; Ouchi et al., 2003; Esposito et al., 2003). Lower level of adiponectin plasma indicated systemic inflammation in obese individuals. On the other hand, increasing adiponectin levels occur, when obese women lost bodyweight through calorie restriction and lifestyle changes. Thus, adiponectin is a unique adipokine, which secreted at the high level by the functional and insulin-sensitive

adipocytes and decreasing in dysfunctional adipocytes frequently found in obese body (Lihn et al., 2005).

Leptin

Leptin was identified in ob/ob mice, which is important in regulating feeding behaviour through central nervous system (Zhang et al., 1994). Contrary to adiponectin, leptin levels, correlate positively with adiposity and therefore considered as a parameter of long term energy reserves. When leptin was knocked out, the ob/ob mice suffer from hyperphagia which resulted in obesity and insulin resistance (Friedman and Halaas, 1998). Furthermore, in leptin deficient animals or humans, administration of recombinant leptin reverses these changes. Nevertheless, in diet induced obesity, increased leptin levels do not exert the expected anorexic responses, which indicates the occurrence of leptin resistance (Cui et al., 2017). In addition, leptin also has multiple roles in the immune system, capable of activating both adaptive and innate immunity (Naylor and Petri., 2016).

Interleukin 6

IL6 is one of pro-inflammatory cytokines, and approximately one third of total produced by AT (Fried et al., 1998). Clinically, plasma IL6 levels positively correlate with fat mass in human and weight loss leads to a decrease in IL6 levels (Esposito et al., 2003; Fried et al., 1998; Ziccardi et al., 2002). IL6 concentration also increases in plasma of type 2 diabetic patients, therefore an increased IL6 in plasma indicated the development of type 2 diabetes (Pradhan et al., 2001). Elevated secretion of IL6 may interrupt proper insulin signalling and thus blunt not only glucose uptake by insulin-sensitive tissues but also increase AT lipolysis, which can lead to redundant lipid accumulation and lipotoxicity (Rotter et al., 2003; Wueest et al., 2016).

I.1.3.2 Function of BAT

I.1.3.2.1 Thermogenesis in BAT

BAT processes non-shivering or adaptive thermogenesis through lipid oxidation, which only exist in mammals to protect species in situations that could dangerously lower body temperature, such as newborns at birth, mammals during hibernation and those exposed to the cold. This function thanks to brown adipocytes that it contains, which differ from the white adipocytes present in the WAT. Brown adipocytes have many mitochondria with a very particular morphology giving them a very high capacity of respiration and oxidation of the substrates, associated with a thermogenic activity.

The majority of cells in human body produce ATP through mitochondria respiration in oxidation reaction. The coenzymes NADH (reduced nicotinamide adenine dinucleotide) and FADH₂ (reduced flavin adenine dinucleotide) are reoxidized by the mitochondrial electron transport chain (respiratory chain) through various complexes with oxygen consumption, which resulted in a proton pumping in the inter membrane space of the mitochondria accompanied with the formation of a proton motive force driving the protons back into the mitochondrial matrix. In a "classical breathing" mechanism, the proton motive force allows the activation of ATP synthase and thus the phosphorylation of ADP to ATP (Figure. 9) (Brondani et al., 2012).

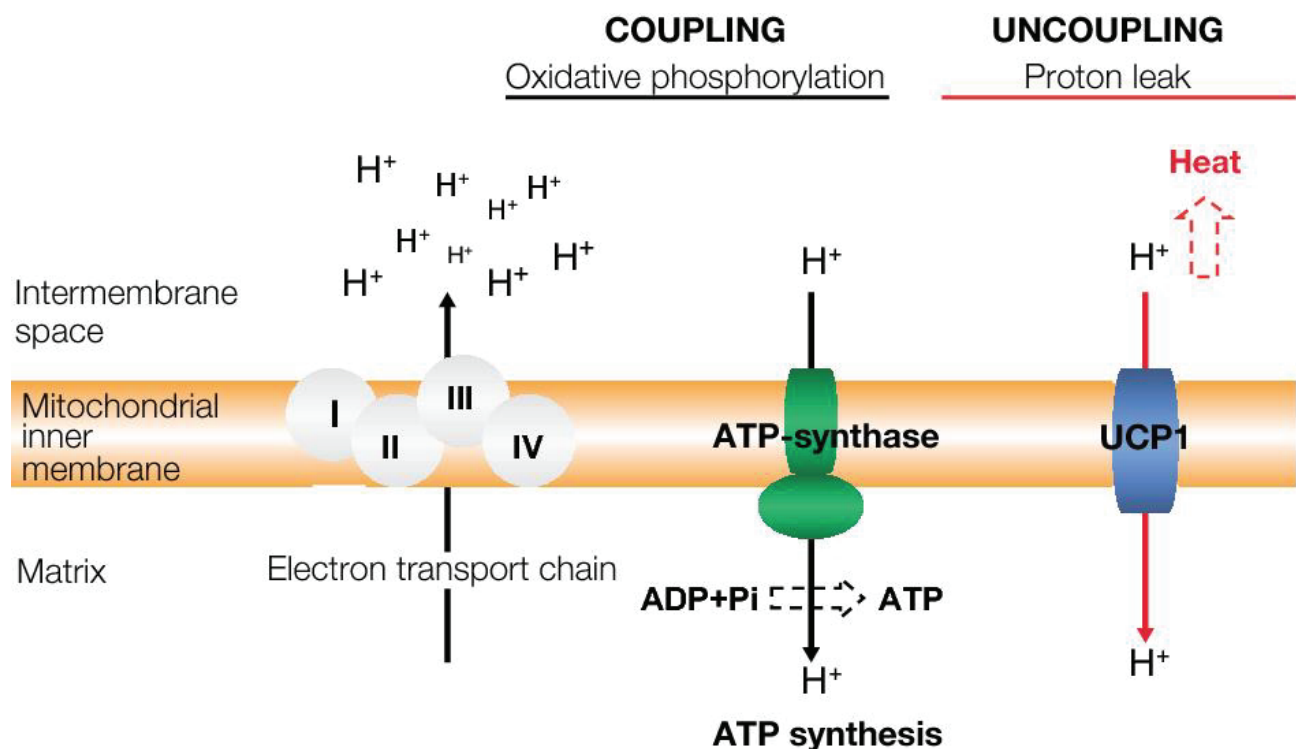


Figure 9. Function in the mitochondrial respiratory chain (MRC). Numbers I-IV corresponds to the MRC complexes. ATP-synthase is the fifth complex of the MRC. During respiration, protons are pumped through the MRC complexes, and a proton gradient is generated. The energy of the proton gradient drives the synthesis of ATP by the ATP-synthase complex. UCP1 catalyzes a regulated re-entry of protons into the matrix, uncoupling the MRC and, consequently, reducing ATP synthesis and generating heat (Brondani et al., 2012).

BAT thermogenesis must be tightly controlled so that heat is only produced under very specific conditions (e.g. falling body temperature). At room temperature (i.e. 20–22 °C), mice need to consume 60% more food to maintain their body weight to compensate for increased energy expenditure mediated by their BAT (Cannon and Nedergaard, 2009). On the contrary, even at thermoneutral temperatures, BAT depletion or dysfunction in rodents results in decreased energy expenditure, leading to an obese phenotype (Feldmann et al., 2009; Lowell et al., 1993). Therefore, increased energy dissipation is not easily compensated by a proportional increase in food intake, which suggests BAT thermogenesis is a promising anti-obesity therapeutic strategy.

In brown adipocytes, the energy obtained through oxidation does not allow the production of ATP, therefore the protons go back into the mitochondrial matrix through the mitochondrial protein Uncoupling protein 1 (UCP1) which allows the release of energy stored in the proton force in the form of heat (Cannon and Nedergaard, 2004; Kuhn et al., 2012) (Figure. 10). The UCP1 promoter has several transcriptional regulatory sequences some of which are activated in response to catecholamines and cAMP (Cassard-Doulcier et al., 1998; Rim and Kozak, 2002).

Activation of brown adipocytes is mainly via the sympathetic innervation and release norepinephrine. The catecholamine binding to the β 3-adrenergic receptor results in the activation of a cascade involving PKA, HSL, production of FFA from TAG and activation of UCP1. Specifically, norepinephrine activates AC causing cAMP production by binding to the β 3-adrenergic receptor. Increasing the level of cAMP activates PKA that will phosphorylate many nuclear and cytosolic proteins. For example, PKA phosphorylates the cAMP response element-binding protein (CREB) that is involved in UCP1 expression (Rim and Kozak, 2002). In addition, PKA induces activation of the P38 MAP kinase pathway that is required for UCP1 expression, and the use of an inhibitor of this kinase in brown adipocytes prevents thermogenesis confirming the importance of PKA (Cao et al., 2001; Fredriksson et al., 2001). At the cytosolic level, PKA plays a major role in lipolysis. It phosphorylates perilipin 1 causing its dissociation of lipid droplets and also activates HSL (Chaudhry and Granneman, 1999). The interaction between HSL and TAG is facilitated to lead to a lipolysis process and causes the release of fatty acids used as a substrate for thermogenesis. Acyl-CoA Activated FFA by ACS (Acyl-CoA Synthesis) is first transferred into Mitochondria. The β -oxidation of Acyl-CoA as well as the activity of the citric acid cycle (CAC) lead to the formation of reduced electron carriers NADH and FADH₂, which followed by oxidation steps creating a proton gradient in the intra membrane of mitochondrial that will be used by UCP1 to dissipate energy in the form of heat (see Figure. 9 and Figure. 10) (Cannon and Nedergaard, 2004).

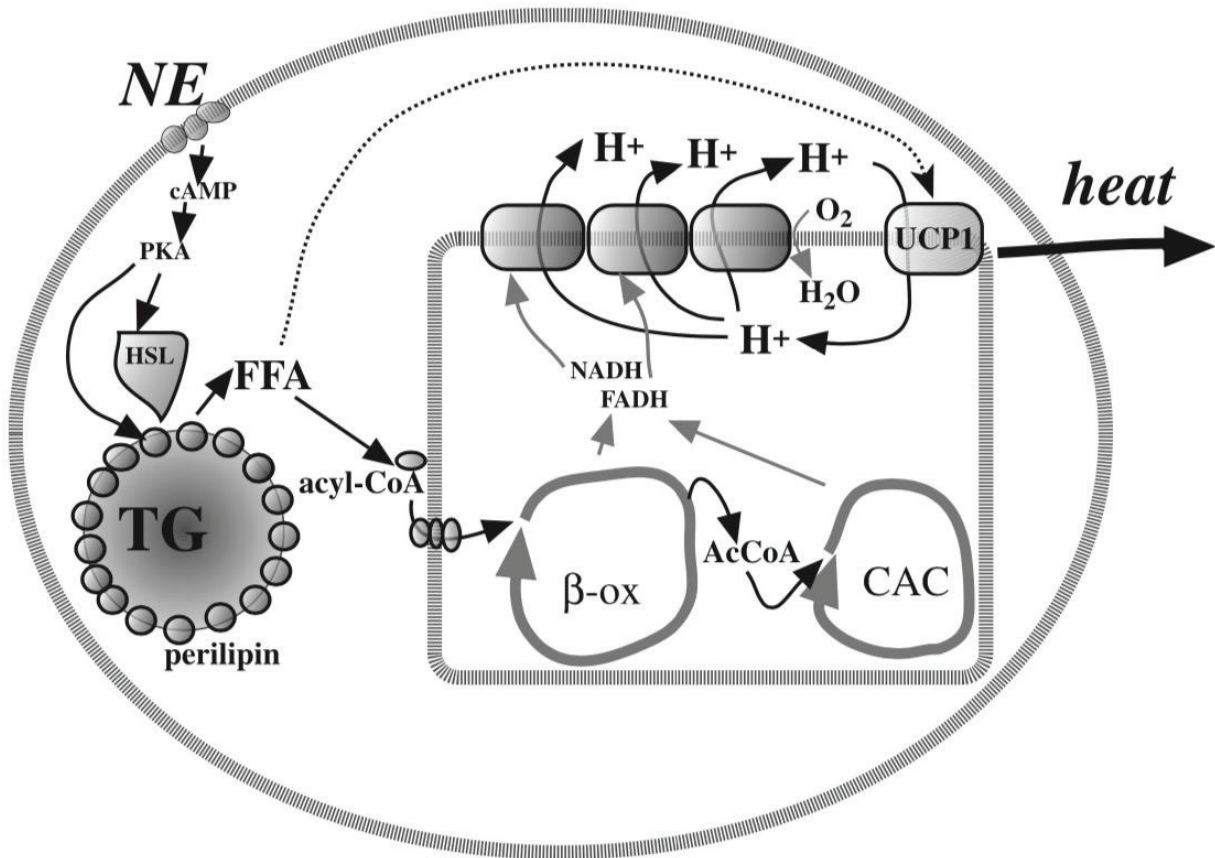


Figure 10. Norepinephrine-induced stimulation of thermogenesis in brown adipocytes: events downstream of the protein kinase A (PKA) activation. HSL, hormone-sensitive lipase; TG, triglyceride droplet; AcCoA, acetyl CoA. Free fatty acids (FFA) activated to acyl CoAs by acyl-CoA synthetase are first transferred to acyl-carnitine by the highly expressed muscle form of carnitine palmitoyltransferase I (M-CPT I), which is the CPT I form found in both brown and white adipose tissue (205) and which is very sensitive to inhibition by malonyl CoA. The acyl-carnitine probably enters the mitochondria through the carnitine transporter (not as yet explicitly described in brown adipose tissue) and is probably reconverted to acyl CoA by CPT II. The ensuing -oxidation (-ox) of the fatty acids (acyl CoAs) as well as the activity of the citric acid cycle (CAC) lead to the formation of the reduced electron carriers FADH and NADH, which are then oxidized by the electron transport chain (respiratory chain; here indicated by the series of gray boxes), ultimately through oxygen consumption. This results in a pumping out of protons from the mitochondria and the formation of a proton-motive force that drives the protons back into the mitochondrial matrix through the uncoupling protein UCPI. The energy stored in the proton-motive force is then released as heat (Cannon and Nedergaard, 2004).

I.1.3.2.2 Endocrine in BAT

BAT also has a secretory role, which could influence systemic metabolism and contribute to BAT activation. Paracrine and autocrine manner have been identified in BAT, which promote hypertrophy and hyperplasia of BAT, vascularization, innervation and blood flow, processes that are all involved with BAT recruitment when thermogenesis is elevated (Figure. 11) (Villarroya et al., 2017). In addition, BAT can also release molecules that influence on other tissues and organs (Figure. 12) (Villarroya et al., 2017). The beneficial effects of BAT transplantation in rodents could be partly due to the secretory capacity of BAT. Fibroblast growth factor 21, IL-6 and neuregulin 4 are among the first BAT-derived endocrine factors, which also called brown adipokines or

batokines, associated in enhancing systemic metabolism and BAT activation. The discovery of such adipokines might be a new approach to counteract obesity and its associated metabolic diseases.

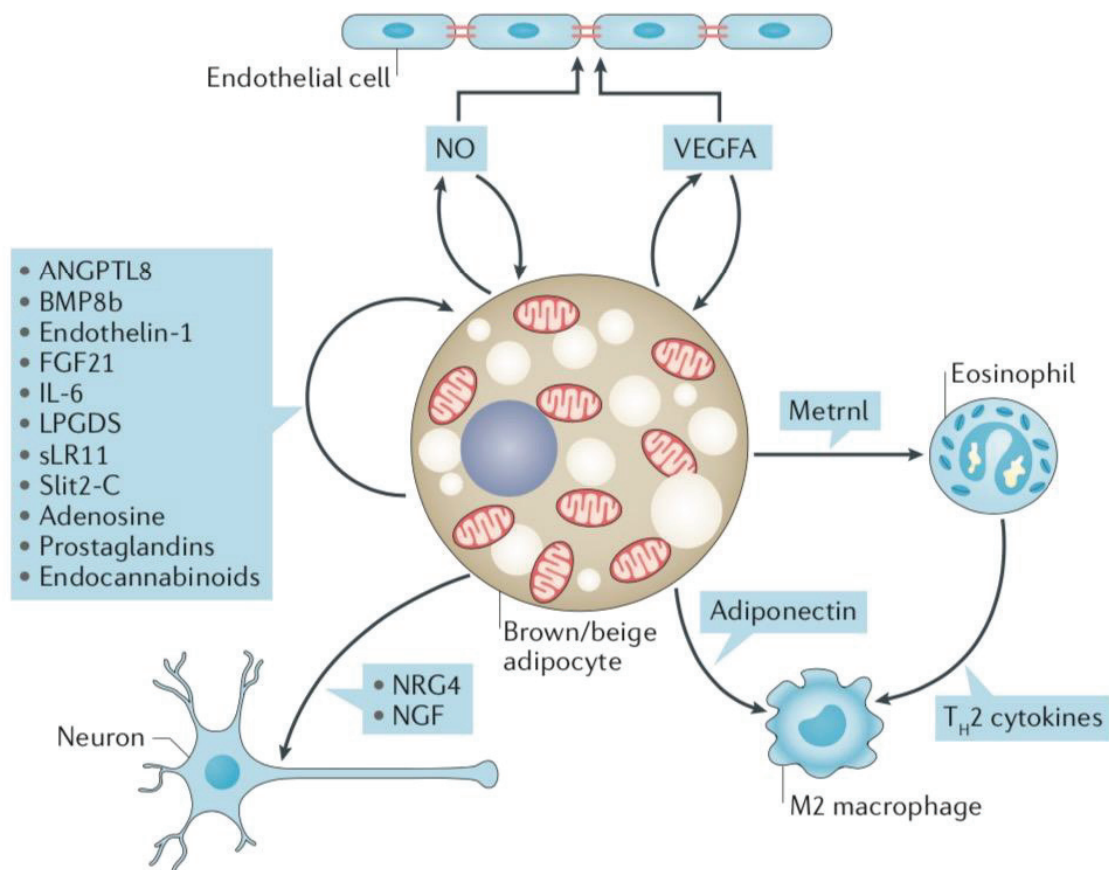


Figure 11. The autocrine and paracrine factors released by brown and beige adipocytes. Brown and beige adipocytes secrete factors with autocrine actions that lead to enhanced (by BMP8b, endothelin-1, FGF21, IL-6, LPGDS) or inhibited (by sLR11) thermogenic activity. Other factors secreted by brown and/or beige adipocytes act locally on other cell types. Nerve growth fibre (NGF) secreted by brown adipocytes promotes sympathetic innervation, secreted vascular endothelial growth factor A (VEGFA) targets endothelial cells to induce vascularization of BAT and nitric oxide (NO) increases blood flow, processes that are associated with brown adipose tissue (BAT) recruitment in response to sustained thermogenic activation. Meteorin-like protein (Metrnl) is secreted by beige, and possibly brown, adipocytes and promotes eosinophil activation, which results in the recruitment of alternatively activated M2 macrophages. The release of adiponectin by beige adipocytes also seems to induce alternative activation and recruitment of M2 macrophages. ANGPTL8, angiopoietin-like8;BMP, bone morphogenetic protein; LPGDS, lipocalin D synthase; NRG4, neuregulin 4; sLR11, soluble LDL receptor 11 (Villarroya et al., 2017).

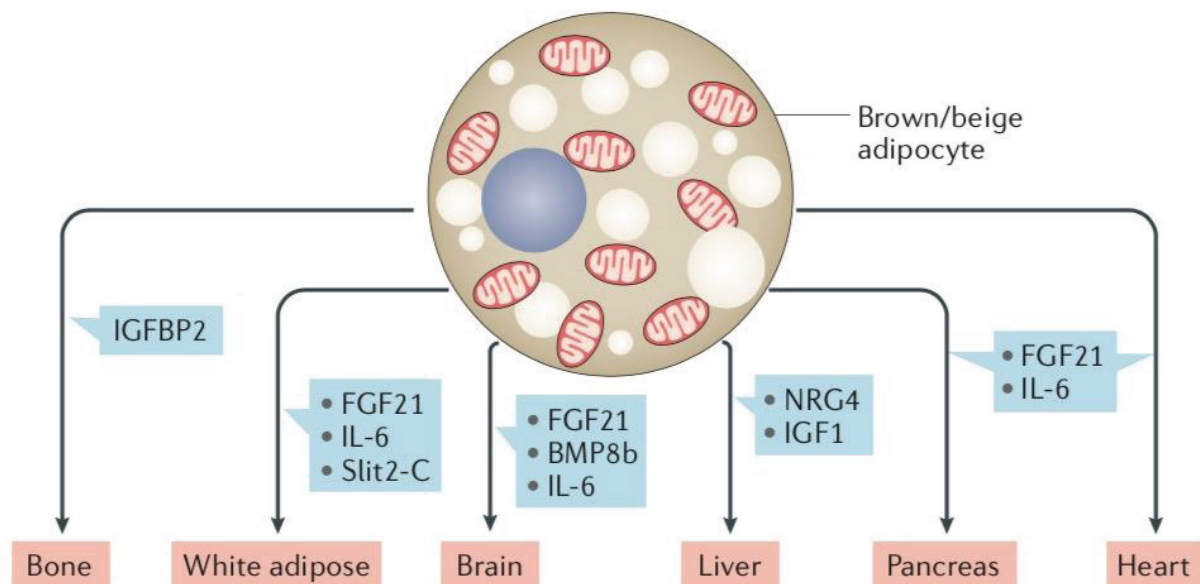


Figure 12. Putative batokines and target organs. Endocrine factors released by brown and beige adipocytes might signal to distinct tissues, including the brain. Some of these factors (fibroblast growth factor 21 (FGF21), Slit2-C) might also target white adipose tissue (WAT) in an endocrine (and autocrine and/or paracrine) mechanism to induce the browning of WAT and the metabolic processes associated with provision of substrates to fuel thermogenesis. In the pancreas, FGF21, IL-6 and possibly angiopoietin-like 8 (ANGPTL8) might improve insulin secretion and β -cell function. Brown adipose tissue (BAT) might also release NRG4 to attenuate lipogenesis in the liver, insulin-like growth factor binding protein 2 (IGFBP2) to promote bone formation and FGF21 and IL-6 to increase cardiac substrate oxidation and protect the heart from hypertrophy and oxidative stress. The endocrine factors released by BAT might modulate systemic metabolism indirectly through the central nervous system, and BAT-released factors such as FGF21, IL-6 and possibly BMP8b might influence sympathetic nervous system activity and other processes such as feeding, circadian behaviour and female endocrine function. IGF1, insulin-like growth factor 1; NRG4, neuregulin 4 (Villarroya et al., 2017).

FGF21

FGF21 is primarily produced by the liver and help maintain the balance of glucose and lipid levels through the use of glucose in AT (Giralt et al., 2015; Markan et al., 2014; Nishimura et al., 2000). FGF21 also causes glucose oxidation in the liver, WAT and pancreas (Coskun et al., 2008). However, when BAT thermogenesis is activated, brown adipocytes produce and secrete a large amount of FGF21, which mainly regulated by cAMP induction (Chartoumpekis et al., 2011; Hondares et al., 2011). FGF21 promoting thermogenesis by lipid oxidation as well as induction of PGC-1 α which will increase UCP1, suggests its autocrine effects (Kleiner et al., 2012; Hondares et al., 2011). Activation of BAT seems to contribute to the systemic levels of FGF21. Upon activation by cold, the expression of FGF21 increases in the BAT but decreased in the liver. In UCP1 deficiency mice, a large amount of FGF21 is found from BAT and muscles, but its level of expression remains stable in the liver. Therefore the expression of FGF21 is independent of the thermogenesis mediated by UCP1 (Hondares et al., 2011; Keipert et al., 2013, 2015). In addition, FGF21 is more expressed in beige adipocytes than brown adipocytes (Sharp et al., 2012). All of its

results indicate that FGF21 has several positive effects on metabolism through the prevention of hyperglycemia and hyperlipidemia and the protection against obesity via energy expenditure (Giralt et al., 2015).

IL-6

The expression and the release of IL-6 by the brown adipocytes is carried out following a thermogenic stimulation. It should be noted that the pro-inflammatory effects of some cytokines in WAT do not have the same physiological consequences in BAT or skeletal muscles. The effects of IL-6 are mainly related to the lipolysis necessary to serve the thermogenic process. It also increases insulin sensitivity (Burysek and Houstek, 1997; Ikeda et al., 2016). IL-6 is important for keeping the beneficial effects during BAT transplantation. There was no improvement in carbohydrate homeostasis and insulin sensitivity in BAT-transplanted IL-6 deficient mice. In addition, this IL-6 disruption prevents the elevation of FGF21 (Stanford et al., 2012).

Bone morphogenetic protein 8b (BMP8b)

BMP8b, unlike other proteins of the BMP family, is not involved in adipocyte differentiation but in the induction of BAT thermogenic activity. Its expression is increased to respond to certain stimuli such as cold exposure or an HFD diet. The secretion of BMP8b by brown adipocytes improves the β -adrenergic response in an autocrine / paracrine manner. This improvement is achieved by an increase in the signaling of certain proteins of the SMAD family (1, 5 and 8 respectively) as well as the p38-MAPK pathway, which increases the expression of UCP1. BMP8b also acts on the hypothalamus to activate thermogenesis via stimulation of the sympathetic nervous system (Whittle et al., 2012). It should be noted that the presence of estrogens induces the expression of BMP8b and its expression is higher in female mice than in males, indicating that the activity of BAT is variable depending on the sex of the individual (Grefhorst et al., 2015).

Neuregulin 4 (NRG4)

NRG4 is a member of the epidermal growth factor family, acting in an autocrine/paracrine or endocrine manner. NRG4 is enriched in brown and beige adipocytes is also thought to promote neurite outgrowth (Rosell et al., 2014). In transcriptomic microarray assays, the *Nrg4* gene is predicted to encode secreted proteins that are induced during brown adipocyte differentiation (Rosell et al., 2014; Wang et al., 2014). It is demonstrated that NRG4 is associated in attenuating hepatic lipogenic signalling in mice based on gain of function and loss of function studies in mice (Wang et al., 2014).

I.2 Development of adipose tissue

I.2.1 Adipogenesis

Adipogenesis is a multi-step process leading to adipocyte development, including two stages of commitment and terminal differentiation. In the first phase, stem cells engage in the adipocyte lineage, thus progressively restrict their potentials for differentiation to generate adipose progenitors. Then during the second stage, these adipose progenitors differentiate into mature and functional adipocytes. The majority of studies on adipogenesis are made from cell models already involved in the adipocyte lineage. Therefore, terminal differentiation is much better characterized than commitment.

I.2.1.1 Commitment

Commitment is the first step in the process of differentiation, from the multipotent stem cells to adipose progenitors. Their morphology can not be distinguished from its precursors, since they have lost the potential to differentiate into cell types other than the adipocyte. Little information is available on the commitment process of the adipocyte development program and nowadays the factors or genes responsible for this stage are still poorly understood. A common theory is that mature adipocyte secretes factors promoting the proliferation of adipose progenitors and their differentiation (Considine et al., 1996; Lau et al., 1990; Marques et al., 1998). However, none of these factors were identified in these studies. The diversity of cells present in the SVF of adipose tissue allows the secretion of many factors that may play a role in adipogenesis. Here are the most important details so far.

The family of Bone Morphogenic Proteins (BMPs)

BMPs are ligands belonging to the TGF- β super family (Transforming Growth Factors), involved in the commitment of stem cells to adipogenic lineage. The BMP signaling pathway has been extensively studied in bone formation during development. However, among BMPs, two are involved in adipocyte differentiation: BMP4 and BMP7. BMP4 has been described to play a role in vivo engagement. In the presence of BMP4, the majority of murine C3H / 10T1 / 2 embryonic cells acquire the features of adipose progenitors. In the presence of a differentiating condition, these cells differentiate into adipocytes (Tang et al., 2004). Therefore, BMP4 allows the commitment of cells into adipose progenitors, and leading to the terminal differentiation. In human MSCs, BMP7 ligand promotes adipogenesis by inhibiting the expression of osteogenesis factors (Neumann et al., 2007). BMP7 triggers the engagement of mesenchymal cells into the brown adipose lineage. Implantation

of BMP7 treated C3H / 10T1 / 2 cells in nude mice leads to adipose tissue development predominantly containing brown adipocytes (Tseng et al., 2008). Furthermore, BMP7 also has an active role in brown adipocyte differentiation. BMP7 treatment on brown adipose progenitors activates the program of brown adipogenesis with induction of early regulatory genes marker of the brown adipocyte (PRDM 16 and PGC-1 α), and results in an increase expression in UCP1, and adipogenic transcript factors PPAR γ and CEBP.

Zfp423

Zfp423 is a transcription factor discovered during the development of the adipogenic potential in embryonic fibroblasts. Those who did not have this protein could not differentiate into adipocytes due to lack of PPAR γ (Gupta et al., 2010). Zfp423 induces adipogenic commitment by amplifying BMP signaling through interacting with SMAD domains. This factor is enriched in high adipogenic fibroblasts compared to murine non-adipogenic fibroblasts. In addition, over expression of ZFP423 in non-adipogenic NIH 3T3 fibroblasts strongly activates the expression of PPAR γ in undifferentiated cells and promotes differentiation of these cells into adipocytes under appropriate conditions. In contrast, the reduction of ZFP423 expression in murine 3T3-L1 APs inhibits the expression of PPAR γ and decreases the ability of these cells to differentiate (Gupta et al., 2010). Therefore, ZFP423 is identified as a transcriptional regulator of the commitment of the adipocyte lineage.

The Wnt signaling pathway

The Wnt pathway is important for maintaining the proper functions of mature tissues. In the absence of ligand, β -catenin is phosphorylated by the enzyme GSK3 (glycogen synthasekinase 3), which leads to its degradation by the proteasome. When the Wnt pathway is active, GSK3 is inhibited and prevents degradation of β -catenin, which will be translocated to the nucleus and bind to the family of TCF transcription factors, and induce the expression of various genes (Logan and Nusse, 2004). Overexpression of Wnt or a mutated form of β -catenin makes it more stable to prevent differentiation of 3T3-L1 cells by inhibiting adipogenic transcription factors such as PPAR γ and CEBP α . In contrast, inhibition of the Wnt pathway in these cells triggers the differentiation process with increased expression of PPAR γ and CEBP α (Ross et al., 2000). Wnt 10B is also involved as a bone mass regulator, promoting osteogenesis at the expense of adipogenesis (Bennett et al., 2005). For transgenic mice expressing Wnt10b in adipocytes, there is a 50% reduction in WAT mass and an absence of BAT (Longo et al., 2004).

Preadipocyte factor 1(Pref-1)

Pref-1 is a transmembrane protein that becomes active after enzymatic cleavage (Villena et al., 2002). The expression of Pref-1 is very high in APs and decreases during adipogenesis. Its involvement in the adipocyte lineage has been studied. Transgenic mice in which cells expressing Pref-1 are labeled were generated. These Pref positive cells appear to be very early adipose progenitors and not expressing Zfp423 and PPAR γ yet. The specific knocking out of Pref1 labeled cells in both the embryonic and adult stages results in loss of adipose tissue. Therefore, progenitors expressing Pref1 are essential for the development and expansion of adipose tissue (Hudak et al., 2014). Flow cytometry experiments in humans showed the presence of Pref1-expressing cells as well as the ASC-specific marker CD34 in the WATsc SVFs. However, when cultured, the cells expressing Pref1 are not able to differentiate into adipocytes (Zwierzina et al., 2015). Indeed, Pref1 is described in humans as a ASCs marker and acts as a negative regulator of adipogenesis (Mitterberger et al., 2012). Its role in humans is still unclear.

I.2.1.2 Terminal differentiation

Terminal differentiation is the process that causes APs to become mature and functional adipocytes. As mentioned previously, more key molecules involved in the differentiation phase are better characterized than the commitment one. Some adipose progenitor models such as murine 3T3-L1 cell line require mitotic clonal expansion (MCE), i.e. one to two cell cycles prior to differentiation. A hypothesis was proposed to explain that mitosis unrests strands of DNA which facilitates access of the transcription factor response elements during adipogenesis (Cornelius et al., 1994). Differentiation requires the activation of many transcription factors that are responsible for coordinating induction and the inhibition, and more than 2,000 genes are involved in adipocyte physiology and morphology (Farmer 2006; Zhu et al., 2015). The main determining factors for terminal adipogenesis are described below:

Peroxisome Proliferator-Activated Receptor- γ (PPAR γ)

PPAR γ has previously been described as a major regulator of differentiation for both white and brown adipocytes (Barak et al., 1999; Rosen et al., 2002). Two isoforms of PPAR γ exist: PPAR γ 1 expresses constitutively in all tissues and PPAR γ 2 is specific for AT (Zhu et al., 1995). These two isoforms are strongly induced during adipogenesis and maintained during differentiation (Morrison and Farmer, 1999). Several studies of gain or loss of function in mice indicate that PPAR γ is associated in the formation of AT. The loss of PPAR γ results in lipodystrophy and insulin resistance (Farmer 2006; Hegele et al., 2002). Furthermore, PPAR γ is necessary for adipogenesis and its potential is strong enough to differentiate non-adipogenic cells such as fibroblasts or myoblasts into adipocytes (Hu et al., 1995; Tontonoz et al., 1994a). PPAR γ controls the

transcription of several genes involved in storage, lipid synthesis, glucose metabolism and adipokine secretion (Barak et al., 1999; Tontonoz et al., 1994b). PPAR γ is also important for maintaining the differentiated state of adipocytes. The use of an adenovirus expressing the dominant negative form of PPAR γ in 3T3-L1 adipocytes causes dedifferentiation and results in loss of lipid accumulation and expression of adipocyte markers (Tamori et al., 2002).

The family of CCAAT-Enhancer-Binding Proteins (CEBP)

The CEBP family is also important for the induction of adipogenesis like PPAR γ , which consists of CEBP α , CEBP β and CEBP γ . This family has a transcriptional activation domain (basic leucine zipper) which makes it possible to dimerize and bind to the CCAAT site of the promoter of several genes involved in adipogenesis (Birkenmeier et al., 1989). CEBP α has a central role in adipocyte differentiation, which promotes the expression of specific adipocyte genes during differentiation in vitro (Garcia de Herreros and Birnbaum, 1989). The ectopic expression of CEBP α in mouse embryonic fibroblasts induces adipogenesis but only in the presence of PPAR γ (Freytag et al., 1994). However, the opposite situation is not observed, since over expression of PPAR γ without CEBP α induces adipocyte differentiation. These results indicate that CEBP α is involved in adipocyte differentiation but not sufficient (Rosen et al., 2002). A positive signaling loop occurs between PPAR γ and CEBP α at first, followed by a second loop between PPAR γ and CEBP β that enhances differentiation (Park et al., 2012, Rosen et al., 2002; Wu et al., 1999). Transcriptional activation by CEBP α induces the transcription of FABP4, GLUT4 transporter, insulin receptor and several other genes (Christy et al., 1989; Kaestner et al., 1990; McKeon and Pham, 1991). A high level of CEBP α activates specific transcription of adipocyte genes and accumulation of lipids in the lack of differentiation-inducing cocktails (Lin and Lane, 1994). In fact, the use of RNAi (interfering RNA) against CEBP α prevents the accumulation of lipids and the conversion of progenitors into adipocytes (Lin and Lane, 1992). However, proteins expressed early in differentiation such as the LPL is not affected by the deletion of CEBP α (Samuelsson et al., 1991). Mice deficient for CEBP α are usually lipodystrophy. They have less WAT, but the effects are lower for brown AT (Linhart et al., 2001).

CEBP β and CEBP γ act at the very beginning of terminal differentiation. The accumulation of these two factors happens in the first 24 hours after the induction of differentiation when the cells are in the MCE (Cao et al., 1991; Tang et al., 2003). CEBP β is induced through activation of the CREB site by cAMP (Zhang et al., 2004). CEBP γ as well as CEBP β are induced by glucocorticoids (Cao et al., 1991). These two proteins directly induce the expression of PPAR γ and CEBP α : two primary transcription factors of adipogenesis (Tang et al., 2005). In fact, the individual deletion of these

two proteins in the mouse has little effect on the development of the adipose mass whereas a double KO strongly reduces the adipocyte development (Tanaka et al., 1997). CEBP β interacting with PDRM16 induces brown adipocyte differentiation from Myf5 progenitors (Kajimura et al., 2009). Their interaction induces the expression of PGC-1 α as well as UCP1 (Barbera et al., 2001, Karamanlidis et al., 2007). In addition, over expression of CEBP β alters the phenotype of white adipocytes to adipocytes with brown adipocyte characteristics.

Sterol Regulatory Element Binding Proteins (SREBPs)

SREBP are zipper basic helix-loop-helix-leucine proteins. SREBP2 regulates the transcription of genes involved in cholesterol metabolism, whereas SREBP1-c controls lipogenesis (Horton, 2002). In the adipocyte differentiation program, the expression of SREBP1-c is activated shortly after the expression of CEBP α and PPAR γ . The over expression of SREBP1-c in the murine 3T3-L1 line in presence of differentiation inducing hormones results in an increase in the expression of adipocyte markers and lipid accumulation. On the other hand, the ectopic expression of this transcription factor in fibroblasts can lead to their conversion to adipocytes but only under certain conditions. The expression of a dominant negative completely abolishes the adipocyte differentiation. These data suggest that, in vitro, SREBP1-c is required for adipogenesis but does not have as much adipogenic capacity as PPAR γ (Kim and Spiegelman, 1996). Finally, SREBP1-c is involved in the activation of lipogenic genes, including those allowing the synthesis of fatty acids and triglycerides. Insulin regulates this transcription factor and thus promotes the energy storage by activating the expression of lipogenic enzymes (Yellaturu et al., 2009).

The Kruppel-like factors (KLF) family

KLFs are a family of "zinc-finger" transcription factors involved in commitment and differentiation terminal. They are involved in the regulation of apoptosis, proliferation and differentiation. Indeed, KLFs play a major role in the regulation of physiological systems including cardiovascular, digestive, respiratory, hematological and immune systems. But they can also be involved in conditions such as obesity, cardiovascular disease, cancer and inflammatory conditions (McConnell and Yang, 2010). Among KLFs, KLF15 promotes adipocyte differentiation and induces expression of the GLUT-4 glucose transporter (Mori et al., 2005; Gray et al., 2002). KLF5 is induced in the early stages of adipocyte differentiation by CEBP β and CEBP δ , and activates the PPAR γ 2 promoter (Oishi et al., 2005). KLF6 inhibits Pref1 expression in murine 3T3-L1 cells. Over expression of KLF6 is not sufficient to promote adipocyte differentiation, but reduced adipogenesis is observed when suppressed (Li et al., 2005). KLF9 regulates the expression of PPAR γ 2 and CEBP α during differentiation. The use of RNAi against KLF9 disrupts adipogenesis (Pei et al., 2011). However,

not all KLFs are necessarily pro-adipogenic. KLF7 and KLF2 are known to inhibit the growth of cancer, and KLF2 is especially to inhibit the PPAR γ 2 promoter (Kanazawa et al., 2005; Wu et al., 2005).

I.2.2 Developmental origin of adipose progenitors

I.2.2.1 Embryonic origin

Mouse embryonic stem cells could differentiate into an adipocyte cell line (Dani et al., 1997). The treatment of embryoid bodies by retinoic acid and then by a specific differentiation medium made it possible to obtain adipocytes. These adipocytes from embryoid bodies have lipid storage, lipolysis and high expression of adipocyte-specific genes. This model was later studied in order to know the various stages of the development of adipocytes. However, it is still necessary to determine the origin of human progenitors capable to differentiate into adipocytes. Initially, APs originate similar to mesenchymal stem cells from mesoderm (Farmer, 2006).

However, during the development of vertebrates, it was established that their origin was not necessarily mesenchymal. A first study showed that the cells from the neural crest could differentiate into adipocytes. However in 2007, my laboratory showed that primary cultures of quail cells isolated from the cephalic neural crest have the ability to differentiate into adipocytes in presence of adipogenic factors (Billon et al., 2007). Subsequently, our team used a CRE system linked to a fluorescent protein for the Sox10 gene (the best marker for cells from the neural crest). During embryonic development, fluorescent staining was found only at the level of the neural crest and not in the mesoderm. This study has shown that there are two origins in APs: an ectodermal for adipose cephalic deposits and the other mesodermal for the rest of adipose deposits of the body. Recently, using human induced pluripotent stem cells (hiPSCs), we have shown that human cells derived from the neuroectoderm are able to differentiate into adipocytes suggesting that some human adipose tissue deposits may also have an origin other than mesodermal (Hafner et al., 2016).

I.2.2.2 Origin of the white adipose progenitor

The development of WAT varies among species. In mice, WAT develops after birth, although white progenitors are detected on days 16.5-17.5 of the embryonic stage (Birsoy et al., 2011). In humans, WAT is formed around weeks 14 and 16 of pregnancy (Poissonnet et al., 1984). The proliferation of APs tends to decrease towards the end of pregnancy, and adipocytes are increased mainly by the filling lipids of the predetermined cells until the age of 10 years. The increase in the

number of APs occurs during adolescence to the adult phase, determining the total number of adipocytes (Knittle et al., 1979). Several studies indicate that APs have a common origin with ECs. APs expressing PPAR γ inside young mice are physically associated with the walls of the blood vessels in adipose tissue (Tang et al., 2008). The use of the promoter of VE-cadherin, an EC-specific protein, to trace the adipocyte lineage shows that the reporter gene is found in ECs as well as in white and brown APs (Tran et al., 2012). In another study, ZFP423, an essential transcriptional regulator for adipocyte lineage commitment, was used to label APs. These cells have a high adipogenic potential and are located within the perivascular compartment. The authors thus hypothesize that a subpopulation of ECs is capable to differentiate into adipocytes (Gupta et al., 2012). However, one study questioned these results since white APs express PDGFR α (Platelet-derived growth factor receptor α) but are different from PDGFR α positive cells located in blood vessels and therefore do not originate from ECs (Berry and Rodeheffer, 2013). On the other hand, PPAR γ KO in EC does not affect AT formation, but only the metabolic response is altered if the animals are on an HFD diet (Kanda et al., 2009). As we have just seen, many hypotheses and studies have tried to define the origin of white APs without obtaining concordant results, which indicates that the origin of the adipocytes is complex. Moreover, it can not be ruled out that, since the different fatty tissue deposits do not share the same characteristics, their origins are varied. Finally, all the results obtained by lineage tracing were carried out on murine models and obviously can not be carried out on human. The immense possibilities of differentiation offered by the hiPSCs could make it possible to provide these responses in humans.

I.2.2.3 Origin of the brown adipose progenitor

BAT has a different origin than those of WAT. In mice and rats, BAT may be identified during embryogenesis but does not express significant amounts of UCP1 until postnatal maturation. In contrast, humans and herbivores are able to switch rapidly to non-shivering thermogenesis after birth. The peak expression of UCP1 thus occurs after birth and slowly decreases as BAT is gradually replaced by WAT (Symonds, 2013). Like white APs, brown APs express PDGFR α and come from mesodermal precursors (Lee et al., 2012). However, brown adipocytes have markers that are very different from white adipocytes. The use of a Cre-Lox system to insert a fluorescence gene into cells shows that brown adipocytes and skeletal smooth muscle cells have common precursors that express Myf5 (Myogenic factor 5) and Pax7 (Paired box 7) (Lepper and Fan, 2010; Lepper et al., 2009; Seale et al., 2008; Tallquist et al., 2000). Myf5 is a transcription factor for muscle differentiation, and Pax7 is also a transcription factor which cooperates with Myf5 to induce muscle formation or myogenesis (Braun and Gautel, 2011; Lang et al., 2005). However, lineage

tracing experiments have detected the presence of a few white adipose progenitors expressing Myf5 (Shan et al., 2013).

Although brown adipocytes and muscle cells have a common precursor, there is a divergence between 9.5 and 12.5 gestation days in mice (Lepper and Fan, 2010). In adulthood, brown adipocytes could come from satellite stem cells present in skeletal muscle (Yin et al., 2013). These data are confirmed by the expression of myogenic cell specific transcription and microRNA factors in brown adipose progenitors, which imply that brown adipocyte progenitors express certain myogenic genes and that they have a different origin than white precursors (Timmons et al., 2007; Walden et al., 2009; Schulz et al., 2011). Just like brown adipocytes, skeletal muscle cells have the possibility of using lipids instead of storing them and consist of a large amount of mitochondria (Billon and Dani, 2012, Tseng et al., 2010). But unlike brown adipocytes, muscle cells do not possess the UCP1 protein that promotes thermogenesis (Farmer, 2008).

I.2.2.4 Origin of the beige adipose progenitor

The origin of the beige adipocytes and their progenitors is the most controversial. Several hypotheses are advanced ranging from a conversion of white to beige adipocytes, the presence of bi-potent progenitors to the existence of progenitors specific to beige adipocytes. Although beige adipocytes have the thermogenic function of brown adipocytes, in mice the majority comes from progenitors do not express Myf5 and Pax7 (Cinti, 2009). However, some studies have demonstrated that in mice the beige adipocytes in some WAT deposits were positive for the Myf5 marker (WAT retroperitoneal and subcutaneous anterior) whereas others were not (WAT inguinal) (Sanchez-Gurmaches et al., 2012; Tallquist et al., 2000). These results indicate that it is very difficult to find specific precursors for each of these adipocytes.

A study has made it possible to determine the origin of the beige adipocytes by means of transdifferentiation. By using a reporter system in which the UCP1 promoter induces the expression of the human estrogen receptor (ER), they found that adipocytes become beige adipocytes expressing this receptor in inguinal WAT after exposure to cold. Rehabilitation at normal temperature results in the disappearance of these beige adipocytes and a return to a white phenotype, which is in favor of bi-directional interconversion (Rosenwald et al., 2013). Another study was carried out thanks to a mouse model in which only the adipocytes are permanently labeled with β -galactosidase (β -Gal) in the presence of doxycycline. In this model, de novo-formed adipocytes do not express β -Gal and cold exposure induces the formation of multilocular adipocytes

in WATsc which have the characteristics of beige adipocytes but which do not express β -Gal, indicating that these adipocytes were produced by clonal expansion of precursors (Wang et al., 2013). Another study showed that beige adipocytes appearing in WAT after adrenergic stimulation containing bromodeoxyuridine, which is in favor of progenitor expansion (Lee et al., 2012). Through lineage tracing, Lee et al showed that progenitors that can differentiate into beige adipocytes expressing PDGFR α . They are said to be bi-potential because they are able to give both beige and white adipocytes after in vitro differentiation (Lee et al., 2012). The hypothesis of the existence of a beige specific adipose progenitor is supported by the characterization of immortalized adipose progenitors from WAT and BAT in vitro. Indeed, some of the adipose progenitors derived from WAT differentiate preferentially into beige adipocytes (Wu et al., 2012). These results suggest different types of adipose progenitors exist in WAT. Some are able to produce beige adipocytes but their origin is still confused.

These different theories are not exclusive and one can imagine that their validity depends on the deposition of WAT. In human, there are several adipose deposits having a heterogeneity for markers such as *PAX3* and *HOXC10* for different WAT deposits (eg, arm vs abdomen vs knee) (Foissac et al., 2017). It can be seen that *PAX3* expression is higher at higher ATs and decreases towards lower ATs. In contrast, *HOXC10* is found only in the lower ATs. It has also been shown that depending on the origin of human ATs (white vs. brown), some genes are higher in the knee compared to chin such as the HOX family (*HOXA9* / *HOXA1* / *HOXC6* / *HOXC8* / *HOXC9*), and that genes such as *ACTA1* / *COL6A6* / *MYH2* / *ZIC1* are found higher in chin AT contrary to that of knee (Kouidhi et al., 2015). The whole of the developmental origins of white, beige and brown adipocytes are summarized in figure 13 (Rosenwald and Wolfrum, 2014).

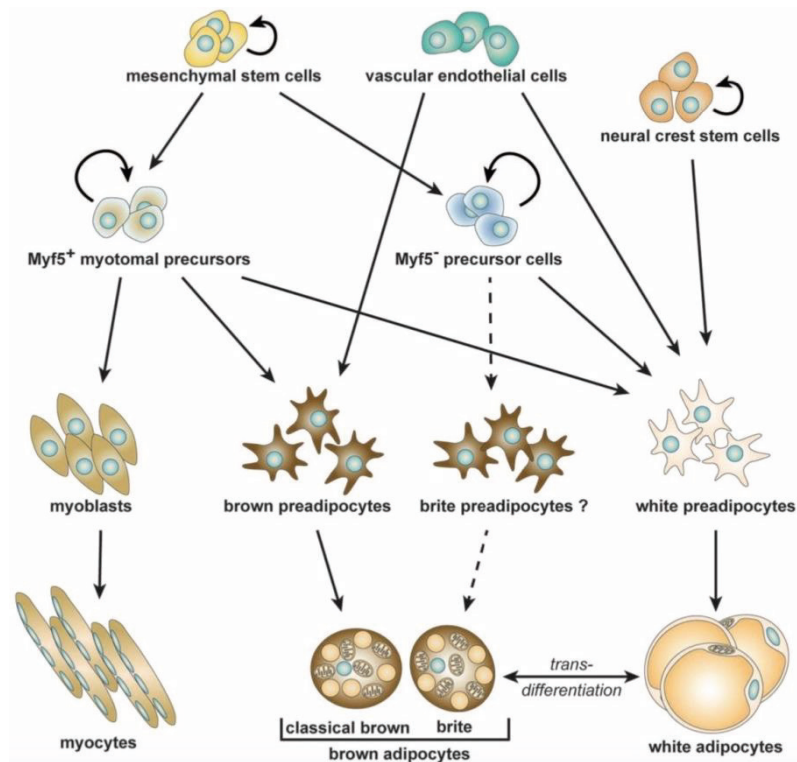


Figure 13. Developmental lineages of adipocytes. Schematic representation of the current knowledge about the possible developmental origins of murine adipocytes, including skeletal myocytes for comparison. At the level of preadipocytes (or myoblasts), the cells are considered committed to a specific differentiation. However, due to the lack of definite molecular markers, it should be noted that precursor cells and preadipocytes can be at least partly overlapping populations. Solid arrows represent conclusions from *in vivo* lineage tracing studies, dotted lines represent conclusions inferred from *ex vivo* or *in vitro* studies (Rosenwald and Wolfrum, 2014).

I.3 Adipose tissue associated pathology

AT is important for energy homeostasis in the body. Nevertheless, there are some diseases that cause disturbances in its size and / or function. Two major disturbances are obesity and lipodystrophy. The causes are different but the consequences remain relatively.

I.3.1 Obesity

Obesity is a disease due to recent changes in lifestyle and results from an imbalance between the intake and the expenditure of energy. According to the World Health Organization (WHO), obesity is defined as "a situation of abnormal or excessive accumulation of fat in adipose tissue leading to health inconveniences". The main associated metabolism diseases are type 2 diabetes, arterial hypertension, dyslipidemia (excess lipids in the blood), cardiovascular disorders, sleep apnea syndrome, other respiratory diseases and joint diseases such as osteoarthritis. Obesity is also associated with an increased risk of certain cancers, such as endometrial cancer. According to the WHO, this disease currently affects almost the entire world, including many emerging countries.

The diagnosis of this disease is mainly through the calculation of the body mass index (BMI). BMI is the weight (in kg) divided by the square of the height (in meters). According to the WHO classification, we are talking about overweight when it is over 25 and obesity when it exceeds 30 (Figure. 14). This indicator is now questioned because it is only the reflection of the total body fat and does not distinguish fat mass from lean mass and their distribution. Another indicator used is waist circumference. When it is greater than 100 cm in men and 88 cm in women, it is called obesity. Indeed, the excess fat located around the belly is associated with greater risks of metabolic disorders. According to Global Health Observatory (GHO) data, in 2016, 39% of women and 39% of men aged 18 and over were overweight, which makes obesity a real public health issue (Figure. 15).

BMI classification	
Underweight	<18.5
Normal range	18.5 – 24.9
Overweight:	>=25.0
<i>Preobese</i>	25.0 – 29.9
Obese:	>=30.0
<i>Obese class I</i>	30.0 – 34.9
<i>Obese class II</i>	35.0 – 39.9
<i>Obese class III</i>	>=40.0

Figure 14. The BMI classification from WHO.

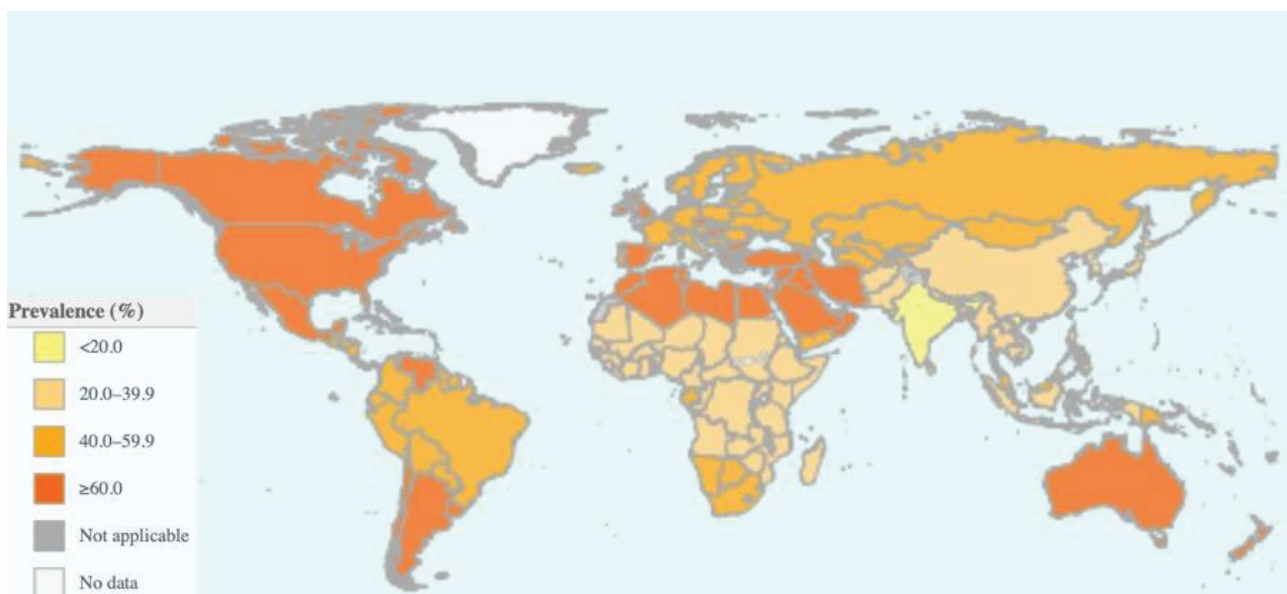


Figure 15. Prevalence of over weight among adults, age 18+: Both sex 2016 adapted from Global Health Observatory (GHO) data.

It is interesting to note that within the WAT itself, different deposits have different metabolic activities depending on their location. Thus, the accumulation of visceral, deep abdominal and subcutaneous WAT is correlated with an increased risk of diabetes, cardiovascular disease and mortality. In contrast, the accumulation of subcutaneous gluteofemoral WAT, which is more important in women, is associated with better insulin sensitivity and decreased metabolic abnormalities (Lee, 2013). One of the possible explanations for this diversity is that the adipocytes from these deposits are not all equivalent and have differences in the secretion of adipokines, levels of lipolysis, and triglyceride synthesis. For this purpose, transplantation experiments were conducted in mice. The visceral tissue graft subcutaneous has no effects, however, the reverse transplantation of subcutaneous tissue in the visceral reduces adiposity and improve carbohydrate homeostasis (Tran and Kahn, 2010). These results demonstrate that there are intrinsic differences between deposits. Similarly, under the same culture conditions, preadipocytes isolated from human subcutaneous abdominal tissue or omental visceral tissue exhibit different proliferation, adipogenesis and apoptosis capacities (Tchkonia et al., 2007). These preadipocytes have distinct gene expression patterns with more than 500 genes that vary. It is interesting to note that among these genes, the category of transcripts that differs the most (about 25%) is that of developmental regulators, which suggests that these distinct properties could be acquired during development.

The medical treatment required for this disease is weight loss (through a control of nutritional intake) with a resumption of physical activity. Specific drug treatments are very limited and are more aimed at treating metabolic complications. Surgery of obesity (or bariatric surgery) allows a significant and lasting loss of weight associated with an improvement of the metabolic abnormalities but this invasive approach has critical side effects and is reserved for the most severe cases. Today, the rediscovery of BAT in adult has become a new approach for treating obesity. This new perspective has reinforced the need for knowledge of the conditions and factors necessary for the recruitment of these cells from the precursors present in the body.

I.3.2 Other diseases associated with obesity

The pathological expansion of adipose tissue causes chronic inflammation with deleterious effects on the homeostasis of the human body. Thus, obesity also leads to adverse consequences for many organs leading to other pathologies, which will be briefly explained in this part.

I.3.2.1 Insulin resistance and type 2 diabetes

Obesity is a strong predictor of insulin resistance in type 2 diabetes. In September 2011, the International Diabetes Federation announced that 336 Millions of people worldwide have type 2 diabetes, which causes 4.6 million deaths each year (Ashcroft and Rorsman, 2012). A study estimates that more than 11% of deaths in the United States are due to this condition (Stokes and Preston, 2017). It is therefore essential to know the mechanisms leading to the appearance of this pathology in order to fight against. Adipose tissue modulates metabolism by releasing FFA, glycerol, cytokines and adipocytokines. During obesity, the production of some of these compounds is increased and causes the appearance of insulin resistance. It releases MCP-1(monocyte chemoattractant protein-1) which recruits macrophages, which in turn will secrete TNF α and IL-6. Both of these molecules are known to induce inflammation and inhibit the action of insulin (Wellen and Hotamisligil, 2005). Inflammation will reduce the storage capacity of FFAs by AT that are involved in insulin resistance (Boden, 1997). FFAs increase the formation of certain acid metabolites such as DAG / Acyl-CoA/ ceramides, which in turn activate a cascade of serine / threonine kinase leading to phosphorylation of the insulin receptor substrate 1 and 2 (IRS1 and IRS2) and a reduced ability of these molecules to activate the P13K pathway. Subsequently, downstream events of insulin receptor signaling are diminished (Shulman, 2000). In addition, the elevation of leptin and resistin as well as the decrease of adiponectin expression in AT also favors the loss of sensitivity to insulin. All of these systemic insulin resistance affect different organs such as muscles and live. To compensate for this loss of sensitivity, pancreatic β cells must secrete a large amount of insulin. Over time, this overproduction induces β -cell depletion, leading to a progressive increase in blood glucose and the development of type 2 diabetes (Poitout and Robertson, 2007; Reaven, 1988).

I.3.2.2 Dyslipidemias

Dyslipidemia associated with obesity causes an increase in TAG, FFA and low density lipoprotein (LDL) as well as a decrease in high density lipoprotein (HDL) (Wang and Peng, 2011). During obesity, the expansion of visceral WAT is accompanied by an increased lipolysis and leads to an increase in FFA that will be delivered directly to the liver via the portal. The FFA intake in the liver induces hepatic resistance, and increases the secretion of TAG-rich lipoproteins (especially very low density lipoproteins - VLDL), thus results in hypertriglyceridemia, and reduces the hepatic degradation of apolipoprotein B (apoB) (Després, 2006). Insulin resistance leads to a decrease in LPL (lipoprotein lipase) activity and consequently a decrease in VLDL catabolism, which also favors hypertriglyceridemia. In addition, obesity induces a change in the secretion of many

adipocytokines that can lead to metabolic disorders. For example, TNF- α , which increases during obesity, decreases LPL expression and stimulates TAG synthesis in the liver (Feingold and Grunfeld, 1987). On the other hand, circulating concentrations of adiponectin are negatively correlated with BMI, is involved in the clearance of VLDLs (Qiao et al., 2008). Finally, the increase of TAG-rich VLDL during obesity leads to an increase exchanges between TAGs and esterified cholesterols, via the CETP (Cholesteryl ester transfer protein), inducing the formation of TAG-enriched HDL particles. The latter are good substrates for hepatic lipase, the activity of which is increased during obesity, and this results in the decrease of HDL in the obese subject (Klop et al., 2013).

I.3.3 Lipodystrophy

Lipodystrophic syndromes represent a heterogeneous group of disease, all defined by a partial or generalized loss of ATs. This deficit is due to a lack of adipocyte differentiation. Most lipodystrophies are caused by an inability to store triglycerides in the lipid droplet. AT is then dysfunctional and leads to metabolic abnormalities, cardiovascular, impaired glucose tolerance and dyslipidemia, which may be due to genetic or acquired origin. The involvement of the different AT deposits varies according to the lipodystrophic syndrome involved suggesting different origins for WAT. Thus, during Berardinelli-Seip syndrome (a generalized lipodystrophy of genetic origin), AT is almost completely absent from subcutaneous, intra-abdominal, trunk and bone marrow deposits. However, patients retained WAT at the retro-orbital level, mouth, palms, soles and other areas. This syndrome is due to a mutation in the gene of seipin (Magré et al., 2001). In contrast, the Dunnigan syndrome (a genetic partial lipodystrophy) is due to a mutation in the lamin A / C gene and is characterized by a decrease AT in the subcutaneous, extremities and trunk, but there is no consequence in visceral, neck or face (Shackleton et al., 2000). It is interesting to note that in partial lipodystrophic syndromes, AT is atrophic in some areas of the body while it accumulates in others. This underlines the different physiology of AT according to its location, since the same alteration induces distinct phenotypes according to the part of the body affected and reinforces the hypothesis of a different developmental origin.

II Human “brite”/brown adipocyte cellular models

It has long been believed that BAT is absent or very scarce in human adult, so its contribution to energy expenditure is not considered relevant. The discovery of thermogenic BAT in human adults provides an innovative strategy for counteract overweight/obesity and related metabolic diseases. The energy consumption in BAT is responsible for the adaptive heat production in response to cold stimulation. In the past 20 years, a large number of mouse models have demonstrated the potential of BAT to counteract metabolic dysfunction. Molecular circuits for differentiation and function of mouse brown adipocytes have been strongly studied due to the availability of primary cell cultures and the existence of many useful cell models. The selection of human adipocyte models derived from adult BAT is limited, therefore hampering the study of molecular control in human brown adipocyte differentiation and function. In human and mouse, BAT have comparable UCP1 functions (Porter et al., 2016), but intrinsic differences between them have been observed (Ramage et al., 2016; Murholm et al., 2013; Kiwaki and Levine, 2003; Kern, 1988), which highlight the relevance of proper human-derived cell models to validate and/or identify key factors involved in inducing thermogenic process in adipocytes. In this section, we will discuss the different human adipocytes cellular models and regulation of their differentiation and/or activation process.

II.1 Immortalized cell lines isolated from human BAT

II.1.1 Immortalized SVF from human infant BAT

The PAZ6 cell line was obtained from the SVF of human infant BAT and immortalized following microinjection of the genes encoding simian virus 40 T and t antigens under the control of the human vimentin promoter (Zilberfarb et al., 1997). The PAZ6 cell line has been described in 1997 as an adipogenic cell line which can form multilocular after a differentiation treatment for 2 weeks (Zilberfarb et al., 1997). PAZ6 cells could be maintained in culture for several months with neither losing their morphological characteristics nor their molecular markers including β 1- and β 2-AR, HSL, adiponin, GLUT1 and GLUT4. Those cells accumulated multilocular fat stores and expressed β 1-, β 2-, β 3- and α 2-AR, lipoprotein lipase (LPL) leptin and UCP1, when exposed to a differentiation cocktail containing insulin, triiodothyronine (T3) dexamethasone and pioglitazone. *UCP1* mRNA level was further increased with a 4-hour-incubation of 10 μ M noradrenalin (Zilberfarb et al., 1997). The gene expression profile during differentiation is similar to human primary adipocytes from subcutaneous adipose tissue (Kazantzis et al., 2012). Thus, PAZ6 cells acquire the characteristics of brown adipocytes throughout differentiation. However various

functions were not investigated in this cellular model. Notably, data on mitochondrial biogenesis and function are lacking, which is importance in brown adipocyte physiology.

II.1.2 Immortalized clonally derived adult human brown adipocytes

Shinoda et al. established sub-cloned human brown-like cell models immortalized following infection with T and t SV40 antigens from non-matched patients (Shinoda et al., 2015). They isolated a total of 65 clonally immortalized preadipocytes obtained from SVF in supraclavicular BAT biopsies of two non-obese individuals, which is considered as a UCP1-positive depot (Jespersen et al., 2013). Seven clonal lines (10.8%) among the 65 clones found to exhibit highly adipogenic properties, which similar to that of a previous report with approximately 6.5% of cloned SVFs (20 out of 305 clonal lines) (Wu et al., 2012). They subsequently analyzed three out of the seven adipogenic lines for globally analyzing their molecular signatures after RNA sequencing and found that a UCP1-positive population in human adipocytes possessed molecular signatures resembling beige adipocytes. In addition, they identified molecular markers in this population, and potassium channel K3 (KCNK3) and mitochondrial tumor suppressor 1 (MTUS1) were found to be required for beige adipocyte differentiation and thermogenic function by using a loss-of-function approach. This study presents new opportunities for human BAT research, and constitutes an important foundation for future human BAT studies like cell-based disease modeling and unbiased screens for thermogenic regulators.

Xue et al. established patient-matched, sub-cloned human brown-like cell models immortalized with telomerase reverse transcriptase (TERT) (Xue et al., 2015). They generated clones of brown preadipocytes from human neck fat and characterized their adipogenic and thermogenic capacity. The variations of thermogenic potentials in these sub-clones demonstrated the heterogeneity of human BAT. Moreover, they introduced a reporter system for monitoring UCP1 expression in the clones and identified expression profiling to define novel sets of gene signatures associated with thermogenic regulations in human preadipocytes once they were mature. They identified two positive UCP1 regulators, *PREX1* and *EDNRB*, by knocking out using CRISPR-Cas9, which abolished UCP1 expression in differentiated brown adipocytes from the preadipocytes. Furthermore, they found those adipose progenitors with great thermogenic potential having the cell surface marker CD29.

These data provide new perspectives into the cellular heterogeneity in human fat and offer potential biomarkers for selecting prime preadipocytes for strong thermogenic differentiation. Although

immortalized clonal lines can provide very important information, they can not reflect the intact tissue due to the absence of heterogeneity in clonal cell models.

II.1.3 Immortalized polyclonal brown preadipocyte cell models

Markussen et al reported the generation of TERT-immortalized polyclonal, patient-matched human preadipocyte cell models from the same patient to further explore the regulation and therapeutic potential (Markussen et al., 2017). The generated cell models, TERT-hBA exhibited high proliferative and adipogenic capacities up to at least passage 20. After differentiation induction, TERT- hBA adipocytes maintain classical features of brown adipocytes, including expressing UCP1 as well as high levels of mitochondrial markers and respiratory capacity. Upon activation of β -adrenergic stimuli, the protein kinase A (PKA)-mitogen-activated protein kinase (MAPK) kinase 3/6 (MKK3/6)-p38 MAPK signaling were phosphorylated along with upregulation of thermogenic genes and increased respiration, indicating hBA adipocytes were receptive and responsive to β -adrenergic stimulation.

II.2 Preadipose cell lines and primary preadipocyte culture

Preadipocytes from human AT can be isolated and differentiated into mature adipocytes in vitro (Figure. 16) (Armani et al., 2010). Primary preadipocyte cultures can reflect adipose functions, representing a suitable cellular system to confirm data from preadipose cell lines, despite the disadvantages e.g. human samples are not easily available and the small mass of biopsies restricts both size and number of experiments. However, the proliferation and differentiation of primary preadipocytes is influenced by anatomic depots as well as the age and sex of donors, which gives a big variation from sample to sample. Thanks to the available cell models of pre-adipocytes, a lot of the knowledge about the molecular pathways that control adipocyte development has been elucidated. There are currently two different cell lines: Pre-adipocytes that have been committed to the adipose cell lineage and multipotent stem cell lines which are able to commit to different lineages, including adipose, bone and muscle lineages. Here, we summary the use of human primary cultures and to study “brite” adipocyte differentiation, as described below.

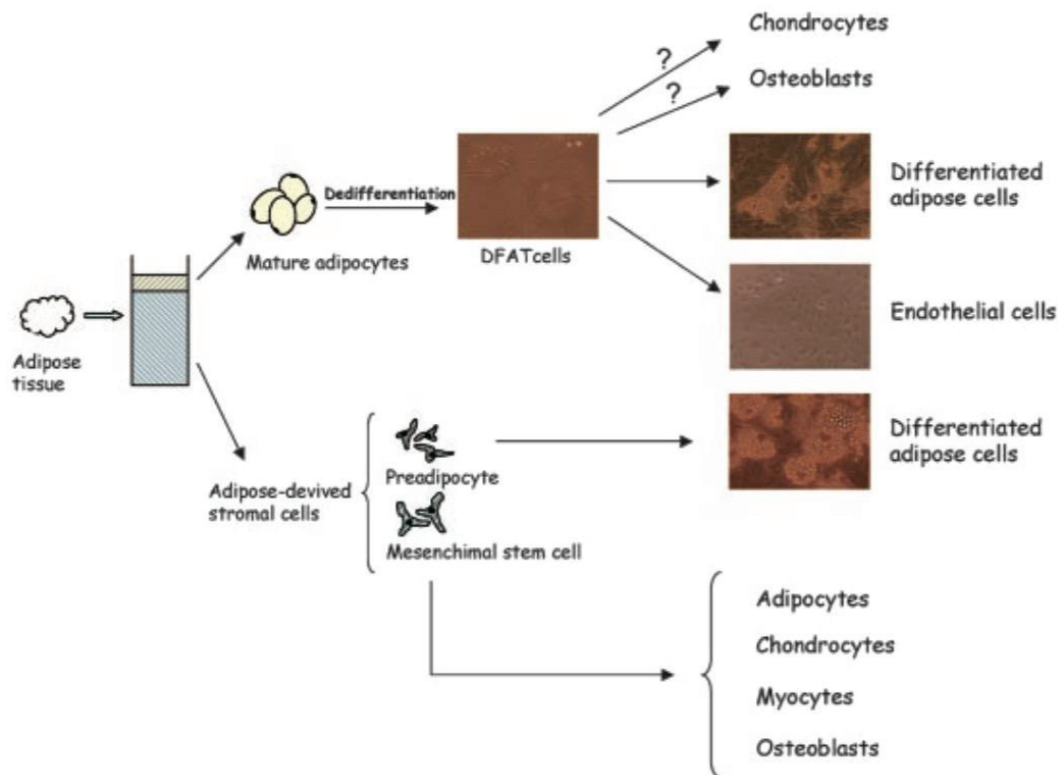


Figure 16. Preadipocytes residing in the stromal vascular fraction of adipose tissue can be easily separated from mature adipocytes by centrifugation, followed by selective purification through appropriate culture techniques or flow cytometric cell sorting. Under opportune culture conditions, preadipocytes are capable of proliferating and differentiating in vitro. Mature adipocytes, through the ceiling culture method, can dedifferentiate into proliferating fibroblast-like cells. Such cells, known as dedifferentiated fat (DFAT) cells, are able to differentiate again into adipocytes as well as to different cell types (Armani et al., 2010).

II.2.1 Primary culture of cells isolated from supraclavicular fat in adults

Since immortalized cell lines do not reliably mimic in vivo situation, primary preadipocytes are used as a cell model to study brown adipocyte cell physiology. Lee et al characterized the progenitors within fat from the supraclavicular region, which were able to differentiate into brown adipocytes expressing UCP1 (Lee et al., 2011). They used PET/CT imaging in order to localize the biopsies from the supraclavicular region, and subcutaneous biopsy from the same patient was obtained as a negative control at the same time. In addition, they compared the supraclavicular fat biopsies between PET-positive (PET+) and PET-negative (PET-) donors, and a higher amount of BAT was found in the positive one. However, UCP1 expression was high in brown adipocytes differentiated in vitro with precursors from both PET+ and PET- samples, which indicates that even though not all the donors have active BAT, the isolated primary preadipocytes in the supraclavicular region were able to differentiate into brown adipocytes expressing high levels of UCP1 (Lee et al., 2011). This suggests an important role of the microenvironment of the tissue for UCP1 expression.

II.2.2 Primary culture of cells isolated from white adipose tissue

PGC-1 α was originally identified as a cold-inducible coactivator of PPAR γ from brown adipocytes (Puigserver et al., 1998), and is now considered as a major transcriptional coactivator involved in mitochondrial and oxidative metabolism in brown fat and skeletal muscle. Therefore, over expression of PGC-1 α has been used as a mean to browning differentiated white adipocytes. Over expression of PGC-1 α for 48 hours in 13-day differentiated preadipocytes isolated from human adipose tissue, induces expression of brown adipocyte markers and enzymes involved in fatty acid oxidation (Tiraby et al., 2003). These transcriptional adaptations have resulted in a higher capacity for oxidation of fatty acids. Furthermore, rosiglitazone and retinoic acid are ligands of PPAR γ and RAR, respectively, which are important factors involved in brown adipogenesis, and over expression of PGC-1 α in combination with them enhances the action of PGC-1 α . In addition to the induction of genes related to mitochondrial oxidative metabolism, glycerol kinase expression is induced by increasing the level of *PPAR α* mRNA (Mazzucotelli et al., 2007). This enzyme allows a key step in the esterification of fatty acids and thus accelerates circulation of glycerol and free fatty acids produced by lipolysis to form new triglycerides. It is interesting to note that the activity of human glycerol kinase is higher in BAT than in WAT (Ryall and Goldrick, 1977), which also favors the conversion of over expressing PGC-1 α white adipocytes to a brown-like phenotype. In the same cellular model, a 48-h treatment with a PPAR α agonist (GW7647) strongly enhanced the catabolism of fatty acids, but no change in UCP1 expression was reported (Ribet et al., 2010). In addition, the activation of PPAR γ induced by rosiglitazone for 48 h had only moderate metabolic effects, contrary to many studies in vivo and in vitro.

In this model, over expression of PGC-1 α promotes a brown-like phenotype, which can be assuming that PGC-1 α -specific genes are induced rather than PPAR γ agonists (such as glycerol kinase or genes involved in catabolism of fatty acids more dependent on PPAR α than PPAR γ) are required for white adipocytes browning (Tiraby et al., 2003; Mazzucotelli et al., 2007). It can also be hypothesized that PPAR γ agonists have the ability to induce a brown phenotype only in uncommitted adipocyte precursors, such as mesenchymal stem cells (MSCs) or in undifferentiated preadipocytes, whereas not sufficient to trigger the conversion from mature white adipocytes to brown. This hypothesis is consistent with the 5-day treatment of rosiglitazone (belongs to the TZD family), which increases UCP1 mRNA expression in preadipocytes isolated from various depots of adult human adipose tissue (Digby et al., 1998).

II.2.3 Human adipose-derived stem cells

Jo et al studied the process of differentiation in human adipose tissue-derived stem cells (ADSC) isolated from subcutaneous adipose tissue in women and cultured under adipogenic conditions (Jo et al., 2011). They observed that ADSC differentiated into multilocular lipid droplets with UCP1 expression after 7 days of differentiation. However, when the differentiation was extended to 14 days, these cells were filled with large individual lipid droplets with reduced UCP1 expression, which indicated a conversion from brown to white adipocytes. This suggests that differentiating adipocytes could shift from white to brown phenotypes during differentiation, which supports the concept of plasticity and transdifferentiation between adipocyte subtypes (Cinti et al., 2009).

Human Multipotent Adipose-Derived Stem Cells (HMADS) were ADSCs taken from subcutaneous adipose tissue from infants (Rodriguez et al., 2004). These cells can proliferate for more than 30 passages while retaining their stem properties and retaining a normal diploid karyotype without forming tumors after transplantation. They are able to self-renew and differentiate into several cell types. In addition to be able to differentiate into adipocytes, HMADS can differentiate into chondrocytes and osteoblasts in vitro (Elabd et al., 2007; Rodriguez et al., 2004; Roux et al., 2013). The transplantation of these cells into dystrophic mouse muscles (mdx model) allows the appearance of the human form of dystrophin, a muscle protein (Rodriguez et al., 2005). The ectopic expression of MyoDI, leads to form myotubes in vitro and in vivo (Goudenege et al., 2009). The high capacity for expansion and differentiation in HMADS makes it considered as an important tool in the study new therapies targeting adipose tissue stem cells.

The use of an adipogenic cocktail makes it possible to differentiate HMADS into cells with a high adipogenic potential. More than 90% of the differentiated cells have lipid droplets highlighted by staining with Oil red O, which labels triglycerides and lipids. The differentiation of HMADS makes it possible to obtain cells with the morphological and functional properties of human white adipocytes. Adipocytes obtained from HMADS express a wide panel of adipocyte-specific genes, ranging from transcription factors such as PPAR γ 2 and CEBP α to genes important for the structure and function of adipocytes such as FABP4 and perilipin. These adipocytes can secrete leptin and adiponectin, uptake glucose in response to insulin, and induce lipolysis after β -adrenergic stimulation (Rodriguez et al., 2004). Adipogenic differentiation of HMADS in the presence of a specific PPAR γ agonist (rosiglitazone) chronically orients the differentiation to cells with thermogenic capacity. They express not only *UCPI* but also *CIDEA*, *PGC-1 α* and *DIO2* (Elabd et al., 2007). Similarly, short-term (2-4 days) treatment of these cells with rosiglitazone is sufficient to induce transdifferentiation to beige adipocytes with increased mitochondrial mass, UCP1 expression and decoupling of respiration (Elabd et al., 2007; Pisani et al., 2011). These cells

represent one of the best human models to study the white-beige conversion of adipocytes. However, the feature of infant hMADS dramatically decreases with aging.

II.3 Adipocyte progenitors derived from human embryonic stem cells (ESCs)

Human ESCs are derived from the inner cell mass of a blastocyst at embryonic day 5.5, having the ability to differentiate and self-renew for a quasi unlimited number of passages in vitro theoretically (Thomson et al., 1998). Given the ability of these cells to generate multiple cell types, ESCs have been recognized as a good model for investigating the mechanisms involved in commitment to a lineage during the course of development. Indeed, their in-vitro culture provides a unique organization to control, and therefore are able to better study the effect of certain factors such as cytokines or growth factors on the differentiation.

The differentiation of ESCs to the adipogenic lineage was first shown in mice (Dani et al., 1997). After adding a medium containing adipogenic factors, the cells can differentiate into functional adipocytes exhibiting lipolysis and lipogenesis activities. Expression of transcription factors involved in preadipocyte differentiation, such as CEBP / β or PPAR γ , are conserved during adipogenesis. Therefore, these cells are a good model for studying all stages of adipocyte differentiation. Moreover, this system has shown the importance of the retinoic acid (RA) signaling pathway. ESCs must be pretreated early with RA to be able to generate adipocytes before the addition of adipogenic factors. The addition of RA also induces the appearance of neural crest markers (FoxD3, Sox9 and Sox10), suggesting that adipocytes derived from ESCs may originate from the neural crest. In-vitro, neuroepithelial cells derived from murine ESCs, in the presence of the appropriate differentiation medium, are capable to differentiate into adipocytes (Billon et al., 2007). These results demonstrate that the adipocytes of the face in the mouse, come from the neural crest. The ESCs model also identified factors and signaling pathways that play a role in the early stages of adipogenesis (Billon et al., 2010).

More recently, it has been shown that human ESCs can also differentiate into adipocytes (Xiong et al., 2005). During the same period, one team successfully isolated neural crest stem cells (or NCSCS) during neural differentiation of ESCs (Lee et al., 2007). These NCSCS are able to differentiate in-vitro towards the mesenchymate lineage generating MSCs capable of differentiating specially into adipocytes. This suggests that human adipocytes can also have a neuroectodermal origin like mice. A few years later, Vodyanik et al direct ESCs to the mesodermal lineage and also

succeed in isolating MSCs through a co-culture system with specific murine feeders (OP9) (Vodyanik et al., 2010). Furthermore, Ahfeldt et al generated adipose progenitors derived from human ESCs which are able to differentiate into brown adipocytes. They were transduced with combinations of PPAR γ 2 with C/EBP β alone or with C/EBP β and PRDM16 in brown adipogenesis. Using this process, the brown human adipocytes exhibited mature functional properties with an increased cellular respiration, and are able to response to β -adrenergic stimulation, indicating elevated thermogenic activity (Ahfeldt et al., 2012).

Therefore, ESCs offer a novel approach for studying the origin of human adipocytes. However, the clinical application of these cells confronts several obstacles. One of them is the risk of tumor formation. The problem of biological incompatibility is another barrier to the use of ESCs in therapy (Fairchild et al., 2005). Indeed, ESCs are isolated from embryos with different immune antigens from the recipient patient. The risk is that the patient's immune system does not recognize injected cells and eliminate them. Therefore, any therapy using ESCs should be accompanied by a heavy immunosuppressive treatment of consequence for the patient.

But the main obstacles, beyond the scientific issue, are the ethical questions. Obtaining these cells requires the destruction of embryos, which is a potential human life. Indeed, religions and cultures oppose the "value" given to the embryo at the stage when it is destroyed and countries differ in their ESCs legislation.

The expectations brought by the discovery of ESCs have been hammered by the obstacles of their use (ethical, scientific and legislative) and have led researchers to question the possibility of reprogramming differentiated cells into pluripotent cells. This has led to the discovery of induced pluripotent stem cells (iPSCs) in 2006.

II.4 Adipocyte progenitors derived from induced Pluripotent Stem Cells (hiPSC)

To date the marketed drugs for BAs activation showed limited efficacy and/or displayed substantial adverse effects. Among the reasons involved in this weak efficacy, one can mention the limitation of the cell models used. Because of the rareness of BAs in adult humans, the cellular models mainly used for drug discovery are murine or human immortalized cell lines. They do not provide relevant models and do not accurately mirror human adipogenic regulatory pathways (Lindroos et al. 2013). Although primary culture and differentiation of human APs is the gold standard for investigating

adipogenic regulations and functions, these cells are difficult to obtain and have a lifetime limitation in culture. Therefore, primary human BAPs can be studied only for short periods before they reach senescence and differentiation failure precluding reproducible in vitro assays and their expansion for cell-based therapy. In addition, the applications of hESCs have ethical, scientific and legislative issues. A cellular source of human BAPs is urgently needed both for in vitro preclinical drug discovery and for the clinic.

IPSCs display a quasi-unlimited self-renewal capacity and are an abundant source of multiple cell types of therapeutic interest for drug screening and drug repositioning. In addition, human iPSCs are outstanding tools in early preclinical phase of drug discovery to perform cytotoxicity assays. They allow autologous transplantation when generated from patient's own cells. To date, autologous transplants are economically expensive, but a recent study reported the possibility of allogenic iPSC transplants, which has a tremendous potential for clinic use (Shiba et al. 2016). Human iPSCs can be cultured for long term and expanded into large numbers under complete defined conditions. Thanks to their high self-renewal capacity, producing sufficient number of cells for an effective treatment does not appear as a critical challenge, but some major concerns remain around the genome instability associated with the reprogramming process. Nevertheless, the use of iPSC-derived cells in clinic has been approved by the FDA for at least two diseases, for iPSC-myogenic progenitors to be delivered to muscular dystrophic patients and phase I/II results are showing promising safety data as well as possible efficacy when used in ocular diseases. One goal of my work thesis has been to propose the use of iPSC-BAs in the obesity field.

II.4.1 IPSC cells

II.4.1.1 Generation of iPSCs

To generate iPSCs, Yamanaka and his team started from the hypothesis that ectopic expression of important factors for ESCs stemness could convert differentiated cells into stem cells including pluripotent and self-renewal capacity.

In the first step, they identified the genes preferentially expressed in the murine ESCs (Takahashi and Yamanaka, 2006). After analyzing the available data, they selected 24 potential candidates. The effect of these factors was tested on murine embryonic fibroblasts (MEFs) carrying the neomycin resistance gene under the control of the promoter of the Fbx15 gene. This gene is only expressed in ESCs but is absent in somatic cells derived from MEFs. If the Fbx15 locus is activated by one of the factors tested, the cells become resistant to neomycin. None of the 24 candidates

were sufficient to induce reprogramming, but following the introduction of all 24 genes, neomycin-resistant colonies with a similar morphology to ESCs were formed. Through addition / withdrawal experiments, they identified 4 necessary and sufficient factors for reprogramming cells: Oct-4, Sox2, Klf4 and c-Myc. These reprogrammed cells have the same characteristics as ESCs in terms of their gene expression profile related to epigenetics and pluripotency (formation of teratomas after injection in mice). These cells were named induced Pluripotent Stem Cells (iPSCs).

Their pluripotency has been confirmed by the formation of chimeras following their injection into a blastocyst where they contribute to the formation of all lineages of the embryo including the germ line. However in this test, the chimeric embryos die prematurely demonstrating an incomplete reprogramming of fibroblasts. They assumed that this defect was due to the choice of the reporter gene. Indeed, Fbx15 is an essential marker of ESCs but not necessary for their maintenance. When replaced by the Oct4 or Nanog genes (identified as essential for the maintenance of pluripotency and self-renew), chimeric embryos survived (Okita et al., 2007). Some iPSCs are even capable of tetraploid complementation (Stadtfeld and Hochedlinger, 2010). Less than a year after iPSC generation in mice, the same combination of factors produced iPSCs from human fibroblasts (Takahashi et al., 2007). The process to generate human iPSCs is described in figure 17 (Rony et al., 2015).

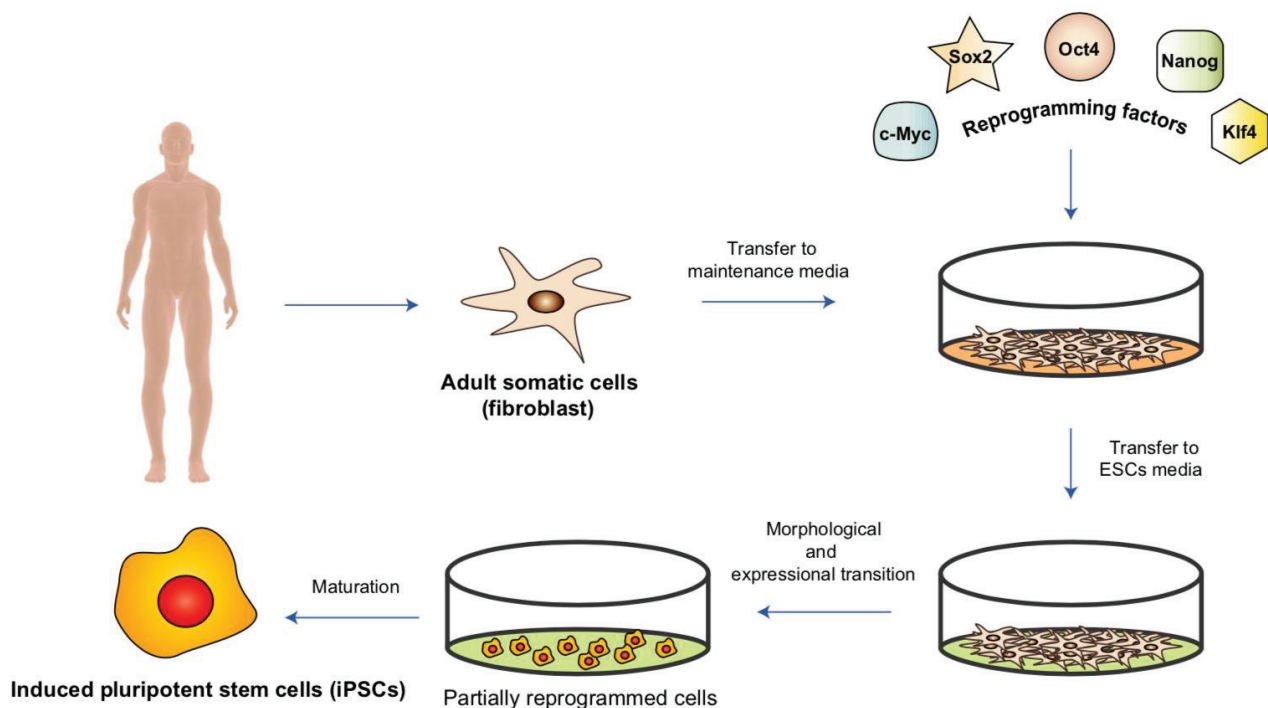


Figure 17. Reprogramming adult somatic cells into induced pluripotent stem cells (iPSCs) through ectopic expression of reprogramming factors. Forced expression of these pluripotency factors resets the epigenetic and transcriptional profile of the specialized cells and reverts them back to their embryonic state (Rony et al., 2015).

II.4.1.2 Applications of iPSCs

iPSCs represent a major scientific advance in the understanding of pluripotency and differentiation, and especially raise great prospects in their therapeutic application. The main advantage of these cells comes from their origin, making it possible to overcome the major problem raised by the use of ESCs. Indeed, these cells are derived from the reprogramming of adult cells, obtained after informed consent of the patient, and therefore do not require the use of embryos. Therefore, their use is not against ethical and legislative restrictions. The application of iPSCs in therapy can be divided into two main areas: cell therapy and disease modeling (Figure. 18) (Stadtfield and Hochedlinger et al., 2010).

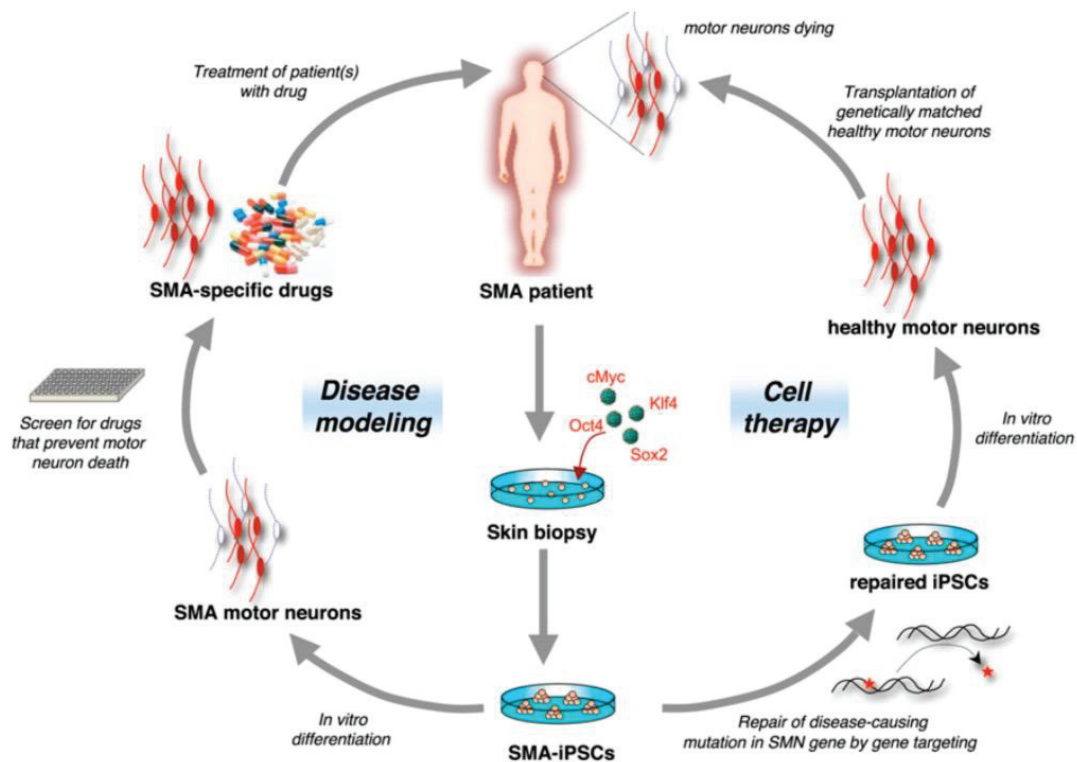


Figure 18. Potential applications of iPSCs. Shown are the potential applications of iPSC technology for cell therapy and disease modeling using SMA as an example. In SMA patients, motor neurons are afflicted and die, causing the devastating symptoms of the disease. SMA-specific iPSCs could be coaxed into motor neurons in vitro in order to establish a culture model of the disease that may lead to the identification of novel drugs that prevent the abnormal death of motor neurons in patients. Alternatively, if known, the disease-causing mutation could be repaired (in this case the SMA gene) in iPSCs by gene targeting prior to their differentiation into healthy motor neurons, followed by transplantation into the patient's brain (Stadtfield and Hochedlinger et al., 2010).

II.4.1.2.1 Cell therapy

iPSCs have been differentiated into many cell types. They represent an unlimited source of healthy differentiated cells for regenerative medicine. In addition to their ethical benefit, iPSCs also solve the problem of rejection by the immune system. Indeed, thanks to current technologies, we can take a patient's somatic cell and reprogram it into a stem cell. This transplant autologous does not require immunosuppressive therapy for the patient.

However, this low immunogenicity of iPSCs was questioned in a study comparing ESCs and iPSCs, and murine iPSC transplants demonstrated there was a rejection by the immune system without immunosuppressive therapy (Zhao et al., 2011). Another study confirmed the immunogenicity of iPSCs in vivo in autologous transplants of mice, and demonstrated that this phenomenon can be only observed in the case of undifferentiated cell transplantation (de Almeida et al., 2014). This does not raise any real contraindications for their clinical use if only the differentiated cells are injected. However, generating iPSCs from each patient would be consuming in time and resources. Therefore, an alternative solution has been proposed. The immune response is decreased if the human leukocyte antigens (HLA) match between the donor and the recipient. The objective is to create "banks" of iPSCs labeled from healthy donors according to their immune profile (HLA), in order to be able to choose therapeutic cells compatible with the profile of the recipient patients (Nakatsuji et al., 2008).

Since the version proposed by Yamanaka, other factors have been identified to allow the generation of iPSCs. Many generation methods have been developed and can make it possible to change the efficiency and quality of the produced iPSCs. Recently, the reprogramming of murine somatic cells through the addition of a combination of chemical molecules has been demonstrated (Hou et al., 2013). Due to the complete lack of introduction of genetic material, this approach makes iPSC safer for clinical use.

It has been shown that there are variations between ES clones (Osafune et al., 2008) and it is possible that some iPS clones also show differences, thus explaining the contradictory results obtained when comparing iPSCs with ESCs at the level of their genomic expression or their potential for differentiation (Miura et al., 2009). These variations between iPS clones appear to be due to differences in methodology between laboratories such as the combination of reprogramming factors used, reprogramming techniques or culture conditions (Yamanaka, 2012). Therefore, it seems necessary to define the criteria for evaluating and selecting the iPS clones that can be used in therapy. While the application of iPSCs in regenerative medicine still requires some checks to be generalized, their use for establishing disease study models is now fully recognized.

II.4.1.2.2 Disease modeling

Study models for diseases are essential tools for understanding the molecular mechanisms responsible for pathology and for the development of new therapies. Obtaining primary cells of the patient may be limited by accessibility to the affected tissues (as in the case of degenerative diseases such as Parkinson's or Alzheimer's) and by the difficulty of keeping them in culture. The models generally used are transformed cell lines or transgenic animals. However, the physiology of the models may be different from that of the patient cells, and partly explains why some selected molecules are not effective in clinical trials.

iPSCs are a new alternative to "modeling" diseases, which are generated from patient skin cells and then differentiated in vitro in the cell type affected by the pathology to replicate the disease phenotype. The in-vitro modeling also makes it possible to identify new molecules to treat the targeted pathology. The first modeled disease was iPSCs derived from cells of patients with spinal muscular atrophy (SMA). Differentiated iPSCs exhibit the same rate of degeneration as control cells (Ebert et al., 2009). Other research groups have used the iPSCs to model a cardiac pathology, long QT syndrome, which including 12 different forms of congenital disorder. The difficulty in obtaining human cardiomyocytes and reproducing all the variants of the disease had considerably slowed the research. The modeling made it possible to identify the mechanisms involved (particularly the effect of mutations in the KCNK1 gene) and to identify new therapeutic targets (Moretti et al., 2010).

The iPSCs allow the modeling of monogenic pathologies as previously described, but also polygenic including Parkinson's disease characterized by the degeneration of dopaminergic neurons. In some cases, this degeneration is due to a mutation on the LRRK2 gene with age-dependent variability that may be affected by unidentified mutations on other locus. Thus, animal models possessing only the mutation on the LRRK2 gene do not have the phenotype of Parkinson's disease. Two studies using iPSCs from patients with Parkinson's disease have shown that the mutation of this gene is the origin of the degeneration of dopaminergic neurons in humans (Nguyen et al., 2011). The neurons from these cells had various phenotypes that could suggest different mechanisms leading to their degeneration in patients. The next step in this approach should lead to a comparison of the different mutations.

However, each patient is a bearer of many genetic variations suggesting a limitation to the use of iPSCs. To be truly representative of a disease, iPSCs will need to be generated from a large number of patients.

II.4.2 HiPSC-APs as a cell model to study adipogenesis

As embryonic stem cells (ESCs) are derived from frozen extra embryos after in vitro fertilization, induced pluripotent stem cells (iPSCs) generated from adult cells represent an abundant source of multiple cell types of therapeutic interest for drug screening as well as for transplantation (Shi et al. 2016; Takahashi et al. 2007). However, in contrast to human ESCs human iPSCs are generated from somatic cells. Their derivation does not require destruction of embryos, thus avoiding ethical problems.

iPSCs can be used to study some cases of lipodystrophy. For this purpose, Taura et al first analyzed and compared the adipogenic potential of iPSCs from cells of healthy individuals with human ESCs (Taura et al., 2009). They used 4 iPSC lines generated with 2 combinations of different reprogramming factors and 2 ES cell lines, which were placed under the conditions of adipocyte differentiation determined previously in the murine ESC model. After 22 days of differentiation, they observed the formation of lipid droplets and evaluated that the accumulation of droplets was equivalent between ESCs and iPSCs. In the same way, they found the expression of adipocyte markers such as PPAR γ 2 or C / EBP α , which was comparable between the two types of pluripotent cells. The authors concluded that iPSCs have the same adipogenic potential as ESCs.

Therefore, the application of iPSCs is not limited to the pathological setting. They are also a good model for studying the mechanisms involved in the white or brown differentiation of adipocytes. Then, Nishio et al. developed a procedure to generate functional brown adipocytes at a high efficiency using a hematopoietic cocktail to induce hiPSC differentiation (Nishio et al., 2012). Interestingly, hiPSC- brown adipocytes were able to improve glucose tolerance after transplantation in mice underlying the therapeutic potential of hiPSCs in the obesity field. However, numerous issues have to be investigated before a therapeutic use of hiPSC-BAs, notably the purification of BA progenitors (BAPs) and their differentiation into functional adipocytes at a high level. In fact, in both works mentioned above, total differentiated hiPSC populations, but not purified progenitors, were transplanted into mice. Indeed, differentiated hiPSC cultures can be enriched with adipocytes but still contain other cell types that are unsuitable for transplantation, including undifferentiated hiPSCs that can form teratomas. An alternative to eliminate hiPSC capacity to form teratomas consists in purifying progenitors of interest during hiPSC differentiation.

This has been done by Ahfeldt et al. who was the first to demonstrate recently that iPSCs had the potential to differentiate into white but also brown adipocytes (Ahfeldt et al., 2012). For this purpose, they have isolated mesenchymate or MPC (mesenchymal progenitor cells) from iPSC,

capable of differentiating into adipocytes, osteoblasts and chondrocytes. These MPCs were then referred to one of the two adipocyte lineages by overexpression of certain factors. The overexpression of PPAR γ 2 induced white differentiation whereas its expression combined with that of C/EBP β and PRDM16 promoted brown differentiation.

Mohsen-Kanson et al. in my laboratory reported a procedure to selectively derive white and brown-like APs from hiPSCs. However, adipogenic cocktails usually used to induce the differentiation of APs derived from adult adipose tissues failed to differentiate hiPSC-BAPs and forced expression of a master adipogenic gene was also required for their differentiation (Mohsen-Kanson et al. 2014). The need to genetically modify hiPSC-APs clearly illustrates their weak adipogenic potential that represents a bottleneck hampering their clinical use.

This feature has been observed by us and others using different approaches to derive progenitors from hiPSCs (Hafner and Dani, 2014). We have recently described a procedure to isolate expandable BAPs from hiPSCs and to generate functional BAs at high levels with no gene transfer (Hafner et al. 2016a; Mohsen-Kanson et al. 2014), opening the opportunity of using hiPSC advantages for anti-obesity drug testing and cell based therapy to increase the BA mass in patients. Moreover, we discovered the critical role of TGF β pathway in switching off hiPSC brown-like adipogenesis and revealed novel factors to unlock their differentiation.

+

More recently, Su et al. generated human beige adipocytes from iPSC-derived FOXF1 mesoderm which express UCP1 and exhibit uncoupled respiration (Su et al., 2018). In agreement with our hypothesis, they also found TGF β pathway involved in iPSC-BAPs differentiation into adipocytes. They even reprogrammed adipocyte precursors from diabetic patients which can also improve beige adipogenesis. Finally, they proved that iPSC-derived beige adipocytes can secrete factors that improve insulin sensitivity.

II.4.3 Small Molecules induce hiPSC-BAP brown-like adipogenesis

Critical pathways regulating hiPSC-BAPs differentiation were recently identified (Hafner et al. 2016a, b; Mohsen-Kanson et al. 2014). It has been shown that Smad2, a potent anti-adipogenic pathway (Dani, 2013), is activated during the differentiation of hiPSC-BAPs, likely thanks to the autocrine expression of TGF β 1 and of activin A. Interestingly, treatment of hiPSC-BAPs with the activin/TGF β inhibitor SB431542 switched on the differentiation process. Other factors such as ascorbic acid, EGF, and hydrocortisone have also been shown to be required for hiPSC-BAPs differentiation. A detailed protocol for the differentiation of hiPSC-BAPs is described in Hafner et

al., 2016b). The molecular pathways mediating the effects of these compounds in hiPSC-BAPs remain to be elucidated.

II.4.3.1 SB431542

Members of the TGF β family are expressed in various tissues where they have been shown to regulate various biological processes including regulation of apoptosis, proliferation and differentiation of different cell types (Phillips, 2005). The TGF β pathway emerged as a critical anti-adipogenic player through the activation of Smad 2/3 (Zamani and Brown, 2010; Zaragosi et al., 2010; Bourlie et al., 2012). Deletion of TGF β receptor 1 in mice has been shown to promote beige adipogenesis within white adipose tissue, supporting a model where TGF β receptor signalling play a role in regulating the pool of beige adipose progenitors (Wankhade et al., 2018). It has been shown that Smad2/3 pathway was active during hiPSC-BAP differentiation suggesting that bioactive TGF β family members were secreted that might lock differentiation (Hafner et al. 2016a). In agreement with this hypothesis, Su et al. showed more recently that expression of TGF β - ligands and receptors increased from the differentiation of FOXF1 mesoderm progenitors towards adipocytes during *in vitro* development of hiPSCs (Su et al., 2018). Then, the anti adipogenic role of the TGF β pathway has been functionally demonstrated thanks to the use of the TGF β inhibitor SB431542 (Inman et al., 2002). Inhibition of active Smad 2/3 pathway upon SB431542 addition during hiPSC-BAP differentiation induced a dramatically increased of UCP1 expression and of the number of mature beige adipocytes (Hafner et al. 2016a,b; Su et al., 2018; Hafner et al. 2018). In addition, inhibition of TGF β signaling in hiPSC- mesenchymal stem cells, i.e., before induction of adipogenic differentiation, promoted the generation of adipocytes (Su et al., 2018). Altogether, these data underline the critical role of TGF β pathway in the commitment of hiPSC into the adipogenic lineage. They indicate that TGF β signalling inhibition enhances the conversion of mesenchymal stem cells into adipogenic progenitors and switches on the differentiation of progenitors into mature beige adipocytes. A review on the role of the TGF β pathway in the adipogenesis of hiPSCs is found below (Yao and Dani, 2019).

Critical Role of TGF β Pathway in the Differentiation of Human Induced Pluripotent Stem Cells into Fat-Burning Adipocytes

Xi Yao and Christian Dani*

*University Côte d'Azur, CNRS, INSERM, iBV, Faculty of Medicine, Nice, France.

Received May 23, 2019; Accepted June 05, 2019; Published July 12, 2019

ABSTRACT

Alternative strategies are urgently required to fight obesity and associated metabolic disorders including diabetes and cardiovascular diseases. Brown and brown-like beige adipocytes (BAs) store fat, but in contrast to white adipocytes, they are equipped to dissipate energy stored. Therefore, BAs represent promising cell targets to counteract obesity. However, the scarcity of BAs in adults is a major limitation for a BA-based therapy of obesity, and the notion to increase the BA mass by transplanting BA progenitors (BAPs) in obese patients recently emerged. The capacity of human induced pluripotent stem cells (hiPSCs) to generate BAPs at a high efficiency offers the opportunity to produce an unlimited number of patient-matched BAs. However, hiPSC-BAPs display a low adipogenic capacity that hampered their use both in cell-based therapy and basic research. Recently we, and others, have identified the critical role of TGF β pathway in switching off differentiation of hiPSC-BAPs in classical 2D culture and also in a 3D beige adiposphere model better mimicking adipocytes *in vivo*. Inhibition of TGF β pathway unlocks differentiation of hiPSC-BAPs making this cell model a suitable tool for therapeutic transplantation. In contrast to BAPs derived from human iPSCs, inhibition of TGF β pathway is not a requisite for differentiation of preadipocytes derived from adult adipose tissues. This observation suggests that hiPSC-BAPs and adult adipose tissue-preadipocytes are at different stages of the adipose progenitor hierarchy.

Keywords: TGF β pathway, Human induced pluripotent stem cells, Beige adipocytes, Adipocyte progenitors, Stem cell-based therapy, Obesity

Abbreviations: TGF: Transforming Growth Factor; BA: Brown and Beige Adipocyte; BAP: Brown and Beige Adipocyte Progenitor; hiPSC: Human Induced Pluripotent Stem Cell

INTRODUCTION

Obesity and associated metabolic disorders such as diabetes and cardiovascular diseases are major health problems. Obesity results from an imbalance between calorie intake and energy expenditure. In mammals, three types of adipocytes coexist, i.e. brown, beige and white, which are all involved in energy balance regulation while having opposite functions. White adipocytes are involved in energy storage and their accumulation marks obesity. Therapies based to reduce energy intake are difficult to follow in our modern life, and current anti-obesity drugs cause important side effects for the patients that limits their use. Bariatric surgery has proven efficiency for obesity, although long-term complications and obesity relapse may appear. Therefore, alternative strategies to increase energy expenditure with the identification of new anti-obesity targets are urgently required. In contrast to white adipocytes, classical brown adipocytes and brown-like adipocytes (BAs), also named beige or brite adipocytes because dispersed in white adipose tissues, are specialized in energy expenditure. Upon activation, BAs consume metabolic substrates and burn fat

via the mitochondrial uncoupling protein-1 (UCP-1). Moreover, the ability of BAs to actively drain circulating glucose and triglycerides to oxidize them can prevent hyperglycemia and hypertriglyceridemia. Therefore, BAs represent promising cell targets to counteract obesity in human. However, there is a major limitation for a BA-based treatment of obesity that is that BAs hold a minor fraction of adipose tissue in human and disappear from most areas with age, persisting only around deeper organs. In addition, BA activity is lower in overweight and obese individuals than in

Corresponding author: Christian Dani, iBV, Faculté de Médecine, Nice, France, Tel: +33 (0)4 93 37 76 47; Fax: +33 (0)4 93 37 70 58; E-mail: dani@unice.fr

Citation: Yao X & Dani C. (2019) Critical Role of TGF β Pathway in the Differentiation of Human Induced Pluripotent Stem Cells into Fat-Burning Adipocytes. *Stem Cell Res Th*, 4(1): 142-145.

Copyright: ©2019 Yao X & Dani C. This is an open-access article distributed under the terms of the Creative Commons Attribution License, which permits unrestricted use, distribution, and reproduction in any medium, provided the original author and source are credited.

leans [1,2]. Hence, the notion to increase the BA mass by transplanting BA progenitors (BAPs) in obese patients as a therapeutic alternative to counteract obesity and its associated metabolic complications recently emerged. The proof-of-concept has been validated in murine models as it has been reported that implants of mouse BAT or of human BAs purified from capillary networks were able to restore normoglycemia in diabetic mice and to reduce obesity in Ob/Ob mice [3-6]. It is interesting to note that small amount of transplants was sufficient to display a beneficial effect, reflecting that in addition to acting as a glucose and energy sink; BAs secrete adipokines that could also contribute to metabolic effects [7]. Therefore, a reliable source of human BAs was urgently needed and induced pluripotent stem cells (iPSCs) appear as a suitable source of BAPs having a high adipogenic capacity only when the TGF β pathway is switch off.

THE TGF β PATHWAY GOVERNS THE DIFFERENTIATION OF hiPSCs INTO BAs

Induced pluripotent stem cells (iPSCs) represent an abundant source of multiple cell types of therapeutic interest for drug screening as well as for transplantation [8,9]. Nakao's group was the first to demonstrate the capacity of hiPSCs to generate white adipocytes [10]. Total differentiated hiPSC populations, but not purified adipose progenitors, were transplanted into mice. Indeed, differentiated hiPSC cultures can be enriched with adipocytes, but still contain other cell types that are unsuitable for transplantation, including undifferentiated hiPSCs that can form teratomas. An alternative to eliminate hiPSC capacity to form teratomas consists in purifying progenitors of interest during hiPSC differentiation. Ahfeldt et al. [11] and Mohsen-Kanson et al. [12] were able to generate pure BAs from hiPSCs that displayed a high adipogenic capacity but only following transduction with adipogenesis master genes. The need to genetically modify hiPSCs-derived progenitors to generate adipocytes clearly illustrates the low adipogenic potential of hiPSCs. This feature represented a bottleneck hampering their clinical use [13].

Several factors, such as ascorbic acid, EGF and hydrocortisone have been shown to regulate hiPSC-BAPs differentiation [12,14,15]. However, TGF β signaling holds a pivotal role. Members of the TGF β family are expressed in various tissues where they have been shown to regulate various biological processes including regulation of apoptosis, proliferation and differentiation of different cell types [16]. The TGF β pathway emerged as a critical anti-adipogenic player through the activation of Smad 2/3 [17-19]. Deletion of TGF β receptor 1 in mice has been shown to promote beige adipogenesis within white adipose tissue, supporting a model where TGF β receptor signalling play a role in regulating the pool of beige adipose progenitors [20]. It has been shown that Smad2/3 pathway was active during

hiPSC-BAP differentiation suggesting that bioactive TGF β family members were secreted that might lock differentiation [14]. In agreement with this hypothesis, Su et al. [21] showed more recently that expression of TGF β -ligands and receptors increased from the differentiation of FOXF1 mesoderm progenitors towards adipocytes during *in vitro* development of hiPSCs [21]. Then, the anti adipogenic role of the TGF β pathway has been functionally demonstrated thanks to the use of the TGF β inhibitor SB431542 [22]. Inhibition of active Smad 2/3 pathway upon SB431542 addition during hiPSC-BAP differentiation induced a dramatically increased of UCP1 expression and of the number of mature beige adipocytes [14,15,21,23]. In addition, inhibition of TGF β signaling in hiPSC-mesenchymal stem cells, i.e., before induction of adipogenic differentiation, promoted the generation of adipocytes [21]. Altogether, these data underline the critical role of TGF β pathway in the commitment of hiPSC into the adipogenic lineage. They indicate that TGF β signalling inhibition enhances the conversion of mesenchymal stem cells into adipogenic progenitors and switches on the differentiation of progenitors into mature beige adipocytes.

INHIBITION OF TGF β PATHWAY IS REQUIRED ONLY DURING THE FIRST DAYS OF DIFFERENTIATION OF hiPSC-3D BEIGE ADIPOSESPHERES

Inhibition of TGF β pathway is required to induce differentiation of hiPSC-derived adipose progenitor cells into adipocytes, whereas is not for the differentiation of progenitors derived from human adult adipose tissues. The low hiPSC-BAP adipogenic capacity compared to adult-BAPs is reminiscent of an observation reported by Han et al. [24]. These authors observed that epididymal adipose tissue, which undergoes early development in mouse, is composed of progenitor cells that lack their adipogenic capacity once isolated from the tissue. In contrast to cells derived from other fat pads that developed later, epididymal fat cells required a 3D structure and a different micro-environment to undergo differentiation. Therefore, among the reasons to explain the weak efficacy of hiPSC-BAP differentiation, one can mention the culture conditions that do not mimic the phenotype of the cells and their physiological microenvironment within the adipose tissue. Cells are classically grown as monolayer, which poorly reflects the *in vivo* situation [25]. In contrast, the cell-cell and cell-extracellular matrix interactions are promoted in 3D configurations. Therefore, 3D cultures represent a bridge between traditional cell culture and live tissue. HiPSC-BAPs can form 3D spheroids able to differentiate into beige adipospheres expressing UCP-1 (**Figure 1B**, Yao X and Dani C, unpublished data). In fact, beige adipospheres revealed a TGF β pathway depend phase only during the first days of spheroid differentiation.

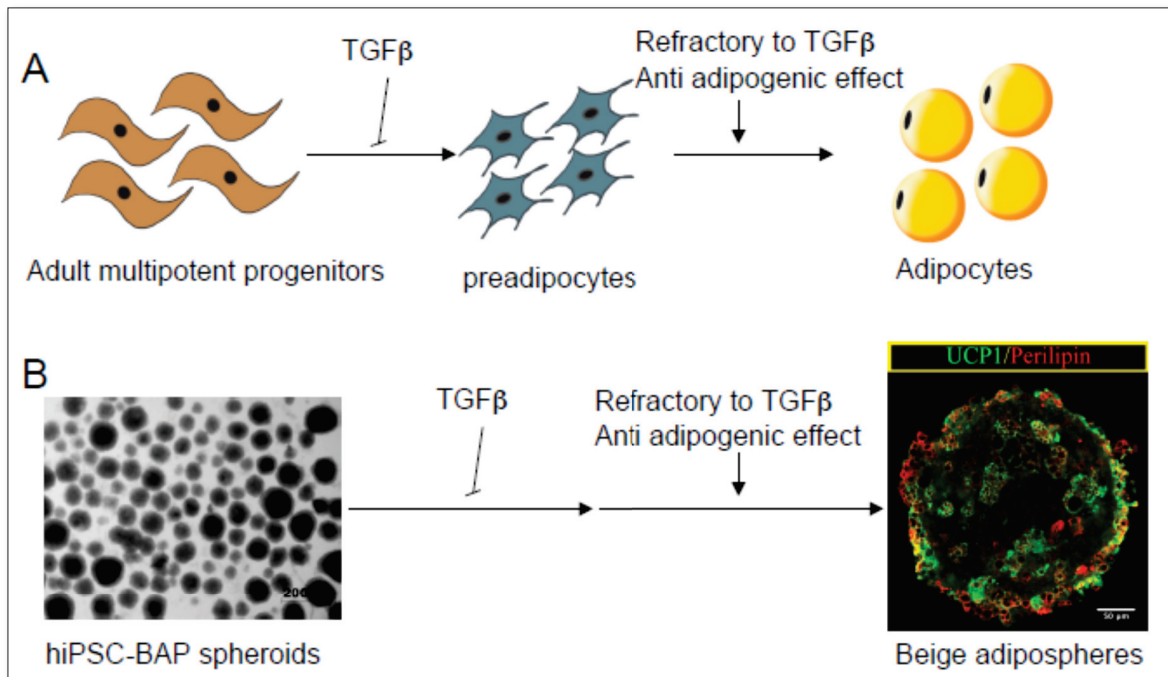


Figure 1. Commitment towards the adipogenic lineage of adult adipose tissues-and of hiPSC-progenitors requires inhibition of TGFβ signalling pathway. A) Multipotent progenitors at the stem of mesenchymal cell hierarchy of adipocyte formation require TGFβ inhibition only for their differentiation into preadipocytes (adapted from [26]). B) Beige progenitors derived from hiPSCs can form spheroids and undergo differentiation into adipospheres expressing UCP1. Only the first days of spheroid differentiation requires TGFβ inhibition.

CONCLUSION

Interestingly, Seale group has recently proposed a mesenchymal progenitor cell hierarchy in adipose tissue where the multipotent progenitor cell required inhibition of TGFβ pathway for its differentiation into preadipocytes. Then, preadipocytes are refractory to the anti adipogenic action of TGFβ to differentiate into adipocytes (Figure 1A, [26]). As discussed above, differentiation of hiPSC-BAP spheroids display also a sensitive and a refractory phase to anti adipogenic effect of TGFβ. It is tempting to speculate that BAPs derived from hiPSCs resemble the multipotent progenitor subpopulation in adult adipose tissue at the origin of preadipocytes. Further analyses are required to test this hypothesis. Numerous other issues have also to be solved before a therapeutic use of iPSCs in the obesity field, but identification of pathways governing the differentiation of BAPs at a high level as well as their capacity to form 3D adipospheres open the opportunity of using hiPSCs advantages for anti-obesity therapy.

REFERENCES

1. Cypess AM, White AP, Vernet C (2013) Anatomical localization, gene expression profiling and functional characterization of adult human neck brown fat. *Nat Med* 19: 635-639.
2. Van Marken Lichtenbelt WD, Vanhommel JW, Smulders NM (2009) Cold-activated brown adipose tissue in healthy men. *N Engl J Med* 360: 1500-1508.
3. Stanford KI, Middelbeek RJ, Townsend KL (2013) Brown adipose tissue regulates glucose homeostasis and insulin sensitivity. *J Clin Invest* 123: 215-223.
4. Gunawardana SC, Piston DW (2010) Reversal of type 1 diabetes in mice by brown adipose tissue transplant. *Diabetes* 61:674-682.
5. Liu X, Wang S, You Y (2015) Brown adipose tissue transplantation reverses obesity in Ob/Ob mice. *Endocrinology* 156: 2461-2469.
6. Min SY, Kady J, Nam M (2016) Human 'brite/beige' adipocytes develop from capillary networks and their implantation improves metabolic homeostasis in mice. *Nat Med* 22: 312-318.
7. Villarroya F, Gavaldà-Navarro A, Peyrou M, Villarroya J, Giralt M (2017) The lives and times of brown adipokines. *Trends Endocrinol Metab* 28: 855-867.
8. Takahashi K, Tanabe K, Ohnuki M (2007) Induction of pluripotent stem cells from adult human fibroblasts by defined factors. *Cell* 131: 861-872.

9. Shi Y, Inoue H, Wu JC, Yamanaka S (2016) Induced pluripotent stem cell technology: A decade of progress. *Nat Rev Drug Discov* 16: 115-130.
10. Taura D, Noguchi M, Sone M (2009) Adipogenic differentiation of human induced pluripotent stem cells: Comparison with that of human embryonic stem cells. *FEBS Lett* 583: 1029-1033.
11. Ahfeldt T, Schinzel RT, Lee YK (2012) Programming human pluripotent stem cells into white and brown adipocytes. *Nat Cell Biol* 14: 209-219.
12. Mohsen-Kanson T, Hafner AL, Wdziekonski B (2014) Differentiation of human induced pluripotent stem cells into brown and white adipocytes: Role of Pax3. *Stem Cells* 32: 1459-1467.
13. Hafner AL, Dani C (2014) Human induced pluripotent stem cells: A new source for brown and white adipocytes. *World J Stem Cells* 6: 467-472.
14. Hafner AL, Contet J, Ravaud C (2016) Brown-like adipose progenitors derived from human induced pluripotent stem cells: Identification of critical pathways governing their adipogenic capacity. *Sci Rep* 6: 32490.
15. Anne-Laure Hafner TM-KACD (2016) A protocol for the differentiation of brown adipose progenitors derived from human induced pluripotent stem cells at a high efficiency with no gene transfer. *Nature Protocol Exchange*.
16. Phillips DJ (2005) Activins, inhibins and follistatins in the large domestic species. *Domest Anim Endocrinol* 28: 1-16.
17. Zamani N, Brown CW (2011) Emerging roles for the transforming growth factor- β superfamily in regulating adiposity and energy expenditure. *Endocr Rev* 32: 387-403.
18. Zaragosi LE, Wdziekonski B, Villageois P (2010) Activin a plays a critical role in proliferation and differentiation of human adipose progenitors. *Diabetes* 59: 2513-2521.
19. Bourlier V, Sengenès C, Zakaroff-Girard A (2012) TGF- β family members are key mediators in the induction of myofibroblast Phenotype of Human Adipose Tissue progenitor cells by macrophages. *PLoS One* 7: e31274.
20. Wankhade UD, Lee JH, Dagur PK (2018) TGF- β receptor 1 regulates progenitors that promote browning of white fat. *Mol Metab* 16: 160-171.
21. Su S, Guntur AR, Nguyen DC (2018) A renewable source of human beige adipocytes for development of therapies to treat metabolic syndrome. *Cell Rep* 25: 3215-3228 e3219.
22. Inman GJ, Nicolas FJ, Callahan JF (2002) SB-431542 is a potent and specific inhibitor of transforming growth factor- β superfamily type I activin receptor-like kinase (ALK) receptors ALK4, ALK5 and ALK7. *Mol Pharmacol* 62: 65-74.
23. Hafner AL, Mohsen-Kanson T, Dani C (2018) Differentiation of brown adipocyte progenitors derived from human induced pluripotent stem cells. *Methods Mol Biol* 1773: 31-39.
24. Han J, Lee J, Jin J (2011) The spatiotemporal development of adipose tissue. *Development* 138: 5027-5037.
25. Horvath P, Aulner N, Bickel M (2016) Screening out irrelevant cell-based models of disease. *Nat Rev Drug Discov* 15: 751-769.
26. Merrick D, Sakers A, Irgebay Z (2019) Identification of a mesenchymal progenitor cell hierarchy in adipose tissue. *Science* 364: 6438.

II.4.3.2 Ascorbic acid

The cell metabolism is closely related to the interaction between different cell types in an organized environment. However, when the cells are isolated from their original tissues and cultured in vitro, the required nutrients are changed and vary from cell to cell (Hosokawa et al., 1971; Eagle, 1955). Ascorbic acid, as one of the stimulatory effect of various nutrients, is critical for the extracellular matrix (ECM) production of cells in vitro, which plays a key role in the post-translational modification of collagen molecules and increases collagen production (Geesin et al., 1991; Chan et al., 1990). Chan et al showed that ascorbic acid had an effect on procollagen synthesis in human skin fibroblast cultures, which increased Collagen I production (Chan et al., 1990). Furthermore, ascorbic acid can modulate cell proliferation in vitro, especially promote proliferation of mesenchyme-derived cell types including osteoblasts, adipocytes, chondrocytes, and odontoblasts (Wang et al., 2006; Sato et al., 2006). Ascorbic acid also regulates cell differentiation, particularly of multilineage mesenchymal cells (adipogenesis, osteogenesis, chondrogenesis, and myogenesis). Ascorbic acid was previously shown to enhance the differentiation of 3T3-L1 mouse cell line, and recent studies attribute this effect to the regulation of type VI collagen (Kim et al., 2013; Liu et al., 2017).

II.4.3.3 Epidermal growth factor (EGF)

The effects of EGF vary from one species to another. However, it has been demonstrated that EGF stimulates hASCs proliferation and modulate their differentiation potentials (Butterwith et al., 1993; Hauner et al., 1995; Tamama et al., 2006; Zaragosi et al., 2006). EGF is a single-chain polypeptide known for proliferative and differentiating effects on many mammalian tissues (Hauner et al., 1995; Kurachi et al., 1993). Tamama et al showed that migration and cell proliferation of bone marrow-derived mesenchymal stem cells can be enhanced by EGF, and their differentiation potentials are maintained at the same time (Tamama et al., 2006). Furthermore, EGF can promote adipocyte development and function in vitro when the concentration is comparable to those found in human serum (Hauner et al., 1995). Kilroy et al observed EGF induced hASC to secrete hepatic growth factor (HGF) in an autocrine manner, which both increased proliferative capacity and adipogenic potential in vitro (Kilroy et al., 2007). Recently, the stimulation of EGR1 (early growth response-1) observed upon treatment of hiPSC-BAPs with EGF is of interest. EGR1 is a zinc finger transcription factor expressed in adult adipose tissue, and it has been reported that Egr1 deficiency induces WAT browning by releasing EGR1-mediated UCP-1 transcription repression in mice (Milet et al. 2017; Zhang et al. 2013). The role of EGR1 in EGF-induced hiPSC-BAPs

differentiation remains to be determined, but these data suggest a dual role of EGF, i.e., required for the commitment of BAPs toward adipocytes and a break for fully expression of UCP-1.

II.4.3.4 Hydrocortisone

Glucocorticoids are involved in regulating energy metabolism, and chronic glucocorticoid excess causes obesity, type 2 diabetes and dyslipidemia (Macfarlane et al., 2008). In rodent, glucocorticoids is known for suppressing UCP1 and thermogenesis in BAT (Hardwick et al., 1989; Strack et al., 1995). However, glucocorticoids have recently been reported to active BAT thermogenesis (Robinson et al., 2016; Ramage et al., 2016). In another human study, acute treatment of glucocorticoid receptor agonist hydrocortisone increased BAT temperature in basal and cold-induced conditions in eight healthy males (Scotney et al. 2017). The yield of both glucocorticoid agonism and antagonism increases in human BAT activity measures, and at least acute effects of hydrocortisone were different between humans and other species. Furthermore, it has been showed that hydrocortisone is involved in initiating adipogenic differentiation (Rosen and Spiegelman, 2000). However, the effect on mature adipocytes is still unknown. Both for pro as well as antilipolytic effects have been reported (Peckett et al., 2011).

II.4.4 Perspectives of hiPSCs in the Obesity Field

The lack of a relevant physiologic cell model for preclinical testing of drugs activating human BAs is a major limitation for a BA-based treatment of obesity. The cellular models mainly used for drug discovery are murine cell lines. They may not provide relevant models as recent findings support species differences for key adipogenic regulatory pathways (Lindroos et al., 2013). Despite their gold standard state, primary human cells derived from adult adipose tissues can be studied only for short periods before they reach senescence and differentiation failure precluding reproducible assays. Because iPSCs display a high self-renewal capacity, they can be cultured for long term and expanded into large numbers under completely defined conditions. In addition, human iPSCs are able to undergo differentiation into hepatocytes and cardiomyocytes, and therefore they are outstanding tools in early preclinical phase of drug discovery to perform toxicity assessment.

Recent studies have clearly established that hiPSC clones can display variable capacities to differentiate into specific lineages (Nishizawa et al., 2016) which complicate the development of universal protocols of differentiation. The identification of the origins of this functional variability is still a file of investigations (Ortmann and Vallier, 2017). An alternative to bypass the hiPSC variability consists in the purification of progenitors from differentiating hiPSCs. Several

approaches have been used for the purification of hiPSC-BAPs (Hafner and Dani, 2014). The purification of hiPSC-BAPs from different hiPSC clones displays various efficiencies, but we showed that progenitors purified from different hiPSC sources have a similar capacity to undergo differentiation when using a unique adipogenic protocol (Hafner et al., 2016a, b). This result strongly supports that the progenitor purification step is a requirement. An advantage to purify progenitors is also to eliminate undifferentiated hiPSCs prone to form teratoma after transplantation.

Another issue is the generation of mutations during hiPSC expansion. Fine genetic analysis and preclinical animal studies should be able to address the safety of hiPSC- BAs to be transplanted, including potential teratoma formation and other cancer development. Finally, the stability of the phenotype of transplanted BAs has to be monitored as dedifferentiation of BAs or transdifferentiation of BAs into white adipocytes after transplantation cannot be ruled out. Tissue engineering aiming to develop tissue-like structures that mimic the *in vivo* situation as closely as possible should prevent this risk. A chapter describing the potential of hiPSCs in the obesity field is found below (Yao et al., 2018).



Brown-Like Adipocyte Progenitors Derived from Human iPS Cells: A New Tool for Anti-obesity Drug Discovery and Cell-Based Therapy?

Xi Yao, Barbara Salingova, and Christian Dani

Contents

- 1 Introduction
 - 2 Capacity of Human-Induced Pluripotent Stem Cells to Generate BAs
 - 3 Pathways Governing hiPSC-BAP Adipogenic Capacity
 - 4 Perspectives of hiPSCs in the Obesity Field
- References

Abstract

Alternative strategies are urgently required to fight obesity and associated metabolic disorders including diabetes and cardiovascular diseases. Brown and brown-like adipocytes (BAs) store fat, but in contrast to white adipocytes, activated BAs are equipped to dissipate energy stored. Therefore, BAs represent promising cell targets to counteract obesity. However, the scarcity of BAs in adults is a major limitation for a BA-based therapy of obesity, and the notion to increase the BA mass by transplanting BA progenitors (BAPs) in obese patients recently emerged. The next challenge is to identify an abundant and reliable source of BAPs. In this chapter, we describe the capacity of human-induced pluripotent stem cells (hiPSCs) to generate BAPs able to differentiate at a high efficiency with no gene transfer. This cell model represents an unlimited source of human BAPs that in a near future may be a suitable tool for both therapeutic transplantation and for the discovery of novel efficient and safe anti-obesity drugs. The generation of a relevant cell model, such as hiPSC-BAs in 3D adipospheres enriched with macrophages and endothelial cells to better mimic the microenvironment within the adipose tissue, will be the next critical step.

X. Yao · B. Salingova · C. Dani (✉)

Faculté de Médecine, Université Nice Sophia Antipolis, iBV, UMR CNRS/INSERM, Nice, Cedex 2, France

e-mail: dani@unice.fr

Keywords

Adipocyte progenitors · Brown adipocytes · Cell-based therapy · Drug discovery · Human-induced pluripotent stem cells · Obesity

1 Introduction

Obesity and associated metabolic disorders such as diabetes and cardiovascular diseases are major health problems. Obesity results from an imbalance between calorie intake and energy expenditure, and three types of adipocytes are the main regulators of this balance. White adipocytes are involved in energy storage and their accumulation marks obesity. Therapies based to reduce energy intake are difficult to follow in our modern life, and current anti-obesity drugs cause important side effects for the patients that limits their use. Bariatric surgery has proven efficiency for obesity, although long-term complications and obesity relapse may appear. Therefore, alternative strategies to increase energy expenditure with the identification of new anti-obesity targets are urgently required. In contrast to white adipocytes, classical brown adipocytes and brown-like adipocytes (BAs) dispersed in white adipose tissues are specialized in energy expenditure. Upon activation, BAs consume metabolic substrates and burn fat via the mitochondrial uncoupling protein-1 (UCP-1). Moreover, the ability of BAs to actively drain circulating glucose and triglycerides to oxidize them can prevent hyperglycemia and hypertriglyceridemia. Therefore, BAs represent promising cell targets to counteract obesity in human. However, there are major limitations for a BA-based treatment of obesity. BAs hold a minor fraction of adipose tissue in human and disappear from most areas with age, persisting only around deeper organs. In addition, BA activity is lower in overweight and obese individuals than in leans (Cypess et al. 2013; van Marken Lichtenbelt et al. 2009). Hence, the notion to increase the BA mass by transplanting BA progenitors (BAPs) in obese patients as a therapeutic alternative to counteract obesity and its associated metabolic complications recently emerged. The proof-of-concept has been validated in murine models as it has been reported that implants of mouse BAT or of human BAs developed from capillary networks were able to restore normoglycemia in diabetic mice and to reduce obesity in Ob/Ob mice (Gunawardana and Piston 2010; Liu et al. 2015; Min et al. 2016; Stanford et al. 2013). It is interesting to note that small amount of transplanted materials was sufficient to display a beneficial effect, reflecting that in addition to acting as a glucose and energy sink, BAs secrete adipokines that could also contribute to metabolic effects (Villarroya et al. 2017).

Therefore, a reliable source of human BAs is urgently needed. Induced pluripotent stem cells appear as a suitable source of BAs for both cell transplantation to increase the BA mass in patients and for anti-obesity drug discovery.

2 Capacity of Human-Induced Pluripotent Stem Cells to Generate BAs

As embryonic stem cells (ESCs) are derived from frozen extra embryos after in vitro fertilization, induced pluripotent stem cells (iPSCs) generated from adult cells represent an abundant source of multiple cell types of therapeutic interest for drug screening as well as for transplantation (Shi et al. 2016; Takahashi et al. 2007). However, in contrast to human ESCs human iPSCs are generated from somatic cells. Their derivation does not require destruction of embryos, thus avoiding ethical problems. Nakao's group was the first to demonstrate the capacity of hiPSCs to generate white adipocytes (Taura et al. 2009). Then, Nishio et al. (2012) developed a procedure to generate functional brown adipocytes at a high efficiency using a hematopoietic cocktail to induce hiPSC differentiation. Interestingly, hiPSC-brown adipocytes were able to improve glucose tolerance after transplantation in mice underlying the therapeutic potential of hiPSCs in the obesity field. However, numerous issues have to be investigated before a therapeutic use of hiPSC-BAs, notably the purification of BA progenitors (BAPs) and their differentiation into functional adipocytes at a high level. In fact, in both works mentioned above, total differentiated hiPSC populations, but not purified progenitors, were transplanted into mice. Indeed, differentiated hiPSC cultures can be enriched with adipocytes but still contain other cell types that are unsuitable for transplantation, including undifferentiated hiPSCs that can form teratomas. An alternative to eliminate hiPSC capacity to form teratomas consists in purifying progenitors of interest during hiPSC differentiation. This has been done by Ahfeldt et al. who purified adipose progenitors (APs) from hiPSCs able to undergo differentiation into BAs but only following forced expression of three adipogenic master genes (Ahfeldt et al. 2012). Mohsen-Kanson et al. reported a procedure to selectively derive white and brown-like APs from hiPSCs. Adipogenic cocktails usually used to induce the differentiation of APs derived from adult adipose tissues failed to differentiate hiPSC-BAPs and forced expression of a master adipogenic gene was also required for their differentiation (Mohsen-Kanson et al. 2014). The need to genetically modify hiPSC-APs clearly illustrates their weak adipogenic potential that represents a bottleneck hampering their clinical use. This feature has been observed by us and others using different approaches to derive progenitors from hiPSCs (Hafner and Dani 2014). These data suggested that the commitment of hiPSC-BAPs toward adipocytes requires activation and/or inhibition of pathways different from those regulating differentiation of BAPs derived from adult adipose tissues.

3 Pathways Governing hiPSC-BAP Adipogenic Capacity

Critical pathways regulating hiPSC-BAPs differentiation were recently identified (Hafner et al. 2016a, b; Mohsen-Kanson et al. 2014). It has been shown that Smad2, a potent anti-adipogenic pathway (Dani 2013), is activated during the differentiation of hiPSC-BAPs, likely thanks to the autocrine expression of TGFb1 and of activin

A. Interestingly, treatment of hiPSC-BAPs with the activin/TGF β inhibitor SB431542 switched on the differentiation process. Other factors such as ascorbic acid, EGF, and hydrocortisone have also been shown to be required for hiPSC-BAPs differentiation. A detailed protocol for the differentiation of hiPSC-BAPs is described in Hafner et al. (2016b). The molecular pathways mediating the effects of these compounds in hiPSC-BAPs remain to be elucidated. Ascorbic acid was previously shown to enhance the differentiation of 3T3-L1 mouse cell line, and recent studies attribute this effect to the regulation of type VI collagen (Kim et al. 2013; Liu et al. 2017). However, the requirement of ascorbic acid for UCP-1 expression would deserve further investigations. EGF is known to stimulate adult-BAPs proliferation (Hebert et al. 2009; Holmstrom et al. 2008); however, its role in the differentiation of human BAPs is not known. The stimulation of EGR1 (early growth response-1) observed upon treatment of hiPSC-BAPs with EGF is of interest. EGR1 is a zinc finger transcription factor expressed in adult adipose tissue, and it has been reported that Egr1 deficiency induces WAT browning by releasing EGR1-mediated UCP-1 transcription repression in mice (Milet et al. 2017; Zhang et al. 2013). The role of EGR1 in EGF-induced hiPSC-BAPs differentiation remains to be determined, but these data suggest a dual role of EGF, i.e., required for the commitment of BAPs toward adipocytes and a break for fully expression of UCP-1. Finally, it appears that the choice of the basal medium enriched with the different factors indicated above is not trivial. Indeed, no differentiation was observed when hiPSC-BAPs were maintained in DMEM. In contrast, hiPSC-BAPs could undergo differentiation at a high level when maintained in a medium developed to support proliferation and differentiation of endothelial cells (Hafner et al. 2016a, b). Interestingly, a common basal medium is used for differentiation of functional endothelial cells, hematopoietic cells, and brown adipocytes from human iPSCs (Hafner et al. 2016a, b; Nishio et al. 2012; Orlova et al. 2014). The reasons why a medium supporting endothelial cells is critical for hiPSC-BAPs differentiation are unknown. Studies showed that adipocytes and endothelial cells surrounding might originate from a common progenitor that could go through adipogenesis or angiogenesis depending on the microenvironment. There are other evidences showing that human adipose-derived stem cells have feature of endothelial progenitor cells (Planat-Benard et al. 2004). Striking similarity between the differentiation conditions suggests a close developmental origin, and the fact that adipocytes may originate from subsets of endothelial cells could be an explanation (Sanchez-Gurmaches and Guertin 2013). Altogether, these data show a functional link between adipogenesis and angiogenesis, and the differentiation of hiPSC-BAPs can constitute a platform for the identification of new pathways regulating the generation of human BAs.

4 Perspectives of hiPSCs in the Obesity Field

The lack of a relevant physiologic cell model for preclinical testing of drugs activating human BAs is a major limitation for a BA-based treatment of obesity. The cellular models mainly used for drug discovery are murine cell lines. They may

not provide relevant models as recent findings support species differences for key adipogenic regulatory pathways (Lindroos et al. 2013). Despite their gold standard state, primary human cells derived from adult adipose tissues can be studied only for short periods before they reach senescence and differentiation failure precluding reproducible assays. Because iPSCs display a high self-renewal capacity, they can be cultured for long term and expanded into large numbers under completely defined conditions. In addition, human iPSCs are able to undergo differentiation into hepatocytes and cardiomyocytes, and therefore they are outstanding tools in early preclinical phase of drug discovery to perform toxicity assessment. A myriad of molecules has been tested as anti-obesity drugs. To date, the marketed drugs for BAs activation showed limited efficacy and/or displayed substantial adverse effects (Giordano et al. 2016). Among the reasons involved in this weak efficacy, one can also mention the limitation of the drug testing models due to the culture conditions that do not mimic the phenotype of the cells and their physiological microenvironment within the adipose tissue. Cells are classically grown as monolayer, which poorly reflects the *in vivo* situation (Horvath et al. 2016). In contrast, the cell–cell and cell–extracellular matrix interactions are promoted in 3D configurations. Therefore, 3D cultures represent a bridge between traditional cell culture and live tissue to overcome the limitations that impaired discovery of efficient and safe drugs. hiPSC-BAPs can form 3D aggregates, also known as spheroids, able to differentiate into UCP-1-expressing adipocytes, therefore named as adipospheres (Yao and Dani, personal observation). Three-dimensional adipospheres formed from hiPSC-BAs could serve as a platform to identify pathways governing the recruitment and the activation of human BAs and for anti-obesity drug discovery (see Fig. 1). On the other hand, the use of iPSC-derived cells in clinic has been approved by the FDA for at least two diseases, for iPSC-myogenic progenitors to be delivered to muscular dystrophic patients, and phase I/II results are showing promising safety data as well as possible efficacy when used in ocular diseases. Therefore, BA adipospheres from obese-iPSCs can be proposed as therapeutic cells (see Fig. 1). Interestingly, it has been recently demonstrated that the therapeutic potential of cells is dramatically improved when transplanted as 3D structures (Petrenko et al. 2017). Indeed, autologous transplantations are not financially feasible at present, but a recent study reported the possibility of allogenic iPSCs transplants, which has a tremendous potential for clinic use (Shiba et al. 2016). Human iPSCs can be cultured for long term and expanded into large numbers under complete defined conditions. Thanks to their high self-renewal capacity, it is not a challenge to produce a sufficient number of cells for an effective treatment. However, crucial points for future applications in humans remain to be solved. Recent studies have clearly established that hiPSC clones can display variable capacities to differentiate into specific lineages (Nishizawa et al. 2016) which complicate the development of universal protocols of differentiation. The identification of the origins of this functional variability is still a file of investigations (Ortmann and Vallier 2017). An alternative to bypass the hiPSC variability consists in the purification of progenitors from differentiating hiPSCs. Several approaches have been used for the purification of hiPSC-BAPs (Hafner and Dani 2014). The

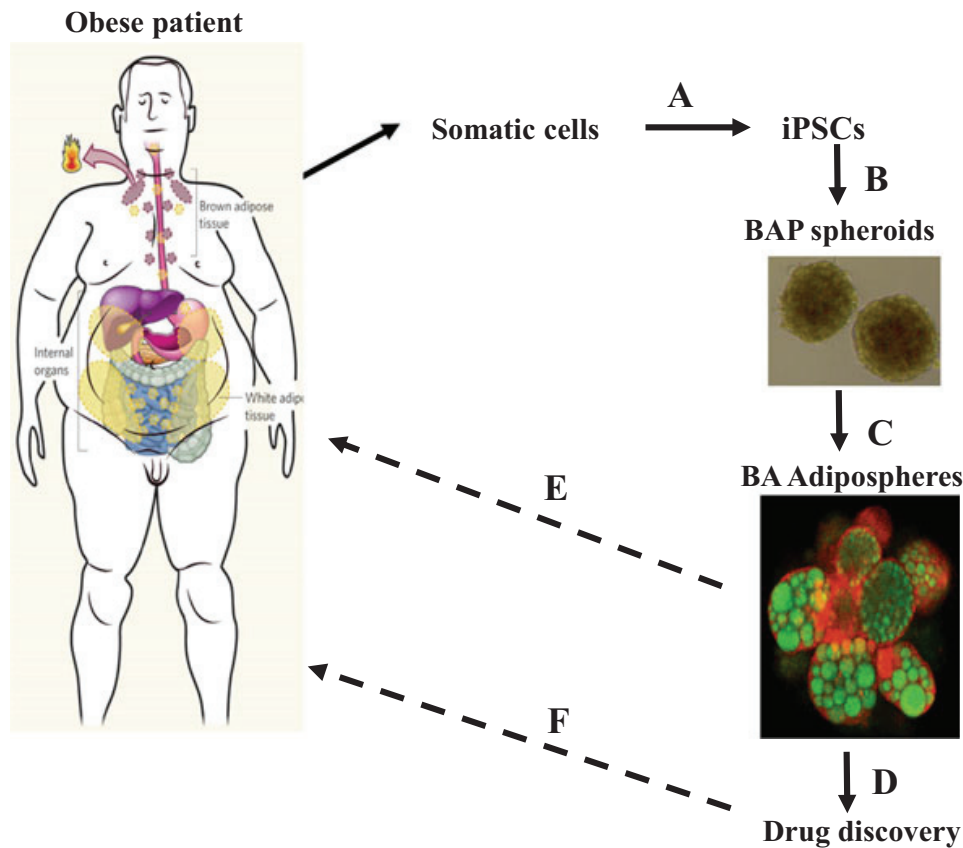


Fig. 1 The main steps of the generation of hiPSC-BA adipospheres for anti-obesity drug discovery and cell-based therapy. (a) Generation of iPSCs from obese patients; (b) derivation of brown-like adipose progenitors and cell culture in spheroids; (c) spheroids induction of differentiation into functional BAs and to mimic the physio- or pathological microenvironments; (d) transplantation of BA adipospheres to increase the BA mass in obese; (e) use the physiological model as a basis for drug discovery or drug repositioning and drug safety; (f) discovery of drugs which could attend patient drug treatment to activate BAs. The cartoon of the man comes from Farmer (2009). Photos of BAP spheroids and of BA adipospheres come from experiments performed by X. Yao in C. Dani's lab

purification of hiPSC-BAPs from different hiPSC clones displays various efficiencies, but we showed that progenitors purified from different hiPSC sources have a similar capacity to undergo differentiation when using a unique adipogenic protocol (Hafner et al. 2016a, b). This result strongly supports that the progenitor purification step is a requirement. An advantage to purify progenitors is also to eliminate undifferentiated hiPSCs prone to form teratoma after transplantation. Another issue is the generation of mutations during hiPSC expansion. Fine genetic analysis and preclinical animal studies should be able to address the safety of hiPSC-BAs to be transplanted, including potential teratoma formation and other cancer development. Finally, the stability of the phenotype of transplanted BAs has to be monitored as dedifferentiation of BAs or transdifferentiation of BAs into white adipocytes after transplantation cannot be ruled out. Tissue engineering aiming to develop tissue-like structures that mimic the in vivo situation as closely as possible should prevent this risk. As hiPSCs can differentiate into cells present in the adipose

tissue, BA adipospheres could be enriched with macrophages and endothelial cells (ECs) to mimic an adipose-like structure and to improve their therapeutic potential. Endothelial growth media supports hiPSC-BAPs differentiation (see above), suggesting the feasibility to coculture BA adipospheres with ECs. Pre-vascularized organoids derived from hiPSCs have been generated including the liver, skeletal, and cardiac muscle. All constructs show incorporation into vascular network and a better viability of the graft after transplantation in animal models (Caspi et al. 2007; Takebe et al. 2013).

Numerous other issues have also to be solved before a therapeutic use of iPSCs in the obesity field, but the derivation of BAPs having a high level of differentiation without gene transfer and their capacity to form 3D adipospheres open the opportunity of using hiPSCs advantages for anti-obesity therapy and for a better understanding of the interactions between different cell types of adipose tissue for BAs recruitment and activation.

References

- Ahfeldt T, Schinzel RT, Lee YK, Hendrickson D, Kaplan A, Lum DH, Camahort R, Xia F, Shay J, Rhee EP, Clish CB, Deo RC, Shen T, Lau FH, Cowley A, Mowrer G, Al-Siddiqi H, Nahrendorf M, Musunuru K, Gerszten RE, Rinn JL, Cowan CA (2012) Programming human pluripotent stem cells into white and brown adipocytes. *Nat Cell Biol* 14:209–219
- Caspi O, Lesman A, Basevitch Y, Gepstein A, Arbel G, Habib IH, Gepstein L, Levenberg S (2007) Tissue engineering of vascularized cardiac muscle from human embryonic stem cells. *Circ Res* 100:263–272
- Cypess AM, White AP, Vernochet C, Schulz TJ, Xue R, Sass CA, Huang TL, Roberts-Toler C, Weiner LS, Sze C, Chacko AT, Deschamps LN, Herder LM, Truchan N, Glasgow AL, Holman AR, Gavrilu A, Hasselgren PO, Mori MA, Molla M, Tseng YH (2013) Anatomical localization, gene expression profiling and functional characterization of adult human neck brown fat. *Nat Med* 19:635–639
- Dani C (2013) Activins in adipogenesis and obesity. *Int J Obes (Lond)* 37:163–166
- Farmer SR (2009) Obesity: be cool, lose weight. *Nature* 458:839–840
- Giordano A, Frontini A, Cinti S (2016) Convertible visceral fat as a therapeutic target to curb obesity. *Nat Rev Drug Discov* 15:405–424
- Gunawardana SC, Piston DW (2010) Reversal of type 1 diabetes in mice by brown adipose tissue transplant. *Diabetes* 61:674–682
- Hafner AL, Dani C (2014) Human induced pluripotent stem cells: a new source for brown and white adipocytes. *World J Stem Cells* 6:467–472
- Hafner AL, Contet J, Ravaut C, Yao X, Villageois P, Suknuntha K, Annab K, Peraldi P, Binetruy B, Slukvin II, Ladoux A, Dani C (2016a) Brown-like adipose progenitors derived from human induced pluripotent stem cells: identification of critical pathways governing their adipogenic capacity. *Sci Rep* 6:32490
- Hafner A-L, Mohsen-Kanson T, Dani C (2016b) A protocol for the differentiation of brown adipose progenitors derived from human induced pluripotent stem cells at a high efficiency with no gene transfer. *Nat Protocol Exchange*. Doi: <https://doi.org/10.1038/protex.2016.067>
- Hebert TL, Wu X, Yu G, Goh BC, Halvorsen YD, Wang Z, Moro C, Gimble JM (2009) Culture effects of epidermal growth factor (EGF) and basic fibroblast growth factor (bFGF) on cryopreserved human adipose-derived stromal/stem cell proliferation and adipogenesis. *J Tissue Eng Regen Med* 3:553–561

- Holmstrom TE, Mattsson CL, Falting JM, Nedergaard J (2008) Differential signalling pathways for EGF versus PDGF activation of Erk1/2 MAP kinase and cell proliferation in brown pre-adipocytes. *Exp Cell Res* 314:3581–3592
- Horvath P, Aulner N, Bickle M, Davies AM, Nery ED, Ebner D, Montoya MC, Ostling P, Pietiainen V, Price LS, Shorte SL, Turcatti G, von Schantz C, Carragher NO (2016) Screening out irrelevant cell-based models of disease. *Nat Rev Drug Discov* 15:751–769
- Kim B, Choi KM, Yim HS, Lee MG (2013) Ascorbic acid enhances adipogenesis of 3T3-L1 murine preadipocyte through differential expression of collagens. *Lipids Health Dis* 12:182
- Lindroos J, Husa J, Mitterer G, Haschemi A, Rauscher S, Haas R, Groger M, Loewe R, Kohrgruber N, Schrogendorfer KF, Prager G, Beck H, Pospisilik JA, Zeyda M, Stulnig TM, Patsch W, Wagner O, Esterbauer H, Bilban M (2013) Human but not mouse adipogenesis is critically dependent on LMO3. *Cell Metab* 18:62–74
- Liu X, Wang S, You Y, Meng M, Zheng Z, Dong M, Lin J, Zhao Q, Zhang C, Yuan X, Hu T, Liu L, Huang Y, Zhang L, Wang D, Zhan J, Jong Lee H, Speakman JR, Jin W (2015) Brown adipose tissue transplantation reverses obesity in Ob/Ob mice. *Endocrinology* 156:2461–2469
- Liu C, Huang K, Li G, Wang P, Liu C, Guo C, Sun Z, Pan J (2017) Ascorbic acid promotes 3T3-L1 cells adipogenesis by attenuating ERK signaling to upregulate the collagen VI. *Nutr Metab (Lond)* 14:79
- van Marken Lichtenbelt WD, Vanhomerig JW, Smulders NM, Drossaerts JM, Kemerink GJ, Bouvy ND, Schrauwen P, Teule GJ (2009) Cold-activated brown adipose tissue in healthy men. *N Engl J Med* 360:1500–1508
- Milet C, Bleher M, Allbright K, Orgeur M, Couplier F, Duprez D, Havis E (2017) Egr1 deficiency induces browning of inguinal subcutaneous white adipose tissue in mice. *Sci Rep* 7:16153
- Min SY, Kady J, Nam M, Rojas-Rodriguez R, Berkenwald A, Kim JH, Noh HL, Kim JK, Cooper MP, Fitzgibbons T, Brehm MA, Corvera S (2016) Human “brite/beige” adipocytes develop from capillary networks, and their implantation improves metabolic homeostasis in mice. *Nat Med* 22:312–318
- Mohsen-Kanson T, Hafner AL, Wdziekonski B, Takashima Y, Villageois P, Carriere A, Svensson M, Bagnis C, Chignon-Sicard B, Svensson PA, Casteilla L, Smith A, Dani C (2014) Differentiation of human induced pluripotent stem cells into brown and white adipocytes: role of Pax3. *Stem Cells* 32:1459–1467
- Nishio M, Yoneshiro T, Nakahara M, Suzuki S, Saeki K, Hasegawa M, Kawai Y, Akutsu H, Umezawa A, Yasuda K, Tobe K, Yuo A, Kubota K, Saito M, Saeki K (2012) Production of functional classical brown adipocytes from human pluripotent stem cells using specific hemopoietin cocktail without gene transfer. *Cell Metab* 16:394–406
- Nishizawa M, Chonabayashi K, Nomura M, Tanaka A, Nakamura M, Inagaki A, Nishikawa M, Takei I, Oishi A, Tanabe K, Ohnuki M, Yokota H, Koyanagi-Aoi M, Okita K, Watanabe A, Takaori-Kondo A, Yamanaka S, Yoshida Y (2016) Epigenetic variation between human induced pluripotent stem cell lines is an Indicator of differentiation capacity. *Cell Stem Cell* 19:341–354
- Orlova VV, van den Hil FE, Petrus-Reurer S, Drabsch Y, Ten Dijke P, Mummery CL (2014) Generation, expansion and functional analysis of endothelial cells and pericytes derived from human pluripotent stem cells. *Nat Protoc* 9:1514–1531
- Ortmann D, Vallier L (2017) Variability of human pluripotent stem cell lines. *Curr Opin Genet Dev* 46:179–185
- Petrenko Y, Sykova E, Kubinova S (2017) The therapeutic potential of three-dimensional multipotent mesenchymal stromal cell spheroids. *Stem Cell Res Ther* 8:94
- Planat-Benard V, Silvestre JS, Cousin B, Andre M, Nibelink M, Tamarat R, Clergue M, Manneville C, Saillan-Barreau C, Duriez M, Tedgui A, Levy B, Penicaud L, Casteilla L (2004) Plasticity of human adipose lineage cells toward endothelial cells: physiological and therapeutic perspectives. *Circulation* 109:656–663
- Sanchez-Gurmaches J, Guertin DA (2013) Adipocyte lineages: tracing back the origins of fat. *Biochim Biophys Acta* 1842:340–351

- Shi Y, Inoue H, Wu JC, Yamanaka S (2016) Induced pluripotent stem cell technology: a decade of progress. *Nat Rev Drug Discov* 16:115–130
- Shiba Y, Gomibuchi T, Seto T, Wada Y, Ichimura H, Tanaka Y, Ogasawara T, Okada K, Shiba N, Sakamoto K, Ido D, Shiina T, Ohkura M, Nakai J, Uno N, Kazuki Y, Oshimura M, Minami I, Ikeda U (2016) Allogeneic transplantation of iPS cell-derived cardiomyocytes regenerates primate hearts. *Nature* 538:388–391
- Stanford KI, Middelbeek RJ, Townsend KL, An D, Nygaard EB, Hitchcox KM, Markan KR, Nakano K, Hirshman MF, Tseng YH, Goodyear LJ (2013) Brown adipose tissue regulates glucose homeostasis and insulin sensitivity. *J Clin Invest* 123:215–223
- Takahashi K, Tanabe K, Ohnuki M, Narita M, Ichisaka T, Tomoda K, Yamanaka S (2007) Induction of pluripotent stem cells from adult human fibroblasts by defined factors. *Cell* 131:861–872
- Takebe T, Sekine K, Enomura M, Koike H, Kimura M, Ogaeri T, Zhang RR, Ueno Y, Zheng YW, Koike N, Aoyama S, Adachi Y, Taniguchi H (2013) Vascularized and functional human liver from an iPSC-derived organ bud transplant. *Nature* 499:481–484
- Taura D, Noguchi M, Sone M, Hosoda K, Mori E, Okada Y, Takahashi K, Homma K, Oyamada N, Inuzuka M, Sonoyama T, Ebihara K, Tamura N, Itoh H, Suemori H, Nakatsuji N, Okano H, Yamanaka S, Nakao K (2009) Adipogenic differentiation of human induced pluripotent stem cells: comparison with that of human embryonic stem cells. *FEBS Lett* 583:1029–1033
- Villarroya F, Gavaldà-Navarro A, Peyrou M, Villarroya J, Giralt M (2017) The lives and times of brown adipokines. *Trends Endocrinol Metab* 28:855–867
- Zhang J, Zhang Y, Sun T, Guo F, Huang S, Chandalia M, Abate N, Fan D, Xin HB, Chen YE, Fu M (2013) Dietary obesity-induced Egr-1 in adipocytes facilitates energy storage via suppression of FOXO2. *Sci Rep* 3:1476

III Three-dimensional (3D) Cell Culture Systems

Research in mammalian cell biology often relies on developing in vitro models to study a specific biological mechanism or process under different test conditions. It is critical that the model represent the cell behavior in vivo, e.g, co-culture model represents more the structure of real tissue. Recently, researchers focus more on creating tissue-like structures, since 3D model better mimic in vivo conditions than 2D, which provides new opportunities for use in basic research and drug discovery. The differences exhibited in 2D and 3D culture systems and the advantage of 3D culture are presented in Figure 19 (Ravi et al., 2015). 3D cultures have numerous applications, such as differentiation Studies, drug discovery and pharmacological applications, cell adhesion and signaling studies, microenvironment studies, drug response studies, and co-cultures, which help understand better the complex cellular physiological mechanisms.

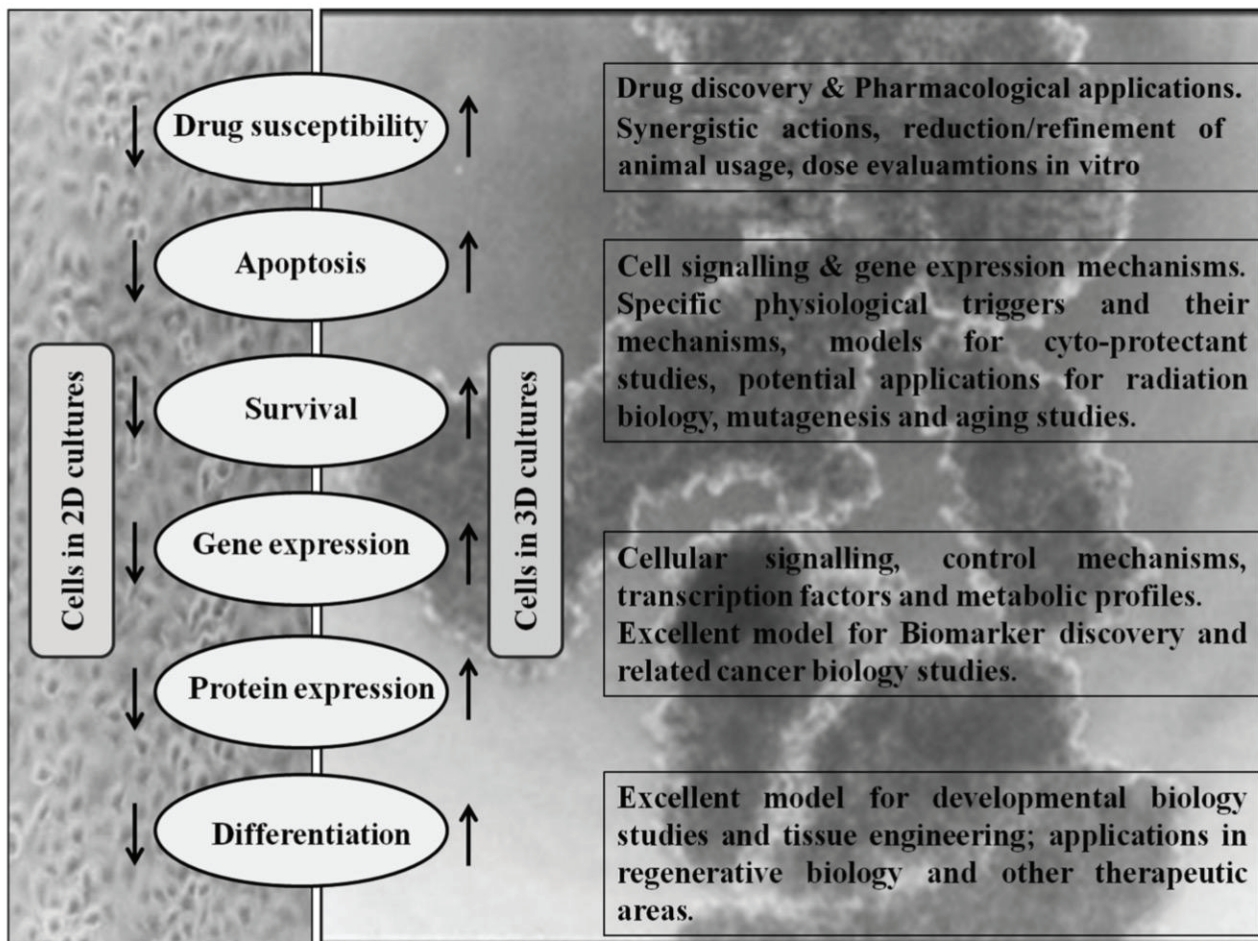


Figure 19. Some of the important areas for which 3D cell culture systems are excellent models include studies involving drug discovery, cytotoxicity, genotoxic, cell growth, apoptosis, survival, gene, and protein expressions, differentiations and developmental changes. Similarly, co-cultures in 3D systems give a better understanding of the cell interactions (Ravi et al., 2015).

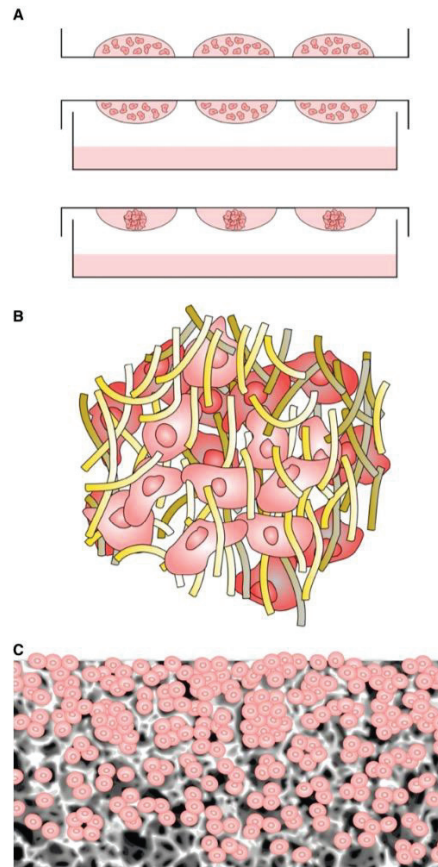


Figure 20. Primary technologies used to culture cells in 3D. (A) Formation of 3D micro-tissues using hanging drop approach. Droplets of cell suspension are placed on the lid of a Petri dish, which is gently inverted and placed on top of the dish containing media to maintain a humid atmosphere. Suspended cells come together in the apex of the drop-let, forming a compact 3D aggregate. (B) 3D culture using hydrogel technology. The cartoon shows cells within a matrix of protein molecules that create a nano-scale micro-environment mimicking the structure of the extracellular matrix. Cells are embedded within the proteinous 3D framework within an aqueous-based gel. (C) Porous solid scaffold supporting 3D cultured cells. Cells enter the porous framework of the solid scaffold where they do not flatten, they maintain their 3D structure, and they bind to one another forming 3D tissue-like masses (Knight and Przyborski, 2015).

III.1 3D cell culture technology

3D cell culture technology can be briefly divided into scaffold-free or scaffold-based culture systems, with scaffolds made from either natural or synthetic materials. In this part, some of the most popular examples currently used will be described, including aggregate cultures and spheroids, hydrogels, and scaffold-based technologies (Figure. 20) (Knight and Przyborski, 2015).

III.1.1 Aggregate cultures and the formation of spheroids

Scaffold-free systems, often referred to as spheroids, is the formation of multi-cellular aggregates, in which cells are able to form their own ECM. Such structures can be produced in many ways, mainly including the hanging drop technique and low adherence substrates. The hanging drop technique is to form spheroids with cells in a drop of media suspended on the lid of a cell culture

dish (Figure. 20A) (Keller, 1995), whereas cells can also form spheroids in suspension with low adherence substrates.

Scaffold-free systems have multiple applications. It has been shown to allow cell survival for long time and maintain the cell phenotype, and the differentiation is more homogeneous than 2D monolayer cells (Banerjee and Bhonde, 2006; De Smedt et al., 2008). Furthermore, Szczepny et al. showed that cells secreted a high concentration of endogenous factors such as the hedgehog proteins, and therefore are able to maintain better tissue function than 2D (Szczepny et al., 2009).

The formation of spheroids is especially critical for stem cell differentiation. In this case, the spheroids are referred as embryoid bodies (EBs), which the size of EB can affect cell differentiation (Messana et al., 2008; Bratt-Leal et al., 2009). ESC-based spheroids are capable of forming simple EBs with morula-like structures or cystic EBs where there is a central cavity resembling the blastula stage (Abe et al., 1996). There are also limitations with scaffold-free systems, including difficulties in nutrient and gaseous diffusion, and the big spheroids (over 500 μm) leads to hypoxia and necrosis in the center (Alvarez-Pérez et al., 2005). However, the hypoxic conditions in 3D models can be used for studying the development and progression of tumors with proliferating cells at the surface and quiescent cells in the center (Mehta et al., 2012).

III.1.2 Scaffold-based technologies for 3D cell culture

3D scaffolds can be produced by natural and synthetic materials. Natural biomaterials are biocompatible and contain cell adhesion sites, based on different components of ECM such as collagen (Baharvand et al., 2006), fibrin (Willerth et al., 2006), hyaluronic acid (Gerecht et al., 2007), or naturally derived materials, including silk (Mauney et al., 2007), gelatin (Awad et al., 2004) and alginate (Li et al., 2010). The limitations may include batch-to-batch variation and limited mechanical properties, and biodegradation which is difficult to control and introduces unknown influence to cells.

Scaffolds made from synthetic materials have defined chemical compositions and tunable mechanical properties, which can affect cell differentiation and cell adhesion (Engler et al., 2006; Hayward et al., 2013). Synthetic materials include biomaterials such as polymers (Gunatillake and Adhikari., 2003) and titanium (van den Dolder et al., 2003), ceramic-based materials such as bioactive glasses (Lu et al., 2003), and self-assembled peptides (Garreta et al., 2006). Synthetic scaffold has advantages like reproducibility, non-degradation and tunable degradability which

materials derived naturally can not provide. However, synthetic materials may not contain cell adhesion sites and need to coat ECM proteins to mimic the naturally cell niche. Scaffold-based 3D cultures have several different methods, and hydrogels and solid scaffolds are the two mainly approaches.

III.1.2.1 Hydrogel technology

Hydrogel technology is to encapsulate cells in a hydrogel composed by a loose scaffold framework with cross-linked natural base materials such as agarose, fibrin, collagen or hyaluronic acid with high water content (Tibbitt and Anseth, 2009) (Figure. 20B). Hydrogels support cell growth by trapping cells in environment with artificial ECM protein or allowing cells to migrate from the surface to the center of the gel (Heywood et al., 2004; Jongpaiboonkit et al., 2008; Topman et al., 2013). However, cells can be only cultured for a relatively short time due to the the lack of nutrients diffusion through the hydrogel (Jongpaiboonkit et al., 2008).

Hydrogels, either Collagen I matrices (Wells et al., 2013) or reconstituted basement membrane extracts (Debnath et al., 2003), are commonly used in models of branching morphogenesis to understand the molecular and cellular mechanisms behind the process of tube formation(Zegers, 2014). It has been demonstrated that cell polarization and lumen formation required different ECM compositions through the comparisons of these two hydrogels (Santos and Nigam, 1993; Campbell and Watson, 2009). More recently, hydrogels are used to combine with bioactive agents in a co-cultured “tumor angiogenesis model” to study the role of ECs in the tumor microenvironment (Chwalek et al., 2014). Hydrogels have also been used to mimic the niche of stem cells with the use of hyaluronic acid, which supports hESCs growth and regulates proliferation and morphogenesis in vivo (Toole, 2009).

III.1.2.2 Solid scaffold-based technology

Solid scaffold provides organized arrangements of cells in vitro, and create natural 3D tissue-like structures (Figure. 20C). Cells can be seeded into the open pore structure of a pre-prepared solid scaffold, which is more controllable and reproducible. Numerous types of solid scaffold are used for different applications. For example, porous scaffold is able to maintain epidermal-like structures of equine keratinocytes, and to produce co-cultures to study tumor invasion into the stromal layer (Sharma et al., 2013; Fischbach et al., 2007).

III.2 3D adipocyte culture systems

III.2.1 3D adipocyte models

3D adipocyte culture systems present several advantages as they offer the microenvironmental niche mimic *in vivo* conditions, which is important for adipocyte development, activation and differentiation. 3D cultures as well as cellular co-culture systems *in vitro* represent a more physiological model for the study of development and activation of thermogenic adipocytes (Figure. 22). In addition, the proper combination of oxygen, cell matrix and growth factors can not only promote the adipocytes differentiation, but also increase cell survival and secretion function (Unser et al., 2015).

Aloysius et al. generated 3D adipose spheroids from primary or immortal human or mouse pre-adipocytes with a scaffold-free method (Aloysius et al., 2018). Spheroids were formed in hanging drops, and then transferred to low adherent plates, which can be maintain for a long time. The spheroids can differentiate into mature adipocytes when exposure to differentiation cues, and are able to accumulate large lipid droplet with expanded time. Expression and secretion of adiponectin is higher in 3D than 2D culture. Furthermore, 3D spheroids derived from BAT can better maintain the BAT markers than 2D cultures derived from the same tissue. Therefore, this model can be used to study adipogenesis which mimic better *in vivo*.

Muller et al. developed a co-cultured 3D model with APs derived from SVF of human subcutaneous white AT and endogenous ECs, which mimic the cellular architecture found in vivo (Muller et al., 2019). They obtained highly vascularized spheroids containing mature adipocytes. Moreover, they transplanted the differentiated spheroids into immune-deficient mice, and chimeric vessels as well as adipocytes of human origin were observed in transplanted mice. This vascularized human AT-like 3D model therefore represents a good tool to understand human AT.

Adipocyte differentiation and homeostasis can be regulated by mechanical signals and ECM changes that represented their physiological environment in vivo. For this reason, organoids or hydrogels are useful because of their controllable rigidity and ECM composition mimicking the microenvironment, which represent good approaches to study cell-cell interactions (Pellegrinelli et al., 2014a; Pellegrinelli et al., 2014b; Geckil et al., 2010; Simunovic and Brivanlou, 2017). Recently, a 3D hydrogel system has been developed to culture adipocytes in 3D, which can keep both function and morphology of the lipid droplets (Pellegrinelli et al., 2014b). Alginate microstands have been used to the culture of brown-like adipocytes derived from mouse ESCs.

Furthermore, a study combined hydrogel consisting of a mixture of hASCs and alginate microspheres containing FGF1 and BMP4, and hASC is able to differentiate into brown-like adipocytes in this 3D culture system (Greenwood-Goodwin M et al., 2014).

With the help of levitated nanoparticles, 3T3- L1 preadipocytes differentiated into mature adipocytes with enhanced differentiation and viability (Daquinag et al., 2012). Adipose organoids are 3D structures formed by levitation, represent human tissues in three dimensional miniatures and recapitulate their physiological characteristics.

Since organoids formed from PSCs can mimic the cell complexity and organisation, they can be good tool to study the development of a given tissue *in vitro* (McCauley and Wells, 2017).

III.2.2 Applications of iPSC-brown-like adipospheres in cell therapy

A myriad of molecules has been tested as anti-obesity drugs. To date, the marketed drugs for BAs activation showed limited efficacy and/or displayed substantial adverse effects (Giordano et al., 2016). Among the reasons involved in this weak efficacy, one can also mention the limitation of the drug testing models due to the culture conditions that do not mimic the phenotype of the cells and their physiological microenvironment within the adipose tissue.

Cells are classically grown as monolayer, which poorly reflects the *in vivo* situation (Horvath et al., 2016). In contrast, the cell–cell and cell–extracellular matrix interactions are promoted in 3D configurations. Therefore, 3D cultures represent a bridge between traditional cell culture and live tissue to overcome the limitations that impaired discovery of efficient and safe drugs.

hiPSC-BAPs can form 3D aggregates, also known as spheroids, able to differentiate into UCP-1-expressing adipocytes, therefore named as adipospheres (Yao and Dani, unpublished data). Three-dimensional adipospheres formed from hiPSC-BAs could serve as a platform to identify pathways governing the recruitment and the activation of human BAs and for anti-obesity drug discovery (Figure. 21) (Yao et al., 2018). On the other hand, BA adipospheres from obese-iPSCs can be proposed as therapeutic cells (Figure. 21).

As hiPSCs can differentiate into cells present in the adipose tissue, BA adipospheres could be enriched with macrophages and endothelial cells (ECs) to mimic an adipose-like structure and to improve their therapeutic potential. Endothelial growth media supports hiPSC-BAPs differentiation,

suggesting the feasibility to coculture BA adipospheres with ECs. Pre-vascularized organoids derived from hiPSCs have been generated including the liver, skeletal, and cardiac muscle. All constructs show incorporation into vascular network and a better viability of the graft after transplantation in animal models (Caspi et al., 2007; Takebe et al., 2013).

Numerous other issues have also to be solved before a therapeutic use of iPSCs in the obesity field, but the derivation of BAPs having a high level of differentiation without gene transfer and their capacity to form 3D adipospheres open the opportunity of using hiPSCs advantages for anti-obesity therapy and for a better understanding of the interactions between different cell types of adipose tissue for BAs recruitment and activation. A chapter describing the potential of hiPSCs in the obesity field is found above (Yao et al., 2018).

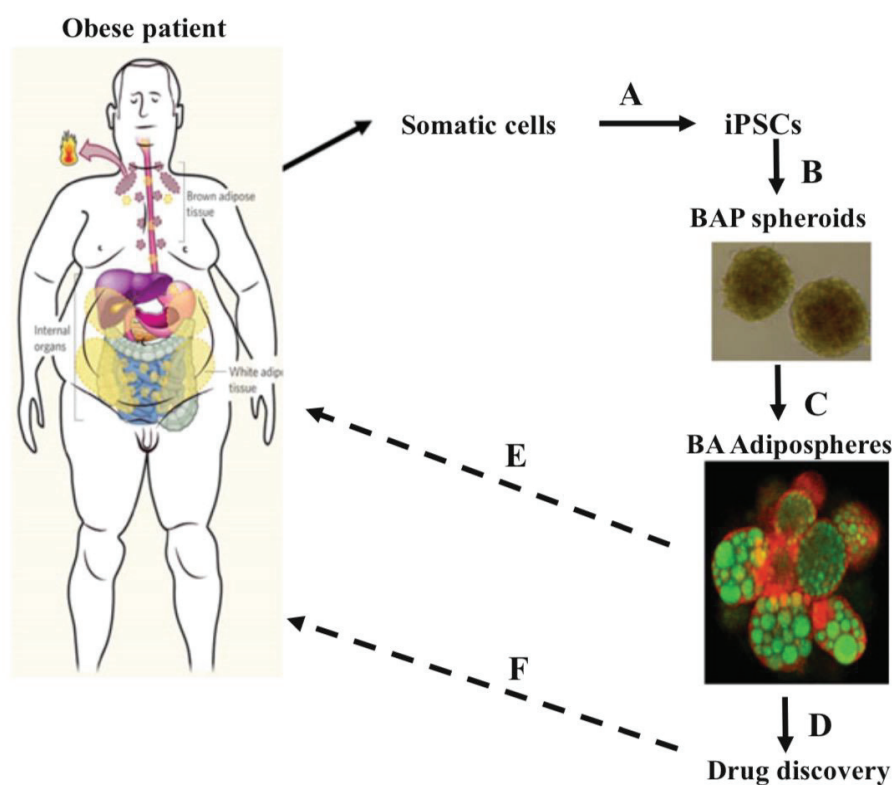


Figure 21. The main steps of the generation of hiPSC-BA adipospheres for anti-obesity drug discovery and cell-based therapy. (a) Generation of iPSCs from obese patients; (b) derivation of brown-like adipose progenitors and cell culture in spheroids; (c) spheroids induction of differentiation into functional BAs and to mimic the physio- or pathological microenvironments; (d) transplantation of BA adipospheres to increase the BA mass in obese; (e) use the physiological model as a basis for drug discovery or drug repositioning and drug safety; (f) discovery of drugs which could attend patient drug treatment to activate BAs. The cartoon of the man comes from Farmer (2009). Photos of BAP spheroids and of BA adipospheres come from experiments performed by X. Yao in C. Dani's lab (Yao et al., 2018).

Cell models and objectives

In our lab, we have several hiPSC-BAPs, and two of which have been used in my thesis (Figure. 22) (Hafner and Dani, 2014). One of hiPSC-BAPs, called MSC3-RA, is derived from the hiPSC line NOK6 from a collaboration (Dr. Austin Smith, University of Cambridge), which are neural stem cells reprogramming by insertion of Nanog, Oct4 and klf4 thanks to the PiggyBac transposon system. HiPSC differentiation was initiated by formation of embryoid bodies (EBs), which are then seeded onto culture dishes and maintained in a mesenchymal culture medium. After serial passages, adherent cells acquire a fibroblast-like morphology and specific MSC markers (Mohsen-Kanson et al., 2014). The other hiPSC-BAP from a collaboration (Dr. Igor I. Slukvin, University of Wisconsin), called 19-9-11T, is generated by reprogramming fetal fibroblasts using lentiviruses containing cDNAs for Oct4, Sox2, Nanog and Lin28. iPSCs were induced to differentiate in coculture with OP9 stromal cells and OP9 cells were depleted by using anti-mouse CD29 antibodies. Cells are maintained in mesenchymal culture medium supplied with FGF2 and VEGF, and then obtain the characterizations of MSCs (Vodyanik et al., 2010).

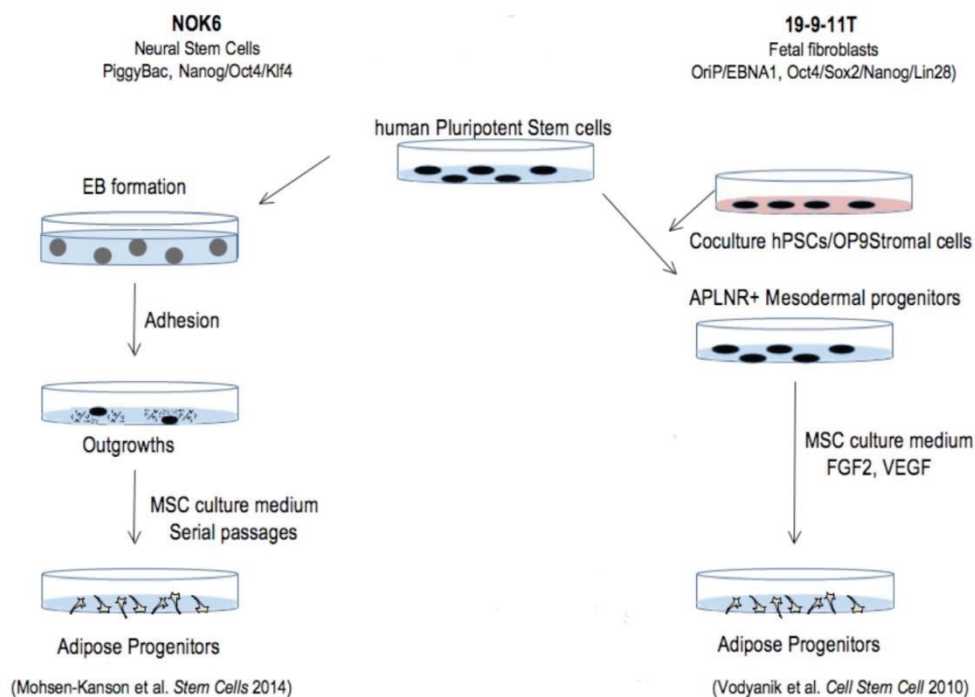


Figure 22. Mesenchymal stem cell derivation strategies. MSCs were derived from hiPSCs following embryoid body formation. Alternatively, hiPSCs were maintained in co-culture with murine stromal cells (Hafner and Dani, 2014).

During my thesis, we used BAPs derived from these two cell lines as cell models to establish 3D model. First, we describe the capacity of hiPSC-BAPS to form spheroids and a method for their differentiation at a high efficiency in hiPSC- adipospheres containing UCP1 expressing cells. Then, we show that expression of UCP1 increased in adipospheres following stimulation with small

molecules or *CDKN2A*-knocked down. Finally, the model was enriched with Human Dermal Microvascular Endothelial Cells (HDMECs) to better mimic the adipose tissue microenvironment and to improve its therapeutic potential.

Results

I 3D brown-like adipocytes derived from human iPSCs to counteract obesity

BAs represent promising cell targets to counteract obesity and type 2 diabetes. However, there are major limitations for a BA-based treatment of obesity, among which the main ones are: 1) The rareness and scarcity of BAs in adult humans and 2) The lack of a relevant physiologic cell model for preclinical testing of drugs activating human BAs. Therefore, an unlimited source of human BAs in a relevant culture condition is needed to lift the barriers to fight obesity.

Following the pioneer work of Yamanaka's group on the generation of patient-specific induced pluripotent stem cells (iPSCs) by reprogramming somatic cells, hiPSCs emerged as an abundant source of cells of therapeutic interest. We were among the first to report the potential of hiPSCs to generate BA progenitors, and to identify critical factors for their differentiation into brown adipocytes at a high level.

In my work of thesis, we generate 3D models hosting functional brown-like adipospheres derived from hiPSCs. We propose it as an innovative model for a better in vitro drug screening and cell therapy of obesity.

I.1 Establish 3D brown-like adipocyte model derived from human iPSCs to counteract obesity

I.1.1 Article "Generation of 3D brown-like adipocytes derived from human iPSCs: A new tool for in vitro preclinical drug discovery and for cell-based therapy to treat obesity"

Article in preparation

Generation of 3D brown-like adipocytes derived from human iPSCs: A new tool for in vitro preclinical drug discovery and for cell-based therapy to treat obesity

Xi YAO¹, Vincent DANI¹, Thorsten Gnad², Alexander Pfeifer², Jean-Sébastien Annicotte³ and Christian DANI¹

1. University Côte d'Azur, CNRS, INSERM, iBV, Faculty of Medicine, Nice, France.
2. Institute for Pharmacology and Toxicology, Biomedical Center, University of Bonn, 53105 Bonn, Germany.
3. Lille University, UMR 8199 e EGID, F-59000 Lille, France

Corresponding author:

Christian Dani, iBV, Faculté de Médecine, Nice, France,

Tel: +33 (0)4 93 37 76 47

Fax: +33 (0)4 93 37 70 58

E-mail: dani@unice.fr

key words: hiPSC, brown-like adiposphere, 3D, co-culture

Abstract

Beige/brite/brown-like adipocytes (BAs), dispersed in white adipose tissue, represent promising cell targets to counteract obesity and associated diseases. However, there are major limitations for a BA-based treatment of obesity, among which the main ones are the rareness of BAs in adult humans and the lack of a relevant cell culture condition for modelling the development of brown-like adipocytes. In this paper we described the capacity of human induced Pluripotent Stem Cells-derived BA progenitors (hiPSC-BAPs) to self-organize in spheroids and a method for their differentiation at a high efficiency in 3D hiPSC-adipospheres containing UCP1-expressing cells.

BAPs derived from two hiPSC clones were maintained in ultra-low attachment plates to form self-organized free-scaffold spheroids. Then, spheroids were induced to undergo adipogenesis at a high level into adipospheres using a novel adipogenic cocktail. Whole-mount immunofluorescence stainings were performed after clearing of hiPSC-adipospheres to visualize brown-like adipocytes during differentiation. Then, hiPSC-adipospheres were compared to adipospheres generated from subcutaneous abdominal adipose stromal cells in terms of distribution of extra cellular matrix proteins and of UCP1 expressing cells.

hiPSC-BAPs self-organized in spheroids within 3 days. Lipid-laden cells and UCP1 expressing cells were detectable 10 days after adipogenesis induction. Differentiation into adipospheres enhanced brown-like adipogenesis compared to conventional monolayer BAP differentiation. UCP1 expression increased in hiPSC-adipospheres upon treatment with cAMP or cGMP analogs or *CDKN2A*-knocked down. Moreover, hiPSC-adipospheres displayed similar extracellular matrix protein profile compared to human subcutaneous abdominal adipospheres.

Finally, hiPSC-BAPs and HDMECs can co-culture in 3D and differentiate into vascularized hiPSC-brown-like adipospheres with functional tubular-like structure formed inside, meanwhile secrete factors to support vascularization which mimic in vivo situation.

The data indicated that 3D hiPSC-adipospheres respond to physiological stimuli and is a relevant model to identify factors regulating the development of human brown-like

adipocytes in white adipose tissue. In a near future, this model may also be a suitable tool for drug screening allowing discovery of novel and safe anti-obesity drugs.

Introduction

The development of obesity and associated metabolic disorders such as diabetes and heart diseases are major health problems. Obesity results from an imbalance between calorie intake and energy expenditure. The scientific community is focusing its attention on white adipose tissue (WAT) that stores energy, and the means to fight its expansion. In contrast to WAT, classical brown adipocytes and brown-like adipocytes (BAs) dispersed in WATs, mainly in the subcutaneous abdominal fat depot, are specialized in energy expenditure by their high mitochondria content with the expression of the uncoupling protein-1 (UCP1) (Rosen and Spiegelman, 2014). Therefore, BAs represent promising cell targets to counteract obesity and type 2 diabetes. However, there are major limitations for a BA-based treatment of obesity, among which the main ones are: 1) The rareness and scarcity of BAs in adult humans and 2) The lack of a relevant physiologic cell model for preclinical testing of drugs activating human BAs. Therefore, an unlimited source of human BAs in a relevant culture condition is needed to lift the barriers to fight obesity.

Induced pluripotent stem cells (iPSCs) display a quasi-unlimited self-renewal capacity and are an abundant source of multiple cell types of therapeutic interest for drug screening and drug repositioning. In addition, human iPSCs are outstanding tools in early preclinical phase of drug discovery to perform cytotoxicity assays. They allow autologous transplantation when generated from patient's own cells. To date, autologous transplants are economically expensive, but a recent study reported the possibility of allogenic iPSC transplants, which has a tremendous potential for clinic use (Shiba et al. 2016). Our laboratory has recently described a procedure to isolate expandable BA progenitors (BAPs) from hiPSCs and to generate functional BAs at high levels with no gene transfer (Hafner 2016a; Hafner et al. 2016b; Mohsen-Kanson et al. 2014), opening the opportunity of using hiPSC advantages for anti-obesity drug testing and cell based therapy to increase the BA mass in patients.

A reason likely involved in this weak efficacy of the drug testing models is the culture conditions that do not mimic the physiological microenvironment in which cells normally reside in vivo. Cells, including hiPSC-derived progenitors, are classically grown as two-dimension (2D) monolayer, which poorly reflects the in vivo situation as adipose tissue exhibits a complex architecture. The generation of 3D spheroids, by cell self-assembly or controlled environment by means of a scaffold, appears as major advance in culture processes

since they offer new models of tissues tightly related to the in vivo context. The formation of spheroids enables cells to form micro-networks and to interact under natural forces. This near-physiological 3D model facilitates an accurate study of a range of biological processes including responses to drugs (Sasai, 2013). Therefore, 3D cultures represent a powerful platform for drug screening to overcome the limitations that impaired discovery of efficient and safe drugs in the obesity field.

Here, we describe the capacity of hiPSC-BAPS to form spheroids and a method for their differentiation at a high efficiency in hiPSC- adipospheres containing UCP1 expressing cells. We show that expression of UCP1 increased in adipospheres following stimulation with small molecules or *CDKN2A*-knocked down. Then, the model was enriched with Human Dermal Microvascular Endothelial Cells (HDMECs) to better mimic the adipose tissue microenvironment and to improve its therapeutic potential. All together, our results indicate that the hiPSC-brown-like adiposphere model better mimics the subcutaneous abdominal adipose tissue than the conventional 2D culture model and that in a near future may be a suitable tool for both therapeutic transplantation and for drug screening allowing discovery of novel and safe anti-obesity drugs.

Materials and Methods

Cell culture

Primary cells derived from adipose tissues and hiPSC-derived cells were grown in standard tissue culture conditions at 37°C with 5% CO₂. MSC3-RA cells, derived from the hiPSC line NOK6 as previously described (Mohsen-Kanson et al., 2014), and 19-9-11T cells derived from Mesoderm-mesenchymal progenitors as described (Vodyanik et al., 2010), were cultured in DMEM supplemented with 10% FCS and with 2.5 ng/ml FGF2. Human Dermal Microvascular Endothelial Cells (HDMECs) were purchased from Promocell and cultured in EGM-MV2 with supplementMix as indicated by the supplier. HDMECs were infected with retrovirus containing the plasmid, MSCV Puro SV40: GFP (Addgene, 68483), which expresses GFP driven by SV40 promoter and further selected upon puromycin resistance.

Spheroid formation and their differentiation into brown-like adipospheres

To generate spheroids, a suspension of hiPSC-BAPs (MSC3-RA or 19-9-11T) at 0.5~1x 10⁶ cells/ml was prepared in growth medium, and 1ml of the cell suspension was seeded in one well of 24 well Ultra-Low Attachment (ULA) plate (Corning 3473). The plate was maintained for 3 days to generate spheroids formed as in Figure 1B. Then, to differentiate spheroids, the proliferation medium was changed to differentiation medium composed of EBM-2 (Lonza) supplemented with 0.1% FCS, IBMX (0.5 mM), dexamethasone (0.25 μM), T3 (0.2 nM), insulin (170 nM), rosiglitazone (1 μM), SB431542 (5 μM), and EGM-2 cocktail (Lonza, CC-3121) including ascorbic acid, hydrocortisone and EGF. IBMX and dexamethasone were maintained only for the first 3 days of differentiation. SB431542 and EGF were removed after the first 7 days of differentiation. Spheroids were maintained in differentiation medium up to 20 to 30 days, with medium changed once a week. To generate co-cultured spheroids of hiPSC-BAPs and HDMECs-GFPs, a suspension including 1ml of hiPSC-BAP and 0.2 ml of HDMECs-GFP both at concentration of 10⁶ cells/ml was seeded in one well of 24 wells ULA plate. Co-cultured spheroids were generated after 3 days in EBM-2 containing 10% serum. Then, medium were changed to hiPSC-brown-like adiposphere differentiation medium supplemented with 2 μg/ ml VEGF and 10 ng/ ml FGF2. Differentiation medium for Abdominal-adipospheres is same as 2D as described previously in(Kouidhi et al., 2005).

Oil Red O staining for adipospheres

Oil Red O working solution was prepared by mixing 6 volumes of 5mg/ml Oil Red O dissolved in isopropanol with 4 volumes of H₂O. Adipospheres were fixed in 4% formaldehyde (Thermo Scientific, 28906) for 1h at room temperature, and stained with Oil Red O working solution for 2 hrs. After washing with 60% isopropanol solution and H₂O, adipospheres stained with DAPI (Invitrogen) were mounted in Grace Bio-Labs FastWell reagent barriers (Sigma, GBL664112). Pictures were taken with LSM 780 confocal microscope in z-stack. The images were reconstructed by imageJ.

Immunofluorescence staining and spheroids clarification

Fixed spheroids were washed 3 times with PBS, and then incubated for 3hr to over night at 4 °C in blocking solution composed of PBS with 1% Triton X-100 and 3%BSA. Spheroids were incubated with primary antibodies diluted in blocking solution over night at 4°C. After 3 times quick washes with PBS only and then 3 times washes with PBS containing 1% Triton X-100 and 1%BSA for 20 mins each, spheroids were incubated with secondary antibodies diluted in blocking solution with DAPI over night at 4 °C. After washing as indicated above, dehydration was done in methanol with 25% MtOH for 15 mins, 50% MtOH for 15 mins, 75% MtOH for 15 mins and 100% MtOH for 15 mins. BABB (Benzyl alcohol: Benzyl benzoate=1:2) was added under the hood, pipetted until the spheroids were transparent. Pictures were chosen in the core of spheroids and taken with LSM 780 confocal microscope. Antibodies are listed in Table S1.

Generation of adipose spheroids in hanging drop cultures

The spheroids are made by 2,000 to 20,000 cells in a volume of 20 µl proliferation medium and placing drops on the inside cover of a petri plate. The cover was then inverted and placed in a humidified chamber for 3 days to allow cells to coalesce. After the spheroids formed, they were transferred to 24-well ULA plates with differentiation medium.

Adiposphere RNA preparation and quantitative RT-PCR

After homogenising spheroids formed by 10⁶ Cells with electric pastel for 30s in 1ml of TRIzol™ Reagent (Sigma), RNAs were extracted twice by chloroform and co-precipitated with 10µg of RNase-free glycogen overnight at -20 °C. The centrifugation was full speed at 4°C during RNA purification. After twice washes with 70% ethanol, the RNA pellet was resuspended in RNase-free H₂O. Total RNA sample concentrations were determined using a Nanodrop spectrophotometer (Thermo Scientific, Waltham, MA, USA). Reverse transcription

was done with M-MLV Reverse Transcriptase (Promega) and qPCR was performed with SYBR green from Takara on a OneStep real-time PCR machine (Applied Life Sciences). *TBP* as the house keeping gene, and delta delta Ct values were used to achieve relative quantification of gene expression. Primer sequences are listed in Table S2.

Comparison of 2D and 3D cultures

5×10^4 cells were plated in one well of 12-well plate for 2D, and 10^6 cells were seeded in one well of 24-well ULA plate for 3D at the same time. Three days later, cells reached confluence on monolayer, and formed spheroids in ULA plate. The proliferation medium were replaced by same differentiation medium on 2D and 3D, and harvested after 24 days of differentiation for later analysis.

Protein preparation and western blot analysis

Spheroids were rinsed with PBS and lysed in stop buffer containing 50 mM Hepes, pH 7.2, 150 mM NaCl, 10 mM EDTA, 10 mM $\text{Na}_4\text{P}_2\text{O}_7$, 2 mM Na_3VO_4 , and 1% Triton X-100 supplemented with Protease Inhibitor Cocktail (Roche). The protein concentration was determined using protein assay dye reagent concentration (Bio-red). Total protein lysates (25 μg) were denatured and loaded on a 12% SDS-PAGE, and subsequently transferred onto PVDF membranes. The blots were blocked in 5% milk in Tris-buffered saline with 0.1% Tween 20 (TBS-T) and incubated overnight with rabbit anti-UCP-1 (1/500, Calbiochem), guinea pig anti-Perilipin1 (1/1000, Acris Antibodies) or mouse anti-Tubulin (1/10000, Sigma) overnight. Secondary horseradish peroxidase-conjugated antibodies were purchased from Promega. The blots were developed with ECL Western blotting detection reagent (GE healthcare) and detected using Amersham Imager 600 (GE healthcare).

GPCR expression analysis

GPCR profiling was performed by our collaborators (Dr. Thorsten Gnad and Dr Alexander Pfeifer).

Acute and chronic cAMP/cGMP treatment

Twenty_one days old hiPSC-adipospheres were acute stimulated with 250 ng/ul 8-CPT-cAMP (Abcam) or 8-Br-cGMP (Abcam) for 3 days in differentiation medium deleted of insulin and hydrocortisone. 250 ng/ul 8-CPT-cAMP or 8-CPT-cAMP were added all along the differentiation for chronic treatment.

LDL Uptake

The LDL-DyLight™ 550 diluted by 1:100 in the differentiation medium was the working solution. At the end of differentiation of hiPSC-BAP and HDMECs-GFP co-cultured adipospheres, the culture medium was replaced by 500 µl/well LDL-DyLight™ 550 working solution in 24 well ULA plate. The adipospheres were incubated in a 37°C incubator for overnight. At the end of the LDL uptake incubation, the culture medium was aspirated and replaced with PBS. The degree of LDL uptake was examined under LSM 780 confocal microscope.

SiRNA transfection

hiPSC-BAPs were incubated under normal growth conditions until reached confluence (typically 37°C and 5% CO₂). 5 x 10⁵ cells was plated per well of a 24-well ULA plate in 400 µl EBM containing 0.5% serum and antibiotics. 750 ng siRNA (Human CDKN2A siRNA-SMART pool, GEHealth Bio-Sciences, Rosersberg, Sweden) was diluted in 100 µl siRNA transfection medium containing 60% DMEM low glucose, 40% MCDB-201, 1× ITS, dexamethasone (10⁻⁹ M), ascorbic sodium acid (100 mM), which gave a final siRNA concentration of 100 nM. 6 µl HiPerFect (Qiagen, France) transfection reagent was added to the diluted siRNA and mixed by pipetting. The mixes were incubated for 5–10 min at room temperature (15–25°C) to allow the formation of transfection complexes. The complexes were added drop-wise onto the cells. The cells and transfection complexes were gently thoroughly mixed by pipetting up and down 4–6 times. Cells were then maintained in conditions to form spheroids and adipospheres as previously described.

Quantification and Statistics analysis

Statistical significance was determined in Microsoft Excel with either a two-tailed Student's t test or a one-way or two-way ANOVA, which can be found in the individual figure panels and figure legends. Probability values < 0.05 were considered as statistically significant and are marked with a single asterisk or with by double asterisks when p < 0.01. Error bars in graphs are defined in the figure legends and represent the mean ± SEM (standard error of mean). All the experiments repeated independently at least 3 times.

Results

Generation and characterization of ULA-plate formed hiPSC-brown-like adipospheres

Because BAs emerge as promising cell targets to counteract obesity and type 2 diabetes, we sought to develop a robust *in vitro* model that mimics as much as possible the *in vivo* situation. The goal is to use it as a relevant physiologic cell model both for preclinical testing of drugs activating human BAs and for cell-based therapy of obesity. To this end, we generated BA adipospheres derived from human induced Pluripotent Stem Cells (hiPSC-BAs). We designed a BA 3D model in which hiPSC-BA Progenitors could self-organize in ultra-low adherent wells (ULA) when maintained in non-differentiation medium within 3 days (Fig. 1A, B). Then, when medium was changed to differentiation medium, the spheroids could differentiate into brown-like adipospheres within around 20-30 days (Fig. 1C, D). Here, we show the 3D model generated from two different hiPSC-BAPs including the MSC3-RA cells derived from the hiPSCs clone NOK6 as previously described (Mohsen-Kanson et al., 2013) and the mesoderm-mesenchymal progenitors derived from the hiPSC-19-9-11T clone (Vodyanik et al., 2010). To investigate the accumulation of lipid droplets, we fixed the spheroids every week following the differentiation, and oil Red O staining in whole-mount was performed. To see the global view of the spheroids, we took z-stack pictures to reconstruct the spheroids surface which showed that the lipid droplets appeared since one week of differentiation, accumulated and increased in size (Fig. 1E). Moreover, the morphology of lipid droplets in MSC3-RA cells is heterogeneous with large droplets (1.5 μm ~20 μm). In contrast 19-9-11T adipospheres contained more homogeneous and smaller lipids droplets. To better explore the differentiation inside the spheroids, we used the whole-mount clearing technique to transparent the spheroids so that we can observe the internal structure without sections (Adavis, 1993). Whole-mount immunofluorescence staining of Perilipin1 and UCP1 as well as clearing were performed on spheroids following the differentiation. The spheroid center picture which can reveal the size of spheroids and differentiation in the core was taken for evaluation (Fig. 1F). Immunofluorescence staining confirmed the spheroids started to undergo differentiation after one week and lipid droplets accumulated from the surface to the core. Mature brown-like adipocytes expressing UCP1 increased at the same time. Interestingly, the pattern of UCP1 expressing adipocytes was different in MSC3-RA and 19-9-11T adipospheres. Together, these data show that ULA-plate formed MSC3-RA and 19-9-11T spheroids are able to differentiate into hiPSC-brown-like adipospheres from the surface to the core.

Adiospheres formed in ultra low attachment plates or by the hanging drop method display a similar adipogenic capacity

The hanging-drop technique, which could generate defined sizes of spheroids, was initially developed for cultivating embryonic stem cell embryoid bodies. It has been previously shown that the number of cells forming the bodies plays a role in the commitment of stem cells toward specific lineages. But labor intensity and massive production could be a hammer for application of this technique. On the other hand, spheroids have limited diffusion of many molecules, especially O₂, which leads to metabolic waste accumulation (Curcio et al., 2005). Spheroids with size over 500 μm in diameter commonly have a necrotic core (Alvarez-Pérez et al., 2005). With our method, spheroids self organized in ultra-low adherent (ULA) plate, we can form 100-150 spheroids in one well of 24 well plate with 10⁶ cells. The most spheroids have sizes between 100 μm-200 μm. To determine if defined sizes are critical for spheroids formation, we first tested extracellular matrix (ECM) formed either by hanging drop or in ULA plate. ECM is well known for its ability to support the structure of organs and tissues, provide the basement membrane for cell layers, and contribute to migration for individual cells (Hynes, 2009), which have effects on spheroids formation and differentiation. We formed spheroids by hanging-drop with 2000 -20000 cells/drop or in ULA plates as describe above. The staining showed the presence of ECM proteins both on the surface and in the core of the spheroids after the formation of spheroids (Fig. 2A). Staining increased after 24 days of differentiation, indicating that the spheroids are secreting their own ECM over time (Fig. 2B). Moreover, the two methods displayed similar patterns on ECM protein expression. To investigate if defined sizes are crucial for spheroids differentiation, we formed the spheroids with hanging drop method described before, and we evaluated the differentiation at D24. We found that different sizes of spheroids showed similar lipid droplets accumulation on the surface and UCP1 expression inside of the spheroids except when the spheroids are formed with 20000 cells (Fig. 2C). Finally, the QPCR results confirmed what we observed with immunofluorescence staining (Fig 2D). Interestingly, transcript level of *Adiponectin* was not affected by the size of spheroids. Together, these results showed that the spheroids generated in ULA plates display comparable pattern regarding to ECM and brown-like adipogenesis, despite the sizes are not defined.

Adiospheres enhanced brown-like adipogenesis compared to monolayer cell differentiation

Cells are classically grown as two-dimension (2D) monolayer, which poorly reflects the *in vivo* situation as adipose tissue exhibits a complex architecture. Three dimension (3D) cell culture associated with the cell self-assembly property of stem cells appear as major advance in culture processes since they offer new tissue-like models tightly related to the *in vivo* context. The formation of spheroids enables cells to form micro-networks and to interact under natural forces. To evaluate whether differentiating adipocytes in 3D would increase brown-like adipogenesis compared to 2D culture, MSC3-RA and 19-9-11T cells were first maintained in proliferation in 2D condition, and then, seeded either into ULA plate (3D) or regular culture plates (2D). Three days later, spheroids were formed in ULA plates and monolayer cells in 2D reached confluence. Differentiation was induced at that time with the same differentiation cocktail, and the protein level of Perilipin1 and UCP1 were analyzed at different time points. As shown, their levels of expression were promoted in 3D condition (Fig. 3A). Immunofluorescence staining showed that increased lipid droplet formation and UCP1 expressing cells are more in 3D conditions (Fig. 3B). Transcription factors that regulate beige and brown adipocyte development, such as *Cidea* also has an increased gene expression compared to 2D condition (Fig. 3C-D). Moreover, we found that brown-like adipospheres encoded more secreted factors like Adiponectin (Fig. 3C-D). These data suggest that our 3D culture model promotes accumulation of brown-like adipocytes that are more biologically active than when cells are maintained in monolayer cells during differentiation. The thermogenic activity of hiPSC-adipospheres remains to be evaluated.

hiPSC-brown-like adipospheres display similar extracellular matrix profile and GPCR gene expression compared adipospheres generated from human subcutaneous abdominal adipose progenitors

Extracellular matrix (ECM) is an important factor for adipose differentiation. The ratio between different types of collagen changes during differentiation, and limiting the amount of Collagen could inhibit differentiation. For example, Collagen IV has been shown to be crucial for pre-adipocytes differentiation (Pierleoni et al., 1998; Iyengar et al., 2005; Khan et al., 2009). In our model, hiPSC-brown-like adipospheres and human adipospheres derived from two different biopsies of abdominal fat displayed similar profile of ECM (Fig.4A). Klepac *et al* showed that twenty-one per cent of the GPCRs link to the Gq family, and inhibition of Gq signalling enhances differentiation of human and murine brown adipocytes (Klepac et al., 2015). Therefore, we compared expression of some GPCR in hiPSC-brown-like adipospheres to that of human adipospheres derived from abdominal fat. We found that similar GPCR

profile in all the cell types (Fig.4B). Interestingly, hiPSC-brown-like adipospheres expressed more UCP1 than subcutaneous abdominal adipospheres. Human APs derived from primary culture of subcutaneous abdominal stromal vascular fraction accurately mirror adipogenic regulatory pathways and are prone for beiging. But they can be studied only for short periods of time before they reach senescence and differentiation failure. These issues preclude reproducible *in vitro* assays and their extensive expansion for cell-based therapy. On the other hand, hiPSC-BAPs display a quasi-unlimited self-renewal capacity, and as we shows the differentiation potential is comparable to human APs derived from abdominal. Therefore, hiPSC-BAPs appears as a novel and promissing tool in the field of obesity. To determine if hiPSC-brown-like adipospheres has more capability to counteract obesity, we investigated the transcript level ratio of *UCP1* and *Perilipin1* in differentiated adipospheres. We induced the differentiation in 3D of two cell lines from hiPSC-BAPs (MSC3-RA and 19-9-11T) and of human adult APs derived from two abdominal biopsies (Abdominal-06/02/12 and Abdominal-17/12/12). Then, *UCP1/Perilipin1* ratio was analyzed at the end of differentiation. Even though Abdominal-17/12/12 fully differentiated, no *UCP1* expression was detectable. In abdominal-06/02/12, we found *UCP1* expression after fully differentiation, but at a lower extend compared to MSC3-RA and 19-9-11T (Fig. 4C). Consistent with the QPCR data, we found same profile displayed in immunofluorescence staining and ratio of UCP1 positive cells was also quantified (Fig. 4D-E). Furthermore, to determine the secretion function of adipospheres, the expression of *Adiponectin*, *FGF21* and *leptin* are also evaluated in four cell types (Fig. 4F). Adipospheres derived from hiPSC express less Adiponectin compared to those derived from abdominal, and leptin can be only detected in one of the abdominal biopsies. Interestingly, FGF21, known as a BAT-derived endocrine factor, which is associated in enhancing systemic metabolism and BAT activation, can be detected more in adipospheres derived from hiPSC.

Altogether, these data demonstrate that hiPSC-brown-like adipospheres have a similar profile of ECM and G Protein-Coupled Receptors (GPCRs) compared with human adipospheres derived from abdominal, suggesting the physiological relevance of the model. In addition, hiPSC-brown-like adipospheres display a more brown-like adipogenic potential that abdominal adipospheres which opening the opportunity of using hiPSC-brown-like adipospheres advantages for anti-obesity drug testing and cell based therapy to increase the BA mass in patients.

hiPSC-brown-like adipospheres respond to small molecules activating UCP1

3',5' -Cyclic Adenosine Monophosphate (cAMP) plays an important role in brown adipocytes, which activates lipolysis, glucose uptake, and thermogenesis (Chernogubova et al., 2004). In murine brown adipocytes differentiation, cAMP signaling increases expression of thermogenesis regulators as well as transcription factors involved in early stage of differentiation (Fredriksson et al., 2000). 3',5' -cyclic guanosine monophosphate (cGMP) has similar functions like cAMP. cGMP signaling is involved in normal adipogenesis and BAT-mediated thermogenesis in mice (Bordicchia et al., 2012). The response to the *in vivo* cold-induced browning could be mimicked by using cAMP and cGMP analogs *in vitro* (Bronnikov et al., 1992). To this end, we stimulated differentiated hiPSC-brown-like adipospheres MSC3-RA with cAMP and cGMP analogs respectively for 3 days to investigate if our 3D models could be able to respond to physiological stimulators. Western blot and immunofluorescence staining both indicated that cAMP and cGMP analogs triggered the expression of UCP1, whereas the expression of Perilipin1, was not modified after the acute stimulation in beige adipospheres generated with MSC3-RA (Fig 5A-D). Moreover, we did chronic stimulation with cAMP and cGMP analogs along the differentiation in MSC3-RA adipospheres. The differentiation was inhibited when cAMP was chronically treated, whereas increased when cGMP was chronically treated, suggesting cAMP and cGMP signaling stimulation display different manners (Fig.5E-H). These data showed that hiPSC-brown-like adipospheres can respond to the stimulation of cAMP and cGMP acutely and chronically, which indicating that our 3D models have the potential to respond to thermogenic activators.

Generation and characterization of vascularized hiPSC-brown-like adipospheres

In human adipose tissue, the vasculature is necessary for adipocyte function. *In vivo*, adipocytes have close contact with the endothelial cells (ECs) nearby which allow the blood flow so that nutrients, oxygen, growth factors, hormones, cytokines and so on can be fetched for AT homeostasis (Cao, 2013). Vascularization is associated in the process of white adipocytes browning (Wang et al., 2017). Recently, a paper has reported the bidirectional interaction between ECs and adipocytes, showing that ECs secrete the ligand for activating PPAR γ in adipocytes (Gogg et al., 2019). Therefore, vascularization is an important parameter for generating a functional 3D model to mimic *in vivo* condition. In addition, enrichment of adipospheres with ECs should improve their grafting. To this end, we aimed to develop a functional 3D model with hiPSC-BAPs and Human Dermal Microvascular Endothelial Cells (HDMECs) co-cultured, which would be closed as possible as the native one. Our strategy was to seed hiPSC-BAPs and HDMECs with ratio of 5-1, respectively, in

ULA plates. This ratio is closed to the *in vivo* one (according to Anne Bouloumié, Toulouse, personal communication). Then, the differentiation was induced three days after spheroids formation (Fig. 6A). Vascular endothelial growth factor (VEGF) and Fibroblast Growth Factor2 (FGF2) which are essential for HDMECs differentiation were added in the adipogenic cocktail. As the pictures showed, the spheroids containing both hiPSC-BAPs and HDMECs can be formed, and can differentiate into adipospheres (Fig. 6B). To investigate how the ECs network formed in the spheroids, we harvested the co-cultured spheroids 3 days after formation and after differentiation for 24 days. Reconstruction of immunofluorescence staining against CD31 showed that HDMECs-GFP were able to form organized vascular network into the spheroids after formation. Anti-GFP antibody was used to confirm that GFP reflects HDMECs by co-staining with CD31 (Data not shown). After differentiation, the co-cultured spheroids were well differentiated and tubular-like structures were also formed which closely resembled the morphology of blood vessels *in vivo*. These data indicate that adipogenesis and angiogenesis were both happening during the differentiation (Fig. 6C). We analysed expression of α SMA, a molecular target of PDGF produced by ECs, and investigated LDL uptake, as two markers of EC functionality. As shown in Figure 6D, α SMA was expressed along the tubular-like structure and LDL was uptake by HDMECs-GFP marked with CD31; These data suggest that , hiPSC-brown-like adipospheres and HDMECs-GFP inside are functional after differentiation (Fig. 6D-E). These data showed also that hiPSC-BAPs and HDMECs-GFP can co-culture in 3D and differentiate into vascularized hiPSC-brown-like adipospheres with functional tubulars-like structure formed inside. To determine if HDMECs-GFP could have an effect on the brown-like adipogenesis, we stained differentiated hiPSC-brown-like adipospheres alone or co-cultured brown-like-adipospheres. Immunofluorescence staining suggested that comparable differentiation capacity (Fig. 6F). QPCR results showed that there was induction of *Perilipin1* and *UCP1* in present of HDMECs-GFP in the adipospheres. The expression of *Adiponectin* was also increased because of the vascularization of adipospheres (Fig. 6H).

VEGF and FGF2 are essential for angiogenesis (Nillesen et al., 2007). To determine if our 3D model could secrete factors to support HDMECs-GFP vascularization, we removed VEGF and FGF2 during the differentiation. As pictures showed, the differentiation was not affected by the removing VEGF and FGF2, meanwhile the vascularization of HDMECs-GFP was still maintained in the adiposphere, despite the morphology is not as complete as the one adding VEGF and FGF2 (Fig.7A). Furthermore, the adipospheres can still form tubular structure

with α SMA expressing in the perivascular cells and LDL uptake (Fig.7B-C). The expression of *CD31* and α SMA are comparable in present or absent of VEGF and FGF2, confirming that the factors secreted by adipospheres are sufficient for maintenance of HDMECs-GFP vascularization. All together, these results indicated that HDMECs-GFP in the adiposphere can promote brown-like adipogenesis, and our co-cultured 3D model can secrete factors to support vascularization which mimic in vivo situation. The impact of enrichment with ECs on hiPSC-adiposphere engraftment in mice remains to be investigated.

Inhibition of *CDKN2A* to enhance hiPSC-brown-like adiposphere therapeutic potential

Genome-wide association studies (GWASs) have showed that *CDKN2A/B* locus has genetic risk influence on cardio-metabolic diseases including type 2 diabetes (T2D), which also modulates fasting insulin and insulin sensitivity in non-diabetic subjects (Hannou et al., 2015; Morris et al., 2012; Voight et al., 2010). In pancreatic beta cells and liver, glucose homeostasis can be affected by rare heterozygous loss-of-function mutations in *CDKN2A* (Pal et al., 2016). Meanwhile, decreased DNA methylation at the *CDKN2A* gene is related to develop obesity during adulthood with a higher risk (Lillycrop et al., 2017). Furthermore, *CDKN2A* deficiency protects mice against high fat diet-induced obesity, increase energy expenditure and improve insulin sensitivity (Rabhi et al., 2018). *P16*^{INK4A}, a CDK inhibitory (CDKI) protein, and *p14*^{ARF} (p19^{ARF} in mice), the p53 regulatory protein, are encoded by human *CDKN2A* locus. We participated by showing that silencing *P16* and *P14* expression during hiPSC-BAP proliferation can promote UCP1 expression in 2D (Rabhi et al., 2018). These data opened the opportunity to modify hiPSC-adipospheres to improve their therapeutic potential. To further understand how *CDKN2A* modulates *UCP1* expression in 3D, we silenced *CDKN2A* during spheroids formation. *P16* and *p14* mRNA levels were significantly reduced in *CDKN2A* siRNA transfected spheroids and adipospheres (Fig. 8A). Meanwhile, mRNA levels of *Perilipin1* and *UCP1* started to appear at D10 with a strong increase in *CDKN2A*-deficient hiPSC-brown-like adipospheres at D17 (Fig. 8B). Moreover, *Dio2* transcriptional level was dramatically decreased at D0 upon *CDKN2A* silencing. These data suggest that *CDKN2A* play an important role in brown-like adipogenic recruitment and maturation. Furthermore, the molecular mechanisms by which *CDKN2A* enhance hiPSC-adiposphere adipogenesis, and the consequences on their therapeutic potential remain to be investigated.

Discussion

To date the marketed drugs for BAs activation showed limited efficacy and/or displayed substantial adverse effects. Among the reasons involved in this weak efficacy, one can mention the limitation of the cell models used. Because of the rareness of BAs in adult humans, the cellular models mainly used for drug discovery are murine or human immortalized cell lines. They do not provide relevant models and do not accurately mirror human adipogenic regulatory pathways (Lindroos et al. 2013). Human iPSCs can be cultured for long term and expanded into large numbers under complete defined conditions. Nevertheless, the use of iPSC-derived cells in clinic has been approved by the FDA for at least two diseases, for iPSC-myogenic progenitors to be delivered to muscular dystrophic patients and phase I/II results are showing promising safety data as well as possible efficacy when used in ocular diseases. Recently, we generated BAPs drives from human iPSC which can be induced to differentiate into brown-like adipocytes. Therefore, we propose the use of iPSC-BAs in the obesity field for autologous transplantation to increase BAs mass in patients and anti-obesity drug screening.

In an effort to improve the physiological relevance of *in vitro* studies, 3D culture technologies and bioengineering methods are attracting a huge interest for the development of microenvironments mimicking the natural ones (Langhans 2018; Liu et al. 2018; Takebe et al. 2017). Proposed approaches allow either the fabrication of artificial scaffolds acting as a mechanical support for soft tissues or the direct printing of cells or organoids seeded within an extracellular matrix. Although 3D system has been used in a variety approaches in attempt to generate adipose tissue-like structures (Abbott et al., 2016; Zhang et al., 2017; Louis et al., 2017), most of these systems do not generate purely cellular models that are in large scale without use of exogenous scaffolding material. While promising, couldn't create tissue-like structures that mimic *in vivo* situation, like secretory function, response to micro environment or histological morphology of native adipose tissue.

Although human adipose spheroids have been generated (Klingelutz et al., 2018, Yang et al., 2017), vascularization was lacked. Abundant literature has already showed there is bi-directional interaction between ECs and APs, including vasculogenesis promoting and modulated secretion of cytokines and ECM proteins (Merfeld-Clauss et al., 2010). Traktuev et al also demonstrated APs can cooperate with ECs to coassemble vessels *in vivo* implants

(Traktuev et al., 2009). Moreover, in mice, proper angiogenesis are mandatory for the development of adipose tissue and vasculature may provide a niche supporting both brown and white APs (Han et al., 2011, Sanchez-Gurmaches and Guertin, 2014). As hiPSCs can differentiate into cells present in the adipose tissue, BA adipospheres could be enriched with endothelial cells (ECs) to mimic an adipose-like structure and to improve their therapeutic potential. Endothelial growth media supports hiPSC-BAPs differentiation, suggesting the feasibility to coculture BA adipospheres with ECs. Pre-vascularized organoids derived from hiPSCs have been generated including the liver, skeletal, and cardiac muscle. All constructs show incorporation into vascular network and a better viability of the graft after transplantation in animal models (Caspi et al. 2007; Takebe et al. 2013). Therefore, preserving ECs within 3D adipospheres can better mimic in vivo situation and promote bio-activities of adipospheres.

To overcome the challenges and shortcomings described above, we developed a scaffold-free approach to generate spheroids in large scale that can differentiate into adipospheres which mimic native adipocytes. We generated BA adipospheres from two different hiPSC-BAP clones, which are able to fully differentiate from the surface to the core. We compared hiPSC-brown-like adipospheres with the ones generated by hanging drop method, and our model displays comparable pattern regarding to extracellular matrix and adipogenesis, despite the sizes are not defined. We also proved that hiPSC-brown-like adipospheres promote accumulation of brown-like adipocytes that are more biologically active compared to cells maintained in conventional monolayer cell cultures. In addition, hiPSC-brown-like adipospheres have a similar expression profile of extracellular matrix and G Protein-Coupled Receptors (GPCRs) compared with human adipospheres derived from sub cutaneous abdominal adipose progenitors, suggested the physiological relevance of the hiPSC-adiposphere model. Moreover, hiPSC-adipospheres display a more brown-like adipogenic potential than abdominal adipospheres opening the opportunity and advantages for anti-obesity drug testing and cell based therapy to increase the BA mass in patients. Furthermore, hiPSC- adipospheres express UCP1 that can response to the stimulation of 8-CPT-cAMP or 8-Br-cGMP acutely and chronically, which indicated that our 3D model display metabolic characteristics of brown-like adipocytes. Finally, enrichment with HDMECs-GFP was performed via co culture in suspension. HDMECs-GFP functionality was tested in vitro by LDL-uptake and expression of α SMA a marker of pericytes. We proved that hiPSC-BAPs and HDMECs-GFP can co-culture in 3D and differentiate into vascularized hiPSC-brown-like

adipospheres with functional tubular-like structure formed inside. Moreover, our co-cultured 3D model can secrete factors to support vascularization which mimic in vivo situation.

All together, we use expandable BAPs from hiPSCs to develop a robust and easy 3D culture condition to generate self-assembled adipospheres in large scale which will be a physiological model for drug screening and for cell based-therapy. Furthermore, we improve the model with the enrichment of adipospheres with endothelial cells to better mimic vascularization of adipocytes in vivo which will also offers a critical advantage for transplantation purposes.

Numerous other issues have also to be solved before a therapeutic use of iPSCs in the obesity field, but the derivation of BAPs having a high level of differentiation without gene transfer and their capacity to form 3D adipospheres open the opportunity of using hiPSCs advantages for anti-obesity therapy and for a better understanding of the interactions between different cell types of adipose tissue for BAs recruitment and activation.

Figure legends

Fig 1. ULA-plate formed hiPSC-BAP spheroids can be formed and differentiated into hiPSC-brown-like adipospheres in suspension

- A. A schematic of spheroid formation in ultra-low adherent well.
- B. Photographs of MSC3-RA and 19-9-11T spheroids after 3 days of formation.
- C. Phase-contrast images of MSC3-RA and 19-9-11T spheroids plated in ultra-low adherent well over 20 days in adipocyte differentiation medium revealing differentiation.
- D. Schematic diagram illustrating the differentiation protocol used for adipogenic differentiation.
- E. Oil Red O staining on surface reconstruction of MSC3-RA and 19-9-11T spheroids following the differentiation. Oil Red O (Red), DAPI (Blue). Scale bars represent 50 μ m or 16.67 μ m.
- F. Immunofluorescence staining of Perilipin1 (Red), UCP1 (Green) and DAPI (Blue) of MSC3-RA and 19-9-11T spheroids following the differentiation after clearing. The core pictures were taken for representing. Scale bars represent 50 μ m or 16.67 μ m.

Fig 2. Comparison between adipospheres formed in ULA plates and hanging drop method

- A. Immunofluorescence staining of Collagen I, Collagen IV, Laminin, Elastin, Fibronectin (Green) and DAPI(Blue) in spheroids generated by ULA plate and hanging drop method with 2000-20000 cells/ drop at D0 after clearing. Scale bars represent 50 μ m or 16.67 μ m.
- B. Immunofluorescence staining of Collagen I, Collagen IV, Laminin, Elastin, Fibronectin (Green) and Perilipin1 (Red) in spheroids generated by ULA plate and hanging drop methods with 2000-20000 cells/ drop at D24 after clearing. Scale bars represent 50 μ m or 16.67 μ m.
- C. Surface construction after Oil Red O staining and core pictures after immunofluorescence staining with clearing of Perilipin1 (Red) , UCP1 (Green) and DAPI (Blue) in adipospheres generated by hanging drop with 2000-20000 cells/ drop D24. Scale bars=50 μ m.
- D. QPCR analysis of *Perilipin1*, *UCP1* and *Adiponectin* in adipospheres generated by hanging drop with 2000-20000 cells/ drop at D24.

Fig 3. 2D and 3D differentiation comparison in MSC3-RA and 19-9-11T

- A. Protein expression kinetics of MSC3-RA and 19-9-11T during differentiation into adipocytes both in 2D and 3D conditions, as determined by western blot. Tubulin serves as a loading control.
- B. Immunofluorescence staining of MSC3-RA and 19-9-11T in 2D and 3D (after clearing) conditions with antibodies against UCP1 (green) and Perilipin1 (red). DAPI is blue. Scale bar=50 μ m.
- C. QPCR analysis of *Perilipin1*, *UCP*, *Cidea* and *Adiponectin* in MSC3-RA after 24 days of differentiation both in 2D and 3D conditions. Values are means \pm SEM. n = 3. *means p < 0.05 and **means p < 0.01.
- D. QPCR analysis of *Perilipin1*, *UCP*, *Cidea* and *Adiponectin* in 19-9-11T after 24 days of differentiation both in 2D and 3D conditions. Values are means \pm SEM. n = 3. *means p < 0.05 and **means p < 0.01.

Fig 4. Adipospheres generated with hiPSC-BAPs or human abdominals display similar gene expression

- A. Surface reconstruction and crops of Immunofluorescence staining and Oil Red O(Red), in adipospheres generated with hiPSC-BAPs (MSC3-RA and 19-9-11T) and human abdominals (Abdominal-06/02/12 and Abdominal-17/12/12) after differentiation 24 days or 17 days, respectively. DAPI(Blue), CollagenI(Green), CollagenIV(Green), Fibronectin(Green), Lamini (Green)and Elastin(Green). Scale bar=50 μ m. Scale bars represent 50 μ m or 16.67 μ m.
- B. GPCR expression of adipospheres generated with hiPSC-BAPs (MSC3-RA and 19-9-11T) and human abdominals (Abdominal-06/02/12 and Abdominal-17/12/12) after differentiation 24 days or 17 days, respectively. Values are means \pm SEM. n = 3. *means p < 0.05 and **means p < 0.01.
- C. QPCR analysis of *UCP1* and *Perilipin1*, and ratio of *UCP1* against *Perilipin1* of adipospheres generated with hiPSC-BAPs (MSC3-RA and 19-9-11T) and human abdominals (Abdominal-06/02/12 and Abdominal-17/12/12) after differentiation 24 days or 17 days, respectively. Values are means \pm SEM. n = 3. *means p < 0.05 and **means p < 0.01.
- D. Immunofluorescence staining of adipospheres generated with hiPSC-BAPs (MSC3-RA and 19-9-11T) and human abdominals (Abdominal-06/02/12 and Abdominal-17/12/12) after differentiation for 24 days, (after clearing) conditions with antibodies against UCP1 (green) and Perilipin1 (red). DAPI is blue. Scale bar=50 μ m.
- E. Quantification of UCP1 positive cells in immunofluorescence staining of adipospheres generated with hiPSC-BAPs (MSC3-RA and 19-9-11T) and human abdominals (Abdominal-06/02/12 and Abdominal-17/12/12) after differentiation for 24 days or 17 days, respectively (n=3).

F. QPCR analysis of Adiponectin, FGF21 and Leptin of adipospheres generated with hiPSC-BAPs (MSC3-RA and 19-9-11T) and human abdominals (Abdominal-06/02/12 and Abdominal-17/12/12) after differentiation 24 days or 17 days, respectively. Values are means \pm SEM. n = 3. *means $p < 0.05$ and **means $p < 0.01$.

Fig 5. hiPSC-brown-like adipospheres can response to cAMP and cGMP stimulation acutely and chronically

A. Immunofluorescence staining after 3 days stimulation of cAMP or cGMP analogs in adipospheres generated with MSC3-RA at 24 days (after clearing) conditions with antibodies against UCP1 (green) and Perilipin1 (red). DAPI is blue. Scale bar=50 μ m.

B. Protein expression of Perilipin1 and UCP1 after 3 days stimulation of cAMP or cGMP analogs in adipospheres generated with MSC3-RA at 24 days. Tubulin serves as a loading control.

C. Quantification of UCP1 positive cells in immunofluorescence staining after 3 days stimulation of cAMP or cGMP analogs in adipospheres generated with MSC3-RA at 24 days (n=3).

D. Protein quantification of UCP1 against Tubulin after 3 days stimulation of cAMP or cGMP analogs in adipospheres generated with MSC3-RA at 24 days (n=3).

E. Immunofluorescence staining after chronic stimulation of cAMP or cGMP analogs in adipospheres generated with MSC3-RA along the differentiation until 24 days (after clearing) conditions with antibodies against UCP1 (green) and Perilipin1 (red). DAPI is blue. Scale bar=50 μ m.

F. Protein expression of Perilipin1 and UCP1 after chronic stimulation of cAMP or cGMP analogs in adipospheres generated with MSC3-RA along the differentiation until 24 days. Tubulin serves as a loading control.

G. Quantification of UCP1 positive cells in immunofluorescence staining after chronic stimulation of cAMP or cGMP analogs in adipospheres generated with MSC3-RA along the differentiation until 24 days (n=3).

H. Protein quantification of UCP1 against Tubulin after chronic stimulation of cAMP or cGMP analogs in adipospheres generated with MSC3-RA along the differentiation until 24 days (n=3).

Fig 6. HDMECs enriched in hiPSC-brown-like adipospheres are functional

A. A schematic of hiPSC-BAP and HDMECs co-cultured spheroid formation in ultra-low adherent well.

B. Phase-contrast images of hiPSC-BAPs and HDMECs-GFP co-cultured spheroids after 3 days of formation and after 24 days of differentiation.

C. Reconstruction after Immunofluorescence staining of MSC3-RA cocultured with HDMECs-GFP by the ratio of 5:0 or 5:1 undifferentiated and differentiated (after clearing) with antibodies against CD31 (green) and Perilipin1 (red). DAPI is blue. Scale bar=50 μ m.

D. Immunofluorescence staining of MSC3-RA cocultured with HDMECs-GFP by the ratio of 5:0 or 5:1 after 24 days of differentiation (after clearing) with antibodies against α SMA(green), Perilipin1 (red) and GFP(grey). DAPI is blue. Scale bar=50 μ m. Reconstruction and one core picture as representative.

E. Immunofluorescence staining of LDL uptake in MSC3-RA cocultured with HDMECs-GFP (5:1) after 24 days of differentiation (after clearing) with antibodies against CD31 (green). LDL-Dylight (Red), DAPI (blue). Scale bars represent 50 μ m or 10 μ m as indicated.

F. Immunofluorescence staining of MSC3-RA co-cultured with HDMECs by the ratio of 5:0 or 5:1 after 24 days of differentiation with antibodies against UCP1 (green), Perilipin1 (red) and CD31 (grey). DAPI is blue. Scale bar=50 μ m.

G. QPCR analysis of *Perilipin1*, *UCP1* and *Adiponectin* of adipospheres generated with MSC3-RA cocultured with HDMECs-GFP by the ratio of 5:0 or 5:1 after differentiation 24 days. Values are means \pm SEM. n = 3. *means $p < 0.05$ and **means $p < 0.01$.

Fig 7. hiPSC-brown-like adipospheres can secrete factors to maintain HDMECs vascularization

A. Immunofluorescence staining of MSC3-RA cocultured with HDMECs-GFP (5:1) with or without VEGF and FGF2 after 24 days of differentiation (after clearing) with antibodies against UCP1 (green), Perilipin1 (red) and CD31 (grey). DAPI is blue. Scale bar=50 μ m.

B. Immunofluorescence staining of MSC3-RA cocultured with HDMECs-GFP (5:1) without VEGF and FGF2 after 24 days of differentiation (after clearing) with antibodies against CD31 (green), LDL-Dylight (Red), DAPI (blue). Scale bars represent 50 μ m or 10 μ m as indicated.

C. Immunofluorescence staining of MSC3-RA cocultured with HDMECs-GFP (5:1) without VEGF and FGF2 after 24 days of differentiation (after clearing) with antibodies against α SMA (green), Perilipin1 (red) and GFP (grey). DAPI is blue. Scale bars represent 50 μ m or 10 μ m as indicated.

D. QPCR analysis of *CD31* and *αSMA* of adipospheres generated with MSC3-RA cocultured with HDMECs-GFP by the ratio of 5:1 after differentiation 24 days with or without VEGF and FGF2. Values are means ± SEM. n = 3. *means p < 0.05 and **means p < 0.01.

Fig 8. Silencing *CDKN2A* in hiPSC-brown-like adipospheres induces UCP1 expression.

A. qPCR analysis of *p16* and *p14* expression kinetics in control or *CDKN2A* silenced hiPSC-brown-like adipospheres (n=3). Values are means ± SEM. n = 3. *means p < 0.05 and **means p < 0.01.

B. qPCR analysis of *Perilipin1*, *UCP1* and *Dio2* expression kinetics in control or *CDKN2A* silenced hiPSC-brown-like adipospheres. Values are means ± SEM. n = 3. *means p < 0.05 and **means p < 0.01.

Figure.1

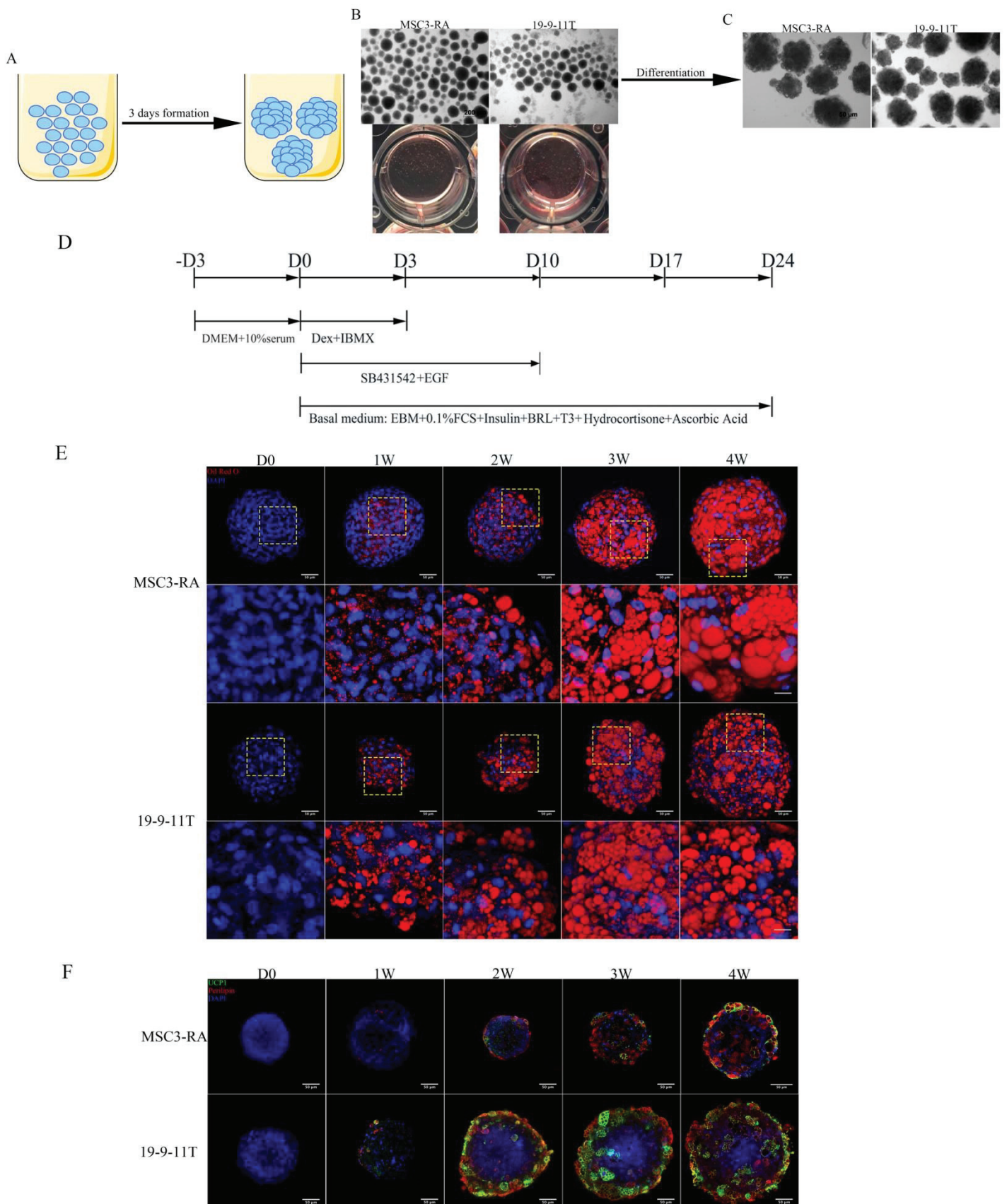
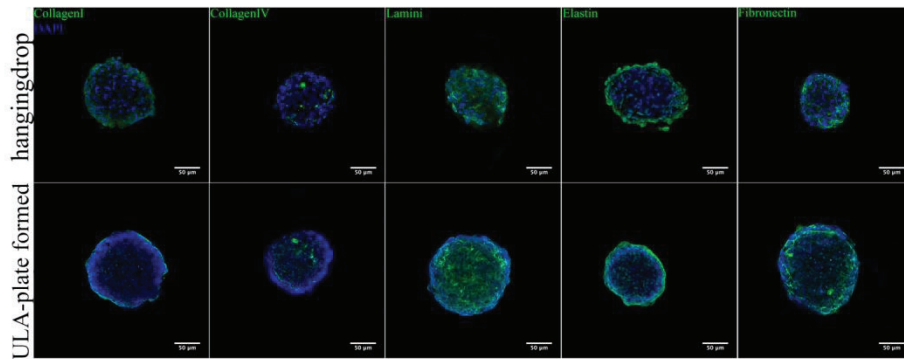
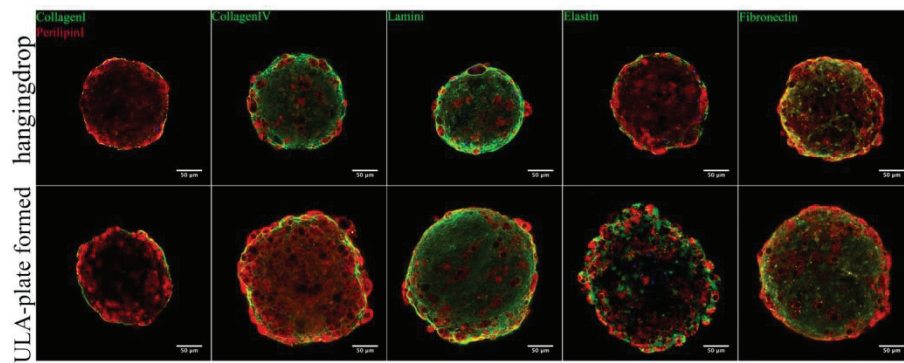


Figure.2

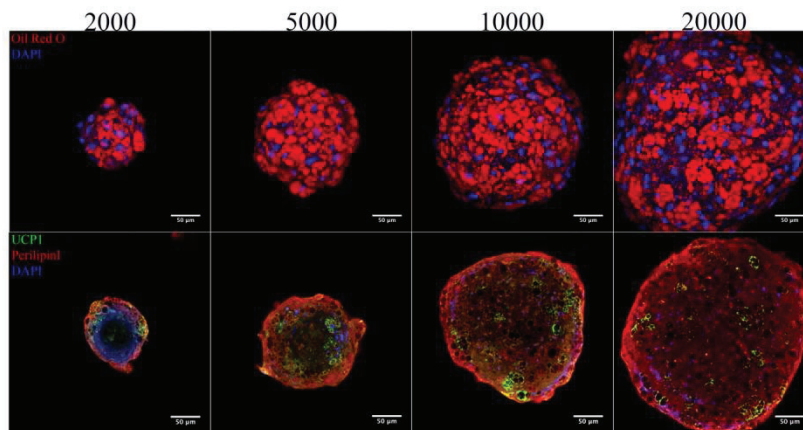
A



B



C



D

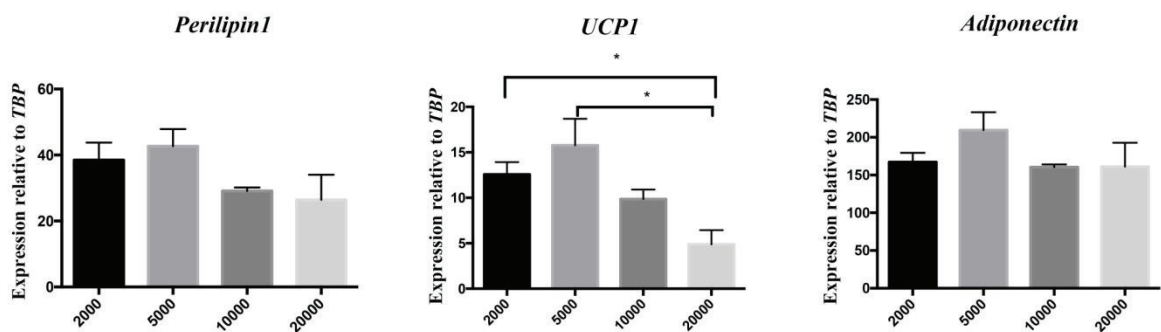


Figure.3

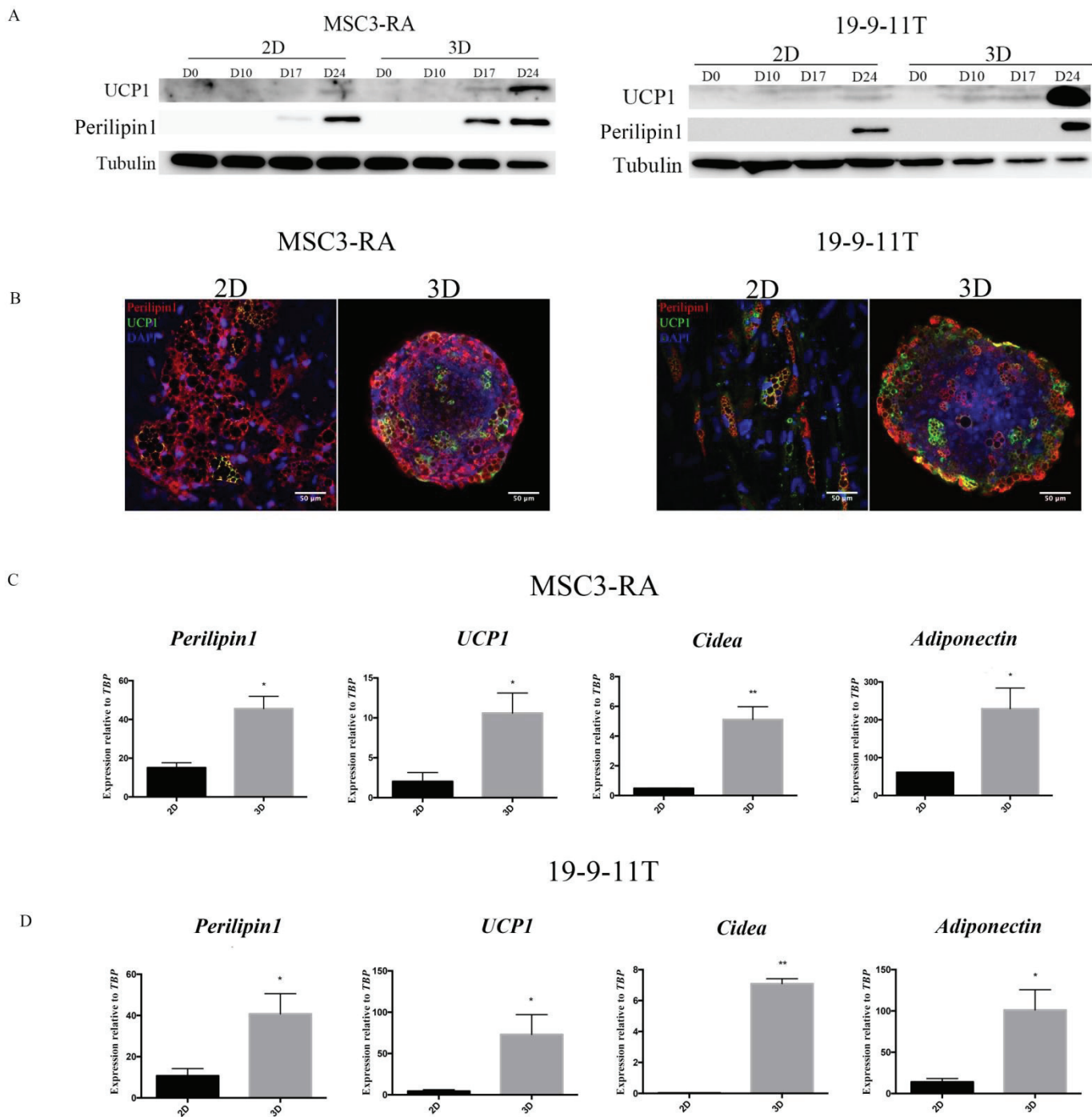


Figure.4

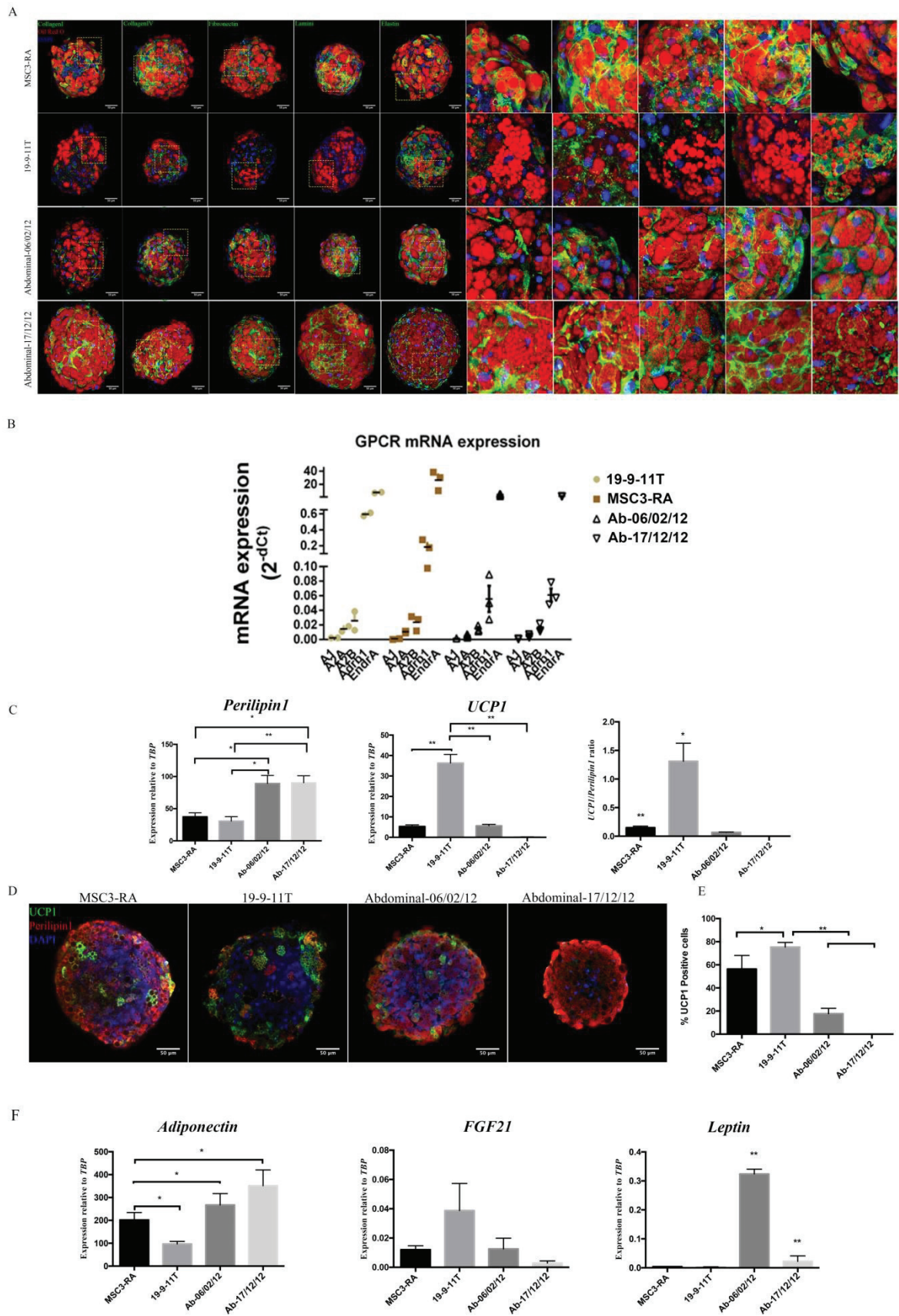


Figure.5

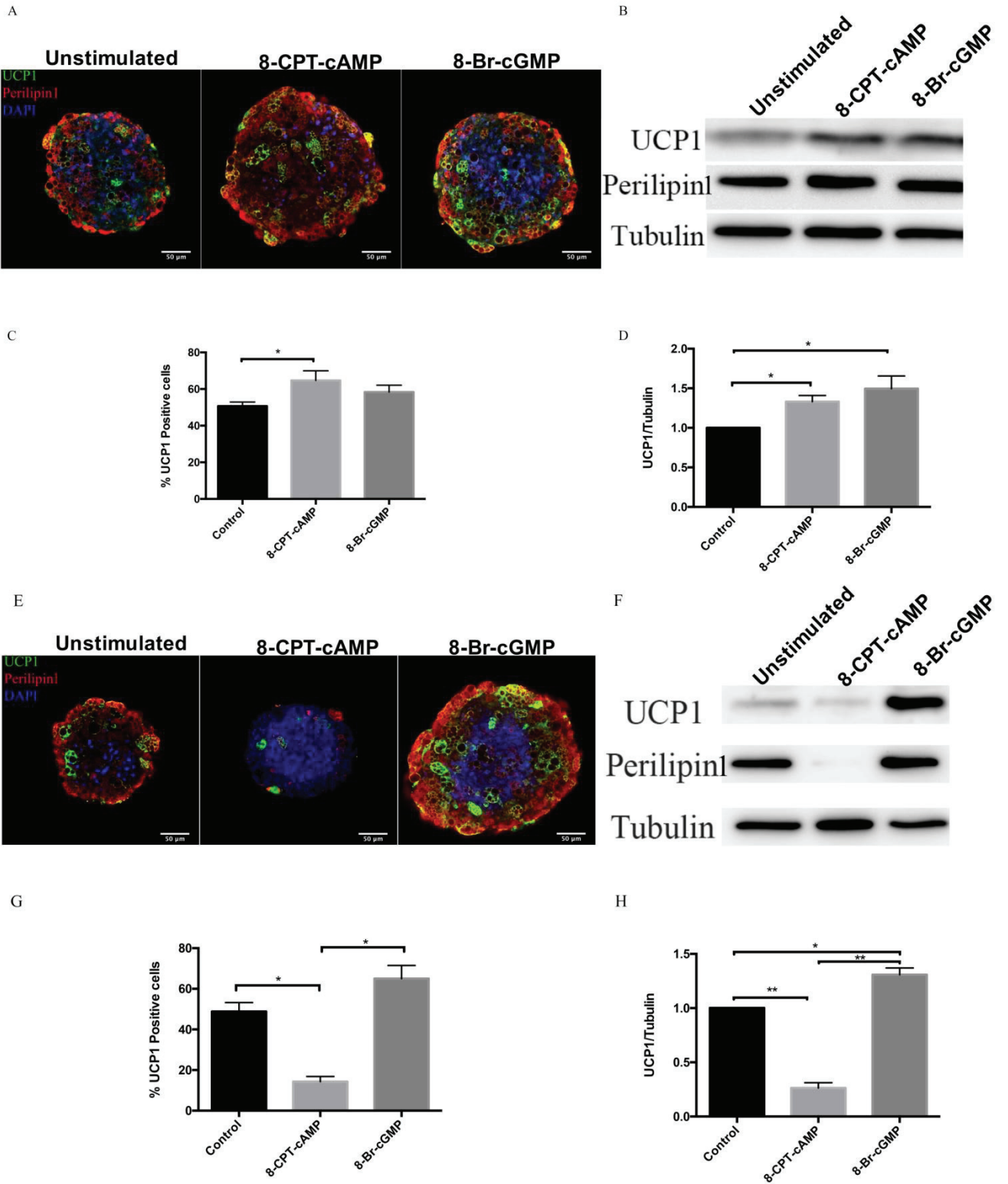


Figure.6

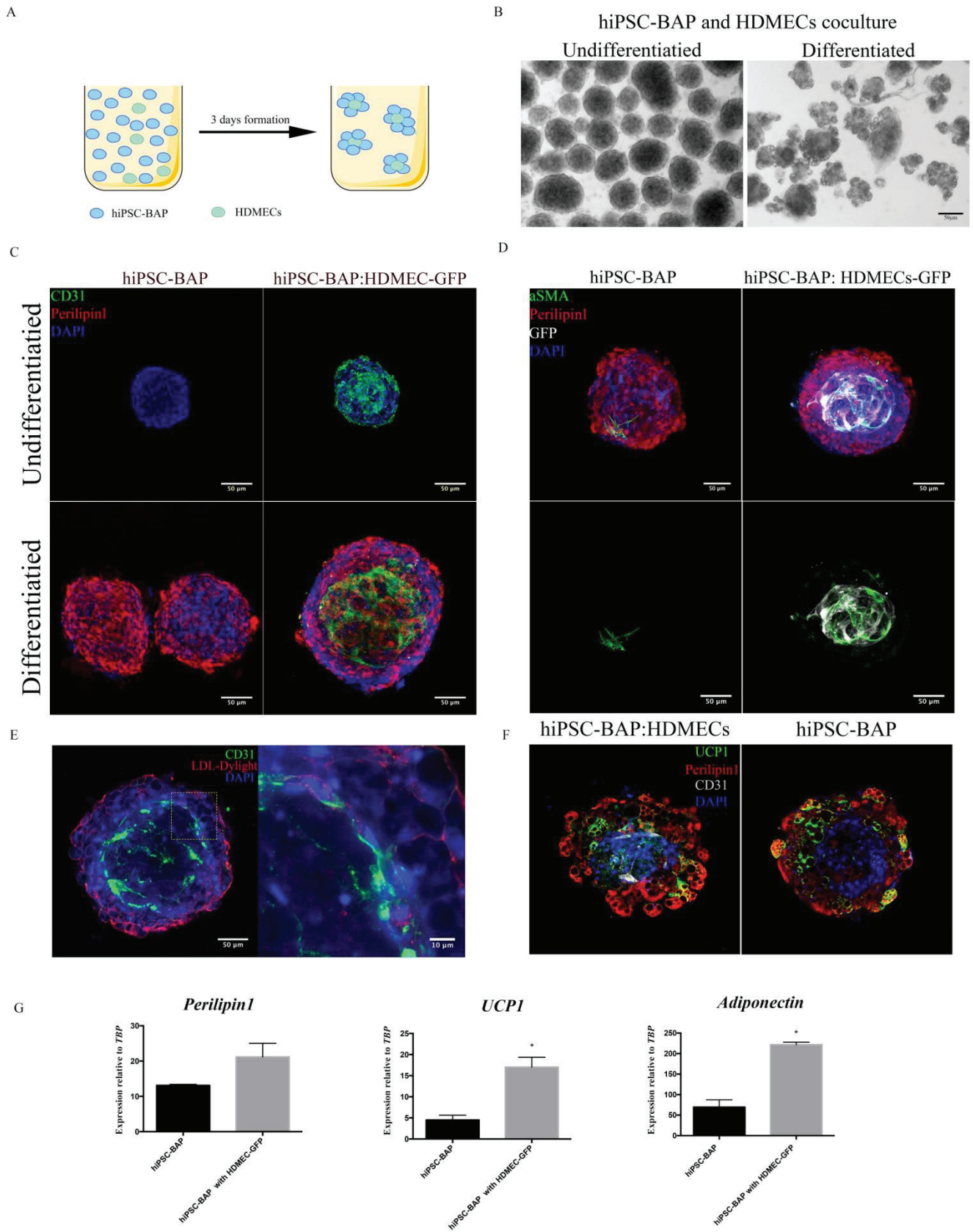


Figure.7

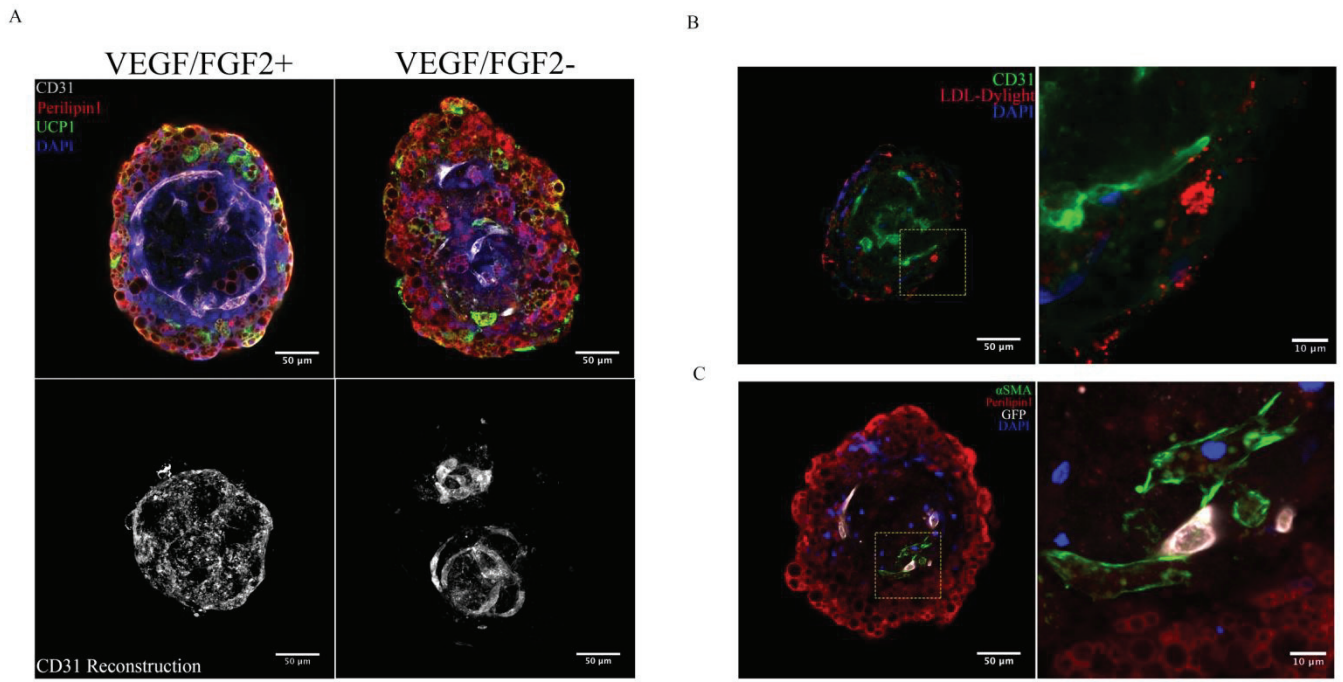


Figure.8

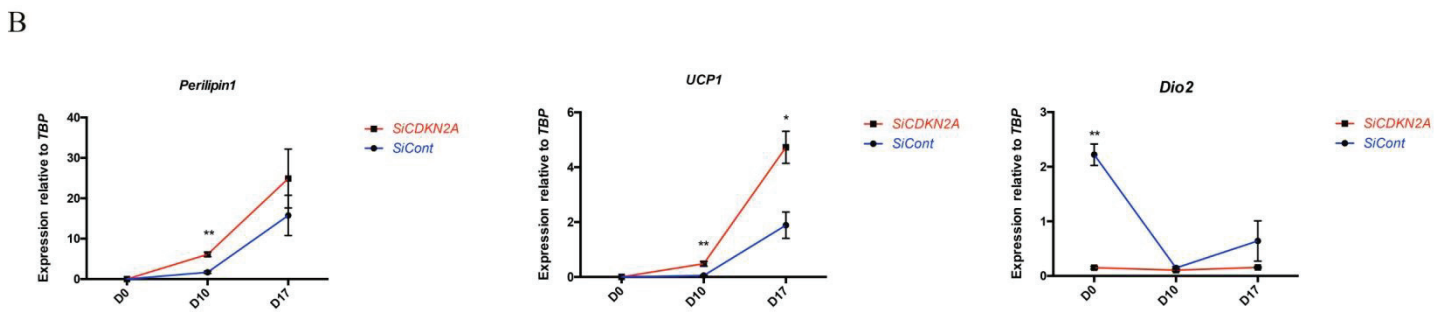
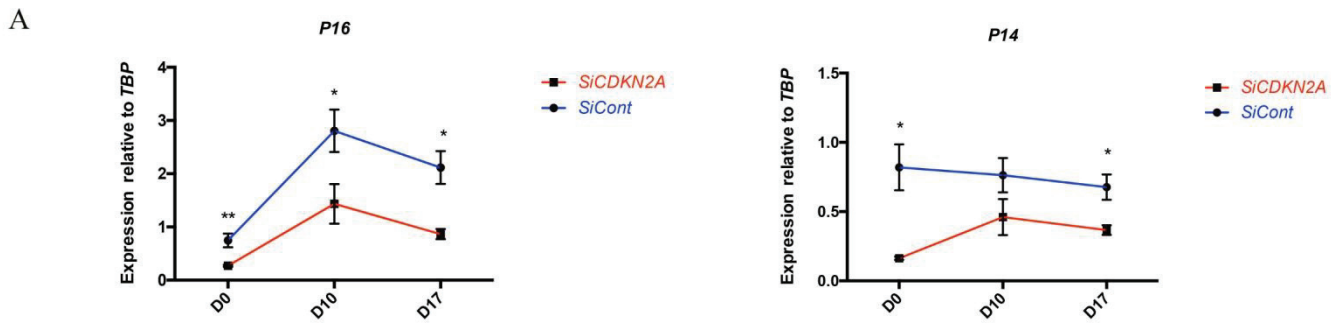


Table S1

ANTIBODY	MANUFACTURER	CATALOG NUMBER
Perilipin1	ACRIS Gmbh	#BP5015
UCP1	Abcam	#ab10983
α SMA	Sigma	#F3777
CD31	DAKO	#JC70A
GFP	ThermoFisher	#A-11122
Collagen I	Sigma	#SAB4500362
Collagen IV	Abcam	#ab6586
Lamini	Abcam	#ab11575
Elastin	Abcam	#ab21610
Fibronectin	Santa Cruz Biothechnology	#SC8422

Table S2

Sequences for the primers used in this study

Gene	Forward primer	Reverse primer
<i>PLIN1</i>	5'-ACCATCTCCACCCGCCTC-3'	5'-GATGGGAACGCTGATGCTGT-3'
<i>UCP1</i>	5'-GTGTGCCCAACTGTGCAATG-3'	5'-CCAGGATCCAAGTCGCAAGA-3'
<i>TBP</i>	5'-ACGCCAGCTTCGGAGAGTTC-3'	5'-CAAACCGCTTGGGATTATATTCG-3'
<i>Adiponectin</i>	5'-GCAGTCTGTGGTTCTGATTCCATAC-3'	5'-GCCCTTGAGTCGTGGTTTCC-3'
<i>Leptin</i>	5'-AGGGAGACCGAGCGCTTTC-3'	5'-TGCATCTCCACACACCAAACC-3'
α SMA	5'-TGCCTGATGGGCAAGTGA-3'	5'-CTGGGCAGCGGAAACG-3'
<i>CD31</i>	5'-CCCACTGAAGACGTCGAATAC-3'	5'-CACCTCAGAACCTCACTTAAC-3'
<i>P16</i>	5'-GAGCAGCATGGAGCCTTC-3'	5'-GGCCTCCGACCGTAACTATT-3'
<i>P14</i>	5'-CCCTCGTGCTGATGCTACTG-3'	5'-CCATCATCATGACCTGGTCTTCT-3'
<i>DiO2</i>	5'-GTCACTGGTCAGCGTGGTTTT-3'	5'-TTCTTCACATCCCCCAATCCT-3'
<i>Cidea</i>	5'-GGCAGGTTACGTGTGGATA-3'	5'-GAAACACAGTGTGGCTCAAGA-3'

References

- Abbott, R.D., R.Y. Wang, M.R. Reagan, Y. Chen, F.E. Borowsky, A. Zieba, K.G. Marra, J.P. Rubin, I.M. Ghobrial, and D.L. Kaplan. 2016. The use of silk as a scaffold for mature, sustainable unilocular adipose 3D tissue engineered systems. *Advanced healthcare materials*. 5:1667-1677.
- Adavis, C. 1993. [31] Whole-mount immunohistochemistry. In *Methods in enzymology*. Vol. 225. Elsevier. 502-516.
- Alvarez-Pérez, J., P. Ballesteros, and S. Cerdán. 2005. Microscopic images of intraspheroidal pH by ¹H magnetic resonance chemical shift imaging of pH sensitive indicators. *Magnetic Resonance Materials in Physics, Biology and Medicine*. 18:293-301.
- Bordicchia, M., D. Liu, E.-Z. Amri, G. Ailhaud, P. Dessi-Fulgheri, C. Zhang, N. Takahashi, R. Sarzani, and S. Collins. 2012. Cardiac natriuretic peptides act via p38 MAPK to induce the brown fat thermogenic program in mouse and human adipocytes. *The Journal of clinical investigation*. 122:1022-1036.
- Bronnikov, G., J. Houstěk, and J. Nedergaard. 1992. Beta-adrenergic, cAMP-mediated stimulation of proliferation of brown fat cells in primary culture. Mediation via beta 1 but not via beta 3 adrenoceptors. *Journal of Biological Chemistry*. 267:2006-2013.
- Cao, Y. 2013. Angiogenesis and vascular functions in modulation of obesity, adipose metabolism, and insulin sensitivity. *Cell metabolism*. 18:478-489.
- Caspi, O., A. Lesman, Y. Basevitch, A. Gepstein, G. Arbel, I.H.M. Habib, L. Gepstein, and S. Levenberg. 2007. Tissue engineering of vascularized cardiac muscle from human embryonic stem cells. *Circulation research*. 100:263-272.
- Chernogubova, E., B. Cannon, and T. Bengtsson. 2004. Norepinephrine increases glucose transport in brown adipocytes via β ₃-adrenoceptors through a cAMP, PKA, and PI3-kinase-dependent pathway stimulating conventional and novel PKCs. *Endocrinology*. 145:269-280
- Curcio, E., Salerno, S., Barbieri, G., De Bartolo, L., Drioli, E. and A. Bader. 2007. Mass transfer and metabolic reactions in hepatocyte spheroids cultured in rotating wall gas-permeable membrane system. *Biomaterials*. 28, 5487-5497.
- Fredriksson, J.M., J.M. Lindquist, G.E. Bronnikov, and J. Nedergaard. 2000. Norepinephrine induces vascular endothelial growth factor gene expression in brown adipocytes through a β -adrenoreceptor/cAMP/protein kinase A pathway involving Src but independently of Erk1/2. *Journal of Biological Chemistry*. 275:13802-13811.
- Gogg, S., A. Nerstedt, J. Boren, and U. Smith. 2019. Human adipose tissue microvascular endothelial cells secrete PPAR γ ligands and regulate adipose tissue lipid uptake. *JCI insight*. 4.
- Hafner, A.-L., J. Contet, C. Ravaut, X. Yao, P. Villageois, K. Suknuntha, K. Annab, P. Peraldi, B. Binetruy, and I.I. Slukvin. 2016a. Brown-like adipose progenitors derived from human induced pluripotent stem cells: identification of critical pathways governing their adipogenic capacity. *Scientific reports*. 6:32490.
- Hafner A-L, Mohsen-Kanson T and C. Dani. 2016b. A protocol for the differentiation of brown adipose progenitors derived from human induced pluripotent stem cells at a high efficiency with no gene transfer. *Nat Protocol Exchange*. Doi: <https://doi.org/10.1038/protex.2016.067>
- Hannou, S.A., K. Wouters, R. Paumelle, and B. Staels. 2015. Functional genomics of the CDKN2A/B locus in cardiovascular and metabolic disease: what have we learned from GWASs? *Trends in Endocrinology & Metabolism*. 26:176-184.
- Hynes, R.O. 2009. The extracellular matrix: not just pretty fibrils. *Science*. 326:1216-1219.

Iyengar, P., V. Espina, T.W. Williams, Y. Lin, D. Berry, L.A. Jelicks, H. Lee, K. Temple, R. Graves, and J. Pollard. 2005. Adipocyte-derived collagen VI affects early mammary tumor progression in vivo, demonstrating a critical interaction in the tumor/stroma microenvironment. *The Journal of clinical investigation*. 115:1163-1176.

Iyengar, P., V. Espina, T.W. Williams, Y. Lin, D. Berry, L.A. Jelicks, H. Lee, K. Temple, R. Graves, and J. Pollard. 2005. Adipocyte-derived collagen VI affects early mammary tumor progression in vivo, demonstrating a critical interaction in the tumor/stroma microenvironment. *The Journal of clinical investigation*. 115:1163-1176.

Kelm, J.M., and M. Fussenegger. 2004. Microscale tissue engineering using gravity-enforced cell assembly. *Trends in biotechnology*. 22:195-202.

Khan, T., E.S. Muise, P. Iyengar, Z.V. Wang, M. Chandalia, N. Abate, B.B. Zhang, P. Bonaldo, S. Chua, and P.E. Scherer. 2009. Metabolic dysregulation and adipose tissue fibrosis: role of collagen VI. *Molecular and cellular biology*. 29:1575-1591.

Klepac, K., A. Kilić, T. Gnad, L.M. Brown, B. Herrmann, A. Wilderman, A. Balkow, A. Glöde, K. Simon, and M.E. Lidell. 2016. The G q signalling pathway inhibits brown and beige adipose tissue. *Nature communications*. 7:10895.

Klingelhutz, A.J., F.A. Gourronc, A. Chaly, D.A. Wadkins, A.J. Burand, K.R. Markan, S.O. Idiga, M. Wu, M.J. Potthoff, and J.A. Ankrum. 2018. Scaffold-free generation of uniform adipose spheroids for metabolism research and drug discovery. *Scientific reports*. 8:523.

Kouidhi, M., P. Villageois, C.M. Mounier, C. Ménigot, Y. Rival, D. Piwnica, J. Aubert, B. Chignon-Sicard, and C. Dani. 2015. Characterization of human knee and chin adipose-derived stromal cells. *Stem cells international*. 2015.

Langhans, S.A. 2018. Three-dimensional in vitro cell culture models in drug discovery and drug repositioning. *Frontiers in pharmacology*. 9:6.

Lillycrop, K., R. Murray, C. Cheong, A.L. Teh, R. Clarke-Harris, S. Barton, P. Costello, E. Garratt, E. Cook, and P. Titcombe. 2017. ANRIL promoter DNA methylation: a perinatal marker for later adiposity. *EBioMedicine*. 19:60-72.

Lindroos, J., J. Husa, G. Mitterer, A. Haschemi, S. Rauscher, R. Haas, M. Gröger, R. Loewe, N. Kohrgruber, and K.F. Schrögenderfer. 2013. Human but not mouse adipogenesis is critically dependent on LMO3. *Cell metabolism*. 18:62-74.

Liu, C., A. Oikonomopoulos, N. Sayed, and J.C. Wu. 2018. Modeling human diseases with induced pluripotent stem cells: from 2D to 3D and beyond. *Development*. 145:dev156166.

Louis, F., P. Pannetier, Z. Souguir, D. Le Cerf, P. Valet, J.P. Vannier, G. Vidal, and E. Demange. 2017. A biomimetic hydrogel functionalized with adipose ECM components as a microenvironment for the 3D culture of human and murine adipocytes. *Biotechnology and bioengineering*. 114:1813-1824.

Merfeld-Clauss, S., N. Gollahalli, K.L. March, and D.O. Traktuev. 2010. Adipose tissue progenitor cells directly interact with endothelial cells to induce vascular network formation. *Tissue Engineering Part A*. 16:2953-2966.

Mohsen-Kanson, T., A.L. Hafner, B. Wdziekonski, Y. Takashima, P. Villageois, A. Carrière, M. Svensson, C. Bagnis, B. Chignon-Sicard, and P.A. Svensson. 2014. Differentiation of human induced pluripotent stem cells into brown and white adipocytes: role of Pax3. *Stem Cells*. 32:1459-1467.

Morris, A.P., B.F. Voight, T.M. Teslovich, T. Ferreira, A.V. Segre, V. Steinthorsdottir, R.J. Strawbridge, H. Khan, H. Grallert, and A. Mahajan. 2012. Large-scale association analysis provides insights into the genetic architecture and pathophysiology of type 2 diabetes. *Nature genetics*. 44:981.

Nillesen, S.T., P.J. Geutjes, R. Wismans, J. Schalkwijk, W.F. Daamen, and T.H. van Kuppevelt. 2007. Increased angiogenesis and blood vessel maturation in acellular collagen–heparin scaffolds containing both FGF2 and VEGF. *Biomaterials*. 28:1123-1131.

Pal, A., T.P. Potjer, S.K. Thomsen, H.J. Ng, A. Barrett, R. Scharfmann, T.J. James, D.T. Bishop, F. Karpe, and I.F. Godsland. 2016. Loss-of-function mutations in the cell-cycle control gene CDKN2A impact on glucose homeostasis in humans. *Diabetes*. 65:527-533.

Pierleoni, C., F. Verdenelli, M. Castellucci, and S. Cinti. 1998. Fibronectins and basal lamina molecules expression in human subcutaneous white adipose tissue. *European journal of histochemistry: EJH*. 42:183-188.

Rabhi, N., S.A. Hannou, X. Gromada, E. Salas, X. Yao, F. Oger, C. Carney, I.C. Lopez-Mejia, E. Durand, and I. Rabearivelo. 2018. Cdkn2a deficiency promotes adipose tissue browning. *Molecular metabolism*. 8:65-76.

Rosen, E.D., and B.M. Spiegelman. 2014. What we talk about when we talk about fat. *Cell*. 156:20-44.

Takebe, T., K. Sekine, M. Enomura, H. Koike, M. Kimura, T. Ogaeri, R.-R. Zhang, Y. Ueno, Y.-W. Zheng, and N. Koike. 2013. Vascularized and functional human liver from an iPSC-derived organ bud transplant. *Nature*. 499:481.

Takebe, T., B. Zhang, and M. Radisic. 2017. Synergistic engineering: organoids meet organs-on-a-chip. *Cell Stem Cell*. 21:297-300.

Traktuev, D.O., D.N. Prater, S. Merfeld-Clauss, A.R. Sanjeevaiah, M.R. Saadatizadeh, M. Murphy, B.H. Johnstone, D.A. Ingram, and K.L. March. 2009. Robust functional vascular network formation in vivo by cooperation of adipose progenitor and endothelial cells. *Circulation research*. 104:1410-1420.

Vodyanik, M.A., J. Yu, X. Zhang, S. Tian, R. Stewart, J.A. Thomson, and I.I. Slukvin. 2010. A mesoderm-derived precursor for mesenchymal stem and endothelial cells. *Cell stem cell*. 7:718-729.

Voight, B.F., L.J. Scott, V. Steinthorsdottir, A.P. Morris, C. Dina, R.P. Welch, E. Zeggini, C. Huth, Y.S. Aulchenko, and G. Thorleifsson. 2010. Twelve type 2 diabetes susceptibility loci identified through large-scale association analysis. *Nature genetics*. 42:579.

Wang, B., X. Fu, X. Liang, J.M. Deavila, Z. Wang, L. Zhao, Q. Tian, J. Zhao, N.A. Gomez, and S.C. Trombetta. 2017. Retinoic acid induces white adipose tissue browning by increasing adipose vascularity and inducing beige adipogenesis of PDGFR α ⁺ adipose progenitors. *Cell discovery*. 3:17036.

Yang, J.P., A.E. Anderson, A. McCartney, X. Ory, G. Ma, E. Pappalardo, J. Bader, and J.H. Elisseeff. 2017. Metabolically active three-dimensional brown adipose tissue engineered from white adipose-derived stem cells. *Tissue Engineering Part A*. 23:253-262.

Zhang, K., L. Song, J. Wang, S. Yan, G. Li, L. Cui, and J. Yin. 2017. Strategy for constructing vascularized adipose units in poly (l-glutamic acid) hydrogel porous scaffold through inducing in-situ formation of ASCs spheroids. *Acta biomaterialia*. 51:246-257.

Conclusion and perspectives

To study and overcome obesity, a relevant cell model which accurately mirrors human adipogenic regulatory pathways is urgently needed. The work of my thesis is to develop a 3D cell model that can differentiate in large scale into adipospheres to better mimic native adipocytes in vivo than the classical 2D culture of adipocytes. We generated fully differentiated adipospheres from two different hiPSC-BAP clones, which are comparable to human adipospheres derived from subcutaneous abdominal adipose progenitors in terms of expression profile of extracellular matrix and of G Protein-Coupled Receptors (GPCRs). Furthermore, hiPSC-brown-like adipospheres can acutely and chronically response to the stimulation of 8-CPT-cAMP or 8-Br-cGMP. This culture model can be genetically modified to enhance UCP1 expression as revealed by the siRNA knocked-down of *CDKN2A*. Finally, hiPSC-BAPs and human endothelial cells (HDMECs) can co-culture in 3D and differentiate into vascularized adipospheres with functional tubular-like structure formed inside. All together, our data strongly suggest that hiPSC-adipospheres could be a physiological model for drug screening and transplantation for cell based-therapy of obesity.

One main characteristic of hiPSC-adipospheres is their inducible character, i.e. their ability to up-regulate the expression of UCP1 and other thermogenic proteins upon noradrenaline/cAMP signaling stimuli. An unbiased analysis of the hiPSC-brown-like adiposphere transcriptomic versus hiPSC-BAs in 2D will be performed by means of RNA-Seq, in order to reveal pathways specifically regulated by the 3D conditions. When available, agonists/antagonists small molecules will be used to investigate the effects of candidate pathways on UCP1 expression. However, the expression of UCP1 mRNA/protein is not sufficient to demonstrate that engineered adipospheres display energy-dissipating properties characteristic of BAs. Mitochondrial oxidative capacity and uncoupled respiration that are the critical metabolic features of BAs that will be tested. On the other hand, high substrate consumption rate is a major metabolic feature of BAs. Glucose consumption will be assessed by measurement of glucose in adiposphere supernatants. Secretion of batokines will be also measured to investigate the endocrine and paracrine activities of hiPSC-brown-like adipospheres.

Meanwhile, the adipose tissue GPCR atlas has identified more than 160 GPCRs regulating the physiological functions of adipocytes (Amisten et al. 2014), thus representing potential anti-obesity drug targets. Importantly, about 25% of the marketed drugs target GPCRs. The G protein coupled receptors (GPCR) has been validated in our model. Pharmacological tools will be used to reveal the effects of a short selection of GPCRs on the expression of UCP1 to validate the usefulness of hiPSC-brown-like adipospheres for the identification of crucial druggable pathways.

In addition, *CDKN2A* locus is related to adipose tissue adaptation to metabolic challenges, which may potentially involve in obesity. It has been observed beige adipocytes appear in *Cdkn2a* invalidated mice without any browning inducing agent, suggesting that this locus may control the browning process by regulating the β 3-adrenergic receptor (β -AR). Especially, the PKA pathway is among the most significantly affected pathway in *Cdkn2a* *-/-* adipocytes. We have demonstrated an induction of UCP1 expression in our 3D model when *CDKN2A* was silenced by siRNA. However, it is necessary to conform *CDKN2A* invalidated hiPSC-brown like adipospheres with a RNA-seq and the kinome analysis to identify the signaling pathways involved in the human model. Then, we are going to transplant *CDKN2A* invalidated hiPSC-brown-like adipospheres in High Fat Diet obese mice to evaluate their therapeutic potentials.

Furthermore, metabolic benefits of hiPSC-brown-like adipospheres enriched with ECs and their ability to counteract metabolic disorders associated with obesity in a cell-based therapeutic assay will be evaluated. We will develop transplantation of adipospheres enriched or not with ECs in NSG mice to determine the effects of ECs to the transplantation outcome. Then, we will investigate the effects on systemic glucose tolerance. We will compare hiPSC-vascularized adipospheres with abdominal-vascularized adipospheres to validate the hiPSC model.

Finally, we will use advanced microfabrication technologies to generate fully controlled 3D microenvironments for vascularized hiPSC-brown-like adipospheres, and to generate engineered microenvironments capable to host functional adipospheres and adipose lobule-like structures by exploiting advanced light-assisted 3D fabrication techniques. The 3D microenvironments hosting the adipospheres will be integrated in 3D bioreactors in order to setup a physiologically relevant drug-screening platform. This project is supported by an ANR grant.

The project addresses one of the biggest health challenges at the moment, which is to fight obesity and associated metabolic disorders including type II diabetes and cardiovascular diseases. One billion people are obese in the world and obesity is responsible for one in 20 deaths. It is timely to propose an innovative and alternative approach to counteract this disease. We propose the use of human iPSC in this field for drug screening and cell-based therapy. At the basic level, the hiPSCs with advanced microfabrication technologies to engineer 3D adipocyte models with fully controlled microenvironments will represent a powerful platform to better understand cellular and molecular mechanisms of human brown like adipogenesis with a relevant model. This is a requirement to identify novel druggable signalling pathways for activation and recruitment of BAs. We will

provide functional and relevant 3D models to test in vitro drug efficiency and safety and to improve BA therapeutic potential after transplantation.

Annexes

SCIENTIFIC REPORTS

OPEN

Brown-like adipose progenitors derived from human induced pluripotent stem cells: Identification of critical pathways governing their adipogenic capacity

Anne-Laure Hafner¹, Julian Contet¹, Christophe Ravaud¹, Xi Yao¹, Phi Villageois¹, Kran Suknuntha², Karima Annab³, Pascal Peraldi¹, Bernard Binetruy³, Igor I. Slukvin², Annie Ladoux¹ & Christian Dani¹

Received: 15 June 2016
Accepted: 08 August 2016
Published: 31 August 2016

Human induced pluripotent stem cells (hiPSCs) show great promise for obesity treatment as they represent an unlimited source of brown/brite adipose progenitors (BAPs). However, hiPSC-BAPs display a low adipogenic capacity compared to adult-BAPs when maintained in a traditional adipogenic cocktail. The reasons of this feature are unknown and hamper their use both in cell-based therapy and basic research. Here we show that treatment with TGF β pathway inhibitor SB431542 together with ascorbic acid and EGF were required to promote hiPSCs-BAP differentiation at a level similar to adult-BAP differentiation. hiPSC-BAPs expressed the molecular identity of adult-UCP1 expressing cells (*PAX3*, *CIDEA*, *DIO2*) with both brown (*ZIC1*) and brite (*CD137*) adipocyte markers. Altogether, these data highlighted the critical role of TGF β pathway in switching off hiPSC-brown adipogenesis and revealed novel factors to unlock their differentiation. As hiPSC-BAPs display similarities with adult-BAPs, it opens new opportunities to develop alternative strategies to counteract obesity.

In mammals, three types of adipocytes coexist, i.e. brown, brite and white, which are all involved in energy balance regulation while having opposite functions. White adipose tissue (WAT) is dispersed throughout the body and is mainly involved in energy storage. In contrast to WAT, brown adipose tissue (BAT) is specialized in energy expenditure. Activated BAT consumes metabolic substrate and burns fat to produce heat via the uncoupling protein (UCP)-1. Brite, also named beige, adipocytes were recently described as brown-like adipocytes and represent a third type of adipocytes recruited in WAT¹. Brown/brite adipocyte recruitment leads to powerful anti-obesity and anti-diabetic effects in mice. It was previously reported that BAT implants were able to restore normoglycemia in diabetic mice and to reduce obesity in Ob/Ob mice²⁻⁴. Hence, the notion of transplanting brown/brite adipose progenitors (BAPs) in obese patients as a therapeutic approach to counteract obesity and its associated metabolic complications recently emerged. However, BAT represents a minor fraction of adipose tissue in humans and disappears from most areas with age, persisting only around deeper organs⁵. Human BAPs are hard to isolate in this regard. Therefore, a cellular source of BAPs is urgently needed for the clinic and to better know human brown adipocyte ontogenesis.

Induced pluripotent stem cells (hiPSCs) can be differentiated into multiple cell types *in vitro*. Following the pioneer work of Yamanaka's group on the generation of patient-specific hiPSCs by reprogramming somatic cells⁶, hiPSCs emerged as an unlimited source of autologous BAPs for cell-based therapy of obesity. However, numerous issues have to be investigated before a therapeutic use of hiPSC-BAPs, including their purification and differentiation into functional adipocytes preferentially at a high level without introduction of exogenous adipogenic genes. The comparison of hiPSC-BAPs with adult-BAPs is also a timely question. Interestingly, white adipocytes generated from hiPSCs can maintain their functional properties for several weeks after transplantation into

¹Université Côte d'Azur, CNRS, Inserm, iBV, Nice, France. ²Department of Pathology and Laboratory Medicine, University of Wisconsin, Madison, WI 53715, USA. ³Inserm U910, Faculty of Medicine La Timone, Marseille, France. Correspondence and requests for materials should be addressed to C.D. (email: dani@unice.fr)

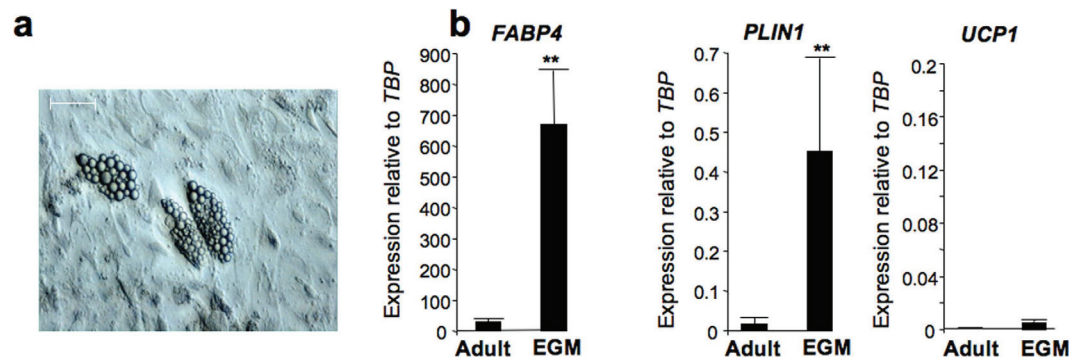


Figure 1. Differentiation of hiPSC-BAPs in EGM adipogenic medium. hiPSC-BAPs were induced to undergo differentiation in a traditional adipogenic medium routinely used for adult APs (Adult) or in the EGM adipogenic medium (EGM). (a) Twenty-five days later, multilocular adipocytes were detectable under the microscope only when cells were maintained in the EGM adipogenic medium; bar scale: 50 μ m. (b) RNAs were prepared and analyzed for adipocyte marker expression. Values are means \pm SEM. n = 6. * means $p < 0.05$ and ** means $p < 0.01$.

nude mice^{7,8}. These data revealed that hiPSCs-white adipocytes could potentially be used to correct metabolic parameters in lipodystrophic patients. Nishio *et al.*⁹ developed a procedure to differentiate hiPSCs into functional brown adipocytes at high efficiency using a hematopoietic cocktail. Remarkably, hiPSCs-brown adipocytes were able to improve glucose tolerance after transplantation in mice. In both works, total differentiated hiPSC cell populations, but not purified APs, were transplanted into mice. Indeed, differentiated hiPSC cultures can be enriched with adipocytes, but also contain other cell types that are unsuitable for transplantation, including undifferentiated iPSCs that can form teratomas. This indicates that purification of hiPSC-BAPs with a high adipogenic capacity is a prerequisite for a hiPSCs-based therapeutic approach. Ahfeldt *et al.*¹⁰ were able to generate pure brown and white APs from hiPSCs that displayed a high adipogenic capacity but only following transduction with adipogenesis master genes. The need to genetically modify hiPSCs-APs to generate adipocytes clearly illustrates the low adipogenic potential of hiPSCs-derived APs. As recently discussed, the bottleneck is the weak adipogenic potential of APs purified from hiPSCs compared to adult adipose tissue-derived APs¹¹. This feature was observed by us and others using different approaches to derive mesenchymal cells from hESCs or hiPSCs¹². Therefore, events required to unlock differentiation of hiPSCs-BAPs have yet to be identified. Here we describe a set of factors capable of governing hiPSC-BAP differentiation, and interestingly, at a level similar to that of BAPs derived from human adult adipose tissue.

Results

An endothelium growth medium and TGF β pathway inhibition were required to switch on hiPSCs-BAP differentiation. We recently reported the procedure to selectively generate BAPs and WAPs from hiPSCs depending on the activation of the retinoic acid pathway early during hiPSC differentiation¹³. In agreement with the observation that APs derived from hiPSCs and from hES cells have a low adipogenic potential (for recent review see ref. 11) the screening of traditional adipogenic factors promoting differentiation of adult APs failed to promote formation of hiPSC-BAP adipocytes (Table supplement 1). However, the screening of other types of media showed that the maintenance of hiPSC-BAPs in an endothelium growth medium (EGM) supplemented with traditional adipogenic factors (see Methods) displayed the potential to induce formation of multilocular adipocytes and to enhance expression of adipogenic markers such as *FABP4* and *PLIN1* (Fig. 1). Expression of *UCP1* was very low at the RNA level (Fig. 1b) and undetectable at the protein level (not shown) in these conditions, indicating that factors present in the EGM medium were able to promote BAP differentiation but not at the level of that of adult-BAPs. We hypothesized that anti-adipogenic factors were secreted by hiPSCs-BAPs, thus precluding their differentiation at a higher level.

The TGF β pathway recently emerged as a critical anti-adipogenic player through the activation of Smad 2/3¹⁴⁻¹⁶. The potent anti-adipogenic effect of TGF β 1 was confirmed on adult-BAPs (Fig. S2B). Interestingly, members of the TGF β family such as *TGF β 1* and *INHBA* were expressed during the first days of hiPSC-BAP differentiation (Fig. 2a). *TGF β 1* and *INHBA* expression was down-regulated in differentiated hiPSC-BAPs compared to the expression levels in undifferentiated cells, but remained at a level sufficient to maintain the Smad2/3 pathway active ((phosphoSmad, Fig. 2b). These data suggested that hiPSC-BAPs secreted bioactive TGF β family members that might lock hiPSC-BAP differentiation. In agreement with this hypothesis, medium conditioned by hiPSCs-BAPs displayed a potent anti-adipogenic effect on adult-BAP differentiation (Fig. S2). An ERK inhibitor (UO126 at 5 μ M) or a p38MAPK inhibitor (SB203580 at 10 μ M) was unable to reverse the anti-adipogenic effect of hiPSCs-BAP conditioned medium on adult-BAPs (not shown). In contrast, the anti-adipogenic effect of the conditioned-medium was inhibited by the addition of 5 μ M SB431542, an inhibitor of the TGF β signalling pathway¹⁷. As shown in Fig. 2b, active Smad 2/3 pathway could be inhibited upon SB431542 addition during the first 4 days of hiPSC-BAP differentiation. Then, a dramatic increase in *FABP4*, *PLIN1* and *UCP1* expression was observed (Fig. 2c). Transient inhibition of the TGF β pathway, during the first 3 days of differentiation only, was sufficient to promote differentiation (Fig. S3). Altogether, these data underline the critical role of TGF β pathway in switching off hiPSC-BAP differentiation.

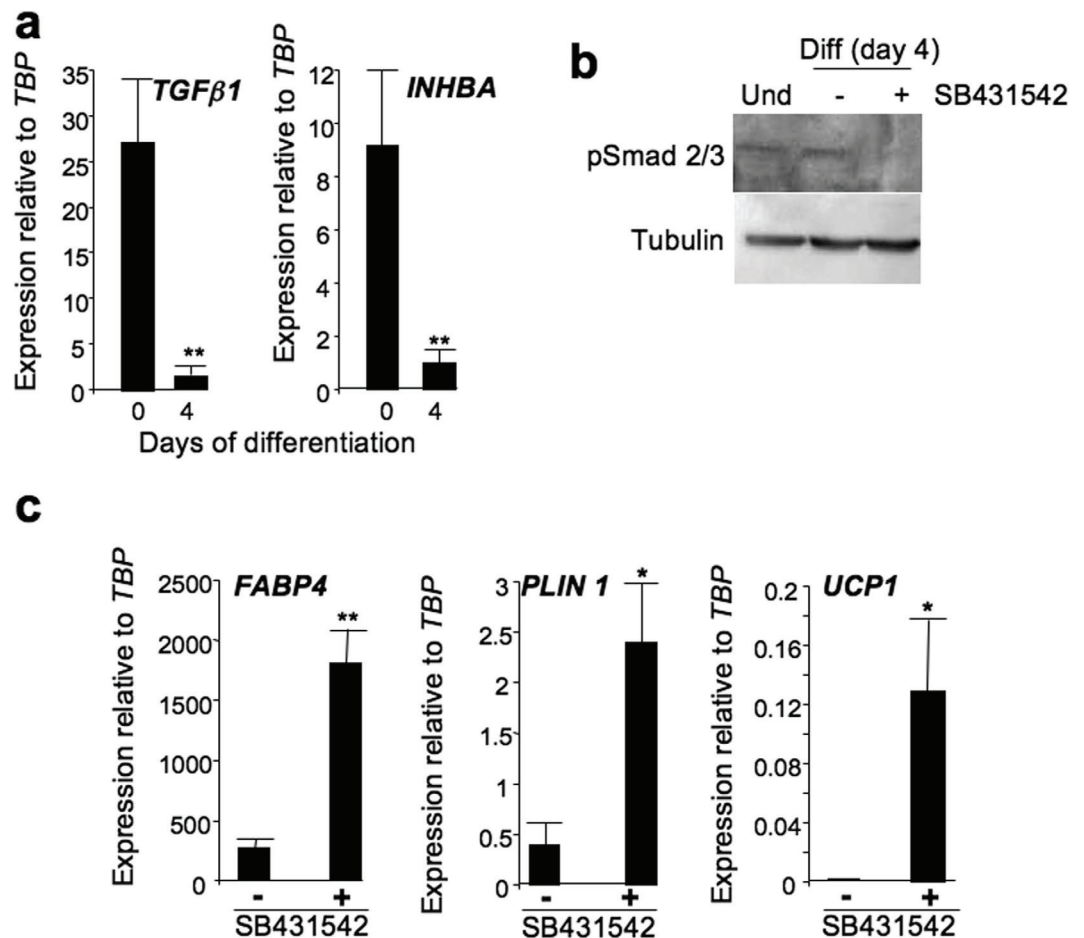


Figure 2. Anti-adipogenic activity secreted by hiPSC-BAPs was reversed by SB431542. (a) Expression of TGFβ family members in undifferentiated (day 0) and differentiated hiPSC-BAPs. (b) Activated Smad2/3 in undifferentiated and differentiated hiPSC-BAPs in the absence or presence of 5 μM of SB431542. (c) hiPSC-BAPs were induced to undergo differentiation in EGM2 adipogenic medium in the absence or presence of 5 μM SB431542. Twenty-five days later, RNAs were prepared and analyzed for the indicated genes. Values are means ± SEM. n = 4. *means p < 0.05 and **means p < 0.01.

Identification of extrinsic factors promoting hiPSCs-BAP differentiation. The commercial EGM medium contains IGF1, FGF2, VEGF, EGF, hydrocortisone and ascorbic acid with no information regarding their concentrations. We showed that FGF2, VEGF and IGF1 were dispensable for hiPSC-BAP differentiation. In contrast, hydrocortisone, ascorbic acid and EGF were required (Fig. S4A). Finally, traditional adipogenic factors supplemented with SB431542 (5 μM) and defined concentrations of ascorbic acid (25.5 μg/ml), hydrocortisone (4 μg/ml) and EGF (10 ng/ml), hereafter named defined hiPSC-adipogenic medium, dramatically enhanced adipocyte formation and expression of adipogenic markers at the protein level (Fig. 3a,b). The defined hiPSC-adipogenic medium supported differentiation at a level identical to that when cells were maintained in complete EGM2 adipogenic medium (Fig. S4B). Except SB431542, none of these essential factors was able to inhibit Smad2/3 activation (Fig. S4C). Importantly, hiPSC-BAP adipocytes were then able to respond to insulin as phosphorylated forms of IRS1, AKT and Erk1/2 were upregulated upon acute insulin administration (Fig. 3c). hiPSC-BAP progenies were also able to respond to forskolin, a chemical mimicking β-adrenergic stimulation, by increasing *UCP1* gene expression and lipolysis (Fig. 3d,e). Overall, these data showed that adipocytes generated from hiPSC-BAPs were responsive to an adrenergic stimulus and displayed an active insulin signaling pathway, the hallmark of functional brown/brite adipocytes. Interestingly, mesenchymal cells originated from two other hiPSC sources and derived by different approaches (see Materials and Methods) were not able to undergo adipocyte differentiation when maintained in a traditional adipogenic medium, as expected. However, their differentiation was dramatically promoted when maintained in the defined hiPSC-adipogenic medium (Fig. 4). Altogether, these data indicated that the set of factors identified was able to switch on differentiation of adipose progenitors derived from different human iPSC sources.

Molecular differentiation of hiPSCs-BAPs and comparison with adipose progenitors derived from human adult adipose tissues. A number of earlier studies have proposed several specific markers for brown, brite and white adipocyte lineages in mouse. Not all of these markers are relevant in humans, but the following ones have been reported in the literature as informative^{1,13,18–21} *ZIC1* (brown), *PAX3*, *DIO2*, *CIDEA*

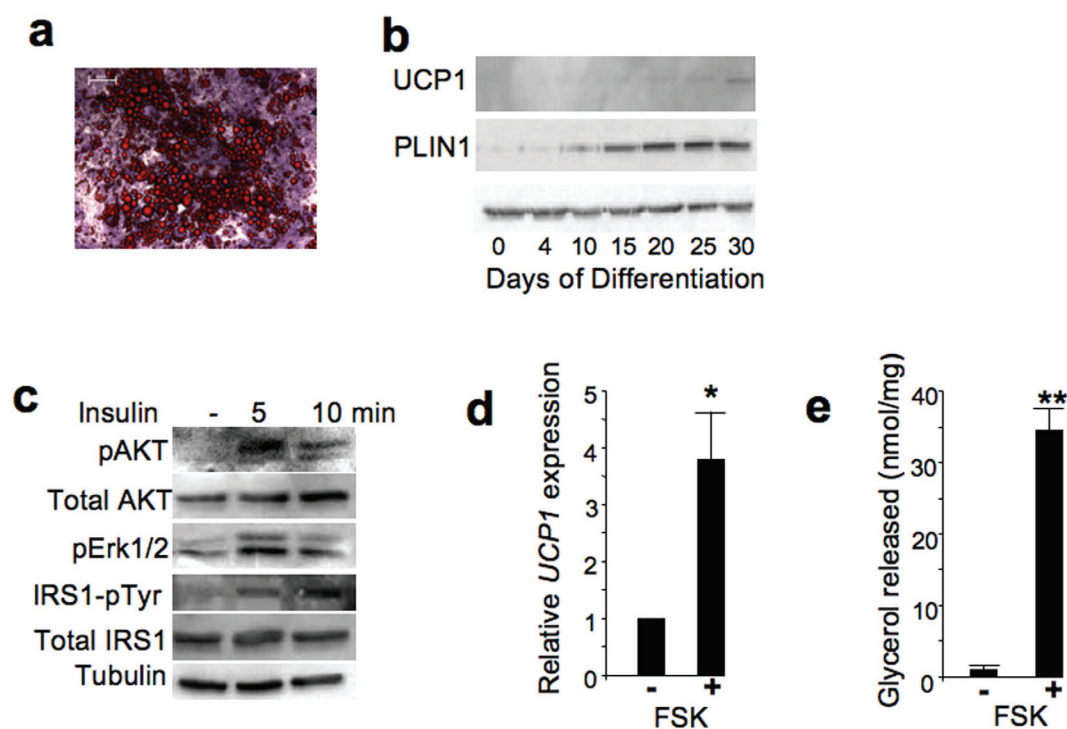


Figure 3. Differentiation of hiPSC-BAPs in optimized conditions. (a) hiPSCs-BAPs were induced to differentiate in the defined medium for 25 days. Then cells were fixed and stained with Oil Red O for lipid droplets. Bar scale: 50 μ m. (b) hiPSCs-BAPs were induced to differentiate in the defined medium and expression of UCP1 and PLIN1 at different time after adipogenic induction was analyzed by Western-blot. (c) Stimulation of insulin pathway: hiPSCs-BAPs were induced to differentiate in the defined adipogenic medium for 28 days as described in the Materials and Methods and then stimulated with 100 nM insulin for 5 or 15 min. Proteins were prepared and analyzed for the indicated markers. (d) Stimulation of UCP1 expression by forskolin. hiPSCs-BAPs were induced to differentiate in the defined adipogenic medium for 25 days, then stimulated with 10 μ M forskolin for 4 h. Values are means \pm SEM. n = 4. (e) Lipolysis induced by forskolin: hiPSCs-BAPs were induced to differentiate for 28 days, then stimulated with 10 μ M forskolin for 5 h. *means $p < 0.05$ and **means $p < 0.01$.

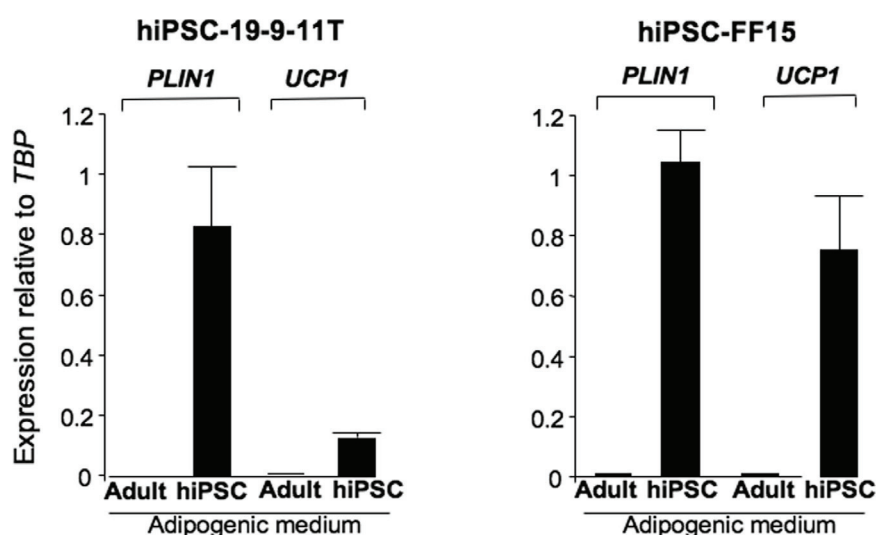


Figure 4. The defined hiPSC-BAP adipogenic medium supported differentiation of mesenchymal cells derived from different hiPSCs. Mesenchymal cells derived from hiPSC-19-9-11T and from hiPSC-FF15 were maintained in the traditional adipogenic medium for adult APs (Adult) or in the defined hiPSC-BAP adipogenic medium (hiPSC) for 25 days. RNAs were prepared and analyzed for expression of adipocyte markers. Values are means \pm SEM. n = 4.

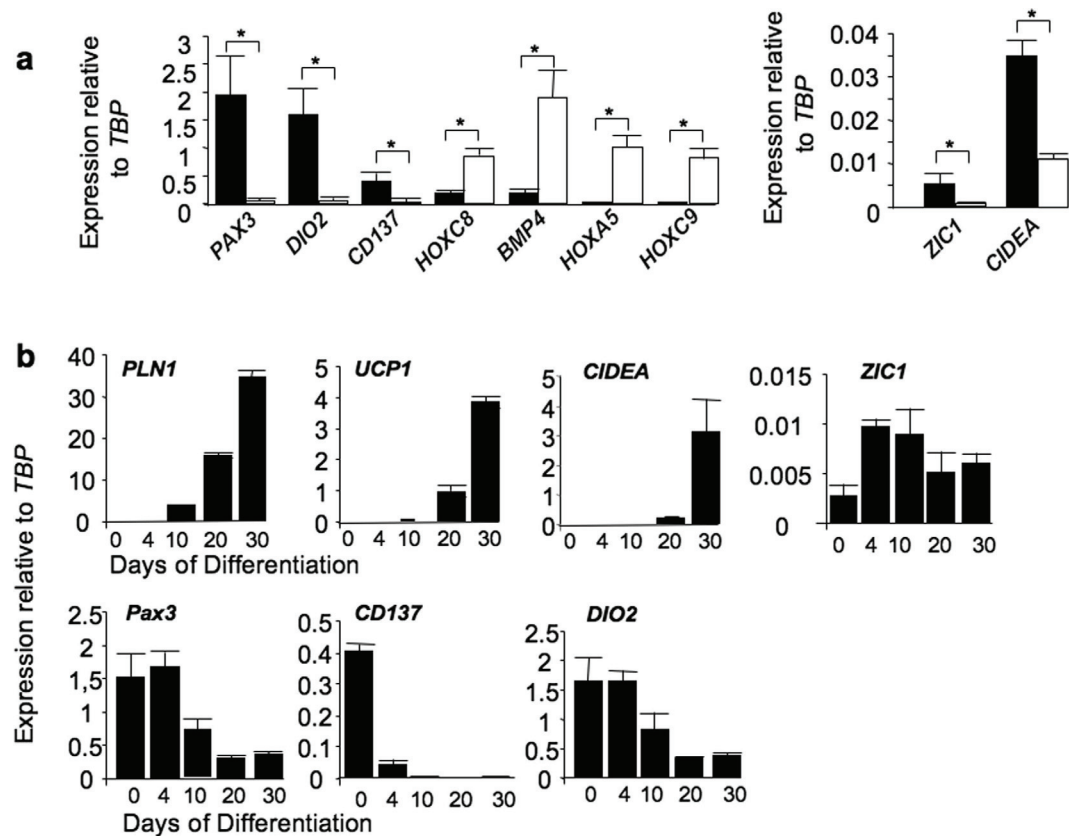


Figure 5. Marker gene expression in hiPSC-BAPs and -WAPs. (a) Expression of indicated markers was analyzed in undifferentiated BAPs (black bars) and WAPs (white bars). (b) hiPSC-BAPs were induced to differentiate in the defined medium and kinetics of expression of indicated markers was analyzed. Values are means \pm SEM. $n = 4$. *means $p < 0.05$.

(brown/brite), *CD137*, *TMEM26*, *TBX1* (brite), *HOXC8*, *BMP4*, *HOXA5*, *HOXC9*, *TCF21* (white). Expression of these markers was investigated both in hiPSC-BAPs and -WAPs. *TMEM26*, *TBX1* and *TCF21* were detected but with no differential expression between both cell types (not shown). In contrast, *PAX3*, *DIO2*, *CD137*, *CIDEA* and *ZIC1* were more expressed in BAPs than in WAPs (Fig. 5a). *HOXC8*, *BMP4*, *HOXA5* and *HOXC9* were weakly, if any, expressed in hiPSC-BAPs. Altogether these data indicate that hiPSC-BAPs expressed both classical brown and brite adipocyte markers. Their kinetics of expression were investigated during hiPSC-BAP differentiation. As shown in Fig. 5b (and see Fig. 3b) expression of *PLN1*, *CIDEA* and *UCP1* increased when cells were maintained in adipogenic medium, whereas expression of *PAX3*, *CD137* and *DIO2* was inhibited. *ZIC1* expression unchanged during differentiation. Finally, this molecular signature and the adipogenic potential of hiPSC-BAPs were compared to those of adult-APs. For that purpose, adult-BAPs and adult-WAPs were isolated from chin and knee paired fat depots, respectively, as we previously described²². As shown in Fig. 6a, no significant differences were observed in the level of expression of BAP markers between hiPSC-BAPs and adult BAPs. After differentiation, similar levels of *UCP1* expression were displayed in hiPSC-BAPs and adult BAPs when normalized to *PLN1* (Fig. 6b,c). Altogether, these data indicate that hiPSC-BAPs and adult-BAPs display similar adipogenic capacity range when maintained in the appropriate adipogenic cocktail.

Discussion

Brown/brite adipose progenitors purified from hiPSC cultures have a low adipogenic capacity compared to adult-BAPs when induced to differentiate using traditional adipogenic media. This bottleneck hampers the use of hiPSC-BAPs both in cell-based therapy and basic research. Here we show that TGF β pathway was activated during hiPSC-BAP differentiation, likely thanks to the expression of TGF β 1 and of activin A, two potent anti-adipogenic factors. Interestingly, treatment with activin/TGF β inhibitor SB431542 during the first days of differentiation only switched on the differentiation process. These data unlighted the critical role of TGF β pathway and reveal a molecular mechanism regulating hiPSC-BAP adipogenesis. We observed that hiPSCs could generate a high number of adipocyte colonies when BAPs were not purified but when BAPs were maintained in the iPSC environment. This strongly suggests that non-adipose cells present in hiPSC differentiated cultures could secrete factors that are required to prime BAPs towards the adipogenic lineage. The identification of non-adipogenic cells and secreted factors supporting brown adipogenesis could be of a great interest for characterizing the brown adipocyte niche during development in humans. Factors identified in this report (EGF, ascorbic acid, TGF β pathway inhibitor) likely belong to the niche. The low hiPSC-BAP adipogenic capacity compared to adult-BAPs is reminiscent of

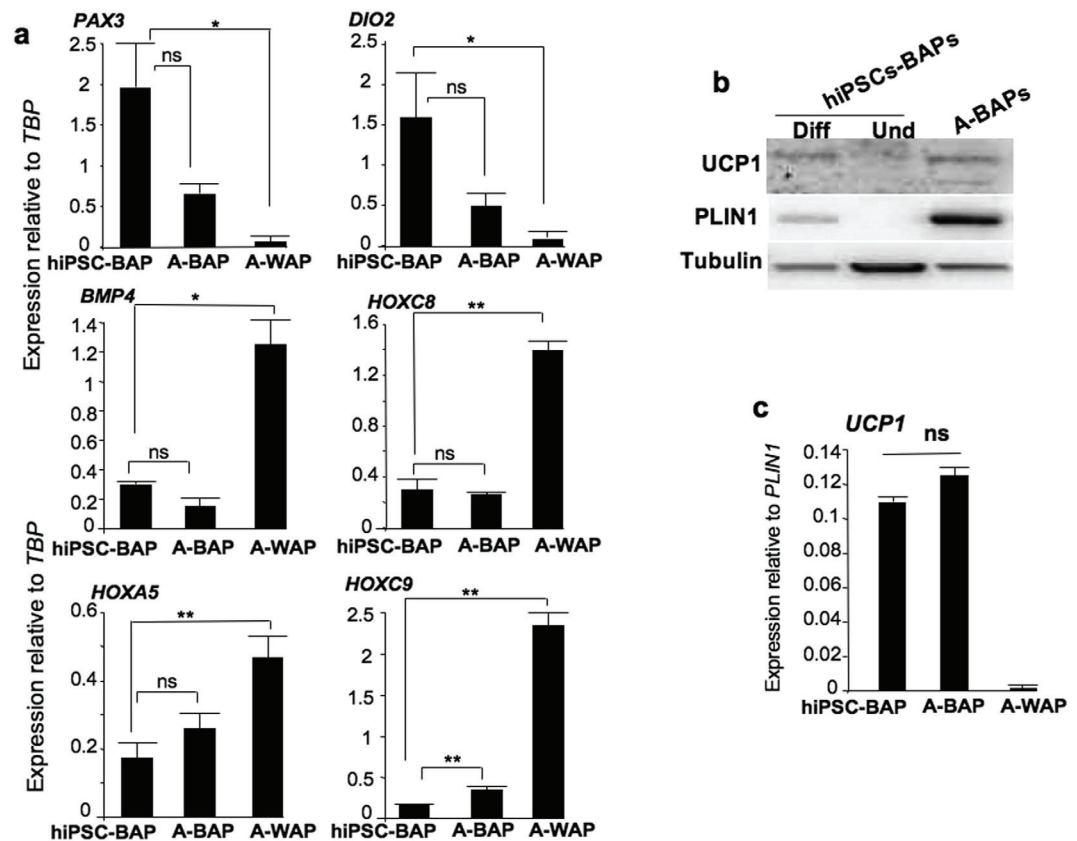


Figure 6. Comparison of gene expression between hiPSC-BAPs and adult-BAPs. (a) Expression of indicated markers was analyzed in undifferentiated hiPSC-BAPs, adult-BAPs, (A-BAPs) adult-WAPs (A-WAPs). Values are means \pm SEM. $n = 5$. (b) hiPSC-BAPs and adult BAPs were differentiated and UCP1 and PLIN1 levels were analyzed by Western-blotting. All protein depots were analyzed on the same gel. (c) Expression of UCP1 normalized to PLIN1 was compared between hiPSC-BAPs, adult-BAPs (A-BAPs) and adult-WAPs (A-WAPs). Values are means \pm SEM. $n = 4$. *means $p < 0.05$ and **means $p < 0.01$.

an observation reported by Han and colleagues²³. These authors observed that epididymal adipose tissue, which undergoes early development in mouse, is composed of progenitor cells that lack their adipogenic capacity once isolated from the tissue. In contrast to cells derived from other fat pads that developed later, epididymal fat cells required a different micro-environment to undergo differentiation. Altogether these results underline that the micro-environment differs for adult and embryonic-like cells and suggest that distinct regulatory mechanisms regulate differentiation of embryonic-like versus adult adipose progenitors as it has been recently reported in rodent²⁴.

Pathways mediating hiPSC-BAP adipogenic effects of hydrocortisone, ascorbic acid and EGF remains to be identified. Each of these factors appeared to be required to switch hiPSC-BAP differentiation on but none of them was sufficient to drive differentiation when added individually. We have previously demonstrated the existence of an autocrine/paracrine loop comprising the TGF β /Smad2 pathway that plays a critical negative role in adipogenesis of human adult APs²⁵. This negative loop is inhibited by dexamethasone contained in the traditional adipogenic cocktail used for the differentiation of adult-APs¹⁵. In contrast, neither dexamethasone nor hydrocortisone was able to switch off activated Smad2 in hiPSC-BAPs and treatment with the TGF β pathway inhibitor SB431542 was required to unlock hiPSCs-BAP differentiation. Dexamethasone is similar to the natural glucocorticoid hydrocortisone. However, dexamethasone included in the basal adipogenic medium could not replace hydrocortisone and vice versa. The molecular reasons of why both glucocorticoids were required for hiPSC-BAP differentiation remain to be investigated. Ascorbic acid was previously shown to enhance mouse adipose progenitor differentiation, and recent studies attribute its effects to the regulation of type V and type VI collagens²⁶. The essential role of collagens for adipogenesis was described several years ago²⁷ but one cannot rule out a metabolic effect of ascorbic acid on UCP1 expression²⁸. The requirement of ascorbic acid for UCP1 expression would deserve further investigation. EGF is known to stimulate adult-BAP proliferation while maintaining their adipogenic differentiation potential^{12,29}. However, its role in human brown adipocyte differentiation is not known. The stimulation of EGR1 expression upon EGF addition is of interest (see Fig. S4C). EGR1 has been shown to play a negative role in adipogenesis of murine 3T3-L1 cell line³⁰. However, more recently it has been reported that EGR1 facilitates fat accumulation in WAT and that EGR1 null WAT express BAT markers³¹. The positive or negative role of EGR1 in EGF-induced hiPSC-BAP differentiation remains to be determined. In conclusion, these data established a defined set of factors that can induce differentiation of human BAPs derived from pluripotent stem

cells at a high rate with no gene transfer. The findings in the present study may constitute a platform for *in vitro* studies and for the screening of drugs against obesity and related metabolic disorders focused on the generation of human white and brown APs. Finally, hiPSC-BAP could undergo differentiation at a level similar to adult-BAPs. This also offers a unique opportunity to investigate in animal models the therapeutic potential of hiPSC-BAPs derived from obese patients, which could lead to the development of autologous transplantation procedures to treat obesity and associated metabolic disorders.

Methods

Derivation of adipose progenitors from hiPSCs and from human adult stromal vascular fraction.

BAPs and WAPs have been derived from the hiPSC line NOK6 as previously described¹³. Briefly, hiPSC differentiation was initiated by floating cultivation to form embryoid bodies (EBs). Retinoic acid (10^{-6} M) was added or not from days 3 to 5 to generate white adipose progenitor (WAPs) or brown-like adipose progenitor (BAPs), respectively. Ten days after EB formation, EB outgrowths, that contain WAPs or BAPs at that stage, were maintained for 1 week in mesenchymal cell growth medium composed of DMEM supplemented with 10% FCS and with 5 ng/ml FGF2. BAPs and WAPs were then trypsinized and passaged with a 1:3 split ratio until achieving homogeneous CD73 labelling. A schematic diagram to explain the generation and differentiation of hiPSC-BAPs is shown in Fig. S1. Mesoderm-mesenchymal progenitors were derived from the hiPSC line 19-9-11T as described in ref. 32. The hiPSC-FF15 cell line was derived and characterized from human adult foreskin fibroblasts (HFF, Millipore) using the CytoTune[®]-iPS Sendai Reprogramming Kit (Thermo Fisher Scientific), as previously described³³. Mesenchymal Stem Cells (MSCs) were obtained after direct differentiation of hiPSC-FF15 in KO-DMEM 10% FBS with Ascorbic Acid-2-P (1 mM) and FGF2 (10 ng/ml) medium for 6 weeks on poly-D-lysine/fibronectin coated plates; cells were trypsinized every week at 1:5 dilution. MSCs were characterized by CD105+/CD73+/CD90+/CD34-/CD45- FACS analysis. Cell cultures were more than 90% double positive after 6 passages. Adult BAPs and WAPs were derived from the stromal vascular fractions of chin and knee paired fat depots, respectively, of Caucasians women who underwent elective liposuction procedures, after obtaining their with informed consent²². Eleven paired chin and knee fat depots was analyzed and a representative paired of BAPs and WAPs was used to compare with hiPSC-APs.

Optimization of hiPSC-BAP differentiation medium. hiPSC-BAPs were plated at 0.5×10^4 cells/cm² and maintained in proliferation in DMEM low glucose medium supplemented with 10% FCS. Then, when cells reached confluence the proliferation medium was changed to differentiation medium composed of EBM-2 (Lonza) supplemented with 0.1% FCS, EGM-2 cocktail (Lonza), IBMX (0.5 mM), dexamethasone (0.25 μ M), T3 (0.2 nM), insulin (170 nM) and rosiglitazone (1 μ M). IBMX and dexamethasone were maintained only for the first 3 days of differentiation. This medium will hereafter be EGM2 adipogenic medium. Because the concentrations of factors contained in EGM-2 were not known, a defined medium was also established. This defined hiPSC- adipogenic medium was composed of EBM-2 (Lonza) supplemented with FCS (0.1%), SB431542 (5 μ M), ascorbic acid (25.5 μ g/ml), hydrocortisone (4 μ g/ml), EGF (10 ng/ml), T3 (0.2 nM), insulin (170 nM), rosiglitazone (1 μ M), IBMX (0.5 mM), dexamethasone (0.25 μ M). IBMX and dexamethasone were maintained for the first 3 days only. The medium was changed once a week. A high differentiation rate was obtained 20–30 days after induction as between 60–80% of hiPSC-BAPs underwent adipocyte differentiation.

RNA preparation and real-time PCR analysis. RNAs were purified on RNeasy Plus Universal columns (Qiagen, France) according to the manufacturer's instructions. Total RNA sample concentrations were determined using a Nanodrop spectrophotometer (Thermo Scientific, Waltham, MA, USA). 1 μ g RNA was used for reverse transcription. Real-time PCR assays were run on a OneStep real-time PCR machine (Applied Life Sciences) and sybergreen was from Applied Biosystems.

Normalization was performed using the geometric averages of the housekeeping gene *TBP*. Delta delta Ct values were used to achieve relative quantification of gene expression when “expression relative to *TBP*” is indicated. The sequences of primers used are in Table S2.

Acute insulin treatment and lipolysis. hiPSC-BAPs cells were induced to differentiate in the defined adipogenic medium for 10 days. Then insulin (170 nM) was replaced by a lower concentration (0.5 nM) until day 28. Cells were maintained in DMEM supplemented with 0.2% BSA for 48 h before stimulation with 100 nM insulin for 5 or 15 min. Glycerol release into cell culture medium was determined as an index of lipolysis using Free Glycerol Reagent (Sigma Aldrich, St. Louis, MO) according to manufacturer instructions. hiPSC-BAPs were induced to differentiate in the defined hiPSC- adipogenic medium for 28 days, then maintained for 3 days in EBM basal medium supplemented with 0.2% BSA. Lipolysis was stimulated with 10 μ M Forskolin for 5 hours.

Preparation of cell extracts and Western blot analysis. Cells were rinsed with PBS and solubilized in stop buffer containing 50 mM HEPES, pH 7.2, 150 mM NaCl, 10 mM EDTA, 10 mM Na₄P₂O₇, 2 mM Na₃VO₄, and 1% Triton X-100 supplemented with Protease Inhibitor Cocktail (Roche). The primary antibodies and dilutions used were: UCP1 (1/500, Calbiochem), Perilipin 1 (1/1000, Acris Antibodies); Tubulin (1/10000, Sigma); AKT (1/1000, Cell Signaling); Phospho-AKT (Thr308) (1/1000, Cell Signaling); Phospho-Erk1/2 (Thr202/Tyr204) (1/1000, Cell Signaling); Phosphotyrosin, clone 4G10 (1/1000, Millipore); IRS1 (1/1000, Millipore); Phospho-Smad2 (1/1000, Cell Signaling); Smad 2/3 ((1/1000, Cell Signaling). Secondary horseradish peroxidase-conjugated antibodies were purchased from Promega.

Statistics analysis. InStat3 software and a nonparametric unpaired test (Mann-Whitney) was used for statistical analysis of the real-time PCR data. Probability values < 0.05 were considered as statistically significant and are marked with a single asterisk or with by double asterisks when $p < 0.01$.

References

1. Wu, J. *et al.* Beige adipocytes are a distinct type of thermogenic fat cell in mouse and human. *Cell* **150**, 366–376 (2012).
2. Stanford, K. I. *et al.* Brown adipose tissue regulates glucose homeostasis and insulin sensitivity. *J Clin Invest* **123**, 215–223 (2013).
3. Gunawardana, S. C. & Piston, D. W. Reversal of type 1 diabetes in mice by brown adipose tissue transplant. *Diabetes* **61**, 674–682 (2010).
4. Liu, X. *et al.* Brown Adipose Tissue Transplantation Reverses Obesity in Ob/Ob Mice. *Endocrinology* **156**, 2461–2469 (2015).
5. Frontini, A. & Cinti, S. Distribution and development of brown adipocytes in the murine and human adipose organ. *Cell Metab* **11**, 253–256 (2010).
6. Takahashi, K. *et al.* Induction of pluripotent stem cells from adult human fibroblasts by defined factors. *Cell* **131**, 861–872 (2007).
7. Taura, D. *et al.* Adipogenic differentiation of human induced pluripotent stem cells: comparison with that of human embryonic stem cells. *FEBS Lett* **583**, 1029–1033 (2009).
8. Noguchi, M. *et al.* *In vitro* characterization and engraftment of adipocytes derived from human induced pluripotent stem cells and embryonic stem cells. *Stem Cells Dev* (2013).
9. Nishio, M. *et al.* Production of Functional Classical Brown Adipocytes from Human Pluripotent Stem Cells using Specific Hemopoietin Cocktail without Gene Transfer. *Cell Metab* **16**, 394–406 (2012).
10. Ahfeldt, T. *et al.* Programming human pluripotent stem cells into white and brown adipocytes. *Nat Cell Biol* (2012).
11. Hafner, A. L. & Dani, C. Human induced pluripotent stem cells: A new source for brown and white adipocytes. *World J Stem Cells* **6**, 467–472 (2014).
12. Holmstrom, T. E., Mattsson, C. L., Falting, J. M. & Nedergaard, J. Differential signalling pathways for EGF versus PDGF activation of Erk1/2 MAP kinase and cell proliferation in brown pre-adipocytes. *Exp Cell Res* **314**, 3581–3592 (2008).
13. Mohsen-Kanson, T. *et al.* Differentiation of human induced pluripotent stem cells into brown and white adipocytes: role of Pax3. *Stem Cells* **32**, 1459–1467 (2014).
14. Zamani, N. & Brown, C. W. Emerging roles for the transforming growth factor- β superfamily in regulating adiposity and energy expenditure. *Endocr Rev* **32**, 387–403 (2011).
15. Zaragosi, L. E. *et al.* Activin a plays a critical role in proliferation and differentiation of human adipose progenitors. *Diabetes* **59**, 2513–2521 (2010).
16. Bourlier, V. *et al.* TGF β Family Members Are Key Mediators in the Induction of Myofibroblast Phenotype of Human Adipose Tissue Progenitor Cells by Macrophages. *PLoS One* **7**, e31274 (2012).
17. Inman, G. J. *et al.* SB-431542 is a potent and specific inhibitor of transforming growth factor- β superfamily type I activin receptor-like kinase (ALK) receptors ALK4, ALK5, and ALK7. *Mol Pharmacol* **62**, 65–74 (2002).
18. Cypess, A. M. *et al.* Anatomical localization, gene expression profiling and functional characterization of adult human neck brown fat. *Nat Med* **19**, 635–639 (2013).
19. Jespersen, N. Z. *et al.* A classical brown adipose tissue mRNA signature partly overlaps with brite in the supraclavicular region of adult humans. *Cell Metab* **17**, 798–805 (2013).
20. Lidell, M. E. *et al.* Evidence for two types of brown adipose tissue in humans. *Nat Med* **19**, 631–634 (2013).
21. de Jong, J. M., Larsson, O., Cannon, B. & Nedergaard, J. A stringent validation of mouse adipose tissue identity markers. *Am J Physiol Endocrinol Metab* **308**, E1085–E1105 (2015).
22. Kouidhi, M. *et al.* Characterization of human knee and chin adipose-derived stromal cells. *Stem Cells Int* **2015**, 592090 (2015).
23. Han, J. *et al.* The spatiotemporal development of adipose tissue. *Development* **138**, 5027–5037 (2011).
24. Wang, Q. A. *et al.* Distinct regulatory mechanisms governing embryonic versus adult adipocyte maturation. *Nat Cell Biol* **17**, 1099–1111 (2015).
25. Dani, C. Activins in adipogenesis and obesity. *Int J Obes (Lond)* **37**, 163–166 (2013).
26. Kim, B., Choi, K. M., Yim, H. S. & Lee, M. G. Ascorbic acid enhances adipogenesis of 3T3-L1 murine preadipocyte through differential expression of collagens. *Lipids Health Dis* **12**, 182 (2013).
27. Ibrahim, A., Bonino, F., Bardon, S., Ailhaud, G. & Dani, C. Essential role of collagens for terminal differentiation of preadipocytes. *Biochem Biophys Res Commun* **187**, 1314–1322 (1992).
28. Carriere, A. *et al.* Browning of white adipose cells by intermediate metabolites: an adaptive mechanism to alleviate redox pressure. *Diabetes* **63**, 3253–3265 (2014).
29. Hebert, T. L. *et al.* Culture effects of epidermal growth factor (EGF) and basic fibroblast growth factor (bFGF) on cryopreserved human adipose-derived stromal/stem cell proliferation and adipogenesis. *J Tissue Eng Regen Med* **3**, 553–561 (2009).
30. Boyle, K. B. *et al.* The transcription factors Egr1 and Egr2 have opposing influences on adipocyte differentiation. *Cell Death Differ* **16**, 782–789 (2009).
31. Zhang, J. *et al.* Dietary obesity-induced Egr-1 in adipocytes facilitates energy storage via suppression of FOXO2. *Sci Rep* **3**, 1476 (2013).
32. Vodyanik, M. A. *et al.* A mesoderm-derived precursor for mesenchymal stem and endothelial cells. *Cell Stem Cell* **7**, 718–729 (2010).
33. Badja, C. *et al.* Efficient and cost-effective generation of mature neurons from human induced pluripotent stem cells. *Stem Cells Transl Med* **3**, 1467–1472 (2014).

Acknowledgements

This work was supported by the French Government (National Research Agency, ANR) through the “Investments for the Future” LABEX SIGNALIFE: program reference number ANR-11-LABX-0028-01, by the Fondation des Gueules Cassées (no. 05-2015) and by the Fondation ARC (fellowship to ALH)

Author Contributions

A.-L.H. conceived and conducted the experiments; J.C., C.R., X.Y., P.V., K.S. and K.A. conducted experiments; P.P., B.B., I.I.S., A.L. and C.D. analyzed the results; C.D. wrote the manuscript. All authors reviewed the manuscript.

Additional Information

Supplementary information accompanies this paper at <http://www.nature.com/srep>

Competing financial interests: The authors declare no competing financial interests.

How to cite this article: Hafner, A.-L. *et al.* Brown-like adipose progenitors derived from human induced pluripotent stem cells: Identification of critical pathways governing their adipogenic capacity. *Sci. Rep.* **6**, 32490; doi: 10.1038/srep32490 (2016).



This work is licensed under a Creative Commons Attribution 4.0 International License. The images or other third party material in this article are included in the article's Creative Commons license, unless indicated otherwise in the credit line; if the material is not included under the Creative Commons license, users will need to obtain permission from the license holder to reproduce the material. To view a copy of this license, visit <http://creativecommons.org/licenses/by/4.0/>

© The Author(s) 2016

SCIENTIFIC REPORTS

OPEN

Platelet-rich plasma respectively reduces and promotes adipogenic and myofibroblastic differentiation of human adipose-derived stromal cells via the TGF β signalling pathway

Bérengère Chignon-Sicard^{1,2}, Magali Kouidhi¹, Xi Yao¹, Audrey Delerue-Audegond³, Phi Villageois¹, Pascal Peraldi¹, Patricia Ferrari⁴, Yves Rival³, David Piwnica³, Jérôme Aubert³ & Christian Dani¹

Autologous fat grafting is a gold standard therapy for soft tissue defects, but is hampered by unpredictable postoperative outcomes. Fat graft enrichment with adipose-derived stromal cell (ASCs) was recently reported to enhance graft survival. Platelet-rich plasma (PRP) has also emerged as a biologic scaffold that promotes fat graft viability. Combined ASC/PRP fat grafting enrichment is thus a promising new regenerative medicine approach. The effects of PRP on ASC proliferation are well documented, but the impact of PRP on ASC differentiation has yet to be investigated in depth to further elucidate the PRP clinical effects. Here we analyzed the human ASC fate upon PRP treatment. PRP was found to sharply reduce the potential of ASCs to undergo differentiation into adipocytes. Interestingly, the PRP anti-adipogenic effect was accompanied by the generation of myofibroblast-like cells. Among the various factors released from PRP, TGF β pathway activators played a critical role in both the anti-adipogenic and pro-myofibroblastic PRP effects. Overall, these data suggest that PRP participates in maintaining a pool of ASCs and in the repair process by promoting ASC differentiation into myofibroblast-like cells. TGF β may provide an important target pathway to improve PRP clinical outcomes.

Autologous fat grafting is a gold standard therapy for soft tissue defects, correction or augmentation in reconstructive and plastic surgery. Autologous fat grafting is particularly useful after tumor removal, in breast reconstruction surgery after mastectomy, as well as in repairing extensive facial deformities caused by injury, illness or congenital abnormalities. This treatment capitalizes on the large quantities of autologous fat that are easy to obtain in various parts of the body with minimum morbidity for patients. However, fat grafting is still controversial due to the postoperative outcome predictability. The main drawbacks of this technique are the variable engraftment results, resorption and cyst formation due to fat necrosis. Platelet-rich plasma (PRP) has recently emerged as an autologous scaffold able to promote neovascularization and fat graft viability^{1,2}. Enrichment with adipose-derived stromal/stem cells (ASCs) has also been shown to enhance fat graft survival, likely through both ASC differentiation and secretion of angiogenic factors³. PRP has also been reported to stimulate ASCs secretion of angiogenic factors^{4,5}. Co-transplantation of ASCs and PRP is thus a promising cell therapy approach in regenerative medicine.

¹Université Côte d'Azur, CNRS, Inserm, iBV, Faculté de Médecine, 06107, Nice Cedex 2, France. ²Plastic, Reconstructive and Hand Surgery Department, Hôpital Pasteur 2, Nice, France. ³Research Galderma, Sophia, Antipolis, France. ⁴Biochemistry Department, Hôpital Pasteur 1, Nice, France. Correspondence and requests for materials should be addressed to C.D. (email: dani@unice.fr)

Received: 22 December 2016
Accepted: 24 April 2017
Published online: 07 June 2017

PRP contains a variety of growth factors, such as platelet-derived growth factors (PDGFs) and vascular endothelial growth factors (VEGFs), with neovascularization properties. PRP also releases factors from members of the transforming growth factor- β (TGF β) family that were shown to be potent anti-adipogenic factors and key mediators in the conversion of human ASCs into myofibroblast-like cells^{6,7}. The functional role of TGF β in PRP effects has, however, not been demonstrated. Myofibroblasts, characterized by alpha-smooth actin (α SMA) expression and collagen secretion, are key partners in the tissue repair process. However, as excessive collagen deposition is associated with fibrotic lesions, we considered it essential to study the TGF β pathway with regard to PRP effects on ASC adipogenic and myofibroblastic differentiation.

In this study, we investigated the effects of individual PRPs prepared from six healthy donors on the differentiation of three different ASC sources (see Materials and Methods). We show that the ASC adipocyte differentiation potential was sharply reduced in the presence of PRP. The PRP anti-adipogenic effect was accompanied by an increase in alpha smooth muscle actin expressing cells and type 1 collagen secretion, the hallmark of myofibroblast-like cells. TGF pathway activators released from PRP were found to have a critical role in this phenomenon as the small SB431542 molecule, i.e. a selective TGF β pathway inhibitor, abolished both the anti-adipogenic and pro-myofibroblastic effects of PRP.

Results

PRP reduced adipogenic differentiation of ASCs. PRPs obtained from six healthy subjects were first tested for their ability to promote ASC proliferation. ASCs derived from paired chin- and knee-fat depots⁸ were maintained in the presence of 20% PRP. In agreement with the findings of previous studies^{4,5,9–11}, the addition of PRP dramatically promoted ASC proliferation (Fig. S1). As the impact of PRP treatment on the ASC fate has yet to be investigated, we analyzed PRP effects on the ASC adipogenic potential. The ratio of PRP used in previous publications is variable. Liao *et al.*⁹ showed that PRP displays an effect on differentiation from 5% to 20%, whereas in a clinical study, Cervelli *et al.*¹¹ showed that 40% PRP was optimal for graft maintenance. We show that the six individually tested PRPs dramatically inhibited knee-ASC adipocyte formation when used at 20%, as revealed by the lower number of adipocytes and lipid contents quantified in the PRP-treated cultures (Fig. S2). Therefore, 20% PRP was used for subsequent experiments. PRPs could have an effect when used at lower concentrations, as suggested by the effects observed when two PRPs were tested at 5% and 10% (Fig. S2). The effects of low PRP concentrations on ASC fate remain to be investigated in more details. The anti-adipogenic effect of 20% PRP was reproduced on three different ASC sources (Fig. 1A). Finally, the effect was confirmed at the molecular level, as shown by the lower expression of adipogenic genes such as *PPAR γ* (an adipogenic master gene), *AdipoQ* (an adipocyte-specific adipokine coding for adiponectin) and *FABP4* (a gene coding for a fatty acid carrier specifically expressed during adipocyte differentiation) in PRP-treated cells (Fig. 1B).

TGF β signalling pathway inhibitor SB431542 reversed PRP anti-adipogenic effects. We profiled PRPs as the first step in identifying molecular mechanisms responsible for the PRP anti-adipogenic effect. An antibody array containing cytokines/growth factors, some of which are known to play a role in adipogenesis, was thus screened. Of the 40 factors in the array (see Methods), eight displayed a fluorescent signal significantly above the background, e.g. EGFR, GM-CSF, IGFBP3, IGFBP6, PDGF-AA, PDGF-AB, PDGF-BB and TGF β 1 (Fig. 2). ELISA assays confirmed that IGFBP3, PDGF-AA, leptin (not spotted in the array) and TGF β 1 were released from PRPs (Table S1). We focused on the potential role of TGF β 1 in the PRP anti-adipogenic effect. The TGF β pathway was a strong candidate for involvement in the PRP effect because this pathway was previously reported to have a potent anti-adipogenic effect mediated by Smad2/3 phosphorylation^{7,12}. As expected, ASC adipocyte differentiation was inhibited in the presence of 2 ng/ml TGF β 1 and the TGF β 1 anti-adipogenic effect was reversed using 5 μ M SB431542, a selective TGF β pathway inhibitor¹³ (Fig. S4). This SB431542 concentration was sufficient to inhibit TGF β 1-induced Smad 2/3 activation (Fig. S4). However, the functional role of TGF β in the PRP mixture has yet to be demonstrated. As shown in Fig. 3A, Smad 2/3 phosphorylation was induced upon PRP treatment and PRP-induced Smad2/3 phosphorylation was reversed in the presence of SB431542. These data strongly suggest that the TGF β pathway was activated by PRP in ASCs and could play a role in the PRP anti-adipogenic effect. To test this hypothesis, ASCs were induced to undergo adipocyte differentiation in the presence of PRP with or without the SB431542 compound. As shown, the lipid content and *FABP4* adipogenic gene expression were restored when cells were treated with 20% PRP in the presence of 5 μ M SB431542 (Fig. 3B–D). Together, these findings supported the hypothesis that the TGF β pathway activators released from PRP are major mediators of the PRP anti-adipogenic effect.

PRP induced myofibroblast-like cell phenotype reversed by SB431542. The TGF β pathway is considered to be the master pathway driving myofibroblast generation in physiological and pathological processes¹⁴. In addition, we previously reported that, in an obesity context, TGF β 1 treatment converts human ASCs into myofibroblast-like cells at the expense of adipocyte differentiation⁶. As expected, ASC myofibroblastic differentiation induced by TGF β 1 was reversed by SB431542 (see Fig. S3). These findings prompted us to investigate the fate of PRP-treated ASCs. ASCs were thus maintained in adipogenic conditions in the absence or presence of PRP and myofibroblastic marker expression was investigated. Interestingly, PRP promoted the generation of α SMA-expressing cells and *alpha-smooth muscle actin* (α SMA) gene expression (Fig. 4A,B, also see Fig. S3). The PRP-induced ASC myofibroblastic-like phenotype was confirmed by overexpression of *α 1 chain 1 of type 1 collagen* (*COL1A1*) genes, as well as by the secretion of type 1 collagen (Fig. 4C,D). Overall, these data indicated that PRP could convert ASCs into a myofibroblast-like phenotype. As for adipogenesis, SB431542 reversed PRP-induced myofibroblastic differentiation, indicating that the TGF β pathway plays a critical role in regulation of the PRP-induced ASC fate.

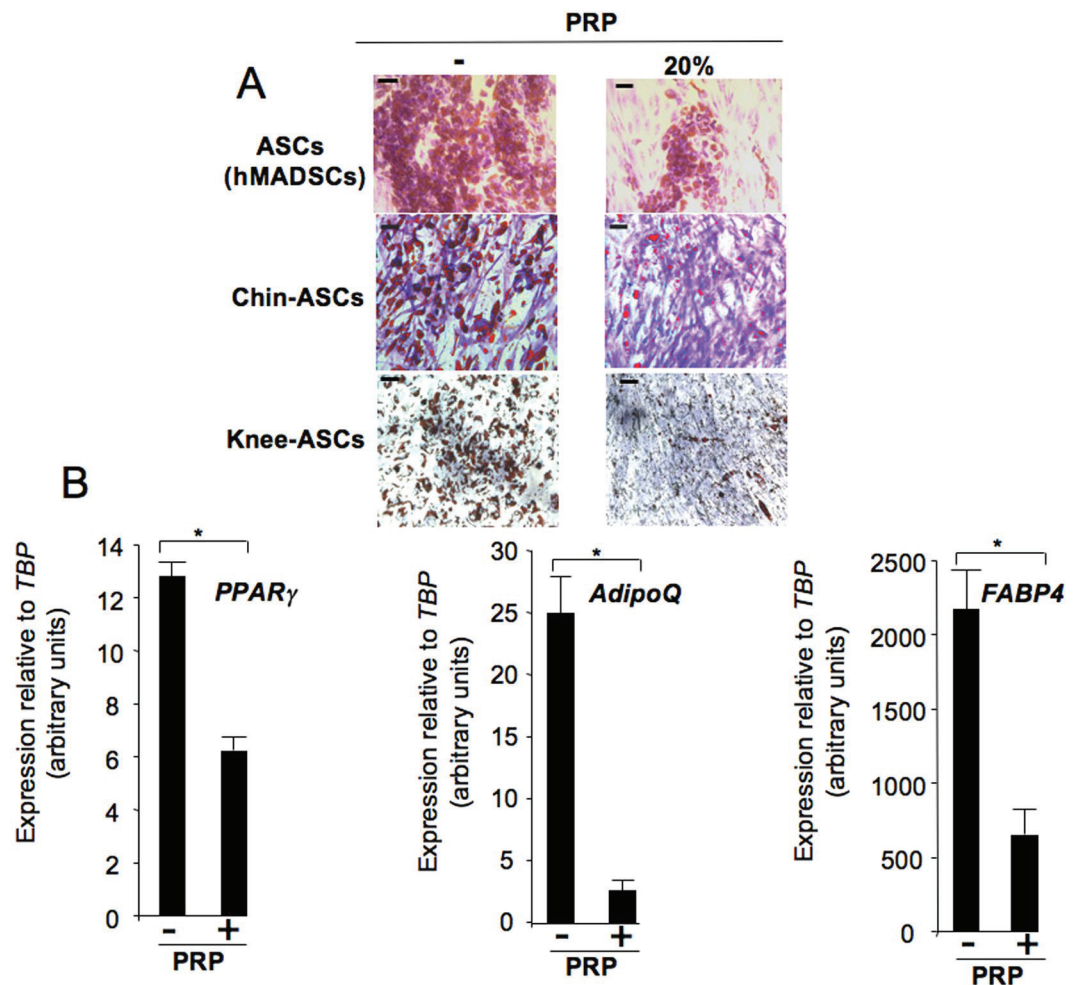


Figure 1. PRP inhibited ASC adipocyte differentiation. (A) ASCs (hMADSCs), chin- and knee-ASC primary cultures were induced to undergo adipocyte differentiation in the absence (–) or presence (+) of 20% PRP. After 10 days, cells were fixed and stained with Oil Red O to visualize lipid droplets, then with nonspecific violet crystals to stain the cell layer. Bar scale: 50 μ m. (B) ASCs were maintained as in (A) and RNAs were prepared to analyse expression of the indicated genes by real-time PCR. Values are means \pm SEM ($n = 3$ individual PRPs). * $p < 0.05$.

Discussion

ASC and PRP-supplemented fat grafts are promising for reconstructive surgery. The beneficial effects of PRP include its potential to promote neovascularization and enhance fat graft viability. PRP profiling data indicated that various factors were released from our PRP preparations, as previously reported. PDGFs and TGF β 1 release have been previously reported and at concentrations similar to those shown in Table S1^{2, 15, 16}. Our experiments also revealed factors released from PRPs that were not previously reported, such as IGFBP3, IGFBP6 and leptin. Note that, in addition to being adipocyte differentiation regulators, these latter factors were also described as being critical modulators of angiogenesis^{17, 18}. The specific role of these factors has yet to be investigated, but they likely play a role in the clinical effects of PRP. One potential beneficial effect of ASC enrichment is the maintenance of a longer-term graft volume. Our data indicated that PRP promotes ASC proliferation, as previously reported, while also inhibiting ASC adipogenic differentiation. We speculate that this phenomenon observed *ex vivo* could participate in maintaining a pool of undifferentiated ASCs to enable adipocyte renewal when PRP growth factors are resorbed. Here, we showed that PRPs had an effect on the ASCs derived from the pubis fat pad from a 4 month-old child, and on ASCs derived from chin and knee adipose tissues from a 72 year-old female subject. We also observed PRP effects on ASCs derived from chin- and knee- fat depots from two 61 year-old female subjects and one 46 year-old female subject (not shown). The effects of PRP on other sources of cells used for autologous fat grafting, such as thigh, hip, and abdominal fat pads, have yet to be analyzed, but it is tempting to propose that PRP effects are age- and fat depot-independent.

It was previously reported that mice treated with PRP displayed increased osteogenesis in bone marrow¹⁹. Interestingly, osteoblast formation was observed at the expense of bone-marrow adipogenesis, in full agreement with the PRP anti-adipogenic effect we observed with human ASCs. PRP anti-adipogenic effects on ASCs were also previously reported⁹. However, the authors of that study did not functionally identify PRP factors mediating

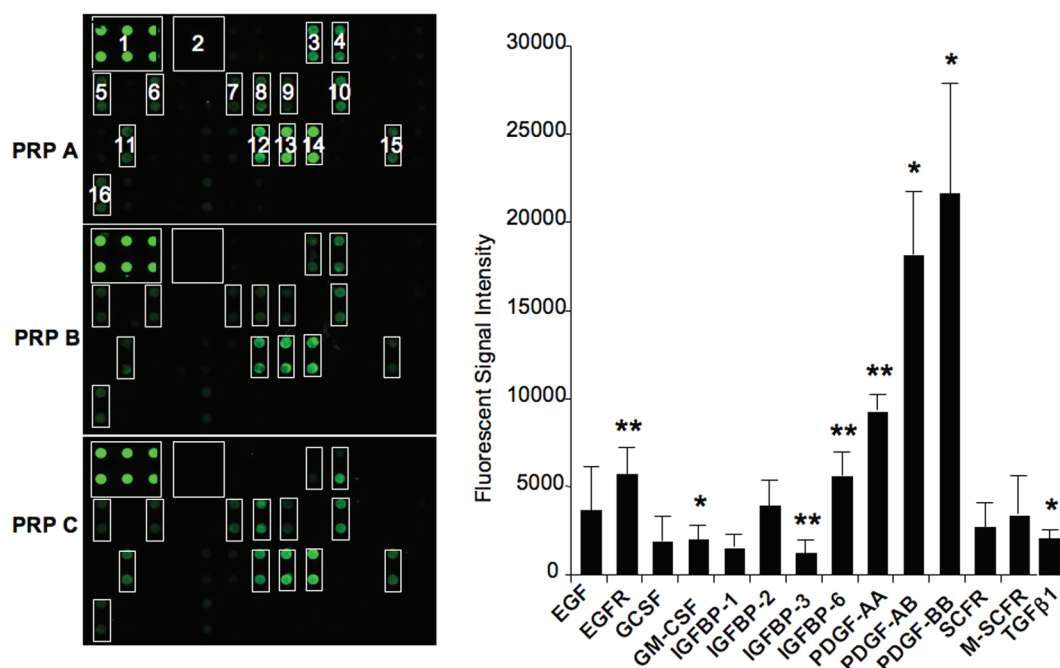


Figure 2. PRP profiling. Cytokines released from PRPs were detected using the RayBio C-Series Human Growth factor Antibody kit. Left panel: Images of arrays probed with indicated PRPs. Cytokines are spotted in duplicate and those released from PRP appear as green dots. The positions and names of cytokines that generated a detectable signal are as follows: 1: Positive control; 2: Negative control; 3: EGF; 4: EGFR; 5: GCSF; 6: GM-CSF; 7: IGFBP-1; 8: IGFBP-2; 9: IGFBP-3; 10: IGFBP-6; 11: M-CSFR; 12: PDGF-AA; 13: PDGF-AB; 14: PDGF-BB; 15: SCFR; 16: TGFb1. Cytokines that were present on the array and non detectable are as follows: amphiregulin (AR, AREG), bFGF, b-NGF, FGF-4, FGF-6, FGF-7, GDNF, HB-EGF, HGF, IGFBP-4, IGF-I, IGF-I R, IGF-II, M-CSF, NT-3, NT-4, PDGF R a, PDGF R b, PLGF, SCF, TGF alpha, TGF beta2, TGF beta3, VEGF-A, VEGFR2, VEGFR3, VEGF-D. Right panel: factors/cytokines presenting a detectable fluorescent signal are indicated. Values are the fluorescence means \pm SEM ($n = 3$ individual PRPs.) * $p < 0.05$; ** $p < 0.01$.

this effect, nor did they investigate the fate of PRP-treated ASCs. It is now essential to identify the signalling pathways responsible for PRP effects to enhance clinical applications. We demonstrated, for the first time, that PRP induced ASC myofibrogenesis differentiation at the expense of adipogenesis and that the TGF β pathway played a critical role in these effects. Pro-adipogenic effects of PRP have also been reported, but only when PRP was associated with high insulin concentrations¹¹. At these concentrations it is known that insulin mimics IGF1 effects. Interestingly, IGF-I signals cross-talk at multiple levels with various components of the TGF β signalling pathway²⁰. Further studies on the cross-talk between IGF1 and TGF β pathways would therefore be of interest, while also analysing their impact on PRP effects.

Finally, the ability of PRP to convert ASCs into myofibroblast-like cells could have clinical consequences. Myofibroblasts are known to participate in tissue repair processes while also being the cellular source of fibrosis when there is excessive collagen deposition. Recently, adipocyte-myofibroblast transition has been proposed as one of the cellular mechanisms leading to cutaneous fibrosis pathogenesis²¹. The PRP-induced ASC myofibroblast-like phenotype would thus require further investigation to assess both the benefits and potential negative outcomes. Our study highlighted a molecular mechanism that might be involved in the clinical effects of PRP when combined with ASC-enriched fat grafting. Note that PRPs can have different properties according to the system used for their purification^{15,16}. The myofibrogenic potential of PRPs from different preparation has yet to be analyzed. The next step would be to investigate our *in vitro* approach in an animal model. *In vivo* analysis of the impact of PRP depleted of TGF β activity by co-injection of PRP with pharmacological molecule inhibitors of the TGF β pathway could provide an opportunity to enhance fat grafting.

Methods

Isolation, characterization and culture of adipose-derived stem/stromal cells. Experiments were carried out using adipose stem cells (ASCs) derived from the pubic region fat pad of a 4-month old male donor. These cells were previously named hMADS3 cells²² and are called ASCs (hMADSCs) here, compliance with the international nomenclature. They were characterized according to the ISCT criteria²³ via the expression of cell surface markers and their potential to differentiate at the single cell level into adipocytes, osteoblasts and chondrocytes as previously described^{22,24}. Their potential to differentiate into myofibroblast-like cells has been more recently reported⁶. PRP effects have also been investigated on adipose-derived stromal cell (ASCs) primary cultures. They were derived from paired chin- and knee-fat depots from a healthy 72 year old female subject as described previously⁸. Briefly, chin- and knee-fat sampling was performed using 10-ml syringes and

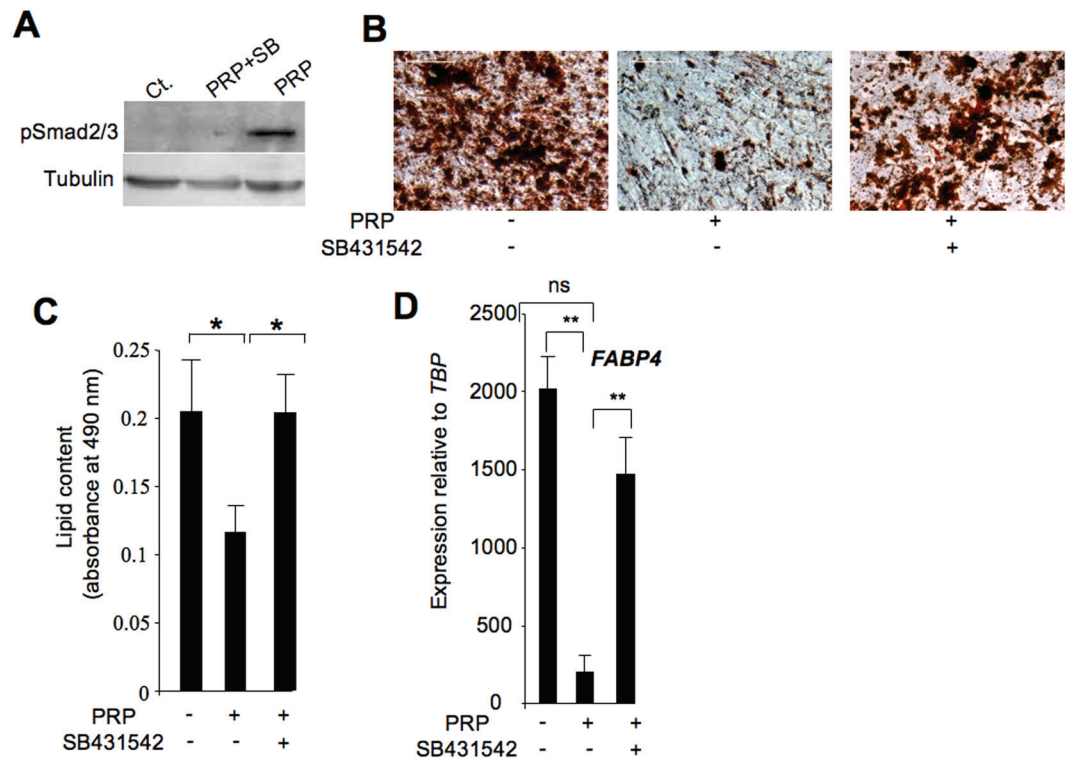


Figure 3. TGF β pathway inhibitor SB 431542 reversed anti-adipogenic PRP effects. **(A)** ASC (hMADSCs) proteins were extracted 1 hour after treatment with 20% PRPs in the absence or presence of 5 μ M SB431542 and analyzed for expression of total Smad2/3 and activated phospho Smad2/3. The blots were cropped. Full-length blots are presented in Supplementary Fig. S5. **(B)** A representative photomicrographic record of ASCs (hMADSCs) treated or not with 20% PRP and 5 μ M SB431542. Bar scale: 50 μ m. **(C)** The lipid content was measured by quantification of Oil Red O staining. Values are the mean \pm SEM ($n = 4$) for individual PRPs. **(D)** ASCs (hMADSCs) and chin-ASCs were induced to undergo adipocyte differentiation in the presence of four individual PRPs. After 10 days, RNAs were prepared and *FABP4* adipogenic gene expression was analyzed by real-time PCR. Values are the mean \pm SEM ($n = 4$ for individual PRPs). ** $p < 0.01$.

was centrifuged at $12,000 \times g$ for 3 min. The lower liquid phase and the oily upper phase were withdrawn. Fat pads were then dissociated with 200 mg/ml collagenase and the stromal vascular fraction (SVF) was separated from the adipocyte fraction by low speed centrifugation. The SVF was then seeded on tissue culture plates and adherent cells were maintained in proliferation medium composed of DMEM (low glucose) containing 10% foetal calf serum, 10 mM HEPES, 100 U/ml penicillin and streptomycin and supplemented with 2.5 ng/ml FGF2, as previously reported²⁴. ASCs were characterized by their capacity to generate adipocytes as previously described⁸. Adipose tissue samples were collected, as scraps from surgical specimens, with the informed consent of the subject, and of the baby's parents for hMADS cells. All methods were approved and performed in accordance with the guidelines and regulations of the Review Board of the Centre Hospitalier Universitaire de Nice.

PRP preparation and profiling. Whole blood was collected from six healthy donors and the six individual PRPs were prepared using the RegenACR-C Extra kit according to the manufacturer's instructions (Regen Lab, Switzerland). The donors' age and gender for the individual PRPs were: PRP A: 19 year old female; PRP B 35 year old: female; PRP C: 31 year old female; PRP D: 48 year old female; PRP F: 72 year old male and PRP G: 67 year old female. PRP was frozen for activation before the first use²⁵. PRP was then diluted at the indicated doses, where 20% represent for a fivefold dilution in the culture medium in the presence of 20 μ g/ml heparin. PRPs were not pooled but used individually. Blood samples were collected with the informed consent of the six blood donors. All methods were approved and performed in accordance with the guidelines and regulations of Review Board of the Centre Hospitalier Universitaire de Nice.

Simultaneous detection of multiple cytokines released from PRP was determined using the RayBio C_Series Human Growth Factor Antibody kit (RayBiotech, Inc, US). The specific antibodies on the array were for the detection of: amphiregulin (AR, AREG), bFGF, b-NGF, EGF, EGF R, FGF-4, FGF-6, FGF-7, GCSF, GDNF, GM-CSF, HB-EGF, HGF, IGFBP-1, IGFBP-2, IGFBP-3, IGFBP-4, IGFBP-6, IGF-I, IGF-I R, IGF-II, M-CSF, M-CSF R, NT-3, NT-4, PDGF R a, PDGF R b, PDGF-AA, PDGF-AB, PDGF-BB, PLGF, SCE, SCF R, TGF alpha, TGF beta 1, TGF beta2, TGF beta3, VEGF-A, VEGFR2, VEGFR3, VEGF-D. PRP profiling was performed by the Tebu-Bio service (France) according to manufacturer's instructions.

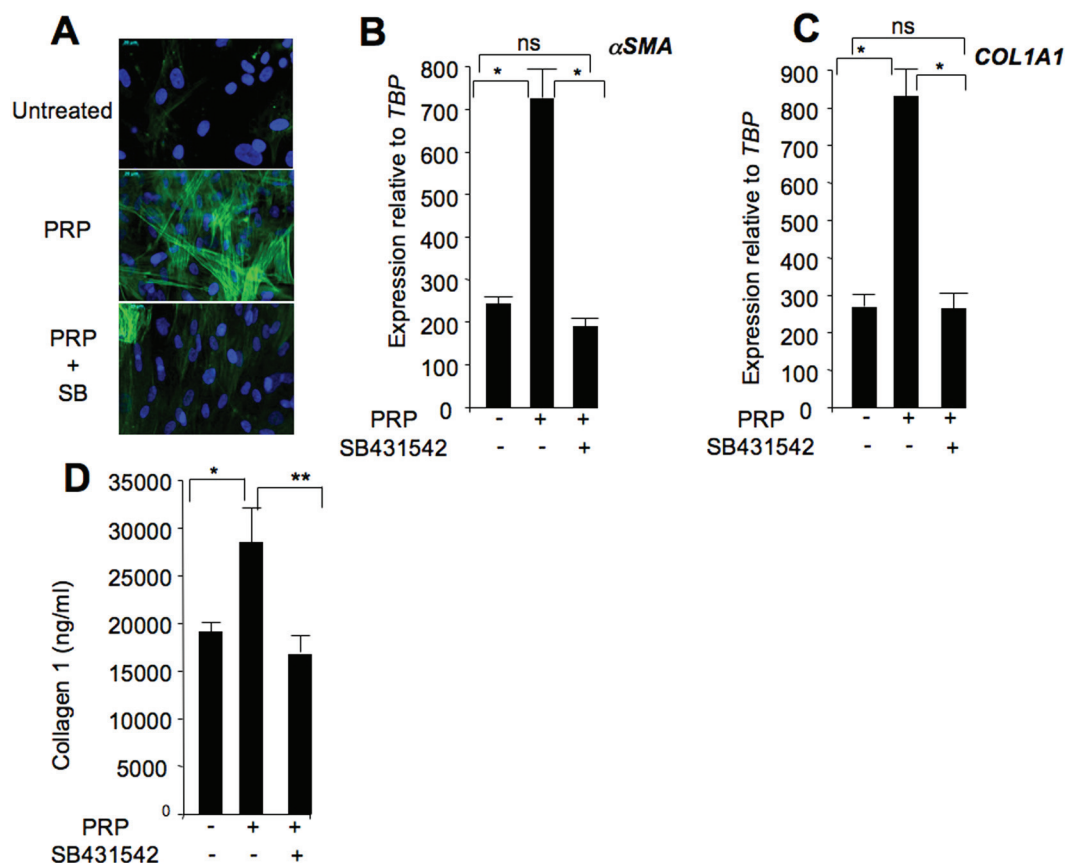


Figure 4. PRP-induced myofibroblast-like phenotype reversed by SB431542. ASCs were induced to undergo adipocyte differentiation for 11 days in the indicated conditions. (A) Generation of α SMA-expressing cells was revealed by immunofluorescence. (B,C) RNAs were prepared and expression of the indicated genes was analyzed by real-time PCR. Values are the mean \pm SEM (n = 4 individual PRPs). (D) Media were collected and collagen type 1 secretion was quantified. Values are the mean \pm SEM (n = 4 individual PRPs). *p < 0.05, **p < 0.01.

ELISA and collagen secretion. IGFBP3 and PDGF-AA were quantified using Sigma-Aldrich (Saint-Louis) ELISA kits and TGF β 1 using the Biosciences (London) ELISA kit. Leptin using the TECO medical ELISA kit (Sissach, Switzerland). Secretion of type I collagen in response to PRP treatment was quantified with an enzyme-linked immunosorbent assay according to the supplier's instructions (PCI C-peptide EIA KIT, Takara Bio Inc, Japan).

Assessment of ASC differentiation. ASCs were maintained in proliferation medium until they reached confluence. Then, cells were induced to undergo differentiation in adipogenic medium composed of DMEM supplemented with 10% FCS, 0.5 mM isobutyl-methylxanthine, 0.25 μ M dexamethasone, 0.2 nM triiodothyronine, 1 μ g/ml insulin and 1 μ M rosiglitazone (BRL49653, a PPAR γ agonist), 20 μ g/ml heparin in the absence or presence of PRP.

Lipid accumulation was assessed by Oil Red O staining. Cells were stained as previously described²⁶ and images were recorded under light microscopy. Then, Oil Red O stained cells were quantified by washing in water and lipid-bound Oil Red-O was dissolved in isopropanol for 15 min. Dissolved Oil Red O absorbance was determined at 490 nm on a microplate reader (BioRad iMark).

Adipogenic-and myofibroblast-gene expression was performed by quantitative PCR. RNAs were purified on RNeasy columns (Qiagen, France). RNA sample concentrations were determined using a Nanodrop spectrophotometer (Thermo Scientific, Waltham, MA, USA). Real-time PCR assays were run on a StepOnePlus system (Applied Biosystems, Life Technologies France). Transcript expression levels were evaluated using the comparative CT method (2-deltaCT). Delta delta Ct values were used when the 'expression relative to TBP' was indicated. The TATA-binding protein gene expression (TBP) was used for sample normalization.

Primer sequences used for real-time PCR were:

PPAR γ : Fw: AGCCTCATGAAGAGCCTTCCA; Rv: TCCGGAAGAAACCCCTTGCA

Adiponectin Fw: GCAGTCTGTGGTTCTGATTCCATAC; Rv: GCCCTTGAGTCGTGGTTTCC

FABP4 Fw: GGGACGTGACCTGGACTGA; Rv: GGGAGAAAATTACTTGCTTGCTAAA

ColA1 Fw: ACCTGCGTGTACCCCACTCA; Rv: CCGCCATACTCGAACTGGAA

Alpha smooth muscle actin Fw: TGGATCAGCAAACAGGAATACG; Rv: GCATTTGCGGTGGACAATG

TBP Fw: ACGCCAGCTTCGGAGAGTTC; Rv: CAAACCGCTTGGGATTATATTCGA

For protein preparation and Western blot analysis cells were rinsed with PBS and solubilized in stop buffer containing 50 mM Hepes, at pH 7.2, 150 mM NaCl, 10 mM EDTA, 10 mM Na₄P₂O₇, 2 mM Na₃VO₄, and 1% Triton X-100 supplemented with Protease Inhibitor Cocktail (Roche). Antibodies against Phospho-Smad2 (Ser465/467) and total Smad2/3 were from Cell Signaling. Anti-Tubulin was from Sigma and used according to the manufacturer's instructions. Western-blots were performed as previously described²⁷.

For immunofluorescence, cells were fixed for 10 min in Roti-Histofix (Roth, Lauterbourg, France). Nonspecific signals were blocked with 3% bovine serum albumin containing 0.1% tween-20 and 0.1% Triton X-100 for 30 min permeabilization. α smooth muscle actin (α SMA) antibody was from BD-Biosciences (Le Pont de Claix, France) and the secondary Alexa Fluor[®] 488 conjugated antibody was purchased from Life Technologies SAS (Saint Aubin, France). Cells were mounted in Mowiol containing Hoechst, and visualized with an Axiovert microscope (Carl Zeiss, Le Pecq, France) under oil immersion. Images were taken on a Zeiss Axio Observer microscope with a EC Plan Neofluar 40X (NA 1.3) oil objective using AxioVision 4.8.2 software and captured using AxioVision software (Zeiss).

Statistical analysis. The data are the means \pm SEM. Statistical analyses were performed using InStat3 software. A nonparametric unpaired test (Mann-Whitney or Student's *t*-test) was used. P values < 0.05 were considered significant.

References

- Blanton, M. W. *et al.* Adipose stromal cells and platelet-rich plasma therapies synergistically increase revascularization during wound healing. *Plast Reconstr Surg* **123**, 56S–64S, doi:10.1097/PRS.0b013e318191be2d (2009).
- Liao, H. T., Marra, K. G. & Rubin, J. P. Application of platelet-rich plasma and platelet-rich fibrin in fat grafting: basic science and literature review. *Tissue Eng Part B Rev* **20**, 267–76, doi:10.1089/ten.teb.2013.0317 (2013).
- Kolle, S. F. *et al.* Enrichment of autologous fat grafts with *ex-vivo* expanded adipose tissue-derived stem cells for graft survival: a randomised placebo-controlled trial. *Lancet* **382**, 1113–20, doi:10.1016/S0140-6736(13)61410-5 (2013).
- D'Esposito, V. *et al.* Platelet-Rich Plasma Increases Growth and Motility of Adipose Tissue-Derived Mesenchymal Stem Cells and Controls Adipocyte Secretory Function. *J Cell Biochem* **116**, 2408–18, doi:10.1002/jcb.v116.10 (2015).
- Willemsen, J. C., Spiekman, M., Stevens, H. P., van der Lei, B. & Harmsen, M. C. Platelet-Rich Plasma Influences Expansion and Paracrine Function of Adipose-Derived Stromal Cells in a Dose-Dependent Fashion. *Plast Reconstr Surg* **137**, 554e–565e, doi:10.1097/01.prs.0000479995.04255.bb (2016).
- Bourlier, V. *et al.* TGFbeta Family Members Are Key Mediators in the Induction of Myofibroblast Phenotype of Human Adipose Tissue Progenitor Cells by Macrophages. *PLoS One* **7**, e31274, doi:10.1371/journal.pone.0031274 (2012).
- Dani, C. Activins in adipogenesis and obesity. *Int J Obes (Lond)* **37**, 163–6, doi:10.1038/ijo.2012.28 (2013).
- Kouidhi, M. *et al.* Characterization of human knee and chin adipose-derived stromal cells. *Stem Cells Int* **2015**, 592090–11, doi:10.1155/2015/592090 (2015).
- Liao, H. T., James, I. B., Marra, K. G. & Rubin, J. P. The Effects of Platelet-Rich Plasma on Cell Proliferation and Adipogenic Potential of Adipose-Derived Stem Cells. *Tissue Eng Part A* **21**, 2714–22, doi:10.1089/ten.tea.2015.0159 (2015).
- Kakudo, N. *et al.* Proliferation-promoting effect of platelet-rich plasma on human adipose-derived stem cells and human dermal fibroblasts. *Plast Reconstr Surg* **122**, 1352–60, doi:10.1097/PRS.0b013e3181882046 (2008).
- Cervelli, V. *et al.* Platelet-rich plasma greatly potentiates insulin-induced adipogenic differentiation of human adipose-derived stem cells through a serine/threonine kinase Akt-dependent mechanism and promotes clinical fat graft maintenance. *Stem Cells Transl Med* **1**, 206–20, doi:10.5966/sctm.2011-0052 (2012).
- Zamani, N. & Brown, C. W. Emerging roles for the transforming growth factor- β superfamily in regulating adiposity and energy expenditure. *Endocr Rev* **32**, 387–403, doi:10.1210/er.2010-0018 (2011).
- Inman, G. J. *et al.* SB-431542 is a potent and specific inhibitor of transforming growth factor-beta superfamily type I activin receptor-like kinase (ALK) receptors ALK4, ALK5, and ALK7. *Mol Pharmacol* **62**, 65–74, doi:10.1124/mol.62.1.65 (2002).
- Meng, X. M., Nikolic-Paterson, D. J. & Lan, H. Y. TGF-beta: the master regulator of fibrosis. *Nat Rev Nephrol* **12**, 325–38, doi:10.1038/nrneph.2016.48 (2016).
- Magalon, J. *et al.* Characterization and comparison of 5 platelet-rich plasma preparations in a single-donor model. *Arthroscopy* **30**, 629–38, doi:10.1016/j.arthro.2014.02.020 (2014).
- Mazzucco, L., Balbo, V., Cattana, E., Guaschino, R. & Borzini, P. Not every PRP-gel is born equal. Evaluation of growth factor availability for tissues through four PRP-gel preparations: Fibrinet, RegenPRP-Kit, Plateletex and one manual procedure. *Vox Sang* **97**, 110–8, doi:10.1111/vox.2009.97.issue-2 (2009).
- Bouloumie, A., Drexler, H. C., Lafontan, M. & Busse, R. Leptin, the product of Ob gene, promotes angiogenesis. *Circ Res* **83**, 1059–66, doi:10.1161/01.RES.83.10.1059 (1998).
- Chan, S. S., Schedlich, L. J., Twigg, S. M. & Baxter, R. C. Inhibition of adipocyte differentiation by insulin-like growth factor-binding protein-3. *Am J Physiol Endocrinol Metab* **296**, E654–63, doi:10.1152/ajpendo.90846.2008 (2009).
- Liu, H. Y. *et al.* The balance between adipogenesis and osteogenesis in bone regeneration by platelet-rich plasma for age-related osteoporosis. *Biomaterials* **32**, 6773–80, doi:10.1016/j.biomaterials.2011.05.080 (2011).
- Danielpour, D. & Song, K. Cross-talk between IGF-I and TGF-beta signaling pathways. *Cytokine Growth Factor Rev* **17**, 59–74, doi:10.1016/j.cytogfr.2005.09.007 (2006).
- Marangoni, R. G. *et al.* Myofibroblasts in murine cutaneous fibrosis originate from adiponectin-positive intradermal progenitors. *Arthritis Rheumatol* **67**, 1062–73, doi:10.1002/art.v67.4 (2015).
- Rodriguez, A.-M. *et al.* Transplantation of a multipotent cell population from human adipose tissue induces dystrophin expression in the immunocompetent mdx mouse. *J. Exp. Med.* **201**, 1397–1405, doi:10.1084/jem.20042224 (2005).
- Dominici, M. *et al.* Minimal criteria for defining multipotent mesenchymal stromal cells. The International Society for Cellular Therapy position statement. *Cytotherapy* **8**, 315–7, doi:10.1080/14653240600855905 (2006).
- Zaragosi, L. E., Ailhaud, G. & Dani, C. Autocrine fibroblast growth factor 2 signaling is critical for self-renewal of human multipotent adipose-derived stem cells. *Stem Cells* **24**, 2412–9, doi:10.1634/stemcells.2006-0006 (2006).
- Roffi, A. *et al.* Does platelet-rich plasma freeze-thawing influence growth factor release and their effects on chondrocytes and synoviocytes? *Biomed Res Int* **2014**, 692913–10, doi:10.1155/2014/692913 (2014).
- Wdziekonski, B., Villageois, P. & Dani, C. Development of adipocytes from differentiated ES cells. *Methods Enzymol* **365**, 268–77, doi:10.1016/S0076-6879(03)65019-6 (2003).
- Hafner, A. L. *et al.* Brown-like adipose progenitors derived from human induced pluripotent stem cells: Identification of critical pathways governing their adipogenic capacity. *Sci Rep* **6**, 32490, doi:10.1038/srep32490 (2016).

Acknowledgements

This study was supported by the French government (ANR) through the “Investments for the future” LABEX Signalife, program reference ANR-11-LABEX-0028-01, by the Agence de Biomédecine Greffe 2016, and the Fondation des Gueules Cassées n°05-2015.

Author Contributions

B.C.-S. and M.K. designed and conducted the experiments; X.Y., P.V., A.D.-A., P.F. and P.P. conducted experiments; Y.R., D.P., J.A., B.C.-S. and C.D. analyzed the results; C.D. wrote the manuscript. All authors reviewed the manuscript.

Additional Information

Supplementary information accompanies this paper at doi:[10.1038/s41598-017-03113-0](https://doi.org/10.1038/s41598-017-03113-0)

Competing Interests: The authors declare that they have no competing interests.

Publisher's note: Springer Nature remains neutral with regard to jurisdictional claims in published maps and institutional affiliations.



Open Access This article is licensed under a Creative Commons Attribution 4.0 International License, which permits use, sharing, adaptation, distribution and reproduction in any medium or format, as long as you give appropriate credit to the original author(s) and the source, provide a link to the Creative Commons license, and indicate if changes were made. The images or other third party material in this article are included in the article's Creative Commons license, unless indicated otherwise in a credit line to the material. If material is not included in the article's Creative Commons license and your intended use is not permitted by statutory regulation or exceeds the permitted use, you will need to obtain permission directly from the copyright holder. To view a copy of this license, visit <http://creativecommons.org/licenses/by/4.0/>.

© The Author(s) 2017

Cdkn2a deficiency promotes adipose tissue browning



Nabil Rabhi^{1,2,3,8,9}, Sarah Anissa Hannou^{1,2,3,8}, Xavier Gromada^{1,2,3,8}, Elisabet Salas^{1,2,3}, Xi Yao⁴, Frédéric Oger^{1,2,3}, Charlene Carney^{1,2,3}, Isabel C. Lopez-Mejia⁵, Emmanuelle Durand^{1,2,3}, Landry Rabearivelo^{1,2,3}, Amélie Bonnefond^{1,2,3}, Emilie Caron⁶, Lluís Fajas⁵, Christian Dani⁴, Philippe Froguel^{1,2,3,7,*,10}, Jean-Sébastien Annicotte^{1,2,3,*,10,11}

ABSTRACT

Objectives: Genome-wide association studies have reported that DNA polymorphisms at the *CDKN2A* locus modulate fasting glucose in human and contribute to type 2 diabetes (T2D) risk. Yet the causal relationship between this gene and defective energy homeostasis remains elusive. Here we sought to understand the contribution of *Cdkn2a* to metabolic homeostasis.

Methods: We first analyzed glucose and energy homeostasis from *Cdkn2a*-deficient mice subjected to normal or high fat diets. Subsequently *Cdkn2a*-deficient primary adipose cells and human-induced pluripotent stem differentiated into adipocytes were further characterized for their capacity to promote browning of adipose tissue. Finally *CDKN2A* levels were studied in adipocytes from lean and obese patients.

Results: We report that *Cdkn2a* deficiency protects mice against high fat diet-induced obesity, increases energy expenditure and modulates adaptive thermogenesis, in addition to improving insulin sensitivity. Disruption of *Cdkn2a* associates with increased expression of brown-like/beige fat markers in inguinal adipose tissue and enhances respiration in primary adipose cells. Kinase activity profiling and RNA-sequencing analysis of primary adipose cells further demonstrate that *Cdkn2a* modulates gene networks involved in energy production and lipid metabolism, through the activation of the Protein Kinase A (PKA), PKG, PPARGC1A and PRDM16 signaling pathways, key regulators of adipocyte beiging. Importantly, *CDKN2A* expression is increased in adipocytes from obese compared to lean subjects. Moreover silencing *CDKN2A* expression during human-induced pluripotent stem cells adipogenic differentiation promoted UCP1 expression.

Conclusion: Our results offer novel insight into brown/beige adipocyte functions, which has recently emerged as an attractive therapeutic strategy for obesity and T2D. Modulating *Cdkn2a*-regulated signaling cascades may be of interest for the treatment of metabolic disorders.

© 2017 The Authors. Published by Elsevier GmbH. This is an open access article under the CC BY-NC-ND license (<http://creativecommons.org/licenses/by-nc-nd/4.0/>).

Keywords Obesity; Type 2 diabetes; Insulin sensitivity; Energy expenditure; *cdkn2a*; Genome-wide association study; Adipose tissue browning

1. INTRODUCTION

Obesity is the main risk factor for type 2 diabetes (T2D) and is due to an imbalance between energy intake and energy expenditure. Current anti-obesity drugs affecting energy intake or intestinal lipid absorption cause important and troublesome side effects for the patient, which limits their use. On the other hand, bariatric surgery has proven efficient for obesity and for diabetes remission with a dramatic effect on

insulin resistance, although long-term complications and obesity relapse may arise. Therefore, understanding the signaling pathways that control fat storage and energy expenditure may open alternative avenues against obesity and linked T2D.

In animal models, genes such as *E2f1* and *Sertad2* (TRIP-Br2) have been shown to prevent fat accumulation and protect against diet-induced obesity (DIO), but they also improve insulin action in metabolic organs including adipose tissue [1–3]. Two major types of

¹Lille University, UMR 8199 — EGID, F-59000 Lille, France ²CNRS, UMR 8199, F-59000 Lille, France ³Institut Pasteur de Lille, F-59000 Lille, France ⁴Université Côte d'Azur, CNRS, INSERM, iBV, Faculté de Médecine, F-06107 Nice Cedex 2, France ⁵Center for Integrative Genomics, Université de Lausanne, CH-1015 Lausanne, Switzerland ⁶INSERM, UMR S-1172, Development and Plasticity of Postnatal Brain, F-59000 Lille, France ⁷Department of Genomics of Common Disease, School of Public Health, Imperial College London, Hammersmith Hospital, London W12 0NN, UK

⁸ These authors contributed equally.

⁹ Present address: Department of Biochemistry, Boston University School of Medicine, MA 02118, USA.

¹⁰ Senior authors.

¹¹ Lead contact.

*Corresponding authors. UMR 8199 (CNRS/Université de Lille 2/Institut Pasteur de Lille), Faculté de Médecine — Pôle recherche, 1 place de Verdun, 59045 Lille Cedex, France. E-mails: p.froguel@imperial.ac.uk (P. Froguel), jean-sebastien.annicotte@inserm.fr (J.-S. Annicotte).

Received November 14, 2017 • Accepted November 23, 2017 • Available online 1 December 2017

<https://doi.org/10.1016/j.molmet.2017.11.012>

adipose tissues exist that are anatomically and functionally distinct: white (WAT) and brown (BAT) adipose tissues. Recent studies have revealed a new distinct type of thermogenic adipocyte intermingled within WAT, named beige cells (also known as brite cells). White adipocytes store excess energy as triacylglycerol and release free fatty acids (FFAs) as energy substrate when required. On the other hand, the catabolic capability of BAT and beige adipocytes to burn fat contributes to reduce circulating FFAs. Indeed, BAT expresses high levels of uncoupling protein 1 (UCP1), leading to substrate oxidation and subsequent heat production and energy expenditure (for review, see Ref. [4]). Beige adipocytes also express UCP1 and develop under cold exposure. This adaptive process is called WAT beiging/browning [5]. In pathological conditions such as obesity, elevated circulating FFAs are associated with insulin resistance and T2D. Since energy balance is modulated by food intake, physical activity, as well as non-shivering thermogenesis in BAT, increasing energy expenditure by classical BAT activation or by promoting browning of WAT have recently emerged as new putative therapy to alleviate the effects of obesity and prevent insulin resistance and T2D [4,6]. Recent reports in humans further confirmed the important function of brown/beige adipocytes in enhancing glucose tolerance and insulin sensitivity [7,8]. Therefore, the identification of selective molecular pathways for beige adipocyte biogenesis would represent a first step towards innovative therapeutic options.

Genome-wide association studies (GWASs) have established the *CDKN2A/B* locus as a hotspot influencing genetic risk for different cardio-metabolic diseases including T2D [9,10]. *CDKN2A/B* single nucleotide polymorphisms associated with T2D also modulate fasting insulin and insulin sensitivity in non-diabetic subjects [11]. In particular, rs10757278-G and rs10811661-T SNPs are situated near the *CDKN2A/B* locus on chromosome 9p21.3 and are respectively associated with the risk for coronary artery disease (CAD) and T2D [12]. The genomic regions containing those SNPs are also in close vicinity of the long non-coding RNA *ANRIL* (Antisense Non-coding RNA in the Inhibitor of CDK4 (INK4) Locus). The function of *ANRIL* is still unknown but it seems to be involved in the epigenetic repression of the *CDKN2A/B* locus [13]. Although rs10757278 and rs10811661 are less than 10 kb away from *CDKN2A/B* genes, those SNPs may affect dynamic chromosome structures and genome activity. Indeed, rs10811661 is negatively associated with a trans-eQTL, presenilin 1 (*PSEN1*), a gene associated in mice with glucose intolerance and insulin resistance [14]. In addition, Lillycrop et al. recently demonstrated that decreased DNA methylation at the *CDKN2A* gene is associated with a higher risk for a child to develop obesity during adulthood [15]. Furthermore, rare heterozygous loss-of-function mutations in *CDKN2A* affect glucose homeostasis through its metabolic role in pancreatic beta cells and liver [16]. Altogether, those results pinpoint the importance of studying the impact of loss-of-function of *CDKN2A* in metabolic tissues.

The human *CDKN2A* locus encodes for p16^{INK4a} a CDK inhibitory (CDKI) protein and the p53 regulatory protein p14^{ARF} (p19^{ARF} in mice), whereas the *CDKN2B* gene encodes another CDKI, p15^{INK4b}. Products of the *CDKN2A/B* locus are involved in apoptosis, senescence, and aging [9]. Whilst p16 and p15 are potent CDKI preventing binding of CDK4/6 to Cyclin D, p14^{ARF} mainly exerts its anti-proliferative activity via the inhibition of MDM2, an ubiquitin-ligase that modulates the activity of the tumor suppressor p53. The *CDKN2A/B* pathway is involved in metabolic control through several ways including adipocyte differentiation [17–19], macrophage polarization [20], fasted–fed transition [21,22], muscle metabolism [1], and pancreatic beta cell proliferation, regeneration, and function [23–25].

While rodent and human studies have highlighted the potential role of *CDKN2A* on insulin secretion [16,26], the contribution of *CDKN2A* to the control of insulin sensitivity is still elusive.

To decipher the link between *Cdkn2a*, obesity and insulin resistance, we analyzed the effect of *Cdkn2a* deficiency in mice on metabolic homeostasis [27]. Here, we demonstrate that the genetic deletion of *Cdkn2a* promotes energy expenditure and improves insulin sensitivity during DIO. We found that the *Cdkn2a* locus modulates signaling pathways in inguinal WAT (ingWAT), where it controls beige adipocyte development. Importantly, we observed that *CDKN2A* expression is increased in adipocytes from obese patients. *CDKN2A* silencing during human-induced pluripotent stem cells adipogenic differentiation promoted UCP1 expression. These data suggest that *Cdkn2a* plays a key role in energy metabolism by regulating a white-to-brown fat transition.

2. MATERIAL AND METHODS

2.1. Materials and oligonucleotides

Chemicals, unless stated otherwise, were purchased from Sigma–Aldrich. Anti-UCP1 antibody was purchased from Abcam, and anti-PKA substrate antibody was from Cell Signaling Technology. The oligonucleotide sequences used for various experiments are listed in Table S5.

2.2. Animals experiments

Cdkn2a^{+/+} and *Cdkn2a*^{-/-} mice were previously described [27] and were maintained on a mixed background according to European Union guidelines for use of laboratory animals. *In vivo* experiments were performed in compliance with the French ethical guidelines for studies on experimental animal (Animal house agreement no. B 59-35015, Authorization for Animal Experimentation no. 59-350294, project approval by our local ethical committee no. CEEA 482012). All experiments were performed with healthy male mice. Animals with detectable tumors were excluded from the study. Mice were housed under a 12 h light–dark cycle and given a regular chow (A04; Safe). For HFD studies, 8-week old mice were placed on D12492 diet (60% cal/fat; Research Diet Inc.) for 13 weeks. Metabolic phenotyping experiments were performed according to the EMPRESS protocols (<http://empress.har.mrc.ac.uk>). Briefly, intraperitoneal glucose (2 g of glucose per kg of body weight) and insulin (0.75 U of insulin per kg of body weight) tolerance tests were performed as previously described [28,29] on 16-h-fasted animals for IPGTT and 5-h-fasted animals for ITT. Glycemia was measured before and at different time after glucose and insulin injections using the Accu-Check Performa (Roche Diagnostics). Circulating insulin levels were measured using the Ultrasensitive Insulin Elisa kit (Mercodia). For cold experiments, mice were maintained at +23 °C or placed at +4 °C for 5h and fasted during the time of the experiment. Body temperature was measured using a rectal probe as described previously [1]. Metabolic rate was measured by indirect calorimetry using the Phenomaster metabolic cage system (TSE Systems). Mice were housed individually and maintained at 23 °C under a 12 h light/12 h dark cycle. Food and water were available *ad libitum*. Mice were sacrificed by cervical dislocation and tissues were harvested and snap-frozen for further processing.

2.3. RNA extraction, measurements, and profiling

Total RNA was extracted from rodent cells and tissues using trizol reagent (Life Technologies) as described previously [1,28]. mRNA expression was measured after reverse transcription by quantitative

real-time PCR (qRT-PCR) with FastStart SYBR Green master mix (Roche) according to the manufacturer's recommendations and gene-specific oligonucleotides. Mouse qRT-PCR results were normalized to endogenous cyclophilin reference mRNA levels. The results are expressed as the relative mRNA level of a specific gene expression using the formula $2^{-\Delta Ct}$. For human cells, RNAs were purified on RNeasy Plus Universal columns (Qiagen, France) according to the manufacturer's instructions. Total RNA sample concentrations were determined using a Nanodrop spectrophotometer (Thermo Scientific, Waltham, MA, USA). 1 μ g RNA was used for reverse transcription. Real-time PCR assays were run on a OneStep real-time PCR machine (Applied Life Sciences) and SYBR green was from Applied Biosystems. Normalization was performed using the geometric averages of the housekeeping gene *TBP*. Delta Ct values were used to achieve relative quantification of gene expression when "expression relative to *TBP*" is indicated.

2.4. Histology, immunofluorescence (IF), and immunohistochemistry (IHC)

IF and IHC were performed exactly as described previously [1,28]. Briefly, deparaffinized adipose tissues sections (5 μ m) were subjected to heat-induced antigen retrieval. The slides were incubated with 0.3% H₂O₂ for 10 min to quench the endogenous peroxidase. The sections were then incubated in 1% BSA/PBS for 10 min, followed by overnight incubation with primary (Rabbit-UCP1) antibodies at 4 °C. Afterward, the slides were incubated at room temperature for 2 h with horseradish peroxidase (HRP)-conjugated (for IHC) or Alexa-conjugated anti-rabbit secondary antibodies (for IF, Fischer Scientific). The IHC staining was developed using fast 3,3'-diaminobenzidine (DAB) tablet sets (D4293; Sigma, St. Louis, MO, USA). The sections were counterstained with hematoxylin and examined by light microscopy. H&E staining was performed using classical protocols. For IF, nuclei were stained with Hoechst. Images were processed using ImageJ software by two observers blinded to experimental groups.

2.5. Protein extracts, PKA activity measurement and immunoblot analysis

Immunoblot was performed as described previously [1,29]. Tissues and cells were washed using cold PBS, and lysis was performed by using 50 mM Tris-HCl pH 8, 137 mM NaCl, 10% glycerol, 1% NP-40 and phosphatase, protease, deacetylase inhibitors (Sigma-Aldrich) on ice. Western blotting was performed using 30 μ g of proteins loaded on SDS-PAGE precast gel (Biorad). After electrotransfer, the membrane was blocked for 1 h at room temperature with 5% nonfat milk in 0.1% Tween-Tris-buffered saline (TTBS) buffer. Membranes were then incubated overnight at 4 °C with primary antibodies as indicated in blocking buffer containing 5% nonfat milk or 0.5% bovine serum albumin at the dilution specified by the manufacturers. Subsequently, membranes were incubated with the secondary antibody conjugated with the horseradish peroxidase enzyme. The visualization of immunoreactive bands was performed using the enhanced chemiluminescence plus western blotting detection system (GE Healthcare). hiPSCs-BAP cells were rinsed with PBS and solubilized in stop buffer containing 50 mM Hepes, pH 7.2, 150 mM NaCl, 10 mM EDTA, 10 mM Na₄P₂O₇, 2 mM Na₃VO₄, and 1% Triton X-100 supplemented with Protease Inhibitor Cocktail (Roche). The primary antibodies and dilutions used were: UCP1 (1/500, Abcam), Tubulin (1/10,000, Sigma); secondary horseradish peroxidase-conjugated antibodies were purchased from Sigma. Quantitation of protein signal intensity was performed by volume densitometry using the ImageJ 1.47t software (National Institutes of Health). PKA activity was

measured on tissue homogenates using the non-radioactive PKA Kinase Activity assay kit following manufacturers' instructions (Abcam).

2.6. Primary adipocyte cell culture

The stromal vascular fraction (SVF) of inguinal adipose or BAT tissues of 8-week old mice was isolated by collagenase (ROCHE) digestion followed by two alternative filtration steps (using 100 and 40 μ m strainers) and centrifugations for 5 min at 700 \times rpm. Cells were then plated and differentiated upon confluence in DMEM/F-12 GlutaMAX with adipogenic cocktail (0.5 mM 3-isobutyl-1-methylxanthine [IBMX], 2.5 μ M dexamethasone, 1 μ M rosiglitazone, 0.02 μ M insulin for inguinal cells and 0.02 μ M insulin, 0.125 μ M indomethacin, 0.5 mM 3-isobutyl-1-methylxanthine [IBMX], 2.5 μ M dexamethasone and 1 nM T3, for BAT cells) for 48 h. Inguinal cells were maintained in 0.02 μ M insulin and BAT cells in 1 nM T3 and 0.02 μ M insulin. Cells were harvested at days 8 post-differentiation. To label lipid droplets, fully differentiated primary adipocytes cells were fixed in 4% PFA then labeled with BODIPY 493/503 lipid probe solution (Molecular Probes/Life Technologies) for 30 min. After PBS wash the staining was examined by fluorescence microscopy.

2.7. Cell culture and siRNA experiments

Brown-like adipose progenitors (BAPs) were derived from human-induced pluripotent stem cells (hiPSCs) and induced to undergo adipocyte differentiation as described in Mohsen-Kanson et al. [65] and Hafner et al. [66]. For more details see <http://www.nature.com/protocolexchange/protocols/5175>. hiPSC-BAPs were transfected with small interfering RNA duplexes (Human CDKN2A siRNA-SMART pool, GEHealth Bio-Sciences, Rosersberg, Sweden) using HiPerfect reagent (Qiagen, France) during the exponential growth phase as described by the supplier.

2.8. Pamgene experiments

For kinase analysis, STK microarrays were purchased from PamGene International BV (STK pamchips, Ref. [32]). Each array contained 140 phosphorylatable peptides as well as 4 control peptides. Sample incubation, detection, and analysis were performed in a PamStation 12 according to the manufacturer's instructions. Briefly, extracts from fully differentiated day 8 (D8) primary adipocytes from *Cdkn2a*^{+/+} and *Cdkn2a*^{-/-} mice were freshly prepared using M-PER mammalian extraction buffer (Thermo Scientific) containing 1:50 Halt phosphatase inhibitor cocktail (Thermo Scientific) and 1:50 Halt protease inhibitor cocktail, EDTA-free (Thermo Scientific) for 20 min on ice. The lysates were then centrifuged at 15,871 g for 20 min to remove all debris. The supernatant was aliquoted, snap-frozen in liquid nitrogen, and stored at -80 °C until further processing. Prior to incubation with the kinase reaction mix, the arrays were blocked with 2% BSA in water for 30 cycles and washed 3 times with the PK assay buffer. Kinase reactions were performed for 1 h with 2.5 μ g of total extract of the mature adipocyte and 400 μ M ATP at 30 °C. Phosphorylated peptides were detected with an anti-rabbit-FITC antibody that recognizes a pool of anti-phospho serine/threonine antibodies. The instrument contains a 12-bit CCD camera suitable for imaging of FITC-labeled arrays. The images obtained from the phosphorylated arrays were quantified using the BioNavigator software (PamGene International BV), and the list of peptides whose phosphorylation was significantly different between *Cdkn2a*^{+/+} and *Cdkn2a*^{-/-} was uploaded to IPA for pathway analysis. The BioNavigator software was used to perform the HPRD based upstream kinase determination that is shown in Figure 4C.

2.9. RNA sequencing

Total RNA was extracted from primary adipocytes 8 days after differentiation using the RNeasy Microkit (Qiagen) following manufacturer's instructions. RNA quality was verified using RNA 6000 nanochips on the Agilent 2100 bioanalyzer. Purified RNA (200 ng) with RNA integrity number ≥ 8 was subsequently used for library preparation (TruSeq Stranded mRNA Library Preparation Kit, Illumina) and sequenced on a HiSeq2500 (Illumina). Three biological replicates per condition were sequenced in paired-end. A mean of 54 million paired-end reads of 75 bp were generated for each sample. After initial checks and validation of sequence quality, RNA-seq reads were aligned to the mouse reference genomes (mm10) using TopHat2 [33]. Subsequently, both quantification and annotation of the reads were performed using Bioconductor package Rsubread [34]. Finally, the differential gene expression analyses were performed using Bioconductor package DESeq2 [35]. Using a $p < 0.05$ adjusted for multiple comparisons as threshold, we then performed pathway analysis using Ingenuity Pathway Analysis (Ingenuity Systems).

2.10. Seahorse experiments

Oxygen consumption rate (OCR) was performed using the XF24e platform from Seahorse Biosciences. Primary adipocytes from *Cdkn2a*^{+/+} and *Cdkn2a*^{-/-} mice were grown and differentiated in a Seahorse plate. Growth medium was replaced with 37 °C seahorse DMEM 1 h before the measurement to allow equilibrium. Measurement was performed at 37 °C, using 3–3–3-min intervals. Basal respiration was measured then uncoupled, and maximal OCR were determined using oligomycin and carbonyl cyanide p-trifluoromethoxyphenylhydrazone (FCCP, 1 μ M each), respectively. Complex I-dependent respiration was inhibited with rotenone (3 μ M). OCR data were normalized using total protein or DNA content as indicated.

2.11. Human adipocyte expression data

Gene Expression Omnibus (GEO) analysis from the NCBI was performed using “adipocytes obese human” as keywords, filtered with “published in the last year” and sorted by the number of samples “high to low”. The dataset GSE94753 [36] was selected and analyzed using GEO2R. The platform GPL11532 was selected and groups were defined using the disease status (lean, WAT, control *versus* obese resistant, WAT OIR). Expression level data were extracted from “profile graph” using *CDKN2A* ID 8160441.

2.12. Statistical analysis

Data are presented as mean \pm SEM. Statistical analyses were performed using unpaired two-tailed Student's *t*-test, one-way ANOVA with least significant difference Bonferroni post hoc test or two-way ANOVA with Bonferroni post hoc tests as appropriate using GraphPad Prism software. Differences were considered statistically significant at $p < 0.05$ (* $p < 0.05$; ** $p < 0.01$ and *** $p < 0.001$).

3. RESULTS

3.1. Germline *Cdkn2a* deficiency improves insulin sensitivity in mice

We first analyzed the metabolic profile of *Cdkn2a*-deficient mice [27]. 9- to 12-week old *Cdkn2a*^{+/+} and *Cdkn2a*^{-/-} mice fed a chow diet (CD) displayed similar body weight (Figure 1A), glucose tolerance (Figure 1B, C) and fasting glycemia (Figure S1A). *In vivo* glucose stimulated insulin secretion (GSIS) was similar in both genotypes under CD (Figure 1D). After 13 weeks of high fat diet (HFD) feeding, body weight of *Cdkn2a*^{-/-} mice was lower than that of age-matched

control mice (Figure 1E), with comparable fasting glucose levels (Figure S1B) and similar glucose clearance during ipGTT tests (Figure 1F, G). As expected, upon HFD feeding *Cdkn2a*^{+/+} had increased basal insulin secretion to maintain normal glucose levels, indicating an insulin-resistant state (Figure 1H). By contrast, HFD *Cdkn2a*-deficient mice displayed lower basal insulin levels and were still responsive to a glucose load (Figure 1H), suggesting that *Cdkn2a* deficiency may affect insulin sensitivity rather than insulin production by the pancreatic beta cells. Consistently, insulin sensitivity was significantly improved in *Cdkn2a*^{-/-} mice under CD (Figure 1I, J) and even more under HFD (Figure 1K, L). These results indicate that *Cdkn2a* deficiency prevents weight gain and improves insulin sensitivity during metabolic stress.

3.2. Increased energy expenditure in *Cdkn2a*^{-/-} mice

To characterize the effect of *Cdkn2a* deficiency on insulin sensitivity and body weight, we monitored energy expenditure using indirect calorimetry measurements. Under CD, *Cdkn2a*^{-/-} mice showed increased food intake only during the second (1AM to 7AM) part of the dark phase compared to controls (Figure 2A and Figure S2A), but this was doubled under HFD during the entire dark phase (Figure 2B and Figure S2B). The reduced body weight gain under HFD (Figure 1) despite an increase in food intake suggests enhanced energy expenditure. The ambulatory activity was similar among all genotypes either under CD (Figure S2C, D) or HFD (Figure S2E, F). Interestingly, *Cdkn2a*^{-/-} mice showed increased energy expenditure measured by heat production, under both CD (Figure 2C and Figure S2G) and HFD (Figure 2D and Figure S2H). This increased metabolic rate was not due to substrate utilization preference (glucose or free fatty acids), since no significant difference in respiratory exchange ratio (RER) was observed between *Cdkn2a*^{+/+} and *Cdkn2a*^{-/-} mice (Figure 2E, F and Figure S2I, J). We then investigated adaptive thermogenesis by either performing a cold test or subjecting mice to 6 h of fasting. During an acute cold stress or under fasting conditions *Cdkn2a*^{-/-} mice maintained a higher body temperature as compared to control animals (Figure 2G, H). Altogether, these findings suggest that the global genetic deletion of *Cdkn2a* locus in mice enhances energy expenditure and adaptive thermogenesis.

3.3. Beige fat programming is dependent on *Cdkn2a*

To determine if *Cdkn2a* regulates brown and beige adipocyte function, we first analyzed BAT thermogenic gene expression in *Cdkn2a*^{+/+} and *Cdkn2a*^{-/-} mice. *Ucp1* and *Prdm16* expression increased in *Cdkn2a*-deficient BAT fed a CD or HFD (Figure 3A, B). *Ppargc1a* expression was similar in control and *Cdkn2a*-deficient BAT under CD, but raised upon HFD in *Cdkn2a*^{-/-} BAT (Figure 3A, B). Mitochondrial content (Figure S3A) and *Ucp1* protein levels (Figure S3B, C) were identical in *Cdkn2a*^{+/+} and *Cdkn2a*^{-/-} BAT tissue homogenates. Total BAT mass was not significantly different in *Cdkn2a*^{+/+} and *Cdkn2a*^{-/-} mice fed CD, but was decreased in HFD-fed *Cdkn2a*^{-/-} mice (Figure S3D, E). When expressed relative to total body weight no difference between genotypes was observed (Figure S3F, G), suggesting that *Cdkn2a* deficiency may have a weak effect on BAT functions. When measuring *p16*, *p19*, and *Ucp1* mRNA levels in different mouse fat depots, we observed that *p16* (Figure 3C) and *p19* (Figure 3D) were mostly expressed in inguinal WAT (ingWAT) compared to epididymal WAT or BAT, whereas *Ucp1* (Figure 3D) was strongly expressed in BAT depots. We then hypothesized that the *Cdkn2a* gene products *p16* and *p19* may promote the WAT beigeing/browning process. To determine if *Cdkn2a* deficiency modifies beige adipocyte differentiation, we compared the expression levels of several

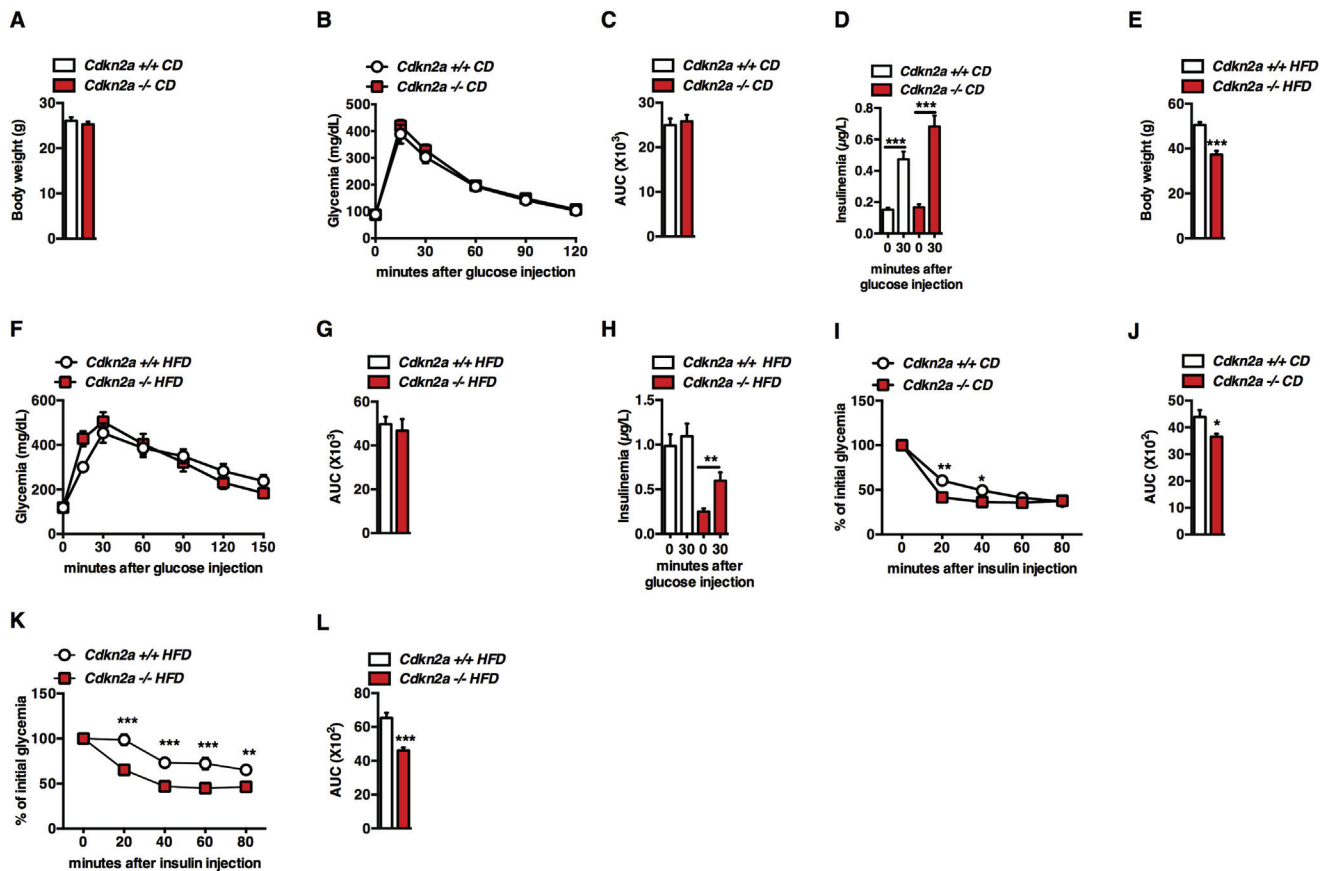


Figure 1: *Cdkn2a*-deficient mice are insulin sensitive during DIO. (A) Body weight of 9- to 12-week old control (*Cdkn2a*^{+/+}) and mutant (*Cdkn2a*^{-/-}) mice fed with chow diet (CD, *n* = 30–32). (B, C) Intraperitoneal glucose tolerance test (ipGTT, B) in *Cdkn2a*^{+/+} and *Cdkn2a*^{-/-} mice fed with CD (*n* = 11–12) and the corresponding area under the curve (AUC, C) of ipGTT. (D) Blood insulin levels as measured during ipGTT in CD-fed mice. (E) Body weight of high fat diet (HFD, *n* = 7–16) fed mice. (F, G) ipGTT in HFD mice (F, *n* = 7) and its AUC (G). (H) Blood insulin levels during ipGTT in HFD-fed mice. (I) Intraperitoneal insulin tolerance test (ipITT) in 8 weeks mice fed with CD (*n* = 7). (J) AUC of ipITT. (K, L) ipITT in HFD-fed mice (K, *n* = 7) and the corresponding AUC of ipITT (L). All values are expressed as means ± SEM; **p* < 0.05, ***p* < 0.01, and ****p* < 0.001.

adipocyte markers between control and *Cdkn2a*-deficient animal's ingWAT. The expression of brown fat-selective genes *Ppargc1a*, *Ucp1*, *Prdm16*, *Tfam*, *Cox5a*, *Cox8a*, and *Dio2* was increased in ingWAT from CD-fed *Cdkn2a*^{-/-} animals (Figure 3F). This effect was more pronounced in HFD-*Cdkn2a*^{-/-} ingWAT (Figure 3G). Hematoxylin and eosin (H&E) staining showed that *Cdkn2a*^{-/-} ingWAT had smaller adipocytes with multilocular lipid droplets (Figure 3H), associated with an increase in UCP1 immunostaining (Figure 3H), further confirmed through immunoblot (Figure 3I, J) and immunofluorescence (Figure S3H) experiments. Mitochondrial content was identical in *Cdkn2a*^{+/+} and *Cdkn2a*^{-/-} ingWAT (Figure S3A). Altogether, these data suggest that *Cdkn2a* deficiency induces a white-to-brown fat conversion in ingWAT.

3.4. The effect of *Cdkn2a* on browning is cell-autonomous and requires the activation of the Protein Kinase A pathway

Stromal vascular cells from ingWAT and BAT can be differentiated into brown-like adipocytes. To determine the cell-autonomous requirement of *Cdkn2a* to the beiging process, we isolated ingWAT and BAT pre-adipocytes from control and *Cdkn2a*-deficient mice and differentiated them for 8 days (Figure S4A). Lipid droplet accumulation was more pronounced in *Cdkn2a*^{-/-} ingWAT and BAT differentiated primary adipocytes, but not in adipocytes differentiated from epididymal pre-adipocytes (eWAT, Figure S4B). We next examined the expression of adipocytes (*Fabp4*) and brown/beige fat markers (*Ppargc1a*, *Ucp1*,

Prdm16, *Cox5a*, *Cidea*, *Elovl3*, *Dio2*) and observed a strong induction of these genes in differentiated ingWAT primary cells upon *p16* and *p19* genetic deletion (Figure 4A), but not in differentiated BAT or eWAT primary cells (Figure S4C and data not shown).

The *Cdkn2a* products *p16*^{ink4a} and *p19*^{ARF} are key regulators of the activity of serine/threonine kinases (STK) involved in cell proliferation and senescence [9]. We postulated that STK may be involved in beige fat programming and performed a global kinome analysis in primary *Cdkn2a*^{+/+} and *Cdkn2a*^{-/-} differentiated adipocytes. We used Pamgene arrays containing 140 serine/threonine peptides that are the substrates of one or multiple kinases. We incubated these chips with protein lysates of primary adipocytes after 8 days of differentiation (D8). We then analyzed the phosphorylation status of these peptides and identified the putative upstream kinases involved. At D8, 47 peptides with significant differences in phosphorylation levels between control and *Cdkn2a*-deficient adipocytes were observed (Figure 4B and Table S1). Using the Human Protein Reference Database (HPRD) [37] to identify potential upstream kinases we identified several signaling pathways that may be affected in *Cdkn2a*-deficient adipocytes, including Protein Kinase A (PKA) and Protein Kinase G (PKG) signaling pathways. Interestingly, PKG is an important regulator of WAT browning [38,39]. For some phosphorylated peptides upstream kinases could not be identified using HPRD analysis (Figure 4B, NA or –). When we analyzed the diseases and/or biological functions affected by the differences in peptide phosphorylation observed upon *Cdkn2a*

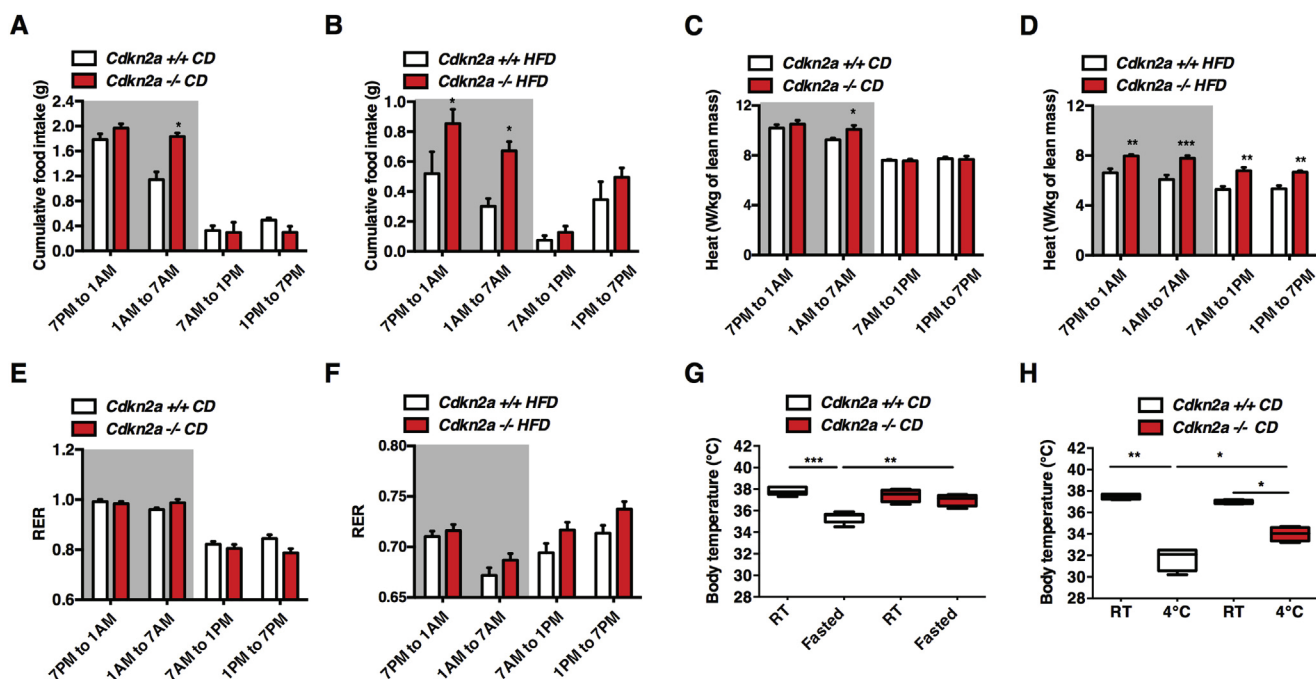


Figure 2: Increased energy expenditure in *Cdkn2a*^{-/-} mice. (A, B) Cumulative food intake in (A) CD and (B) HFD-fed control (*Cdkn2a*^{+/+}) and mutant (*Cdkn2a*^{-/-}) mice ($n = 4$) measured during the dark (7PM to 1AM and 1AM to 7AM) and the light (7AM to 1PM and 1PM to 7PM) periods. (C, D) Heat production in (C) chow diet and (D) HFD-fed mice. (E, F) Respiratory exchange ratio (RER) in (E) CD and (F) HFD-fed mice. (G, H) Body temperature in CD-fed *Cdkn2a*^{+/+} and *Cdkn2a*^{-/-} mice after 5 h fasting (G, $n = 4$) and 5 h of cold exposure (H, $n = 4$). All values are expressed as means \pm SEM; * $p < 0.05$, ** $p < 0.01$, and *** $p < 0.001$.

genetic deficiency through Ingenuity Pathway Analysis (IPA), we found networks related to “Cancer,” “Organismal Injury and Abnormalities,” and “Developmental Disorders,” but also to “Cardiovascular Disease” (Table S2). Then we found a significant enrichment of potential signaling pathways upstream kinases involved in “Protein Kinase A Signaling” in *Cdkn2a*-deficient cells ($P = 1.07 \times 10^{-15}$; Figure 4C), confirming HPRD analysis. In addition, “AMPK signaling” ($P = 4.96 \times 10^{-12}$; Figure 4C), “synaptic long-term potentiation” ($P = 1.28 \times 10^{-10}$; Figure 4C), “prostate cancer signaling” ($P = 9.26 \times 10^{-10}$; Figure 4C) or “Molecular Mechanisms of Cancer” ($P = 3.92 \times 10^{-09}$; Figure 4C) were canonical pathways also affected in *Cdkn2a*^{-/-} primary adipocytes. These analyses prompted us to focus on dissecting the contribution of PKA to our phenotype. Increased PKA activity was confirmed in *Cdkn2a*^{-/-} ingWAT homogenates, whereas no changes were found in BAT or eWAT (Figure 4D and data not shown). The increased PKA activity was further confirmed in *Cdkn2a*^{-/-} ingWAT using protein homogenates and an anti-PKA phospho-substrate antibody (Figure S4D, E). The increase in PKA activity was associated with a significant raise in basal and maximal respiration, as well as basal proton leak of *Cdkn2a*^{-/-} primary ingWAT cells, as measured by oxygen consumption rate (OCR, Figure 4E, F). The PKA inhibitor H89 completely abolished PKA activity in tissue homogenates (Figure 4D) as well as the increase of oxygen consumption observed in *Cdkn2a*^{-/-} primary cells (Figure 4E, F). Altogether, these findings indicate that *Cdkn2a* modulates PKA activity in adipocytes, oxygen consumption and promotes being in ingWAT. Our results also suggest that *Cdkn2a* may regulate other pathways, such as PKG, that can further contribute to adipose being.

3.5. *Cdkn2a* modulates a regulatory gene network involved in brown adipocyte function

We next carried out RNA-sequencing (RNA-seq) analysis in *Cdkn2a*^{+/+} and *Cdkn2a*^{-/-} primary adipocytes at D8 of differentiation. We

found 11,855 transcripts differentially expressed (Table S3). IPA highlighted the presence of a network of 98 genes associated to *Cdkn2a* deletion which was involved in “energy production, lipid metabolism and small molecule biochemistry,” including *Ppargc1a* and *Prdm16* (Figure S5A). Subsequently, we analyzed the diseases and/or functions associated to *Cdkn2a* deficiency. The main differences between *Cdkn2a*^{+/+} and *Cdkn2a*^{-/-} primary adipocytes were included into “carbohydrate metabolism” ($P = 1.67 \times 10^{-3}$) or “cellular development, connective tissue development and function, tissues development” ($P = 4.36 \times 10^{-3}$; Table S4). Next, we used the “upstream regulator analysis” function of IPA to identify potential contributors to the phenotype of *Cdkn2a*^{+/+} and *Cdkn2a*^{-/-} primary adipocytes. Among the most significant upstream regulators, tumor necrosis factor (TNF) and promyelocytic leukemia (PML) signaling pathways were activated (Table 1). Interestingly, norepinephrine, which acts on β -AR receptors in BAT [40] and WAT [41,42], was also activated (Table 1). This analysis further revealed a potential inhibition of the NR1H2 pathway, which has been associated to severe obesity [43] (Table 1). Transcription factor network analyses revealed that PPARGC1A and PRDM16 were activated in *Cdkn2a*^{-/-} cells (Table 2). The period circadian clock 2 (PER2) transcription factor was also activated (Table 2). This is consistent with the observation that PER2 is necessary for adaptation to cold temperature in mice through the regulation of *Ucp1* expression [44]. Moreover, Aryl hydrocarbon receptor nuclear translocator like (ARNTL) activity is potentially inhibited in our model (Table 2), in agreement with its antagonistic role on PER2 in the control of the circadian rhythm. Finally, the marked inhibition of inhibitor of DNA (ID1) further confirmed the brown-like features of *Cdkn2a*^{-/-} primary adipocytes. Indeed, germline deficient *Id1* mice are protected against DIO through enhanced energy expenditure [45]. These RNA-seq data further suggest that *Cdkn2a* is a crucial regulator of effectors controlling the expression of brown-like markers.

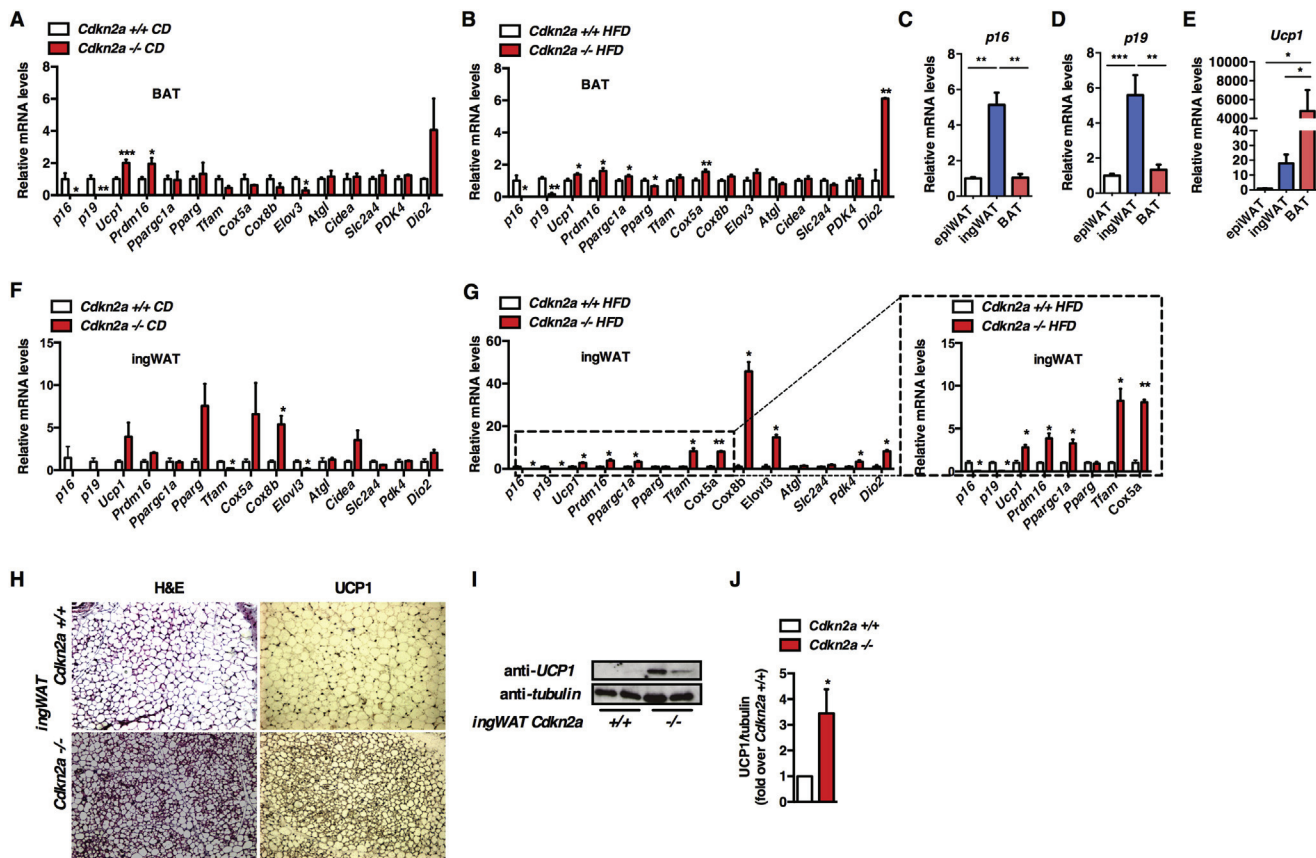


Figure 3: *Cdkn2a* deficiency promotes the browning process *in vivo*. (A, B) mRNA level of thermogenic genes in BAT from *Cdkn2a*^{+/+} and *Cdkn2a*^{-/-} mice fed chow (A) or HFD (B, $n = 5-6$). (C-E) mRNA levels of *p16* (C), *p19* (D) and *Ucp1* (E) in epididymal WAT (epiWAT), inguinal WAT (ingWAT) and BAT. (F, G) mRNA levels for adipogenic and thermogenic genes in ingWAT from *Cdkn2a*^{+/+} and *Cdkn2a*^{-/-} mice fed CD (F) or HFD (G, $n = 5-6$). An inset of some genes is represented. (H) Hematoxylin and eosin (H&E) staining and UCP1 immunohistochemistry of representative sections of ingWAT from *Cdkn2a*^{+/+} and *Cdkn2a*^{-/-} mice fed CD. (I, J) Western blot assay (I) and quantification (J) showing UCP1 protein levels in ingWAT of *Cdkn2a*^{+/+} and *Cdkn2a*^{-/-} mice. Tubulin was used as a loading control. Quantification was performed using the ImageJ software. All values are expressed as means \pm SEM; * $p < 0.05$, ** $p < 0.01$, and *** $p < 0.001$.

3.6. *CDKN2A* modulates adipose tissue browning in human adipocytes

We next questioned whether deregulated expression of *CDKN2A* could be associated to obesity in humans. Interestingly, using global transcriptome profiling of adipocytes from lean and obese subjects (GEO: GSE94752; Ref. [36]) we observed a significant increase of *CDKN2A* mRNA expression levels in obese insulin-resistant adipocytes compared to lean controls (Figure 5A). We next wondered whether decreasing *CDKN2A* levels in human adipocytes could recapitulate some of the effects we observed in mice and induce browning in human cells. Recent reports demonstrated that human-induced pluripotent stem cells (hiPSCs) could be differentiated into brown/brite adipose progenitors (hiPSCs-BAP, Refs. [30,31]). To further analyze whether *CDKN2A* modulates UCP1 expression in human cells, we silenced *CDKN2A* expression during the exponential growth phase of hiPSCs and differentiated them into brown/brite adipose cells during 22 days as described previously [30,31]. As shown in Figure 5B, C, *p16* and *p14* mRNA levels were significantly reduced after silencing of the *CDKN2A* gene. In addition, *UCP1* mRNA levels were strongly induced in hiPSCs-BAP upon *CDKN2A* silencing (Figure 5D). This transcriptional effect was associated with a strong increase of UCP1 protein levels in hiPSCs-BAP *CDKN2A*-deficient cells (Figure 5E, F). Moreover, silencing *CDKN2A* increased lipid droplet accumulation and

adipocyte differentiation in hiPSCs-BAP cells (Figure 5G). Altogether, our data indicate that *CDKN2A* is an important mediator of human adipose tissue browning.

4. DISCUSSION

Our results demonstrate that *CDKN2A* gene products *p16*^{INK4a} and *p19*^{ARF} are, beside their known role as cell cycle regulatory proteins, crucial regulators of adipocyte function and adaptation to metabolic stress. Previous studies have linked the *CDKN2A* locus to diabetes pathophysiology through its putative role on pancreatic islet biology [16,25]. Here, we show that *CDKN2A*-loss may also impact energy balance and metabolic homeostasis *via* non-pancreatic dependent mechanisms. First, we observed that *CDKN2A* expression is increased in human obese adipocytes, and deletion of both *p16*^{INK4a} and *p19*^{ARF} protect mice from diet-induced obesity and associated insulin resistance by enhancing energy expenditure. Second, *Cdkn2a* invalidation enhances ingWAT plasticity, facilitating the acquisition of beige adipocytes phenotype. Increasing energy expenditure is associated with decreased blood glucose and triglycerides and improving hyperglycemia and dyslipidemia in both mice and humans [8,46]. In humans, BAT activation by cold exposure positively affects body weight and insulin sensitivity [7,47-49]. In addition, the implantation of human

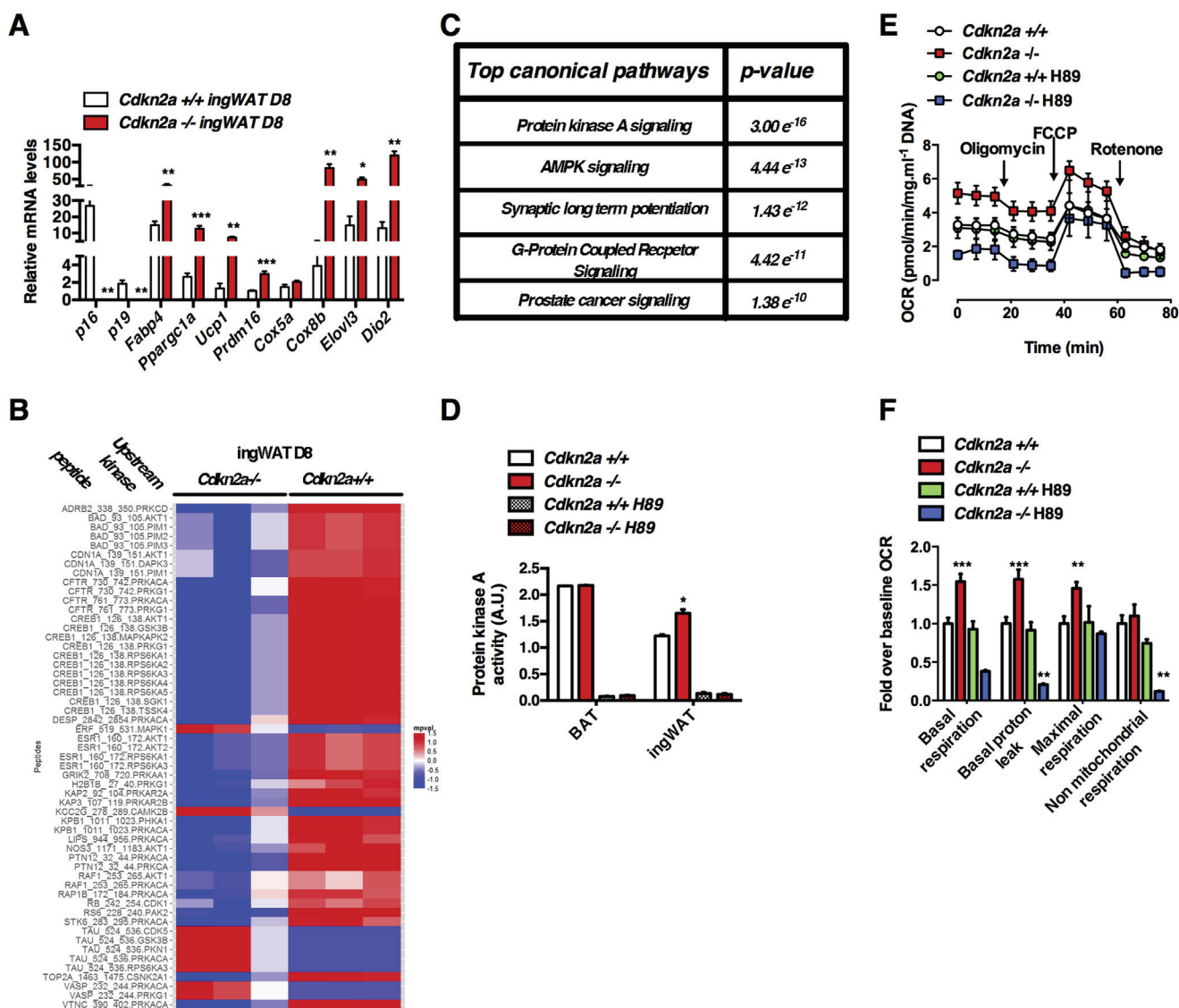


Figure 4: Activation of the Protein Kinase A pathway in *Cdkn2a*^{-/-} adipocytes induces white adipose tissue browning. (A) mRNA levels for adipogenic and thermogenic genes in ingWAT primary differentiated adipocytes isolated from *Cdkn2a*^{+/+} and *Cdkn2a*^{-/-} mice ($n = 3$). (B) Heatmap showing differences in peptide phosphorylation between primary differentiated adipocyte from *Cdkn2a*^{+/+} and *Cdkn2a*^{-/-} inguinal fat depots ($n = 3$). Upstream kinases were identified using the Human Protein Reference Database. (C) Pangene results were analyzed using Ingenuity Pathway Analysis (IPA) to identify the top activated canonical pathways in *Cdkn2a*^{-/-} primary differentiated adipocyte compared to *Cdkn2a*^{+/+}. (D) PKA activity measurement in tissue homogenates from BAT and ingWAT isolated from *Cdkn2a*^{+/+} and *Cdkn2a*^{-/-} mice ($n = 3$) treated with DMSO or the PKA inhibitor H89 at 10 μM . (E, F) Oxygen consumption rate (OCR) was measured using the Seahorse XFe24 platform. After 8 days of differentiation (D8), OCR was measured in *Cdkn2a*^{+/+} and *Cdkn2a*^{-/-} differentiated adipocytes (E) and quantification of basal respiration, basal proton leak (by blocking ATP synthase activity with oligomycin), maximal respiration by stimulating uncoupling process with FCCP (carbonyl cyanide *p*-trifluoromethoxyphenylhydrazone) and non-mitochondrial respiration (with rotenone) is represented (F, $n = 5$). *Cdkn2a*^{-/-} cells were treated 1 h with 10 μM of PKA inhibitor H89 before the experiment ($n = 5$). All values are expressed as means \pm SEM; * $p < 0.05$, ** $p < 0.01$, and *** $p < 0.001$.

beige adipocytes in mice improves metabolic homeostasis [50]. Interestingly, besides its classical BAT feature, human adult BAT also has some beige-like characteristics [5.51,52]. Altogether these data suggest that beige adipocyte activation may be useful against obesity and related metabolic disorders. In this broad context, our data show that *CDKN2A* locus is involved in adipose tissue adaptation to metabolic challenges in mice and humans that may have potential implications for human obesity.

Although it is not yet clear whether short-term cold acclimation induces browning in humans [7], severe adrenergic stress does activate

human WAT browning [53,54]. In mice, beige adipocytes appear after cold exposure or other inducers [4]. In our model, we observed the presence of beige adipocytes in *Cdkn2a* invalidated mice in the absence of any browning inducing agent, suggesting that this locus may act as modulator of the β -adrenergic receptor (β -AR) that controls the browning process. The link between β -AR signaling pathway, *CDKN2A* and the browning process remains yet to be elucidated.

Using a multiplex method for global kinase activity profiling in ingWAT, we identified the PKA pathway among the most significantly affected

Table 1 — Pathway analysis of RNA-sequencing data in *Cdkn2a*^{+/+} and *Cdkn2a*^{-/-} primary adipocytes.

Upstream regulator	Exp log ratio	Molecule type	Predicted activation state	Activation z-score	p-Value of overlap	Target molecules in dataset
CIDEA		Other		0.786	6.82E-03	ACADL, COX4I2, CYCS, DGAT2, EBF2, FOXC2, PNPLA2, PPARG, PPARGC1A, PPARGC1B
CCDC3		Other			9.86E-03	ACACA, DGAT2, FASN
PPARGC1B	-1.230	Transcription regulator			9.86E-03	EGLN3, ER01A, VEGFA
Melatonin		Chemical — endogenous mammalian			9.86E-03	ACACA, FASN, IRS1
ARNTL	-0.518	Transcription regulator			2.18E-02	DBP, ELOVL6, PER2, PER3
PTPN1		Phosphatase		-1.387	2.62E-02	IRS1, IRS2, PPARGC1A, PRDM16, TMEM26
SGCB	0.379	Other			3.31E-02	DAG1, SGCD, SGCE
SGCD	1.385	Other			3.31E-02	DAG1, SGCB, SGCE
IL1B		Cytokine			3.31E-02	IRS1, SERPINE1, VEGFA
PNPLA2	-0.896	Enzyme		-1.131	4.23E-02	ACADL, FASN, Gk, PPARG
FFAR4		G-protein coupled receptor			4.60E-02	INSR, IRS1
TNFRSF1B	0.504	Transmembrane receptor			4.60E-02	SERPINE1, SOCS3
STAT1		Transcription regulator			4.60E-02	PPARG, SOCS3
EGR1		Transcription regulator			4.60E-02	CSF1, F3
TGFB1		Growth factor			4.60E-02	F3, SERPINE1
TNFRSF1A		Transmembrane receptor			4.60E-02	SERPINE1, SOCS3
Norepinephrine		Chemical — endogenous mammalian		1.930	2.03E-01	ELOVL6, PPARGC1A, RBP4, SLC2A1, VEGFA
TNF		Cytokine	Activated	2.048	2.27E-01	AOC3, APLN, Celf1, DBI, F3, FABP5, FASN, FOS, INSR, NRIP1, PPARG, RELA, SERPINE1, SOCS3, TALDO1
NR1H2	0.471	Ligand-dependent nuclear receptor	Inhibited	-2.449	2.42E-01	ELOVL6, FASN, PNPLA2, PRDM16, RB1, Saa3, SLC16A2
PML		Transcription regulator	Activated	2.000	3.52E-01	ACACA, ACOX1, FASN, PPARGC1A

Table 2 — Analysis of upstream transcription factors in RNA-sequencing data from *Cdkn2a*^{+/+} and *Cdkn2a*^{-/-} primary adipocytes.

Molecules in network	Score	Focus molecules	Top diseases and functions
CEBPA, FOXC2, ID1, KLF11, MDM2, PPARGC1A, PPARGC1B, PRDM16, RB1, SREBF1, STAT6, TP53	3	9	Cellular Development, Connective Tissue Development and Function, Tissue Development
ARNTL, DBP, PER2	2	3	Behavior, Nervous System Development and Function, Organ Morphology
ID3, TCF3	0	1	Hematological System Development and Function, Lymphoid Tissue Structure and Development, Tissue Morphology
HDAC3, RELA	0	1	Cell Death and Survival, Neurological Disease, Organismal Injury and Abnormalities

pathway in *Cdkn2a*^{-/-} adipocytes. Furthermore we demonstrated that loss of *p16*^{INK4a} and *p19*^{ARF} expression is sufficient to activate the thermogenic program in ingWAT. We also confirmed that PKA activity was higher in *Cdkn2a*-deficient ingWAT, suggesting an *in vivo* activation of this pathway. Interestingly in the liver, *p16*^{INK4A} controls gluconeogenesis and PKA activation in a CDK4-dependent manner [22]. In contrast in ingWAT, our kinome analysis revealed that CDK4 kinase activity, which is regulated by *p16*^{INK4A}, is not modulated in the absence of *Cdkn2a*. Therefore, the effect on PKA signaling in ingWAT may be independent of the activation of CDK4. In agreement with this, the analysis of adipose tissues depots from mice expressing a constitutively active CDK4 form (CDK4^{R24C}, Ref. [55]) did not show any signs of browning (data not shown). Moreover, PKA activity is increased in epididymal WAT from *Cdk4*-deficient mice [56]. Although we cannot rule out that other key signaling pathways, including PKG, could contribute to the phenotype observed in *Cdkn2a*-deficient mice, our observations suggest that the molecular mechanisms controlled by *p16*^{INK4A} and *p19*^{ARF} may be tissue-specific and independent of the *bona fide* cell cycle regulation, as previously described in the liver for other cell cycle regulators [21]. As demonstrated for *p16*^{INK4A}/CDK4 and *p19*^{ARF}/mdm2 in the control of cell proliferation or senescence, respectively, it is tempting to speculate that *p16*^{INK4A} and *p19*^{ARF} may

act as direct repressors of the PKA complex to regulate its activity. The potential interaction of these proteins with different yet specific partners may subsequently dictate metabolic *versus* proliferative functions of *p16*^{INK4A} and *p19*^{ARF}.

It is noteworthy that *CDKN2A* loss-of-function is involved in cancer development, particularly melanoma [57]. Recent reports shed light on the contribution of adipose tissue browning process in cancer-associated cachexia in rodents and humans [58–62]. Here we describe a novel metabolic function for this key tumor suppressor gene in energy expenditure and adipose tissue browning. The activation of the β 3-AR pathway during cachexia [63,64], and the putative tight relationship between *CDKN2A* and β 3-AR, further suggests that *CDKN2A* deficiency in cancer cells may profoundly affect energy homeostasis facilitating the development of cachexia.

In conclusion, our results demonstrate that the *Cdkn2a* locus is an important regulator of energy homeostasis and adipose tissue function in response to metabolic stress in mice. Mice model approaches can be useful to elucidate and further carefully dissect the molecular mechanisms underlying the pleiotropic impact of GWAS on T2D associated genes. Modulating *Cdkn2a*-regulated signaling cascades may constitute novel targetable pathways for treating metabolic disorders.

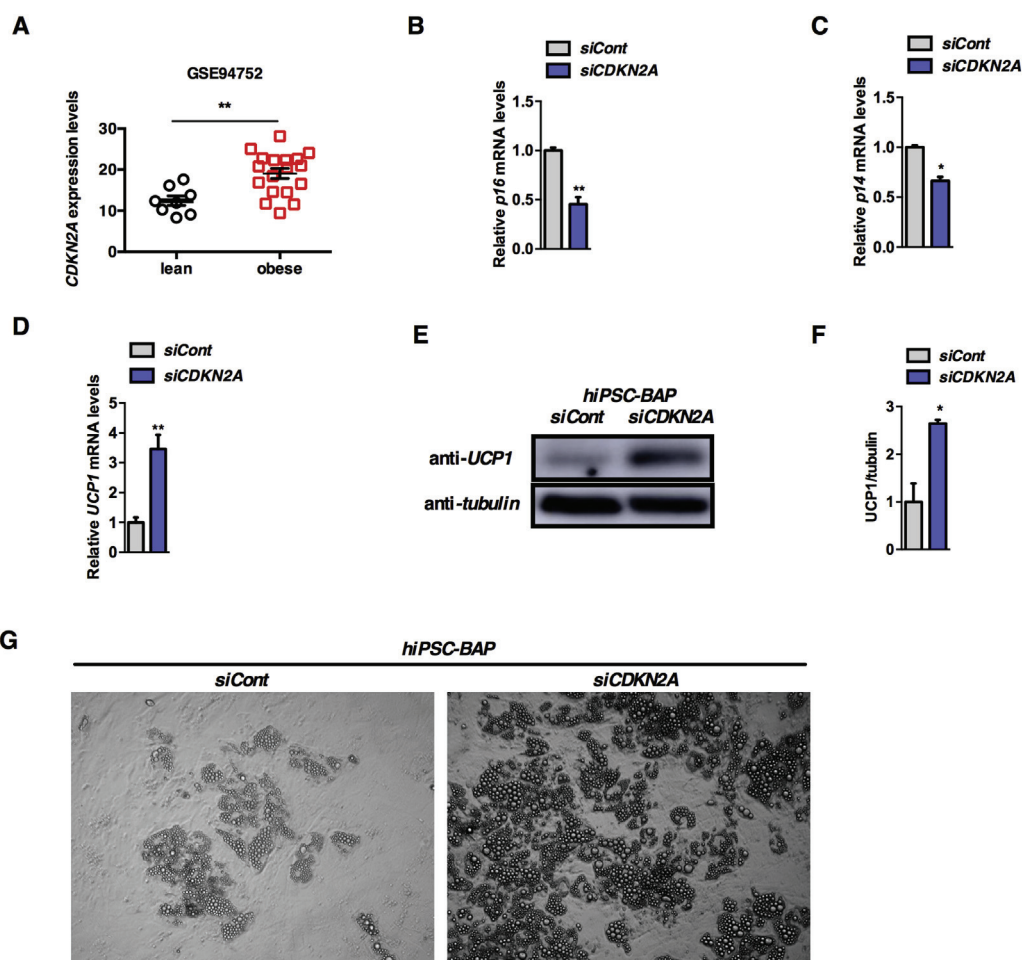


Figure 5: *CDKN2A* is increased in obese insulin-resistant adipocytes and its silencing in hiPSCs-BAP cells induces UCP1 expression. (A) Correlation between *CDKN2A* and human obesity. *CDKN2A* expression is upregulated in adipocytes from obese insulin-resistant patients. Analyses are based on the human dataset GEO: GSE94752. (B–D) Relative expression of *p16* (B), *p14* (C), and *UCP1* (D) genes in control (siCont) or *CDKN2A* silenced (si*CDKN2A*) hiPSCs-BAPs ($n = 3$). (E, F) Western blot assay (E) and quantification (F) showing UCP1 protein levels in control (siCont) or *CDKN2A* silenced (si*CDKN2A*) hiPSCs-BAPs ($n = 3$). Tubulin was used as a loading control. Quantification was performed using the ImageJ software. (G) Representative microscopy analysis of siCont and si*CDKN2A* hiPSCs-BAPs after differentiation showing increased lipid droplets upon *CDKN2A* silencing. All values are expressed as means \pm SEM; * $p < 0.05$ and ** $p < 0.01$.

AUTHORS' CONTRIBUTION

NR, SAH, and XG performed most of the experiments. ES, XY, CC, FO, ICL-M, and EC contributed to the *in vivo* and cellular experiments. ICL-M and LF performed and/or analyzed the Pamgene experiments and provided reagents and data. ED, IR, and AB performed the RNA-sequencing experiments. XY and CD performed the hiPSCs experiments and analyzed the data. PF discussed and interpreted the results from the study. J-SA designed the study, supervised the project and contributed to experiments and/or their analysis. NR, SAH, PF, and J-SA wrote the manuscript.

ACKNOWLEDGMENTS

We thank Dr. Manuel Serrano for providing us with the *Cdkn2a*^{-/-} mice. We thank Carine de Bettignies and Olivier Sand from UMR 8199 for helpful discussions and technical assistance. We thank Estelle Le Borgne for help with illustrations. We thank Dr. David Blum for sharing reagents. The authors thank the Experimental Resources platform from Lille 2 University, especially Yann Lepage, Ludovic Mercier, Kelly Timmerman, Mélanie Besegher, and Delphine Taillieu for animal care. We thank the

Department of Histology from the Lille Medicine Faculty, in particular M.H. Gevaert and R.M. Siminski, for histological preparations. We are indebted to the RHEM network (Réseau d'Histologie Expérimentale de Montpellier, IFR122, France) for histology and, in particular, for tissue and slide preparations. This work was supported by grants from «European Genomic Institute for Diabetes» (EGID, ANR-10-LABX-46 to PF and J-SA), Agence Nationale pour la Recherche (BETAPLASTICITY, ANR-17-CE14-0034 to PF and J-SA; Equipex 2010 ANR-10-EQPX-07-01; 'LIGAN-PM' Genomics platform), European Foundation for the Study of Diabetes (EFSD, to J-SA), European Commission, European Research Council (GEPIDIAB 294785 to PF), Institut National de la Santé et de la Recherche Médicale, Centre National de la Recherche Scientifique, Association pour la Recherche sur le Diabète (to J-SA), Lille 2 University (to NR, XG, ES, and J-SA), Conseil Régional Hauts de France and Métropole Européenne de Lille (to NR, XG, and J-SA), FEDER (Fonds Européen de Développement Régional, to NR, PF, J-SA) and Société Francophone du Diabète/Servier (to SAH and J-SA).

CONFLICT OF INTEREST

The authors declare no competing financial interests.

APPENDIX A. SUPPLEMENTARY DATA

Supplementary data related to this article can be found at <https://doi.org/10.1016/j.molmet.2017.11.012>.



REFERENCES

- [1] Blanchet, E., Annicotte, J.-S., Lagarrigue, S., Aguilar, V., Clapé, C., Chavey, C., et al., 2011. E2F transcription factor-1 regulates oxidative metabolism. *Nature Cell Biology* 13:1146–1152.
- [2] Fajas, L., Landsberg, R.L., Huss-Garcia, Y., Sardet, C., Lees, J.A., Auwerx, J., 2002. E2Fs regulate adipocyte differentiation. *Developmental Cell* 3:39–49.
- [3] Liew, C.W., Boucher, J., Cheong, J.K., Vernochet, C., Koh, H.J., Mallol, C., et al., 2013. Ablation of TRIP-Br2, a regulator of fat lipolysis, thermogenesis and oxidative metabolism, prevents diet-induced obesity and insulin resistance. *Nature Medicine* 19:217–226.
- [4] Kajimura, S., Spiegelman, B.M., Seale, P., 2015. Brown and beige fat: physiological roles beyond heat generation. *Cell Metabolism* 22:546–559.
- [5] Wu, J., Bostrom, P., Sparks, L.M., Ye, L., Choi, J.H., Giang, A.H., et al., 2012. Beige adipocytes are a distinct type of thermogenic fat cell in mouse and human. *Cell* 150:366–376.
- [6] Wu, J., Cohen, P., Spiegelman, B.M., 2013. Adaptive thermogenesis in adipocytes: is beige the new brown? *Genes & Development* 27:234–250.
- [7] Hanssen, M.J., Hoeks, J., Brans, B., van der Lans, A.A., Schaart, G., van den Driessche, J.J., et al., 2015. Short-term cold acclimation improves insulin sensitivity in patients with type 2 diabetes mellitus. *Nature Medicine* 21:863–865.
- [8] Lee, P., Smith, S., Linderman, J., Courville, A.B., Brychta, R.J., Dieckmann, W., et al., 2014. Temperature-acclimated brown adipose tissue modulates insulin sensitivity in humans. *Diabetes* 63:3686–3698.
- [9] Hannou, S.A., Wouters, K., Paumelle, R., Staels, B., 2015. Functional genomics of the CDKN2A/B locus in cardiovascular and metabolic disease: what have we learned from GWASs? *Trends in Endocrinology & Metabolism* 26:176–184.
- [10] Morris, A.P., Voight, B.F., Teslovich, T.M., Ferreira, T., Segre, A.V., Steinthorsdottir, V., et al., 2012. Large-scale association analysis provides insights into the genetic architecture and pathophysiology of type 2 diabetes. *Nature Genetics* 44:981–990.
- [11] Voight, B.F., Scott, L.J., Steinthorsdottir, V., Morris, A.P., Dina, C., Welch, R.P., et al., 2010. Twelve type 2 diabetes susceptibility loci identified through large-scale association analysis. *Nature Genetics* 42:579–589.
- [12] Dauriz, M., Meigs, J.B., 2014. Current insights into the joint genetic basis of type 2 diabetes and coronary heart disease. *Current Cardiovascular Risk Reports* 8:368.
- [13] Wan, G., Mathur, R., Hu, X., Liu, Y., Zhang, X., Peng, G., et al., 2013. Long non-coding RNA ANRIL (CDKN2B-AS) is induced by the ATM-E2F1 signaling pathway. *Cellular Signalling* 25:1086–1095.
- [14] Mody, N., Agouni, A., McLroy, G.D., Platt, B., Delibegovic, M., 2011. Susceptibility to diet-induced obesity and glucose intolerance in the APP (SWE)/PSEN1 (A246E) mouse model of Alzheimer's disease is associated with increased brain levels of protein tyrosine phosphatase 1B (PTP1B) and retinobinding protein 4 (RBP4), and basal phosphorylation of S6 ribosomal protein. *Diabetologia* 54:2143–2151.
- [15] Lillycrop, K., Murray, R., Cheong, C., Teh, A.L., Clarke-Harris, R., Barton, S., et al., 2017. ANRIL promoter DNA methylation: a perinatal marker for later adiposity. *EBioMedicine* 19:60–72.
- [16] Pal, A., Potjer, T.P., Thomsen, S.K., Ng, H.J., Barrett, A., Scharfmann, R., et al., 2016. Loss-of-function mutations in the cell-cycle control gene CDKN2A impact on glucose homeostasis in humans. *Diabetes* 65:527–533.
- [17] Svensson, P.A., Wahlstrand, B., Olsson, M., Froguel, P., Falchi, M., Bergman, R.N., et al., 2014. CDKN2B expression and subcutaneous adipose tissue expandability: possible influence of the 9p21 atherosclerosis locus. *Biochemical and Biophysical Research Communications* 446:1126–1131.
- [18] Horswell, S.D., Fryer, L.G., Hutchison, C.E., Zindrou, D., Speedy, H.E., Town, M.M., et al., 2013. CDKN2B expression in adipose tissue of familial combined hyperlipidemia patients. *Journal of Lipid Research* 54:3491–3505.
- [19] Abella, A., Dubus, P., Malumbres, M., Rane, S.G., Kiyokawa, H., Sicard, A., et al., 2005. Cdk4 promotes adipogenesis through PPARgamma activation. *Cell Metabolism* 2:239–249.
- [20] Fuentes, L., Wouters, K., Hannou, S.A., Cudejko, C., Rigamonti, E., Mayi, T.H., et al., 2011. Downregulation of the tumour suppressor p16INK4A contributes to the polarisation of human macrophages toward an adipose tissue macrophage (ATM)-like phenotype. *Diabetologia* 54:3150–3156.
- [21] Lee, Y., Dominy, J.E., Choi, Y.J., Jurczak, M., Tolliday, N., Camporez, J.P., et al., 2014. Cyclin D1-Cdk4 controls glucose metabolism independently of cell cycle progression. *Nature* 510:547–551.
- [22] Bantubungi, K., Hannou, S.A., Caron-Houde, S., Vallez, E., Baron, M., Lucas, A., et al., 2014. Cdkn2a/p16ink4a regulates fasting-induced hepatic gluconeogenesis through the PKA-CREB-PGC1alpha pathway. *Diabetes* 63:3199–3209.
- [23] Krishnamurthy, J., Ramsey, M.R., Ligon, K.L., Torrice, C., Koh, A., Bonner-Weir, S., et al., 2006. p16INK4a induces an age-dependent decline in islet regenerative potential. *Nature* 443:453–457.
- [24] Salas, E., Rabhi, N., Froguel, P., Annicotte, J.S., 2014. Role of Ink4a/Arf locus in beta cell mass expansion under physiological and pathological conditions. *Journal of Diabetes Research* 2014:873679.
- [25] Helman, A., Klochendler, A., Azazmeh, N., Gabai, Y., Horwitz, E., Anzi, S., et al., 2016. p16(Ink4a)-induced senescence of pancreatic beta cells enhances insulin secretion. *Nature Medicine* 22:412–420.
- [26] Dimas, A.S., Lagou, V., Barker, A., Knowles, J.W., Magi, R., Hivert, M.F., et al., 2014. Impact of type 2 diabetes susceptibility variants on quantitative glycemic traits reveals mechanistic heterogeneity. *Diabetes* 63:2158–2171.
- [27] Serrano, M., Lee, H., Chin, L., Cordon-Cardo, C., Beach, D., DePinho, R.A., 1996. Role of the INK4a locus in tumor suppression and cell mortality. *Cell* 85:27–37.
- [28] Annicotte, J.S., Blanchet, E., Chavey, C., Iankova, I., Costes, S., Assou, S., et al., 2009. The CDK4-pRB-E2F1 pathway controls insulin secretion. *Nature Cell Biology* 11:1017–1023.
- [29] Rabhi, N., Denechaud, P.D., Gromada, X., Hannou, S.A., Zhang, H., Rashid, T., et al., 2016. KAT2B is required for pancreatic beta cell adaptation to metabolic stress by controlling the unfolded protein response. *Cell Reports* 15:1051–1061.
- [30] Tyler, D.S., Vappiani, J., Caneque, T., Lam, E.Y.N., Ward, A., Gilan, O., et al., 2017. Click chemistry enables preclinical evaluation of targeted epigenetic therapies. *Science* 356:1397–1401.
- [31] Larrieu, D., Britton, S., Demir, M., Rodriguez, R., Jackson, S.P., 2014. Chemical inhibition of NAT10 corrects defects of laminopathic cells. *Science* 344:527–532.
- [32] Hillhorst, R., Houkes, L., Mommersteeg, M., Musch, J., van den Berg, A., Ruijtenbeek, R., 2013. Peptide microarrays for profiling of serine/threonine kinase activity of recombinant kinases and lysates of cells and tissue samples. *Methods in Molecular Biology* 977:259–271.
- [33] Kim, D., Pertea, G., Trapnell, C., Pimentel, H., Kelley, R., Salzberg, S.L., 2013. TopHat2: accurate alignment of transcriptomes in the presence of insertions, deletions and gene fusions. *Genome Biology* 14:R36.
- [34] Liao, Y., Smyth, G.K., Shi, W., 2013. The Subread aligner: fast, accurate and scalable read mapping by seed-and-vote. *Nucleic Acid Research* 41:e108.
- [35] Love, M.I., Huber, W., Anders, S., 2014. Moderated estimation of fold change and dispersion for RNA-seq data with DESeq2. *Genome Biology* 15:550.
- [36] Kulyte, A., Ehlund, A., Arner, P., Dahlman, I., 2017. Global transcriptome profiling identifies KLF15 and SLC25A10 as modifiers of adipocytes insulin sensitivity in obese women. *PLoS One* 12:e0178485.

- [37] Peri, S., Navarro, J.D., Kristiansen, T.Z., Amanchy, R., Surendranath, V., Muthusamy, B., et al., 2004. Human protein reference database as a discovery resource for proteomics. *Nucleic Acid Research* 32:D497–D501.
- [38] Jennissen, K., Haas, B., Mitschke, M.M., Siegel, F., Pfeifer, A., 2013. Analysis of cGMP signaling in adipocytes. *Methods in Molecular Biology* 1020:175–192.
- [39] Mitschke, M.M., Hoffmann, L.S., Gnad, T., Scholz, D., Kruihoff, K., Mayer, P., et al., 2013. Increased cGMP promotes healthy expansion and browning of white adipose tissue. *FASEB Journal* 27:1621–1630.
- [40] Cannon, B., Nedergaard, J., 2004. Brown adipose tissue: function and physiological significance. *Physiological Reviews* 84:277–359.
- [41] Grujic, D., Susulic, V.S., Harper, M.E., Himms-Hagen, J., Cunningham, B.A., Corkey, B.E., et al., 1997. Beta3-adrenergic receptors on white and brown adipocytes mediate beta3-selective agonist-induced effects on energy expenditure, insulin secretion, and food intake. A study using transgenic and gene knockout mice. *The Journal of Biological Chemistry* 272:17686–17693.
- [42] Jimenez, M., Barbatelli, G., Allevi, R., Cinti, S., Seydoux, J., Giacobino, J.P., et al., 2003. Beta 3-adrenoceptor knockout in C57BL/6J mice depresses the occurrence of brown adipocytes in white fat. *European Journal of Biochemistry* 270:699–705.
- [43] Bell, C.G., Benzinou, M., Siddiq, A., Lecoq, C., Dina, C., Lemainque, A., et al., 2004. Genome-wide linkage analysis for severe obesity in French Caucasians finds significant susceptibility locus on chromosome 19q. *Diabetes* 53:1857–1865.
- [44] Chappuis, S., Ripperger, J.A., Schnell, A., Rando, G., Jud, C., Wahli, W., et al., 2013. Role of the circadian clock gene *Per2* in adaptation to cold temperature. *Molecular Metabolism* 2:184–193.
- [45] Satyanarayanan, A., Klarmann, K.D., Gavrilo, O., Keller, J.R., 2012. Ablation of the transcriptional regulator *Id1* enhances energy expenditure, increases insulin sensitivity, and protects against age and diet induced insulin resistance, and hepatosteatosis. *FASEB Journal* 26:309–323.
- [46] Chondronikola, M., Volpi, E., Borsheim, E., Porter, C., Annamalai, P., Enerback, S., et al., 2014. Brown adipose tissue improves whole-body glucose homeostasis and insulin sensitivity in humans. *Diabetes* 63:4089–4099.
- [47] Blondin, D.P., Labbe, S.M., Tingelstad, H.C., Noll, C., Kunach, M., Phoenix, S., et al., 2014. Increased brown adipose tissue oxidative capacity in cold-acclimated humans. *The Journal of Clinical Endocrinology & Metabolism* 99:E438–E446.
- [48] van der Lans, A.A., Hoeks, J., Brans, B., Vijgen, G.H., Visser, M.G., Vosselman, M.J., et al., 2013. Cold acclimation recruits human brown fat and increases nonshivering thermogenesis. *Journal of Clinical Investigation* 123:3395–3403.
- [49] Yoneshiro, T., Aita, S., Matsushita, M., Kayahara, T., Kameya, T., Kawai, Y., et al., 2013. Recruited brown adipose tissue as an antiobesity agent in humans. *Journal of Clinical Investigation* 123:3404–3408.
- [50] Min, S.Y., Kady, J., Nam, M., Rojas-Rodriguez, R., Berkenwald, A., Kim, J.H., et al., 2016. Human 'brite/beige' adipocytes develop from capillary networks, and their implantation improves metabolic homeostasis in mice. *Nature Medicine* 22:312–318.
- [51] Jespersen, N.Z., Larsen, T.J., Pejts, L., Daugaard, S., Homoe, P., Loft, A., et al., 2013. A classical brown adipose tissue mRNA signature partly overlaps with brite in the supraclavicular region of adult humans. *Cell Metabolism* 17:798–805.
- [52] Shinoda, K., Luijten, I.H., Hasegawa, Y., Hong, H., Sonne, S.B., Kim, M., et al., 2015. Genetic and functional characterization of clonally derived adult human brown adipocytes. *Nature Medicine* 21:389–394.
- [53] Patsouris, D., Qi, P., Abdullahi, A., Stanojic, M., Chen, P., Parousis, A., et al., 2015. Burn induces browning of the subcutaneous white adipose tissue in mice and humans. *Cell Reports* 13:1538–1544.
- [54] Sidossis, L.S., Porter, C., Saraf, M.K., Borsheim, E., Radhakrishnan, R.S., Chao, T., et al., 2015. Browning of subcutaneous white adipose tissue in humans after severe adrenergic stress. *Cell Metabolism* 22:219–227.
- [55] Rane, S.G., Dubus, P., Mettus, R.V., Galbreath, E.J., Boden, G., Reddy, E.P., et al., 1999. Loss of *Cdk4* expression causes insulin-deficient diabetes and *Cdk4* activation results in beta-islet cell hyperplasia. *Nature Genetics* 22:44–52.
- [56] Lagarrigue, S., Lopez-Mejia, I.C., Denechaud, P.D., Escote, X., Castillo-Armengol, J., Jimenez, V., et al., 2016. *CDK4* is an essential insulin effector in adipocytes. *Journal of Clinical Investigation* 126:335–348.
- [57] Cannon-Albright, L.A., Goldgar, D.E., Meyer, L.J., Lewis, C.M., Anderson, D.E., Fountain, J.W., et al., 1992. Assignment of a locus for familial melanoma, *MLM*, to chromosome 9p13-p22. *Science* 258:1148–1152.
- [58] Tsoli, M., Moore, M., Burg, D., Painter, A., Taylor, R., Lockie, S.H., et al., 2012. Activation of thermogenesis in brown adipose tissue and dysregulated lipid metabolism associated with cancer cachexia in mice. *Cancer Research* 72:4372–4382.
- [59] Shellock, F.G., Riedinger, M.S., Fishbein, M.C., 1986. Brown adipose tissue in cancer patients: possible cause of cancer-induced cachexia. *Journal of Cancer Research and Clinical Oncology* 111:82–85.
- [60] Kir, S., White, J.P., Kleiner, S., Kazak, L., Cohen, P., Baracos, V.E., et al., 2014. Tumour-derived PTH-related protein triggers adipose tissue browning and cancer cachexia. *Nature* 513:100–104.
- [61] Petruzzelli, M., Schweiger, M., Schreiber, R., Campos-Olivas, R., Tsoli, M., Allen, J., et al., 2014. A switch from white to brown fat increases energy expenditure in cancer-associated cachexia. *Cell Metabolism* 20:433–447.
- [62] Kir, S., Komaba, H., Garcia, A.P., Economopoulos, K.P., Liu, W., Lanske, B., et al., 2016. PTH/PTHrP receptor mediates cachexia in models of kidney failure and cancer. *Cell Metabolism* 23:315–323.
- [63] Das, S.K., Eder, S., Schauer, S., Diwoky, C., Temmel, H., Guertl, B., et al., 2011. Adipose triglyceride lipase contributes to cancer-associated cachexia. *Science* 333:233–238.
- [64] Fearon, K.C., Glass, D.J., Guttridge, D.C., 2012. Cancer cachexia: mediators, signaling, and metabolic pathways. *Cell Metabolism* 16:153–166.
- [65] Mohsen-Kanson, T., Hafner, A.L., Wdziekonski, B., Takashima, Y., Villageois, P., Carrière, A., et al., 2014. Jun. Differentiation of human induced pluripotent stem cells into brown and white adipocytes: role of *Pax3*. *Stem Cells* 32(6):1459–1467. <https://doi.org/10.1002/stem.1607>.
- [66] Hafner, A.L., Contet, J., Ravaut, C., Yao, X., Villageois, P., Suknuntha, K., et al., 2016 Aug 31. Brown-like adipose progenitors derived from human induced pluripotent stem cells: identification of critical pathways governing their adipogenic capacity. *Science Reports* 6:32490. <https://doi.org/10.1038/srep32490>.

ORIGINAL RESEARCH ARTICLE

Resveratrol and HIV-protease inhibitors control UCP1 expression through opposite effects on p38 MAPK phosphorylation in human adipocytes

Christophe Ravaut^{1*} | Martin Paré^{1*} | Xi Yao¹ | Stéphane Azoulay² |
Nathalie M. Mazure³ | Christian Dani¹  | Annie Ladoux¹ 

¹Université Côte d'Azur, INSERM, iBV, France

²Université Côte d'Azur, ICN, France

³Université Côte d'Azur, Centre Antoine Lacassagne, CNRS-UMR 7284-Inserm U1081, Nice, France

Correspondence

Annie Ladoux, PhD, iBV, Institut de Biologie Valrose, Univ. Nice Sophia Antipolis, Tour Pasteur; UFR Médecine; 28, avenue de Valombrose, 06107 Nice Cedex 2, France.
Email: ladoux@unice.fr

Present address

Christophe Ravaut, University of Oxford, Department of Physiology Anatomy & Genetics, Sherrington Building, Parks Road, Oxford OX1 3PT, UK.

Nathalie M. Mazure, University of Côte d'Azur (UCA), INSERM U1065, C3M, 151 Route de St Antoine de Ginestière, BP2 3194, 06204 Nice Cedex 03, France.

Funding information

Fondation ARC pour la Recherche sur le Cancer, Grant/Award Number: 2016 1204713; Agence Nationale de Recherches sur le Sida et les Hépatites Virales, Grant/Award Number: # AO 2013-1 CSS3; Agence Nationale de la Recherche, Grant/Award Number: # ANR-11-LABX-0028-01

Abstract

Brown and brown-like adipocytes (BBAs) control thermogenesis and are detected in adult humans. They express UCP1, which transforms energy into heat. They appear as promising cells to fight obesity. Deciphering the molecular mechanisms leading to the browning of human white adipocytes or the whitening of BBAs represents a goal to properly and safely control the pathways involved in these processes.

Here, we analyzed how drugs endowed with therapeutic potential affect the differentiation of human adipose progenitor-cells into BBAs and/or their phenotype. We showed that HIV-protease inhibitors (PI) reduced UCP1 expression in BBAs modifying their metabolic profile and the mitochondria functionality. Lopinavir (LPV) was more potent than darunavir (DRV), a last PI generation. *PPAR γ* and *PGC-1 α* were decreased in a PI or cell-specific manner, thus altering *UCP1*'s constitutive expression.

In addition, LPV altered p38 MAPK phosphorylation, blunting then the β -adrenergic responses. In contrast, low doses of resveratrol stimulated the activatable expression of UCP1 in a p38 MAPK-dependent manner and counteracted the LPV induced loss of UCP1. This effect was independent of the resveratrol-induced sirtuin-1 expression. Altogether our results uncover how drugs impact crucial components of the networks regulating the expression of the thermogenic signature. They provide important information to control the relevant pathways involved in energy expenditure.

KEYWORDS

adipose tissue, aging, brown adipocytes, energy metabolism, HIV protease inhibitors, p38 mitogen-activated kinase, resveratrol, sirtuin-1, UCP1, white adipocytes

1 | INTRODUCTION

Adipose tissue (AT) is composed of two distinct entities with opposite functions that play a crucial role in the control of energy balance. While white adipose tissue (WAT) consists in a safe energy-storing reservoir of lipids, brown/beige adipose tissue (BAT)

*Christophe Ravaut and Martin Paré contributed equally to this study.

†Christian Dani and Annie Ladoux are senior co-authors.

promotes energy dissipation and produces heat. BAT was considered for long to be present exclusively in rodents and human neonates. Its presence was established in adult humans in 1972 (Heaton, 1972) and further confirmed, thanks to positron-emission tomography (Cypess et al., 2009; van Marken Lichtenbelt et al., 2009). In adults, the major depots are localized in the cervical-supraclavicular region and in a region extending from the neck to the thorax. In addition to these brown adipocytes (Sanchez-Gurmaches et al., 2012; Seale et al., 2007), brown-like (or beige/brite) adipocytes (BBAs) bearing brown properties were detected in WAT depots. BBAs display distinct molecular signatures with brown adipocytes (Peirce, Carobbio, & Vidal-Puig, 2014), but are metabolically active as they respond to cold stimulus or β 3-adrenergic stimulation (Barbatelli et al., 2010), contributing then to energy homeostasis. BAT depots and BBAs are reduced in obese humans or during aging. This is accompanied by defects that fetch up in metabolic disorders (Cypess et al., 2009; Graja & Schulz, 2015; Lean, James, Jennings, & Trayhurn, 1986).

A better comprehension of the mechanisms involved in acquisition (browning) or the loss (whitening) of the thermogenic signature is of interest since an increase in the energy expenditure emerged as a possible strategy to treat obesity or to prevent metabolic disorders including those occurring in the elderly.

BBAs contain high amounts of mitochondria, which express the uncoupling protein-1 (UCP1) at their inner membrane. This protein dissipates the mitochondrial proton gradient and converts the energy of substrate oxidation into heat instead of ATP (Klingenberg, 1999) and it represents the functional hallmark for these cells. In addition to UCP1, the thermogenic signature includes cell death activator CIDE-A (*CIDEA*), a protein that modulates the uncoupling action of UCP1 and lipolysis in adipocytes and two transcriptional coactivators: PR domain containing-16 (*PRDM16*) and PPAR γ coactivator-1 α (*PGC-1 α* ; Cohen & Spiegelman, 2015). Several transcription factors control *UCP1* expression: PPAR γ 2, a master transcriptional regulator of adipocyte differentiation (Tontonoz, Hu, & Spiegelman, 1994), *PGC-1 α* (Cohen & Spiegelman, 2015), retinoid-X-receptor, and thyroid receptor. A region located 3.9 kb upstream of the transcription start of the human *UCP1* gene contains response elements for these nuclear hormone receptors (Villarroya, Peyrou, & Giralt, 2017). Moreover, *UCP1* expression in response to cold exposure and catecholamines is triggered by an increase in intracellular cAMP and phosphorylation of p38 MAPK, thus indicating the existence of an actionable pathway. In addition to these pathways, sirtuins (SIRT), the mammalian homologs of *sir2* (silent information regulators), play a crucial role in the maintenance of AT and adipocytes including BBAs. They belong to the third class of deacetylase enzymes that bind NAD⁺ (Landry et al., 2000) and they are known to promote longevity in invertebrates (Tissenbaum & Guarente, 2001). For instance, diet-induced obesity was accompanied by a loss of brown fat in SIRT1-deficient mice (Xu et al., 2016), while gain of function of SIRT1 promotes murine WAT browning (Qiang et al., 2012). In parallel, SIRT1 controls *UCP1* expression in murine immortalized brown adipocytes as it promotes

deacetylation of PPAR γ (Nohr, Bobba, Richelsen, Lund, & Pedersen, 2017). SIRT2, the most abundant sirtuin in adipocytes, regulates also adipose differentiation in rodents (Jing, Gesta, & Kahn, 2007). Its expression decreases in the AT of obese individuals (Krishnan et al., 2012) and increases in the AT of mice exposed to caloric restriction (Wang, Nguyen, Qin, & Tong, 2007). Note that resveratrol (5-[(E)-2-(4-hydroxyphenyl)ethenyl]benzene-1,3-diol; RESV), a natural polyphenolic compound endowed with antiaging properties and which is able to activate SIRT1, was reported to display beneficial effects and to induce brown-like adipocytes formation in mice (Wang et al., 2016).

In contrast, some molecules are known to alter AT and mitochondria integrity. Besides its valuable efficiency in treating patients with AIDS, the highly active antiretroviral therapy (ART) has been reported to display unwanted side effects, that is, selective loss of fat depots, lipodystrophies, dyslipidemia, hypertriglyceridemia, insulin resistance, and premature aging (Caron-Debarle et al., 2010; Torres & Lewis, 2014). This therapy is composed of several classes of antiretroviral drugs that hinder the formation of infectious viral particles, including inhibitors of the HIV protease (PI) and of the reverse transcriptase (NRTI). PIs were shown to alter adipose differentiation in vitro and to decrease the expression of white adipose markers as well as genes controlling these processes: *C/EBP α* and PPAR γ (Bastard et al., 2002; Gallego-Escuredo et al., 2010; Kim, Wilson, Wabitsch, Lazar, & Steppan, 2006; Vernochet et al., 2005). Information concerning PIs' effect on BBAs properties including mitochondrial dysfunction and aging is limited.

Hence, a properly controlled thermogenic signature remains a challenge for both treatment of obesity and prevention of metabolic disorders. To decipher the complex network that governs *UCP1* expression, we challenged BBAs obtained from distinct human adipose progenitors (APs; Elabd et al., 2009; Kouidhi et al., 2015) with PIs and RESV and we further analyzed how these drugs impacted BBAs' features. We focused on two PIs: Lopinavir (LPV), one of the most widely used PI and darunavir (DRV), a new generation-PI renowned to display few secondary effects. The concentrations used are consistent with those measured in the plasma of AIDS-treated patients (Darini et al., 2013; Lopez-Cortes et al., 2013). In all BBAs models used here, chronic or short-term treatment with LPV promoted adipose whitening as it dramatically repressed *UCP1* and *CIDEA* expressions. hMADS-adipocytes were more sensitive than chin-adipocytes. LPV, but not DRV, decreased the expression of PPAR γ 2 and *PGC-1 α* in hMADS-adipocytes. LPV increased reactive oxygen species (ROS) production in mitochondria while it decreased superoxide dismutase-2 (SOD2). In addition, LPV blocked the β 3-adrenergic responses through p38 MAPK inhibition. It also reduced the expression of sirtuins. RESV promoted *UCP1* expression and browning. It partially reversed LPV's effects in a p38 MAPK-dependent but SIRT1-independent manner.

Our results pointed out that the thermogenic signature was controlled by both basal and actionable components that may be

targeted in a cell-specific or drug-specific manner in human cells. Their relevance is discussed in the context of metabolic disorders.

2 | MATERIAL AND METHODS

2.1 | Reagents

Unless specified otherwise, reagents were obtained from Sigma (Saint-Quentin Fallavier, France), tissue culture media from LONZA (Levallois-Perret, France) and fetal calf serum from Dutscher (Brumath, France). PIs were obtained by extraction from commercially available tablets and capsules. Their purity was assessed by ^1H and ^{13}C nuclear magnetic resonance and mass spectrometry.

2.2 | Cell culture

hMADS cells were isolated more than 15 years ago from adipose tissue, as surgical scraps from surgical specimen of various surgeries of young donors, with the informed consent of the parents. All methods were approved and performed in accordance with the guidelines and regulations of the Centre Hospitalier Universitaire de Nice Review Board. Chin APs were derived from the stroma vascular fraction of Caucasians women who underwent elective liposuction procedures. Informed consent was obtained from all patients.

hMADS cells and chin-APs were grown, maintained, and differentiated as previously described (Kouidhi et al., 2015; Rodriguez et al., 2004). They express a thermogenic signature upon appropriate differentiation conditions (referred as hMADS-adipocytes; Elabd et al., 2009). Chin-derived adipocytes (referred as chin-adipocytes) express UCP1 after differentiation (Kouidhi et al., 2015). Cells were tested every other week for the absence of mycoplasma.

2.3 | Gene expression analysis

Total RNA was extracted using the TRI-Reagent kit (Euromedex, Soufflweyersheim, France). Reverse-transcription (RT) was performed using MMLV reverse transcriptase (Promega, Charbonnières, France), as recommended by the manufacturer. Primer sequences are described in the supplementary section. Real-time polymerase chain reaction (PCR) assays were run on an ABI Prism One step real-time PCR machine (Applied-Biosystems, Courtaboeuf, France). Normalization was performed using *36B4* as a reference gene. Quantification was performed using the comparative Ct method.

2.4 | Protein expression

Cells were rinsed in ice-cold phosphate-buffered saline (PBS) and whole cell extracts were prepared as described (Ravaud et al., 2015).

Thirty micrograms of proteins were resolved by sodium dodecyl sulfate-polyacrylamide gel electrophoresis under reducing conditions and transferred to Immobilon-P membranes (Millipore, Molsheim,

France). The detection antibodies (see supplementary section) were used according to the manufacturer's instructions.

The bound primary antibody was detected by horseradish peroxidase-conjugated secondary antibody and visualized using an enhanced chemiluminescence detection kit (Millipore, Molsheim, France).

Chemiluminescence was observed using a molecular imager ChemiDoc XRS system (Bio-Rad, Marne la Coquette, France). The band intensity was quantified using Bio-Rad QuantityOne software.

2.5 | UCP1 promoter analysis

hMADS cells were infected with a lentivirus containing the plasmid, pLV.ExBi.P/Puro-hUCP1promoter-Luc(firefly)-T2A-hrGFP, which expresses luciferase and GFP driven by the human UCP1 promoter (4,148 bp; Xue et al., 2015) and further selected upon puromycin resistance.

They were differentiated for 23 days in 12-well plates and further incubated or not in the presence of 20 μM DRV or LPV. Cells were rinsed with PBS and lysed. The luciferase activity was assessed using the luciferase assay system (Promega) and was normalized to the protein concentration of each sample.

2.6 | Mitochondrial-specific dye staining

Differentiated cells were stained with MitoTracker dyes (MtT) for 25 min at 37°C in a humidified atmosphere containing 5%CO₂. MtT-Green (M7514, CMXRos, 200 nM) and MtT-Orange (M7511, CMH2 TMRos, 1 μM) solutions were added at time zero in the presence or the absence of PIs. Acquisitions were performed every 2 min on five different fields for 25 min. Signals were quantified using the ImageJ software from three independent experiments.

2.7 | Microscopic analysis

The spinning-disk experiments were done on an inverted IX81 Olympus microscope (Olympus, Center Valley, PA) at 37°C in a CO₂-controlled atmosphere. Separation of the emission signals was done using a GFP/mCherry filter cube containing a beam splitter 580 and two emission filters, BP 525/50 and LP 600, respectively. The LASER lines were at 405 nm (diode), 488 nm (DPSS), 561 nm (DPSS), and 640 nm (Diode; Andor Technology, Belfast, UK). The system was controlled using MetaMorph software (Molecular Devices, Sunnyvale, CA).

2.8 | Statistical analysis

The results are shown as mean \pm standard error of the mean (SEM), with the number of experiments indicated. Statistical significance was determined by *t* tests using BiostaTGV (INSERM and Sorbonne University, PARIS, France). Probability (*p*) values < .05 were considered statistically significant and are marked with a single asterisk, <.01 with double asterisks, and <.001 with triple asterisks.

3 | RESULTS

3.1 | LPV and DRV displayed distinct effects on UCP1 and the thermogenic signature expressions

The time course for the thermogenic signature expression indicated that UCP1 was detected after 15 days of differentiation, in contrast to adipocyte structural proteins (PLIN1 and FABP4) which appeared earlier (Figure S1). Thus, cells differentiated for at least 17 days were further used. We analyzed the impact of a chronic PI-treatment on this process using hMADS-adipocytes. Increasing concentrations of DRV up to 50 μ M had no significant effect on the expression of *PLIN1*, while LPV (10 μ M) reduced it significantly (Figure 1a).

In contrast, both PIs dose-dependently and significantly reduced the expression of brown adipocyte markers, *UCP1* and *CIDEA* (Figure 1b,c), even at concentrations that did not impair *PLIN1* expression (10 μ M DRV and 5 μ M LPV, respectively) indicating that PIs preferentially affect BBAs markers. In addition, DRV as well as LPV lowered *PPAR γ 2* expression in a dose-dependent manner in hMADS-adipocytes (Figure 1d). While DRV had no effect on *PGC-1 α* , low concentrations of LPV decreased significantly its mRNA expression (Figure 1e). Thus, LPV and DRV had distinct effects on genes controlling *UCP1*.

These results were further confirmed at the protein level. *UCP1* expression was impaired at low doses of PIs while *PLIN1* expression was only suppressed for the highest LPV concentration (Figure 1f).

These observations also applied to chin-adipocytes, which exhibited a preferential brown/beige phenotype. DRV (20–50 μ M) impaired brown markers expressions, while 5 μ M LPV was sufficient (Figure S2). *PPAR γ 2* expression was reduced only when differentiation was carried out in the presence of 20 μ M LPV. PIs did not impact *PGC-1 α* expression. Thus, the decreased-*UCP1* expression did not directly result from defects in *PPAR γ 2* and/or *PGC-1 α* expressions in chin-adipocytes. Note that PIs did not alter *PRDM16* expression in both cell types (Figure S3).

These results indicated that chronic treatment with PIs altered the thermogenic signature and induced whitening in distinct cell models of BBAs.

3.2 | PIs inhibited browning and UCP1 expression

We then determined how PIs impacted the brown/beige phenotype in cells treated with 10 μ M PIs at late stages of differentiation that is, from Days 15 to 17 or from Days 15 to 22 (Figure 2a–d). When DRV was applied from Days 15 to 17 or 15 to 22, *UCP1*, *PLIN1*, and *FABP4* expressions were not modified. LPV dramatically impaired *UCP1*, but not *PLIN1* and *FABP4* expressions, indicating that a short-term treatment was sufficient to modify the BBA phenotype. The impact of LPV was higher when cells were treated from Days 15 to 22 compared with treatment from Days 15 to 17 (Figure 2a,b). Similar results were observed in chin-adipocytes (Figure S4).

We then analyzed *UCP1* promoter activity using hMADS-adipocytes expressing a construct containing the firefly luciferase gene under the control of the *UCP1* promoter (Xue et al., 2015). A 4-day treatment of hMADS-adipocytes with DRV produced no

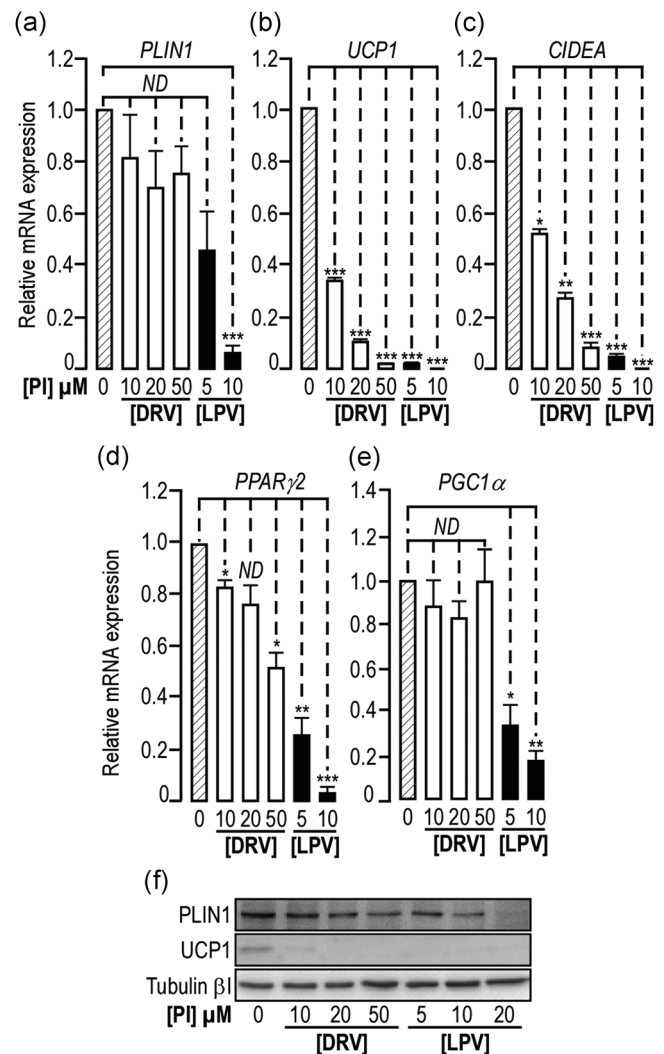


FIGURE 1 Effects of PIs treatment on differentiation of hMADS cells. (a–e) Expression of the adipogenic/thermogenic markers *PLIN1*, *UCP1*, *CIDEA*, *PPAR γ 2*, and *PGC1 α* after 17 days of differentiation in the absence or the presence of increasing concentrations of PIs. Expression of the markers was assessed by the real-time RT-PCR and normalized for the expression of *36B4* mRNA. It was measured in cells grown in the differentiation medium in absence of PIs (dashed bar), in presence of DRV (white bars) or LPV (black bars). The means \pm SEM were calculated from three independent experiments, with determinations performed in duplicate (* p < .05, ** p < .01, *** p < .001, ND means “not significantly different”). (f) Expression of *PLIN1* and *UCP1* after 17 days of differentiation in the absence or the presence of increasing concentrations of PIs. Expression of the proteins was measured in cells grown in the differentiation medium in the absence or in the presence of increasing concentrations of PIs. Expressions of *PLIN1* (upper panel) and *UCP1* (middle panel) and *Tubulin β 1* used as a loading control (lower panel) were analyzed by western blot using specific antibodies. Representative western blots are shown. Thirty micrograms of proteins were loaded in each lane. DRV, darunavir; LPV, lopinavir; PIs, protease inhibitors; RT-PCR, reverse-transcription polymerase chain reaction

significant change, while LPV reduced the luciferase activity two times onwards (Figure 2e). Indeed a two-day treatment of hMADS-adipocytes with LPV between days 15 and 17 of differentiation significantly reduced the expression of *PPAR γ 2* and *PGC-1 α* (Figure 2f,g) while DRV was less efficient.

Altogether these results showed that both DRV and mainly LPV-induced whitening of BBAs by decreasing UCP1 expression through a reduced expression of the transcription factors *PPAR γ 2* and *PGC-1 α* , hMADS-adipocytes being more sensitive than chin-adipocytes.

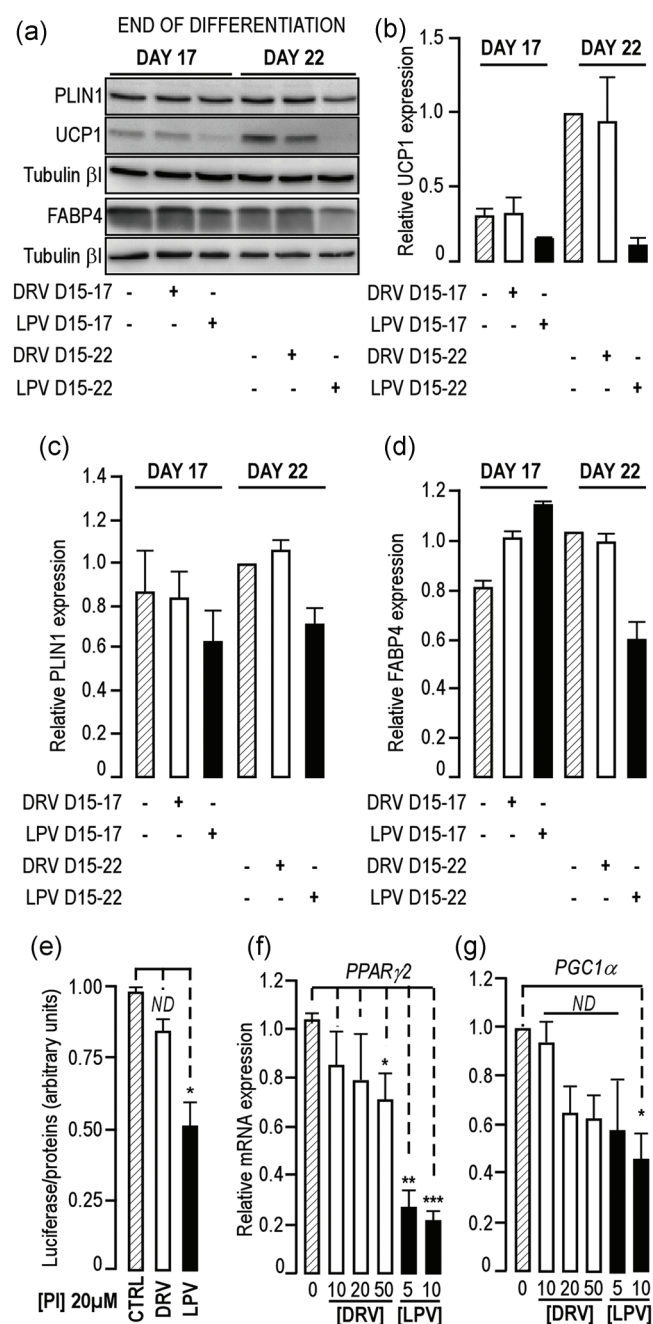


FIGURE 2 Continued.

3.3 | LPV impaired forskolin-induced UCP1 expression

As catecholamines induce browning, we measured p38 MAPK phosphorylation and UCP1 expression in hMADS-adipocytes treated or not with PIs and stimulated by forskolin to mimic the β -adrenergic response. The DRV treatment had no significant effect, while a 4-day treatment with LPV reduced forskolin-induced p38 MAPK phosphorylation two times onwards, compared with control (Figure 3a,b). UCP1 mRNA expression was slightly reduced by DRV and LPV in the absence of forskolin stimulation. A 4-hr stimulation with forskolin increased UCP1 mRNA expression 10 times onwards in control cells. The LPV treatment (20 μ M) blunted this effect hindering then the response to a β -adrenergic stimulation (Figure 3c).

Altogether these data indicated that LPV dramatically impaired expression of thermogenic genes by altering the actionable signaling pathway induced by elevated-cAMP levels.

3.4 | LPV impaired mitochondrial function and metabolism in different models of human BBAs

We then analyzed the PI-induced oxidative damage in mitochondria with MitoTracker Orange. MitoTracker Green was used to label all mitochondria. Note that MtT-Orange labeling was detected after

FIGURE 2 PIs induced a blockade of UCP1 expression in hMADS-adipocytes. (a) Expression of PLIN1, UCP1, and FABP4 in cells treated with LPV or DRV. Thirty micrograms of proteins prepared from hMADS differentiated for the indicated period of time and treated during the last 2 days or more as indicated with 20 μ M of LPV or DRV were loaded onto a 10% acrylamide gel to measure the expressions of PLIN1 and UCP1 and onto a 15% acrylamide gel to measure the expression of FABP4. Expression of Tubulin- β I was used as a loading control (lower panel). A representative western blot analysis is shown. (b-d) Quantification of the signals. Expression of the proteins was quantified using the Quantity One Program and compared with the expression of Tubulin β I. Two independent experiments performed in duplicate were analyzed. (e) Transcriptional inhibition of UCP1 promoter in response to PIs. The luciferase expression was driven by the human UCP1 promoter. Luciferase activity was determined after 4 days of incubation with 20 μ M of PIs. The means \pm SEM were calculated from four independent experiments performed in triplicate. (* p < .05 as compared with untreated cells, ND means "not significantly different"). (f,g) Expression of *PPAR γ 2* and *PGC1 α* after 2 days of treatment in the absence or the presence of increasing concentrations of PIs (Days 15–17 of differentiation). Expression of the markers was assessed by the real-time RT-PCR and normalized for the expression of *36B4* mRNA. It was measured in cells grown in the differentiation medium in the absence of PIs (dashed bar), in the presence of DRV (white bars) or LPV (black bars). The means \pm SEM were calculated from three independent experiments, with determinations performed in duplicate (* p < .05, ** p < .01, *** p < .001, ND means "not significantly different"). DRV, darunavir; LPV, lopinavir; mRNA, messenger RNA; PIs, protease inhibitors; RT-PCR, reverse-transcription polymerase chain reaction

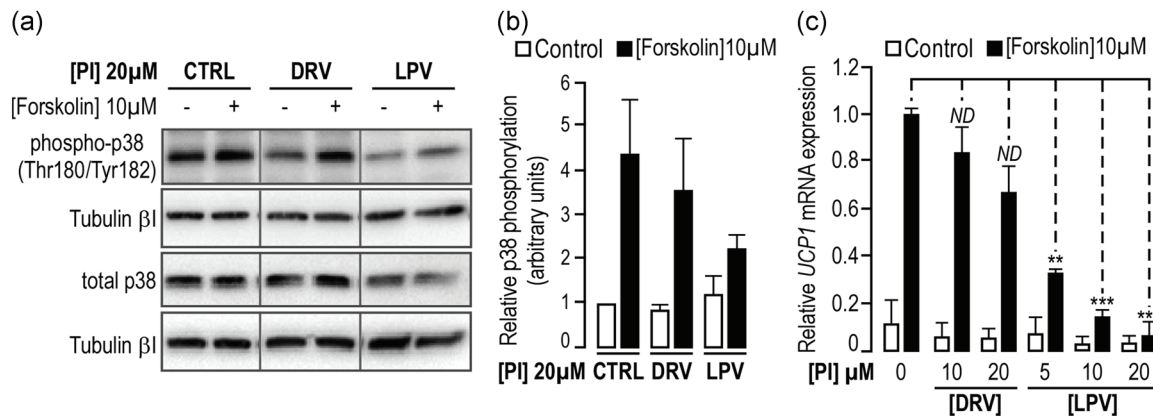


FIGURE 3 Lopinavir treatment blocked β -adrenergic responses. (a) Forskolin-induced p38 MAPK phosphorylation in cells treated for 4 days with 20 μ M DRV or LPV. Proteins were prepared from hMADS adipose progenitors differentiated for 21 days and further treated during 4 days with LPV or DRV and then submitted to a 15 min stimulation with 10 μ M forskolin as indicated. Thirty micrograms of proteins were loaded onto a 10% acrylamide gel to measure the expressions of phosphorylated or total p38 MAPK. Expression of Tubulin- β I was used as a loading control (lower panel). Representative western blots are shown. (b) Quantification of the signals. Expression of the proteins was quantified using the Quantity One Program and compared with the expression of Tubulin β . Two independent experiments performed in duplicate were analyzed. (c) UCP1 mRNA expression of differentiated hMADS cells, exposed or not to DRV or LPV at the indicated concentrations for 1 day prior forskolin stimulation. UCP1 expression was assessed by the real-time RT-PCR and normalized to the expression of 36B4 mRNA. Comparison of the PI-induced alteration in control cells (white histograms) or in cells stimulated for 4 hr with 1 μ M forskolin (black histograms). Results are reported as the means \pm SEM calculated from three independent experiments, with determinations performed in duplicate (** p < .01; *** p < .001, ND means "not significantly different"). DRV, darunavir; LPV, lopinavir; mRNA, messenger RNA; PIs, protease inhibitors; RT-PCR, reverse-transcription polymerase chain reaction

8 min of incubation and was more pronounced after 20 min in both control and PI-treated cells (Figure S5).

Qualitative analysis revealed a very weak red labeling in untreated or DRV-treated hMADS-adipocytes (Figure 4a; Figure S6a). A significant increase in the oxidative stress was measured after quantification of the fluorescent signals only in LPV-treated cells compared with control (Figure 4b; Figure S6b). In addition, LPV decreased significantly SOD2 expression, a major enzyme involved in clearing superoxide ions. This may account for the observed-ROS accumulation (Figure 4c,d and Figure S6c).

We then compared the oxygen consumption rates (OCR) in control cells or cells treated with PIs. A 72-hr DRV treatment had no significant effect compared with control (Figure S6d). Indeed, similar treatment with LPV produced a robust decrease of both basal and FCCP maximal mitochondrial respiration as compared with control or DRV-treated cells. ATP production measured with oligomycin (OLIGO), an inhibitor of the FOF1-ATP synthase, was similar in all cells. The spare mitochondrial capacity was 2.8 times lower in LPV-treated cells than in control cells. Rotenone/AntimycinA reduced oxygen consumption to a similar level in all cases. These results indicated that LPV altered the mitochondria and caused metabolic dysfunctions.

3.5 | LPV modulated the expression of antiaging markers

As expression of the thermogenic signature declines with age, we aimed to evaluate the effect of PIs on sirtuins expressions. Among the distinct sirtuins, SIRT2 was the most expressed in both hMADS and chin-adipocytes (Figure S7a,b). We focused on the expressions of

SIRT1, SIRT2, and SIRT6 which are relevant for adipocytes and SIRT3 since it localizes in mitochondria. A 2-day treatment with LPV but not DRV was sufficient to reduce significantly the expression of these all four sirtuins in hMADS-adipocytes (Figure 5a,d). The chronic treatment of hMADS cells with PIs during the differentiation process gave similar results (Figure 5e-h). Chin-adipocytes were less sensitive as SIRT1-2-3 expressions were only altered by the highest LPV dose (Figure S7).

Altogether these results indicated that PIs decrease the expression of antiaging markers, as it has been observed during aging (Torres & Lewis, 2014).

3.6 | Effect of resveratrol on UCP1 expression

3.6.1 | Distinct concentrations of resveratrol induced UCP1, CIDEA, and SIRT1 expressions

We analyzed the effects of RESV a commercially available SIRT1 inducer. In hMADS-adipocytes submitted to increasing doses of RESV, UCP1 expression was induced at doses comprised between 0.1 μ M and 3 μ M (Figure 6a,b) with the maximum effect observed at 1 μ M (induction factor = 1.95 ± 0.33 ($n = 10$, $p = .018$)). Higher doses inhibited its expression (Figure 6a-c). While we noticed a slight increase for UCP1 mRNA expression (Figure 6c), RESV had a more clear effect on protein expression (Figure 6a,b), suggesting that both transcriptional and posttranscriptional effects were involved. Low doses of RESV modulated CIDEA expression in a similar manner. Concentrations higher than 30 μ M induced SIRT1 but robustly inhibited UCP1 and CIDEA expressions (Figure 6c).

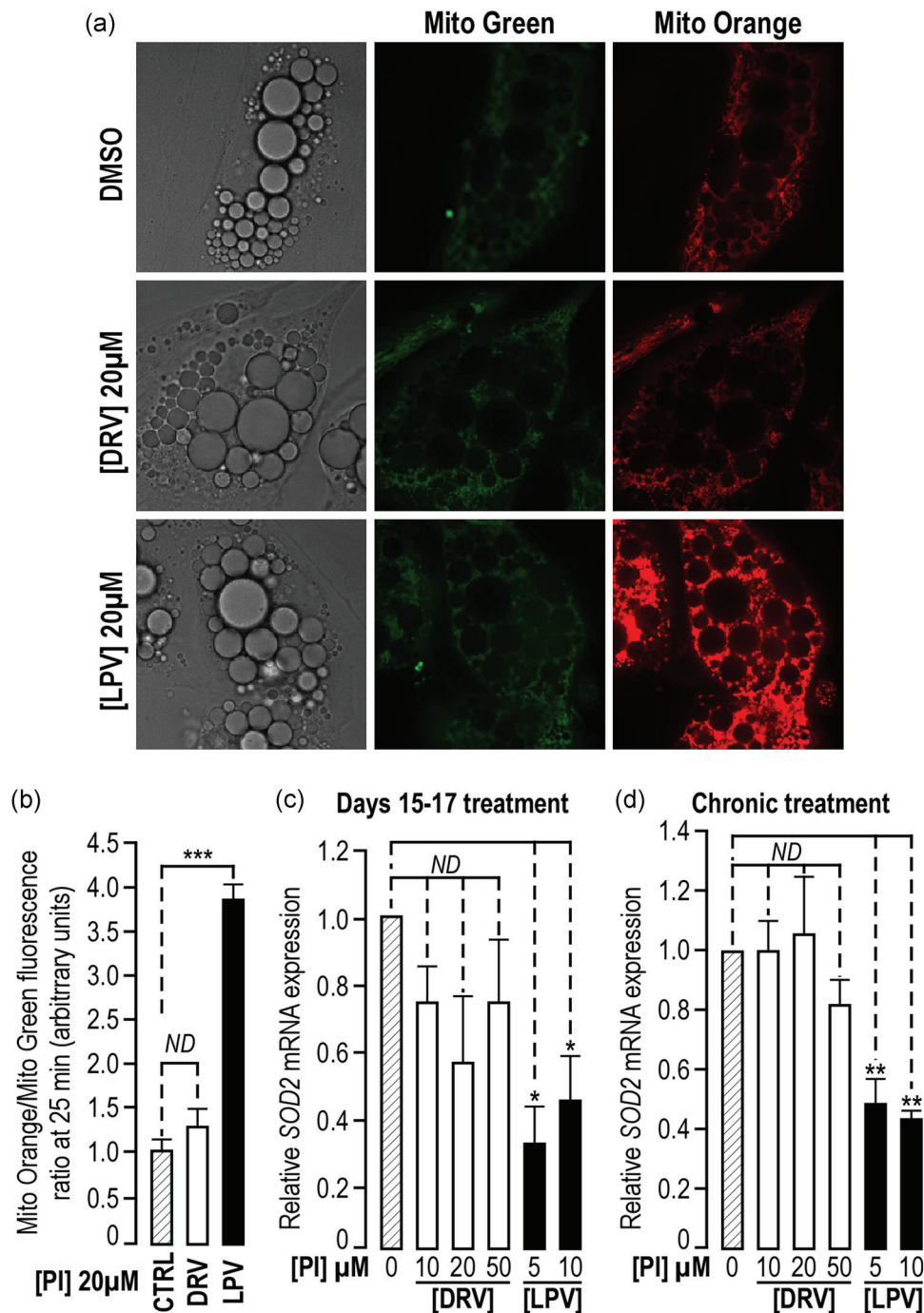


FIGURE 4 Lopinavir induced ROS production in differentiated hMADS cells. (a) LPV induced a significant and time dependent production of ROS. hMADS-adipocytes were visualized during incubation with both MitoTracker Green and MitoTracker Orange, in the presence or the absence of PIs as indicated, using an IX81Olympus microscope under brightfield, or with a GFP/mCherry filter cube. Cells showed cytoplasmic labeling and nuclear sparing, consistent with mitochondrial localization. Magnification $\times 100$. (b) Quantification of the signals. LPV induced a significant and time dependent ROS production as measured from the ratio of orange versus green fluorescence. The means \pm SEM were calculated from three independent experiments, with determinations performed in quintuplicate ($***p < .001$, ND means "not significantly different"). (c,d) Effect of PIs treatment on SOD2 expression. SOD2 expression was assessed by the real-time RT-PCR and normalized for the expression of 36B4 mRNA. SOD2 expression was measured in cells treated for 2 days (c) or grown in the differentiation medium (d) in the absence of PIs (dashed bar), in the presence of DRV (white bars) or LPV (black bars). The means \pm SEM were calculated from three independent experiments, with determinations performed in duplicate ($*p < .05$; $**p < .01$, ND means "not significantly different"). DRV, darunavir; LPV, lopinavir; mRNA, messenger RNA; PIs, protease inhibitors; ROS, reactive oxygen species; RT-PCR, reverse-transcription polymerase chain reaction [Color figure can be viewed at wileyonlinelibrary.com]

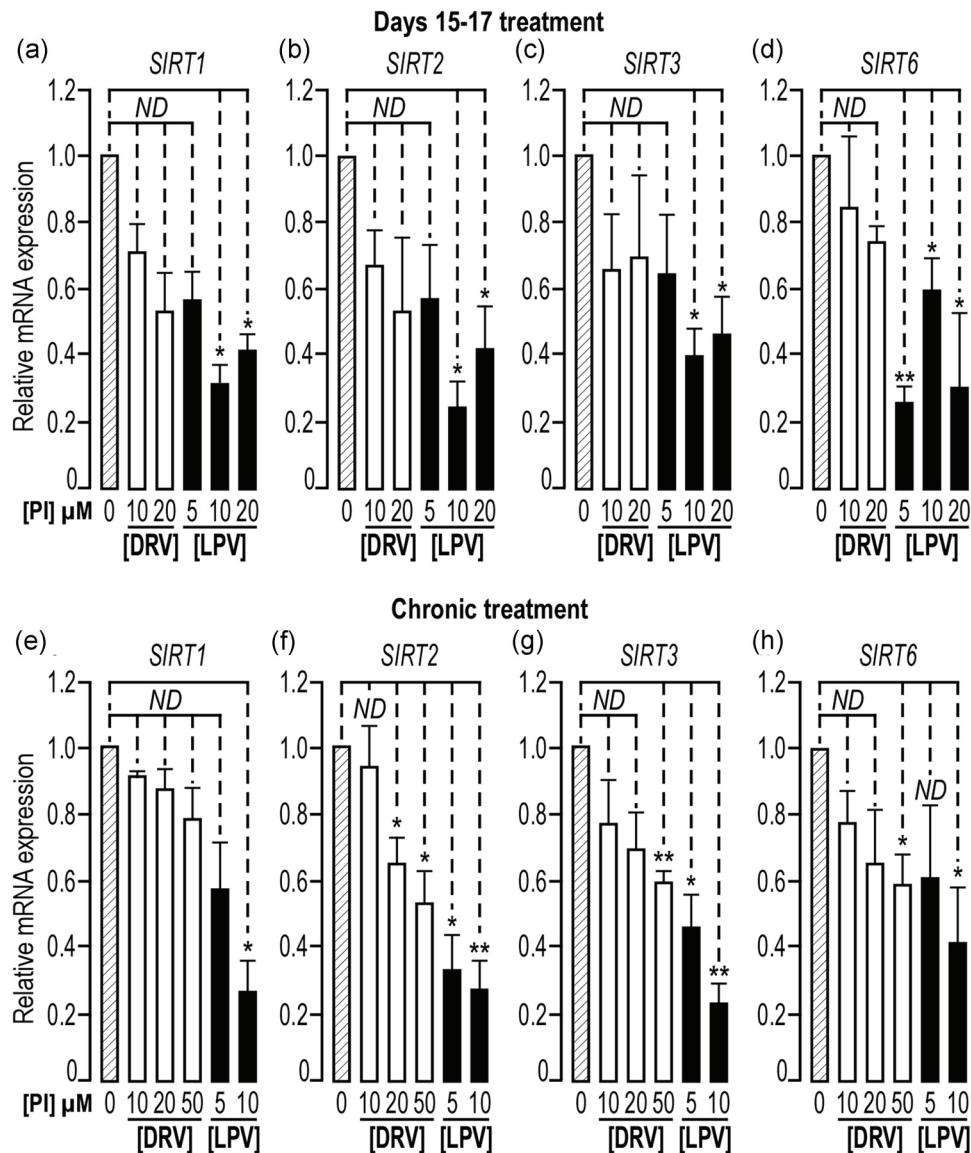


FIGURE 5 PIs modified the expression of genes associated with senescence in adipocytes. *Sirtuins* expression was measured after 17 days of differentiation in the absence or the presence of increasing concentrations of PIs. *SIRT* expressions were assessed by real-time RT-PCR and normalized for the expression of *36B4* mRNA. *SIRT* expressions were measured in cells treated for 2 days (a–d) or grown in the differentiation medium (e–h) in the absence of PIs (dashed bar), in the presence of DRV (white bars), or LPV (black bars). The means \pm SEM were calculated from three independent experiments, with determinations performed in duplicate (* $p < .05$, ** $p < .01$, ND means “not significantly different”). DRV, darunavir; LPV, lopinavir; mRNA, messenger RNA; PIs, protease inhibitors; RT-PCR, reverse-transcription polymerase chain reaction

These results pointed out a clear discrepancy between the doses of RESV promoting the thermogenic signature and those fighting aging in human cells.

3.6.2 | Inhibition of p38-MAPK activity blocked resveratrol-induced UCP1 expression

In search of common molecular targets to LPV and RESV, hMADS-adipocytes were treated with 5 μM SB203580 (SB) to block the activity of p38 MAPK, previously identified as a LPV target. They were further challenged for 4 days with 1 μM RESV. Inhibiting the activity of p38 MAPK prevented RESV to induce UCP1 expression

(Figure 6d,e). Thus, p38 MAPK emerged as a common target to RESV and LPV.

3.6.3 | Resveratrol partially reversed LPV's effect on UCP1 expression

A 4-day stimulation of hMADS-adipocytes with RESV (1 μM) in the presence of LPV (10 μM) partially restored the LPV-reduced UCP1 expression. However it remained below the induction observed in control conditions (Figure 6f,g). This indicated that activation of p38 MAPK by RESV was sufficient to increase UCP1 expression through an actionable pathway.

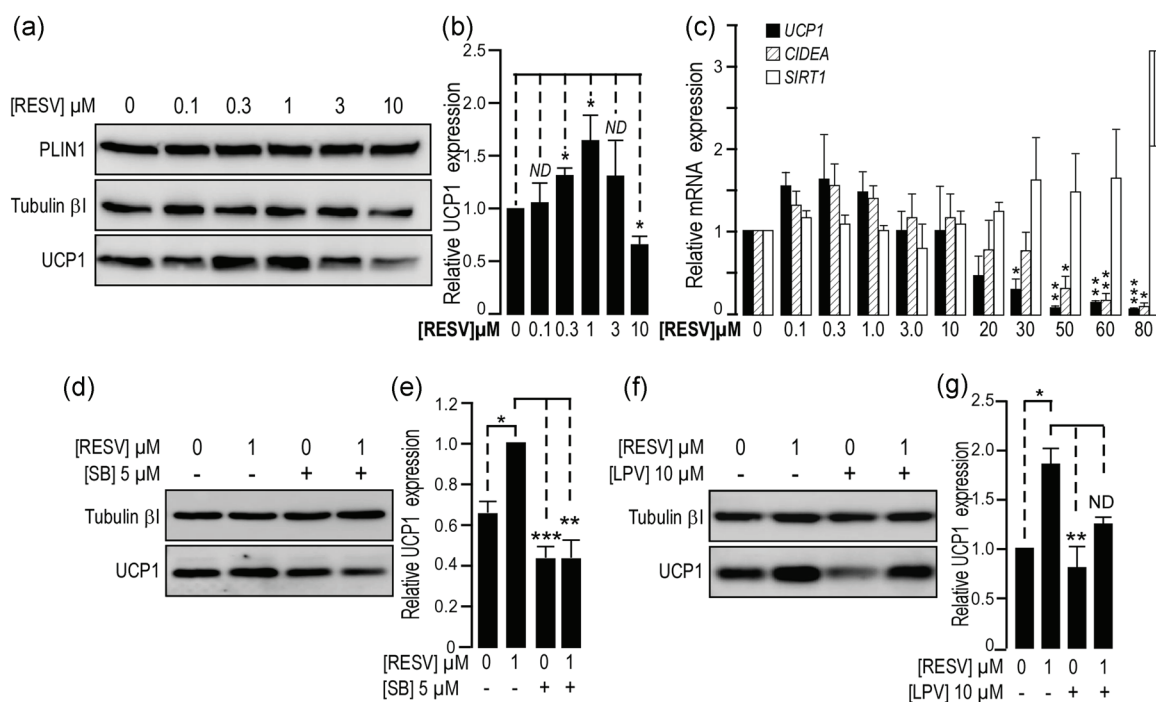


FIGURE 6 Resveratrol induces UCP1 in a p38 MAPK-dependent manner and counterbalance LPV's effect. (a) RESV increased UCP1 expression in a dose-dependent manner. Protein expression was measured in hMADS-adipocytes grown in the differentiation medium in the absence or in the presence of increasing concentrations of RESV during the last 4 days. Expressions of UCP1 (lower panel), PLIN1 (upper panel), and Tubulin- β 1 used as a loading control (intermediate panel) were analyzed by western blot using specific antibodies. Representative western blots are shown. (b) Quantification of the signals. Expression of the proteins was quantified using the Quantity One Program and compared with the expression of Tubulin- β 1. The means \pm SEM were calculated from four independent experiments ($*p < .05$, ND means "not significantly different"). (c) RESV has opposite effects on UCP1 expression depending on its concentration UCP1 (black bars), CIDEA (dashed bars), and SIRT1 (white bars) expressions were assessed by the real-time RT-PCR and normalized for the expression of 36B4 mRNA. Expression was measured in cells grown in the differentiation medium in the absence or in the presence of increasing doses of RESV between Days 17 and 21. The means \pm SEM were calculated from three independent experiments, with determinations performed in duplicate ($*p < .05$, $**p < .01$, $***p < .001$, ND means "not significantly different"). (d) SB203580 blocks RESV-induced UCP1 expression. Protein expression was measured in hMADS-adipocytes differentiated for 17 days. They were treated or not with SB203580 (5 μ M) and further incubated for 4 days in the absence or in the presence of RESV (1 μ M). Expression of UCP1 (lower panel), and Tubulin- β 1 used as a loading were analyzed by western blot using specific antibodies. Representative western blots are shown. (e) Quantification of the signals. Expression of UCP1 was quantified using the Quantity One Program and compared with the expression of Tubulin β 1. The means \pm SEM were calculated from six independent experiments ($*p < .05$, $**p < .01$, $***p < .001$). (f) RESV partially restored the LPV impaired UCP1 expression. Protein expression was measured in hMADS-adipocytes differentiated for 17 days. They were treated or not with 1 μ M RESV and further incubated for 4 days in the absence or in the presence of LPV (10 μ M). Expressions of UCP1 (lower panel), Tubulin- β 1 used as a loading control (upper panel) were analyzed by western blot using specific antibodies. Representative western blots are shown. (g) Quantification of the signals. Expression of the proteins was quantified using the Quantity One Program and compared with the expression of Tubulin β 1. The means \pm SEM were calculated from three independent experiments ($*p < .05$, $**p < .01$, ND means "not significantly different"). DRV, darunavir; LPV, lopinavir; mRNA, messenger RNA; RT-PCR, reverse-transcription polymerase chain reaction

4 | DISCUSSION

We aimed to decipher how the pathways that control the thermogenic signature can be modulated by drugs to promote either whitening or browning of BBAs. In human cells, PIs decreased brown adipocyte differentiation, altered BBAs' functionality, and affected their phenotype. In contrast, RESV a natural polyphenol with beneficial effects on metabolism, which is also able to induce SIRT1 expression, increased UCP1 expression, and counteracted the LPV induced loss of UCP1.

Adipose tissue is the main target for unwanted side effects of ART therapy. Indeed, an important remodeling of adipose tissue and

lipodystrophies develop in patients with AIDS treated with ART. Many studies conducted using murine or human models of adipose differentiation reproduced the impairments observed in patients with AIDS in the absence of HIV infection. For instance, PIs inhibit adipose differentiation of both murine and human adipose progenitors (Bastard et al., 2002; Vernochet et al., 2005). These models allowed the identification of many pathways sensitive to ART. Chronic treatment of hMADS- and chin-adipocytes with LPV or DRV dramatically and dose-dependently decreased UCP1 and CIDEA expressions, while only high doses of LPV reduced the expression of PLIN1, an adipocyte structural protein. These observations unambiguously indicate that PIs preferentially hindered the formation of cells able to expend energy and favored

the whitening of BBAs. They are in line with previously reported observations on the effects of indinavir in murine models (Viengchareun et al., 2007). However, these two PIs harbored differences in the alteration of the thermogenic signature. DRV did not modify the expression of genes essential for the adipocyte function and higher doses were requested to reduce the expression of *UCP1* and *CIDEA* as compared with LPV. In hMADS-adipocytes, PIs decreased the mRNA expression of *PPAR γ 2* and *C/EBP α* (Ravaud, Pare, Azoulay, Dani, & Ladoux, 2017), while similar concentrations did not significantly lower the expression of these two genes in chin-adipocytes. LPV, even when applied for 2 days, diminished *PPAR γ 2* and *PGC-1 α* expressions. This may account for the reduction of the thermogenic signature and the very weak ability for uncoupled respiration in hMADS-adipocytes. All the experiments were carried out in presence of rosiglitazone. Hence one can assume that *PPAR γ 2* was not produced, precluding then any activation by its ligand. Of note, PIs had no effect on *PRDM16* expression indicating that its presence was not sufficient to maintain *UCP1* expression in humans, unlike observed in murine models (Cohen & Spiegelman, 2015). LPV also impaired the expression of many sirtuins. Altogether these observations are in line with those reported in mice indicating that *SIRT6* depletion decreases the expression of *PGC-1 α* and other thermogenic genes, as well as the mitochondrial respiratory capacity (Yao et al., 2017). Thus, PIs induced whitening of BBAs through the inhibition of the *PPAR γ 2/PGC-1 α* and *SIRT* pathways upon transcriptional and putative epigenetic regulations.

Short-term treatment with LPV reduced the transcriptional activity of *UCP1* promoter and turned down *UCP1* without modifying *PLIN1* and *FABP4* protein expressions. It blunted the β -adrenergic/cAMP induction of *UCP1* mRNA. This processes occurred through an impairment of p38 MAPK phosphorylation. Transcriptional control of *UCP1* relies on regulatory regions present in the 5'-end of the gene, where a region immediately upstream of the transcription start site contains a CREB binding site. It likely upregulates *UCP1* transcription in response to cAMP production (Cao et al., 2004). Note that in accordance with its lower unwanted side effects as compared with LPV, short-term treatment with DRV did not display any significant reduction of the forskolin-induced expression of *UCP1*. Thus LPV, but not DRV, promoted BBAs whitening by impeding the activatable catecholamine pathway that produces cAMP, phosphorylates p38 MAPK, and activates CREB.

Many studies have reported the pleiotropic effects of RESV and its efficiency especially to reverse metabolic disorders or to prevent some features of aging (Chachay et al., 2011; Marchal, Pifferi, & Aujard, 2013). Administration of RESV to mice increased the presence of BBAs in the inguinal WAT pointing out beneficial changes of the metabolic parameters (S. Wang et al., 2016). In parallel, concentrations of RESV higher than 10 μ M, reduced the differentiation of 3T3-L1 cells (Chang, Lin, Peng, Day, & Hung, 2016), while they elevated *SIRT1* expression in normal keratinocytes (Wu, Uchi, Morino-Koga, Shi, & Furue, 2014). In good agreement with these observations, we measured an increase in *UCP1* expression when lipid-laden cells were treated for 2 or 4 days with concentrations of RESV below 10 μ M. In contrast to RESV-reported effects in HIB-1B murine cells (Nohr et al., 2017), higher RESV

concentrations strongly decreased *UCP1* and *CIDEA* expressions, reducing then the thermogenic ability of hMADS-adipocytes. *SIRT1* expression was induced by RESV concentrations higher than 20 μ M in hMADS-adipocytes, as in others cell types. This underlines that in humans, the RESV-induced browning is likely independent of its antiaging properties mediated through *SIRT1* expression, albeit this remains to be expressly established. Indeed activation of *SIRT1* was reported to inhibit white adipose differentiation in mice (Fang et al., 2017). Altogether these data sustained that *SIRT1* impeded the acquisition of both white and brown/beige adipocyte features. In this regard, a recent study showing that caloric restriction does not induce WAT browning in obese humans is in line with our observations although no information on *SIRT1* expression is provided (Barquissau et al., 2018).

In our model SB203580 was efficient to block RESV-induced *UCP1* expression, pointing out the importance of an active p38 MAPK in this process. Thus, RESV activated an actionable pathway able to promote *UCP1* expression. Indeed, RESV was reported to competitively inhibit cAMP-phosphodiesterases (PDE; Park et al., 2012), preventing then cAMP degradation. Elevation of cAMP levels activates PKA and p38 MAPK and increases *UCP1* expression. In this regard, PDE inhibitors were shown to promote *UCP1* expression in vitro (Kraynik, Miyaoka, & Beavo, 2013) and the use of PDE inhibitors such as roflumilast unexpectedly and significantly lowers glucose in individuals with type 2 diabetes (Wouters et al., 2012). Such a mechanism is suitable to account, at least in part, for the induction of *UCP1* and further metabolic benefits of RESV.

While LPV inhibited *UCP1* expression through basal and activatable components, RESV displayed more limited potential in controlling *UCP1* expression. When cells were incubated with RESV before the LPV treatment, *UCP1* expression was partially restored as RESV acted on the p38 MAPK activatable pathway only. From this observation RESV displayed beneficial outcome to prevent some of the deleterious effects of PIs on adipose tissue. Thus, in addition to a cell-specific regulation, *UCP1* was targeted in a drug-specific manner: PIs and RESV displaying opposite effects on its expression. LPV remains one of the recommended treatments by the World Health Organization for children exposed to HIV. Then, a RESV cotreatment, provided that suitable plasma concentrations are reached (Calvo-Castro et al., 2018), may help to overcome the side effects. Of note, RESV was reported to attenuate the effects of PIs on rat body weight while improving the cardiac parameters (Symington, Mapanga, Norton, & Essop, 2017). A putative role of *UCP1* may account in part for these observations although no information regarding its expression is provided. The pertinence of the association of PIs with RESV remains to be evaluated for an in vivo use. In such a context, the impact of RESV on HIV replication and/or latency in infected individuals should also be clarified.

5 | CONCLUSION

In conclusion, we show the importance of p38 MAPK to control the balance between browning and whitening of adipocytes. It is targeted

by distinct drugs, that is, LPV and RESV which displayed opposite effects on UCP1 expression. While p38 MAPK was requested for RESV to induce UCP1, LPV reduced its phosphorylation, blunting then the activatable component of the thermogenic response.

These observations may be relevant in the obesity context: A proper control of UCP1 induction is possible and may apply to propose safe antiobesity therapies. They may also be of interest to restrain the loss of brown cells in the elderly. They may also apply to thwart systemic metabolic disorders characterized by an increased catabolism of stored nutrients such as cachexia. In this regard, an efficient reduction of UCP1 expression may consist in a therapeutic strategy with expected beneficial effects.

ACKNOWLEDGMENTS

We thank our colleagues for helpful suggestions and discussions. We are indebted to Dr. Pascal Peraldi for a careful reading of this manuscript.

The microscopy was done in the Prism facility, "Plateforme PRISM - IBV- CNRS UMR 7277- INSERM U1091-UNS." The help of Magali Mondin is acknowledged. The UCP1 construct was a gift from Pr. Y.-H. Tseng (Joslin Diabetes Center, USA).

FUNDING STATEMENT

This study was supported by ANRS (French National Agency for Research on AIDS and Viral Hepatitis; grant number # AO 2013-1 CSS3), Fondation ARC (grant number: 2016 1204713), and the French Government (National Research Agency, ANR) through the "Investments for the Future" LABEX SIGNALIFE: program reference #ANR-11-LABX-0028-01.

C. R. is recipient of a pre-doctoral fellowship from ANRS and then from SIDACTION, M. P. is a pre-doctoral fellow from LABEX SIGNALIFE. X. Y. is recipient of a pre-doctoral fellow from the China Scholarship Council.

CONFLICT OF INTERESTS

The authors declare that they have no conflict of interests.

AUTHOR CONTRIBUTIONS

C. R. design of experiments, data research, and contributed to discussion; M. P. design of experiments, data research, and contributed to discussion; X. Y. data research; S. A. chemical synthesis and purification and contributed to discussion; N. M. design of experiments and contributed to discussion; C. D. design of experiments and contributed to discussion; and A. L. design of experiments, data research, contributed to discussion, and wrote the manuscript. All authors approved the manuscript.

ORCID

Christian Dani  <http://orcid.org/0000-0003-3228-0230>

Annie Ladoux  <http://orcid.org/0000-0003-3857-2621>

REFERENCES

- Barbatelli, G., Murano, I., Madsen, L., Hao, Q., Jimenez, M., Kristiansen, K., ... Cinti, S. (2010). The emergence of cold-induced brown adipocytes in mouse white fat depots is determined predominantly by white to brown adipocyte transdifferentiation. *American Journal of Physiology, Endocrinology and Metabolism*, 298(6), E1244–E1253. <https://doi.org/10.1152/ajpendo.00600.2009>
- Barquissau, V., Leger, B., Beuzelin, D., Martins, F., Amri, E. Z., Pisani, D. F., ... Langin, D. (2018). Caloric Restriction and diet-induced weight loss do not induce browning of human subcutaneous white adipose tissue in women and men with obesity. *Cell Reports*, 22(4), 1079–1089. <https://doi.org/10.1016/j.celrep.2017.12.102>
- Bastard, J. P., Caron, M., Vidal, H., Jan, V., Auclair, M., Vigouroux, C., ... Capeau, J. (2002). Association between altered expression of adipogenic factor SREBP1 in lipoatrophic adipose tissue from HIV-1-infected patients and abnormal adipocyte differentiation and insulin resistance. *Lancet*, 359(9311), 1026–1031.
- Calvo-Castro, L. A., Schiborr, C., David, F., Ehrh, H., Voggel, J., Sus, N., ... Frank, J. (2018). The oral bioavailability of trans-resveratrol from a grapevine-shoot extract in healthy humans is significantly increased by micellar solubilization. *Molecular Nutrition & Food Research*, 62(9), e1701057. <https://doi.org/10.1002/mnfr.201701057>
- Cao, W., Daniel, K. W., Robidoux, J., Puigserver, P., Medvedev, A. V., Bai, X., ... Collins, S. (2004). p38 mitogen-activated protein kinase is the central regulator of cyclic AMP-dependent transcription of the brown fat uncoupling protein 1 gene. *Molecular and Cellular Biology*, 24(7), 3057–3067.
- Caron-Debarle, M., Boccara, F., Lagathu, C., Antoine, B., Cervera, P., Bastard, J. P., ... Capeau, J. (2010). Adipose tissue as a target of HIV-1 antiretroviral drugs. Potential consequences on metabolic regulations. *Current Pharmaceutical Design*, 16(30), 3352–3360.
- Chachay, V. S., Kirkpatrick, C. M. J., Hickman, I. J., Ferguson, M., Prins, J. B., & Martin, J. H. (2011). Resveratrol—pills to replace a healthy diet? *British Journal of Clinical Pharmacology*, 72(1), 27–38. <https://doi.org/10.1111/j.1365-2125.2011.03966.x>
- Chang, C. C., Lin, K. Y., Peng, K. Y., Day, Y. J., & Hung, L. M. (2016). Resveratrol exerts anti-obesity effects in high-fat diet obese mice and displays differential dosage effects on cytotoxicity, differentiation, and lipolysis in 3T3-L1 cells. *Endocrine Journal (Kyoto Japan)*, 63(2), 169–178. <https://doi.org/10.1507/endocrj.EJ15-0545>
- Cohen, P., & Spiegelman, B. M. (2015). Brown and beige fat: Molecular parts of a thermogenic machine. *Diabetes*, 64(7), 2346–2351. <https://doi.org/10.2337/db15-0318>
- Cypess, A. M., Lehman, S., Williams, G., Tal, I., Rodman, D., Goldfine, A. B., ... Kahn, C. R. (2009). Identification and importance of brown adipose tissue in adult humans. *New England Journal of Medicine*, 360(15), 1509–1517. <https://doi.org/10.1056/NEJMoa0810780>
- Darini, C. Y., Martin, P., Azoulay, S., Drici, M. D., Hofman, P., Obba, S., ... Ladoux, A. (2013). Targeting cancer stem cells expressing an embryonic signature with anti-proteases to decrease their tumor potential. *Cell Death & Disease*, 4, e706–e706. <https://doi.org/10.1038/cddis.2013.206>
- Elabd, C., Chiellini, C., Carmona, M., Galitzky, J., Cochet, O., Petersen, R., ... Amri, E. Z. (2009). Human multipotent adipose-derived stem cells differentiate into functional brown adipocytes. *Stem Cells*, 27(11), 2753–2760.
- Fang, J., Ianni, A., Smolka, C., Vakhrusheva, O., Nolte, H., Krüger, M., ... Bober, E. (2017). Sirt7 promotes adipogenesis in the mouse by inhibiting autocatalytic activation of Sirt1. *Proceedings of the National Academy of Sciences of the United States of America*, 114(40), E8352–E8361. <https://doi.org/10.1073/pnas.1706945114>

- Gallego-Escuredo, J. M., Del Mar Gutierrez, M., Diaz-Delfin, J., Domingo, J. C., Mateo, M. G., Domingo, P., ... Villarroya, F. (2010). Differential effects of efavirenz and lopinavir/ritonavir on human adipocyte differentiation, gene expression and release of adipokines and pro-inflammatory cytokines. *Current HIV Research*, 8(7), 545–553.
- Graja, A., & Schulz, T. J. (2015). Mechanisms of aging-related impairment of brown adipocyte development and function. *Gerontology*, 61(3), 211–217. <https://doi.org/10.1159/000366557>
- Heaton, J. M. (1972). The distribution of brown adipose tissue in the human. *Journal of Anatomy*, 112(Pt 1), 35–39.
- Jing, E., Gesta, S., & Kahn, C. R. (2007). SIRT2 regulates adipocyte differentiation through FoxO1 acetylation/deacetylation. *Cell Metabolism*, 6(2), 105–114. <https://doi.org/10.1016/j.cmet.2007.07.003>
- Kim, R. J., Wilson, C. G., Wabitsch, M., Lazar, M. A., & Stepan, C. M. (2006). HIV protease inhibitor-specific alterations in human adipocyte differentiation and metabolism. *Obesity (Silver Spring)*, 14(6), 994–1002. <https://doi.org/10.1038/oby.2006.114>
- Klingenberg, M. (1999). Uncoupling protein—a useful energy dissipator. *Journal of Bioenergetics and Biomembranes*, 31(5), 419–430.
- Kraynik, S. M., Miyaoka, R. S., & Beavo, J. A. (2013). PDE3 and PDE4 isozyme-selective inhibitors are both required for synergistic activation of brown adipose tissue. *Molecular Pharmacology*, 83(6), 1155–1165. <https://doi.org/10.1124/mol.112.084145>
- Krishnan, J., Danzer, C., Simka, T., Ukropec, J., Walter, K. M., Kumpf, S., ... Krek, W. (2012). Dietary obesity-associated Hif1alpha activation in adipocytes restricts fatty acid oxidation and energy expenditure via suppression of the Sirt2-NAD+ system. *Genes and Development*, 26(3), 259–270. <https://doi.org/10.1101/gad.180406.111>
- Landry, J., Sutton, A., Tafrov, S. T., Heller, R. C., Stebbins, J., Pillus, L., & Sternglanz, R. (2000). The silencing protein SIR2 and its homologs are NAD-dependent protein deacetylases. *Proceedings of the National Academy of Sciences of the United States of America*, 97(11), 5807–5811. <https://doi.org/10.1073/pnas.110148297>
- Lean, M. E. J., James, W. P. T., Jennings, G., & Trayhurn, P. (1986). Brown adipose tissue uncoupling protein content in human infants, children and adults. *Clinical Science (London)*, 71(3), 291–297.
- Lopez-Cortes, L. F., Ruiz-Valderas, R., Sanchez-Rivas, E., Lluch, A., Gutierrez-Valencia, A., Torres-Cornejo, A., ... Viciano, P. (2013). Lopinavir plasma concentrations and virological outcome with lopinavir-ritonavir monotherapy in HIV-1-infected patients. *Antimicrobial Agents and Chemotherapy*, 57(8), 3746–3751. <https://doi.org/10.1128/AAC.00315-13>
- Marchal, J., Pifferi, F., & Aujard, F. (2013). Resveratrol in mammals: Effects on aging biomarkers, age-related diseases, and life span. *Annals of the New York Academy of Sciences*, 1290, 67–73. <https://doi.org/10.1111/nyas.12214>
- vanMarken Lichtenbelt, W. D., Vanhommel, J. W., Smulders, N. M., Drossaerts, J. M., Kemerink, G. J., Bouvy, N. D., ... Teule, G. J. (2009). Cold-activated brown adipose tissue in healthy men. *New England Journal of Medicine*, 360(15), 1500–1508. <https://doi.org/10.1056/NEJMoa0808718>
- Nøhr, M., Bobba, N., Richelsen, B., Lund, S., & Pedersen, S. (2017). Inflammation downregulates UCP1 expression in brown adipocytes potentially via SIRT1 and DBC1 interaction. *International Journal of Molecular Sciences*, 18(5), 1006. <https://doi.org/10.3390/ijms18051006>
- Ouidhi, M., Villageois, P., Mounier, C. M., Menigot, C., Rival, Y., Piwnica, D., ... Dani, C. (2015). Characterization of human knee and chin adipose-derived stromal cells. *Stem Cells International*, 2015, 592090–11. <https://doi.org/10.1155/2015/592090>
- Park, S. J., Ahmad, F., Philp, A., Baar, K., Williams, T., Luo, H., ... Chung, J. H. (2012). Resveratrol ameliorates aging-related metabolic phenotypes by inhibiting cAMP phosphodiesterases. *Cell*, 148(3), 421–433. <https://doi.org/10.1016/j.cell.2012.01.017>
- Peirce, V., Carobbio, S., & Vidal-Puig, A. (2014). The different shades of fat. *Nature*, 510(7503), 76–83. <https://doi.org/10.1038/nature13477>
- Qiang, L., Wang, L., Kon, N., Zhao, W., Lee, S., Zhang, Y., ... Accili, D. (2012). Brown remodeling of white adipose tissue by SirT1-dependent deacetylation of Ppargamma. *Cell*, 150(3), 620–632. <https://doi.org/10.1016/j.cell.2012.06.027>
- Ravaud, C., Esteve, D., Villageois, P., Bouloumie, A., Dani, C., & Ladoux, A. (2015). IER3 promotes expansion of adipose progenitor cells in response to changes in distinct microenvironmental effectors. *Stem Cells*, 33(8), 2564–2573. <https://doi.org/10.1002/stem.2016>
- Ravaud, C., Paré, M., Azoulay, S., Dani, C., & Ladoux, A. (2017). Impairment of the activin A autocrine loop by lopinavir reduces self-renewal of distinct human adipose progenitors. *Scientific Reports*, 7(1), 2986. <https://doi.org/10.1038/s41598-017-02807-9>
- Rodriguez, A. M., Elabd, C., Delteil, F., Astier, J., Vernochet, C., Saint-Marc, P., ... Ailhaud, G. (2004). Adipocyte differentiation of multipotent cells established from human adipose tissue. *Biochemical and Biophysical Research Communications*, 315(2), 255–263.
- Sanchez-Gurmaches, J., Hung, C. M., Sparks, C. A., Tang, Y., Li, H., & Guertin, D. A. (2012). PTEN loss in the Myf5 lineage redistributes body fat and reveals subsets of white adipocytes that arise from Myf5 precursors. *Cell Metabolism*, 16(3), 348–362. <https://doi.org/10.1016/j.cmet.2012.08.003>
- Seale, P., Kajimura, S., Yang, W., Chin, S., Rohas, L. M., Uldry, M., ... Spiegelman, B. M. (2007). Transcriptional control of brown fat determination by PRDM16. *Cell Metabolism*, 6(1), 38–54.
- Symington, B., Mapanga, R. F., Norton, G. R., & Essop, M. F. (2017). Resveratrol co-treatment attenuates the effects of HIV protease inhibitors on rat body weight and enhances cardiac mitochondrial respiration. *PLoS One*, 12(1), e0170344. <https://doi.org/10.1371/journal.pone.0170344>
- Tissenbaum, H. A., & Guarente, L. (2001). Increased dosage of a sir-2 gene extends lifespan in *Caenorhabditis elegans*. *Nature*, 410(6825), 227–230. <https://doi.org/10.1038/35065638>
- Tontonoz, P., Hu, E., & Spiegelman, B. M. (1994). Stimulation of adipogenesis in fibroblasts by PPAR gamma 2, a lipid-activated transcription factor. *Cell*, 79(7), 1147–1156.
- Torres, R. A., & Lewis, W. (2014). Aging and HIV/AIDS: Pathogenetic role of therapeutic side effects. *Laboratory Investigation*, 94(2), 120–128. <https://doi.org/10.1038/labinvest.2013.142>
- Vernochet, C., Azoulay, S., Duval, D., Guedj, R., Cottrez, F., Vidal, H., ... Dani, C. (2005). Human immunodeficiency virus protease inhibitors accumulate into cultured human adipocytes and alter expression of adipocytokines. *Journal of Biological Chemistry*, 280(3), 2238–2243.
- Viengchareun, S., Caron, M., Auclair, M., Kim, M. J., Frachon, P., Capeau, J., ... Lombes, A. (2007). Mitochondrial toxicity of indinavir, stavudine and zidovudine involves multiple cellular targets in white and brown adipocytes. *Antiviral Therapy*, 12(6), 919–929.
- Villarroya, F., Peyrou, M., & Giral, M. (2017). Transcriptional regulation of the uncoupling protein-1 gene. *Biochimie*, 134, 86–92. <https://doi.org/10.1016/j.biochi.2016.09.017>
- Wang, F., Nguyen, M., Qin, F. X. F., & Tong, Q. (2007). SIRT2 deacetylates FOXO3a in response to oxidative stress and caloric restriction. *Aging cell*, 6(4), 505–514. <https://doi.org/10.1111/j.1474-9726.2007.00304.x>
- Wang, S., Liang, X., Yang, Q., Fu, X., Zhu, M., Rodgers, B. D., ... Du, M. (2016). Resveratrol enhances brown adipocyte formation and function by activating AMP-activated protein kinase (AMPK) α 1 in mice fed high-fat diet. *Molecular Nutrition & Food Research*, 61(4), 1600746(1600741-1600711)
- Wouters, E. F. M., Bredenbröker, D., Teichmann, P., Brose, M., Rabe, K. F., Fabbri, L. M., & Göke, B. (2012). Effect of the phosphodiesterase 4 inhibitor roflumilast on glucose metabolism in patients with treatment-naïve, newly diagnosed type 2 diabetes mellitus. *Journal of Clinical Endocrinology and Metabolism*, 97(9), E1720–E1725. <https://doi.org/10.1210/jc.2011-2886>
- Wu, Z., Uchi, H., Morino-Koga, S., Shi, W., & Furue, M. (2014). Resveratrol inhibition of human keratinocyte proliferation via SIRT1/ARNT/ERK

- dependent downregulation of aquaporin 3. *Journal of Dermatological Science*, 75(1), 16–23. <https://doi.org/10.1016/j.jdermsci.2014.03.004>
- Xu, F., Zheng, X., Lin, B., Liang, H., Cai, M., Cao, H., ... Weng, J. (2016). Diet-induced obesity and insulin resistance are associated with brown fat degeneration in SIRT1-deficient mice. *Obesity (Silver Spring)*, 24(3), 634–642. <https://doi.org/10.1002/oby.21393>
- Xue, R., Lynes, M. D., Dreyfuss, J. M., Shamsi, F., Schulz, T. J., Zhang, H., ... Tseng, Y. H. (2015). Clonal analyses and gene profiling identify genetic biomarkers of the thermogenic potential of human brown and white preadipocytes. *Nature Medicine (New York, NY, United States)*, 21(7), 760–768. <https://doi.org/10.1038/nm.3881>
- Yao, L., Cui, X., Chen, Q., Yang, X., Fang, F., Zhang, J., ... Chang, Y. (2017). Cold-inducible SIRT6 regulates thermogenesis of brown and beige fat. *Cell Reports*, 20(3), 641–654. <https://doi.org/10.1016/j.celrep.2017.06.069>

SUPPORTING INFORMATION

Additional supporting information may be found online in the Supporting Information section.

How to cite this article: Ravaud C, Paré M, Yao X, et al. Resveratrol and HIV-protease inhibitors control UCP1 expression through opposite effects on p38 MAPK phosphorylation in human adipocytes. *J Cell Physiol.* 2019;1–13. <https://doi.org/10.1002/jcp.29032>

References

- Abe, K., H. Niwa, K. Iwase, M. Takiguchi, M. Mori, S.-I. Abé, K. Abe, and K.-I. Yamamura. 1996. Endoderm-specific gene expression in embryonic stem cells differentiated to embryoid bodies. *Experimental cell research*. 229:27-34.
- Ahfeldt, T., R.T. Schinzel, Y.-K. Lee, D. Hendrickson, A. Kaplan, D.H. Lum, R. Camahort, F. Xia, J. Shay, and E.P. Rhee. 2012. Programming human pluripotent stem cells into white and brown adipocytes. *Nature cell biology*. 14:209.
- Ahima, R.S., and J.S. Flier. 2000. Adipose tissue as an endocrine organ. *Trends in Endocrinology & Metabolism*. 11:327-332.
- Alvarez-Pérez, J., P. Ballesteros, and S. Cerdán. 2005. Microscopic images of intraspheroidal pH by ¹H magnetic resonance chemical shift imaging of pH sensitive indicators. *Magnetic Resonance Materials in Physics, Biology and Medicine*. 18:293-301.
- Armani, A., C. Mammi, V. Marzolla, M. Calanchini, A. Antelmi, G.M. Rosano, A. Fabbri, and M. Caprio. 2010. Cellular models for understanding adipogenesis, adipose dysfunction, and obesity. *Journal of cellular biochemistry*. 110:564-572.
- Asahara, T., T. Murohara, A. Sullivan, M. Silver, R. van der Zee, T. Li, B. Witzenbichler, G. Schatteman, and J.M. Isner. 1997. Isolation of putative progenitor endothelial cells for angiogenesis. *Science*. 275:964-966.
- Ashcroft, F.M., and P. Rorsman. 2012. Diabetes mellitus and the β cell: the last ten years. *Cell*. 148:1160-1171.
- Awad, H.A., M.Q. Wickham, H.A. Leddy, J.M. Gimble, and F. Guilak. 2004. Chondrogenic differentiation of adipose-derived adult stem cells in agarose, alginate, and gelatin scaffolds. *Biomaterials*. 25:3211-3222.
- Badimon, L., B. Oñate, and G. Vilahur. 2015. Adipose-derived mesenchymal stem cells and their reparative potential in ischemic heart disease. *Revista Española de Cardiología (English Edition)*. 68:599-611.
- Baharvand, H., S.M. Hashemi, S.K. Ashtiani, and A. Farrokhi. 2004. Differentiation of human embryonic stem cells into hepatocytes in 2D and 3D culture systems in vitro. *International Journal of Developmental Biology*. 50:645-652.
- Banerjee, M., and R.R. Bhonde. 2006. Application of hanging drop technique for stem cell differentiation and cytotoxicity studies. *Cytotechnology*. 51:1-5.
- Barak, Y., M.C. Nelson, E.S. Ong, Y.Z. Jones, P. Ruiz-Lozano, K.R. Chien, A. Koder, and R.M. Evans. 1999. PPAR γ is required for placental, cardiac, and adipose tissue development. *Molecular cell*. 4:585-595.
- Barbe, P., L. Millet, J. Galitzky, M. Lafontan, and M. Berlan. 1996. In situ assessment of the role of the β 1, β 2-and β 3-adrenoceptors in the control of lipolysis and nutritive blood flow in human subcutaneous adipose tissue. *British journal of pharmacology*. 117:907-913.
- Barberá, M.J., A. Schlüter, N. Pedraza, R. Iglesias, F. Villarroya, and M. Giralt. 2001. Peroxisome Proliferator-activated Receptor α Activates Transcription of the Brown Fat Uncoupling Protein-1 Gene A LINK BETWEEN REGULATION OF THE THERMOGENIC AND LIPID OXIDATION PATHWAYS IN THE BROWN FAT CELL. *Journal of Biological Chemistry*. 276:1486-1493.
- Bennett, C.N., K.A. Longo, W.S. Wright, L.J. Suva, T.F. Lane, K.D. Hankenson, and O.A. MacDougald. 2005. Regulation of osteoblastogenesis and bone mass by Wnt10b. *Proceedings of the National Academy of Sciences*. 102:3324-3329.
- Berry, R., and M.S. Rodeheffer. 2013. Characterization of the adipocyte cellular lineage in vivo. *Nature cell biology*. 15:302.
- Billon, N., and C. Dani. 2012. Developmental origins of the adipocyte lineage: new insights from genetics and genomics studies. *Stem Cell Reviews and Reports*. 8:55-66.
- Billon, N., P. Iannarelli, M.C. Monteiro, C. Glavieux-Pardanaud, W.D. Richardson, N. Kessar, C. Dani, and E. Dupin. 2007. The generation of adipocytes by the neural crest. *Development*. 134:2283-2292.

- Billon, N., R. Kolde, J. Reimand, M.C. Monteiro, M. Kull, H. Peterson, K. Tretyakov, P. Adler, B. Wdziekonski, and J. Vilo. 2010. Comprehensive transcriptome analysis of mouse embryonic stem cell adipogenesis unravels new processes of adipocyte development. *Genome biology*. 11:R80.
- Birkenmeier, E.H., B. Gwynn, S. Howard, J. Jerry, J.I. Gordon, W.H. Landschulz, and S.L. McKnight. 1989. Tissue-specific expression, developmental regulation, and genetic mapping of the gene encoding CCAAT/enhancer binding protein. *Genes & Development*. 3:1146-1156.
- Birsoy, K., R. Berry, T. Wang, O. Ceyhan, S. Tavazoie, J.M. Friedman, and M.S. Rodeheffer. 2011. Analysis of gene networks in white adipose tissue development reveals a role for ETS2 in adipogenesis. *Development*. 138:4709-4719.
- Björntorp, P., and L. Sjöström. 1978. Carbohydrate storage in man: speculations and some quantitative considerations. *Metabolism*. 27:1853-1865.
- Boden, G. 1997. Role of fatty acids in the pathogenesis of insulin resistance and NIDDM. *Diabetes*. 46:3-10.
- Boquest, A.C., A. Shahdadfar, K. Frønsdal, O. Sigurjonsson, S.H. Tunheim, P. Collas, and J.E. Brinchmann. 2005. Isolation and transcription profiling of purified uncultured human stromal stem cells: alteration of gene expression after in vitro cell culture. *Molecular biology of the cell*. 16:1131-1141.
- Bourlier, V., C. Sengenès, A. Zakaroff-Girard, P. Decaunes, B. Wdziekonski, J. Galitzky, P. Villageois, D. Esteve, P. Chiotasso, and C. Dani. 2012. TGFbeta family members are key mediators in the induction of myofibroblast phenotype of human adipose tissue progenitor cells by macrophages. *PLoS One*. 7:e31274.
- Bratt-Leal, A.M., R.L. Carpenedo, and T.C. McDevitt. 2009. Engineering the embryoid body microenvironment to direct embryonic stem cell differentiation. *Biotechnology progress*. 25:43-51.
- Braun, T., and M. Gautel. 2011. Transcriptional mechanisms regulating skeletal muscle differentiation, growth and homeostasis. *Nature reviews Molecular cell biology*. 12:349.
- Brondani, L.d.A., T.S. Assmann, G.C.K. Duarte, J.L. Gross, L.H. Canani, and D. Crispim. 2012. The role of the uncoupling protein 1 (UCP1) on the development of obesity and type 2 diabetes mellitus. *Arquivos Brasileiros de Endocrinologia & Metabologia*. 56:215-225.
- Burýšek, L., and J. Houštek. 1997. β -Adrenergic stimulation of interleukin-1 α and interleukin-6 expression in mouse brown adipocytes. *FEBS letters*. 411:83-86.
- Butterwith, S., C. Peddie, and C. Goddard. 1993. Regulation of adipocyte precursor DNA synthesis by acidic and basic fibroblast growth factors: interaction with heparin and other growth factors. *Journal of endocrinology*. 137:369-374.
- Campbell, J.J., and C.J. Watson. 2009. Three-dimensional culture models of mammary gland. *Organogenesis*. 5:43-49.
- Cannon, B., and J. Nedergaard. 2004. Brown adipose tissue: function and physiological significance. *Physiological reviews*. 84:277-359.
- Cannon, B., and J. Nedergaard. 2009. Thermogenesis challenges the adipostat hypothesis for body-weight control: Symposium on 'Frontiers in adipose tissue biology'. *Proceedings of the Nutrition Society*. 68:401-407.
- Cao, W., A.V. Medvedev, K.W. Daniel, and S. Collins. 2001. β -adrenergic activation of p38 MAP kinase in adipocytes cAMP induction of the uncoupling protein 1 (UCP1) gene requires p38 map kinase. *Journal of Biological Chemistry*. 276:27077-27082.
- Cao, Y. 2013. Angiogenesis and vascular functions in modulation of obesity, adipose metabolism, and insulin sensitivity. *Cell metabolism*. 18:478-489.
- Cao, Z., R.M. Umek, and S.L. McKnight. 1991. Regulated expression of three C/EBP isoforms during adipose conversion of 3T3-L1 cells. *Genes & development*. 5:1538-1552.
- Caspi, O., A. Lesman, Y. Basevitch, A. Gepstein, G. Arbel, I.H.M. Habib, L. Gepstein, and S. Levenberg. 2007. Tissue engineering of vascularized cardiac muscle from human embryonic stem cells. *Circulation research*. 100:263-272.

- CASSARD-DOULCIER, A.-M., C. GELLY, F. BOUILLAUD, and D. RICQUIER. 1998. A 211-bp enhancer of the rat uncoupling protein-1 (UCP-1) gene controls specific and regulated expression in brown adipose tissue. *Biochemical journal*. 333:243-246.
- Chaldakov, G., I. Stankulov, M. Hristova, and P. Ghenev. 2003. Adipobiology of disease: adipokines and adipokine-targeted pharmacology. *Current pharmaceutical design*. 9:1023-1031.
- Chan, D., S.R. Lamande, W. Cole, and J.F. Bateman. 1990. Regulation of procollagen synthesis and processing during ascorbate-induced extracellular matrix accumulation in vitro. *Biochemical journal*. 269:175-181.
- Charrière, G., B. Cousin, E. Arnaud, M. André, F. Bacou, L. Pénicaud, and L. Casteilla. 2003. Preadipocyte conversion to macrophage Evidence of plasticity. *Journal of Biological Chemistry*. 278:9850-9855.
- Chartoumpakis, D.V., I.G. Habeos, P.G. Ziros, A.I. Psyrogiannis, V.E. Kyriazopoulou, and A.G. Papavassiliou. 2011. Brown adipose tissue responds to cold and adrenergic stimulation by induction of FGF21. *Molecular medicine*. 17:736-740.
- Chaudhry, A., and J.G. Granneman. 1999. Differential regulation of functional responses by β -adrenergic receptor subtypes in brown adipocytes. *American Journal of Physiology-Regulatory, Integrative and Comparative Physiology*. 277:R147-R153.
- Christy, R., V. Yang, J. Ntambi, D. Geiman, W. Landschulz, A.D. Friedman, Y. Nakabeppu, T. Kelly, and M. Lane. 1989. Differentiation-induced gene expression in 3T3-L1 preadipocytes: CCAAT/enhancer binding protein interacts with and activates the promoters of two adipocyte-specific genes. *Genes & development*. 3:1323-1335.
- Chwalek, K., M.V. Tsurkan, U. Freudenberg, and C. Werner. 2014. Glycosaminoglycan-based hydrogels to modulate heterocellular communication in in vitro angiogenesis models. *Scientific reports*. 4:4414.
- Cinti, S. 2009. Transdifferentiation properties of adipocytes in the adipose organ. *American Journal of Physiology-Endocrinology and Metabolism*. 297:E977-E986.
- Considine, R.V., M.R. Nyce, L.M. Morales, S.A. Magosin, M.K. Sinha, T.L. Bauer, E.L. Rosato, J. Colberg, and J.F. Caro. 1996. Paracrine stimulation of preadipocyte-enriched cell cultures by mature adipocytes. *American Journal of Physiology-Endocrinology And Metabolism*. 270:E895-E899.
- Cornelius, P., O.A. MacDougald, and M.D. Lane. 1994. Regulation of adipocyte development. *Annual review of nutrition*. 14:99-129.
- Coskun, T., H.A. Bina, M.A. Schneider, J.D. Dunbar, C.C. Hu, Y. Chen, D.E. Moller, and A. Kharitonov. 2008. Fibroblast growth factor 21 corrects obesity in mice. *Endocrinology*. 149:6018-6027.
- Cui, H., M. López, and K. Rahmouni. 2017. The cellular and molecular bases of leptin and ghrelin resistance in obesity. *Nature Reviews Endocrinology*. 13:338.
- Cypess, A.M., A.P. White, C. Vernochet, T.J. Schulz, R. Xue, C.A. Sass, T.L. Huang, C. Roberts-Toler, L.S. Weiner, and C. Sze. 2013. Anatomical localization, gene expression profiling and functional characterization of adult human neck brown fat. *Nature medicine*. 19:635.
- Dani, C., A. Smith, S. Dessolin, P. Leroy, L. Staccini, P. Villageois, C. Darimont, and G. Ailhaud. 1997. Differentiation of embryonic stem cells into adipocytes in vitro. *Journal of cell science*. 110:1279-1285.
- Daquinag, A.C., G.R. Souza, and M.G. Kolonin. 2012. Adipose tissue engineering in three-dimensional levitation tissue culture system based on magnetic nanoparticles. *Tissue Engineering Part C: Methods*. 19:336-344.
- Das, U.N. 2002. Is metabolic syndrome X an inflammatory condition? *Experimental Biology and Medicine*. 227:989-997.
- De Almeida, P.E., E.H. Meyer, N.G. Kooreman, S. Diecke, D. Dey, V. Sanchez-Freire, S. Hu, A. Ebert, J. Odegaard, and N.M. Mordwinkin. 2014. Transplanted terminally differentiated induced pluripotent stem cells are accepted by immune mechanisms similar to self-tolerance. *Nature communications*. 5:3903.
- de Herreros, A.G., and M. Birnbaum. 1989. The acquisition of increased insulin-responsive hexose transport in 3T3-L1 adipocytes correlates with expression of a novel transporter gene. *Journal of Biological Chemistry*. 264:19994-19999.

- de la Concepcion, M.R., P. Yubero, J.C. Domingo, R. Iglesias, P. Domingo, F. Villarroya, and M. Giral. 2005. Reverse transcriptase inhibitors alter uncoupling protein-1 and mitochondrial biogenesis in brown adipocytes. *Antiviral therapy*. 10:515-526.
- De Smedt, A., M. Steemans, M. De Boeck, A.K. Peters, F. Van Goethem, A. Lampo, and P. Vanparys. 2008. Optimisation of the cell cultivation methods in the embryonic stem cell test results in an increased differentiation potential of the cells into strong beating myocard cells. *Toxicology in Vitro*. 22:1789-1796.
- Debnath, J., S.K. Muthuswamy, and J.S. Brugge. 2003. Morphogenesis and oncogenesis of MCF-10A mammary epithelial acini grown in three-dimensional basement membrane cultures. *Methods*. 30:256-268.
- Digby, J.E., C.T. Montague, C.P. Sewter, L. Sanders, W.O. Wilkison, S. O'Rahilly, and J.B. Prins. 1998. Thiazolidinedione exposure increases the expression of uncoupling protein 1 in cultured human preadipocytes. *Diabetes*. 47:138-141.
- Divoux, A., S. Moutel, C. Poitou, D. Lacasa, N. Veyrie, A. Aissat, M. Arock, M. Guerre-Millo, and K. Clément. 2012. Mast cells in human adipose tissue: link with morbid obesity, inflammatory status, and diabetes. *The Journal of Clinical Endocrinology & Metabolism*. 97:E1677-E1685.
- Du, M., X. Liu, X. Liu, X. Yin, S. Han, Q. Song, and S. An. 2015. Glycerol-3-phosphate O-acyltransferase is required for PBAN-induced sex pheromone biosynthesis in *Bombyx mori*. *Scientific reports*. 5:8110.
- Eagle, H. 1955. Nutrition needs of mammalian cells in tissue culture. *Science*. 122:501-504.
- Ebert, A.D., J. Yu, F.F. Rose Jr, V.B. Mattis, C.L. Lorson, J.A. Thomson, and C.N. Svendsen. 2009. Induced pluripotent stem cells from a spinal muscular atrophy patient. *Nature*. 457:277.
- Elabd, C., C. Chiellini, A. Massoudi, O. Cochet, L.-E. Zaragosi, C. Trojani, J.-F. Michiels, P. Weiss, G. Carle, and N. Rochet. 2007. Human adipose tissue-derived multipotent stem cells differentiate in vitro and in vivo into osteocyte-like cells. *Biochemical and biophysical research communications*. 361:342-348.
- Elgazar-Carmon, V., A. Rudich, N. Hadad, and R. Levy. 2008. Neutrophils transiently infiltrate intra-abdominal fat early in the course of high-fat feeding. *Journal of lipid research*. 49:1894-1903.
- Engler, A.J., S. Sen, H.L. Sweeney, and D.E. Discher. 2006. Matrix elasticity directs stem cell lineage specification. *Cell*. 126:677-689.
- Esposito, K., A. Pontillo, C. Di Palo, G. Giugliano, M. Masella, R. Marfella, and D. Giugliano. 2003. Effect of weight loss and lifestyle changes on vascular inflammatory markers in obese women: a randomized trial. *Jama*. 289:1799-1804.
- Fairchild, P.J., N.J. Robertson, S. Cartland, K.F. Nolan, and H. Waldmann. 2005. Cell replacement therapy and the evasion of destructive immunity. *Stem cell reviews*. 1:159-167.
- Farmer, S.R. 2006. Transcriptional control of adipocyte formation. *Cell metabolism*. 4:263-273.
- Farmer, S.R. 2008. Brown fat and skeletal muscle: unlikely cousins? *Cell*. 134:726-727.
- Feldmann, H.M., V. Golozoubova, B. Cannon, and J. Nedergaard. 2009. UCP1 ablation induces obesity and abolishes diet-induced thermogenesis in mice exempt from thermal stress by living at thermoneutrality. *Cell metabolism*. 9:203-209.
- Ferrante Jr, A.W. 2013. The immune cells in adipose tissue. *Diabetes, Obesity and Metabolism*. 15:34-38.
- Fischbach, C., R. Chen, T. Matsumoto, T. Schmelzle, J.S. Brugge, P.J. Polverini, and D.J. Mooney. 2007. Engineering tumors with 3D scaffolds. *Nature methods*. 4:855.
- Foissac, R., P. Villageois, B. Chignon-Sicard, C. Georgiou, O. Camuzard, and C. Dani. 2017. Homeotic and embryonic gene expression in breast adipose tissue and in adipose tissues used as donor sites in plastic surgery. *Plastic and reconstructive surgery*. 139:685e-692e.
- Fredriksson, J.M., H. Thonberg, K.B. Ohlson, K.-i. Ohba, B. Cannon, and J. Nedergaard. 2001. Analysis of inhibition by H89 of UCP1 gene expression and thermogenesis indicates protein kinase A mediation of β 3-adrenergic signalling rather than β 3-adrenoceptor antagonism by H89. *Biochimica et Biophysica Acta (BBA)-Molecular Cell Research*. 1538:206-217.

- Freytag, S.O., D.L. Paielli, and J.D. Gilbert. 1994. Ectopic expression of the CCAAT/enhancer-binding protein alpha promotes the adipogenic program in a variety of mouse fibroblastic cells. *Genes & development*. 8:1654-1663.
- Fried, S.K., D.A. Bunkin, and A.S. Greenberg. 1998. Omental and subcutaneous adipose tissues of obese subjects release interleukin-6: depot difference and regulation by glucocorticoid. *The Journal of Clinical Endocrinology & Metabolism*. 83:847-850.
- Friedman, J.M., and J.L. Halaas. 1998. Leptin and the regulation of body weight in mammals. *Nature*. 395:763.
- Friedman, J.M., R. Leibel, D. Siegel, J. Walsh, and N. Bahary. 1991. Molecular mapping of the mouse obesity mutation. *Genomics*. 11:1054-1062.
- Galitzky, J., C. Sengenès, C. Thalamas, M.A. Marques, J.-M. Senard, M. Lafontan, and M. Berlan. 2001. The lipid-mobilizing effect of atrial natriuretic peptide is unrelated to sympathetic nervous system activation or obesity in young men. *Journal of lipid research*. 42:536-544.
- Galli, S.J., N. Borregaard, and T.A. Wynn. 2011. Phenotypic and functional plasticity of cells of innate immunity: macrophages, mast cells and neutrophils. *Nature immunology*. 12:1035.
- Galli, S.J., S. Nakae, and M. Tsai. 2005. Mast cells in the development of adaptive immune responses. *Nature immunology*. 6:135.
- Garreta, E., E. Genové, S. Borrós, and C.E. Semino. 2006. Osteogenic differentiation of mouse embryonic stem cells and mouse embryonic fibroblasts in a three-dimensional self-assembling peptide scaffold. *Tissue engineering*. 12:2215-2227.
- Geckil, H., F. Xu, X. Zhang, S. Moon, and U. Demirci. 2010. Engineering hydrogels as extracellular matrix mimics. *Nanomedicine*. 5:469-484.
- Geesin, J.C., L.J. Hendricks, J.S. Gordon, and R.A. Berg. 1991. Modulation of collagen synthesis by growth factors: the role of ascorbate-stimulated lipid peroxidation. *Archives of biochemistry and biophysics*. 289:6-11.
- Gerecht, S., J.A. Burdick, L.S. Ferreira, S.A. Townsend, R. Langer, and G. Vunjak-Novakovic. 2007. Hyaluronic acid hydrogel for controlled self-renewal and differentiation of human embryonic stem cells. *Proceedings of the National Academy of Sciences*. 104:11298-11303.
- Gesta, S., Y.-H. Tseng, and C.R. Kahn. 2007. Developmental origin of fat: tracking obesity to its source. *Cell*. 131:242-256.
- Giordano, A., A. Frontini, and S. Cinti. 2016. Convertible visceral fat as a therapeutic target to curb obesity. *Nature Reviews Drug Discovery*. 15:405.
- Giralt, M., A. Gavaldà-Navarro, and F. Villarroya. 2015. Fibroblast growth factor-21, energy balance and obesity. *Molecular and cellular endocrinology*. 418:66-73.
- Gogg, S., A. Nerstedt, J. Boren, and U. Smith. 2019. Human adipose tissue microvascular endothelial cells secrete PPAR γ ligands and regulate adipose tissue lipid uptake. *JCI insight*. 4.
- Goudenege, S., D.F. Pisani, B. Wdziekonski, J.P. Di Santo, C. Bagnis, C. Dani, and C.A. Dechesne. 2009. Enhancement of myogenic and muscle repair capacities of human adipose-derived stem cells with forced expression of MyoD. *Molecular Therapy*. 17:1064-1072.
- Goudriaan, J.R., V.E. Dahlmans, M. Febbraio, B. Teusink, J.A. Romijn, L.M. Havekes, and P.J. Voshol. 2002. Intestinal lipid absorption is not affected in CD36 deficient mice. In *Cellular Lipid Binding Proteins*. Springer. 199-202.
- Gray, S., M.W. Feinberg, S. Hull, C.T. Kuo, M. Watanabe, S.S. Banerjee, A. DePina, R. Haspel, and M.K. Jain. 2002. The Krüppel-like factor KLF15 regulates the insulin-sensitive glucose transporter GLUT4. *Journal of Biological Chemistry*. 277:34322-34328.
- Greenwood-Goodwin, M., E.S. Teasley, and S.C. Heilshorn. 2014. Dual-stage growth factor release within 3D protein-engineered hydrogel niches promotes adipogenesis. *Biomaterials science*. 2:1627-1639.

- Grefhorst, A., J.C. van den Beukel, E.L.A. van Houten, J. Steenbergen, J.A. Visser, and A.P. Themmen. 2015. Estrogens increase expression of bone morphogenetic protein 8b in brown adipose tissue of mice. *Biology of sex differences*. 6:7.
- Gunatillake, P.A., and R. Adhikari. 2003. Biodegradable synthetic polymers for tissue engineering. *Eur Cell Mater*. 5:1-16.
- Gupta, R.K., Z. Arany, P. Seale, R.J. Mepani, L. Ye, H.M. Conroe, Y.A. Roby, H. Kulaga, R.R. Reed, and B.M. Spiegelman. 2010. Transcriptional control of preadipocyte determination by Zfp423. *Nature*. 464:619.
- Gupta, R.K., R.J. Mepani, S. Kleiner, J.C. Lo, M.J. Khandekar, P. Cohen, A. Frontini, D.C. Bhowmick, L. Ye, and S. Cinti. 2012. Zfp423 expression identifies committed preadipocytes and localizes to adipose endothelial and perivascular cells. *Cell metabolism*. 15:230-239.
- Hafner, A.-L., J. Contet, C. Ravaud, X. Yao, P. Villageois, K. Suknuntha, K. Annab, P. Peraldi, B. Binetruy, and I.I. Slukvin. 2016a. Brown-like adipose progenitors derived from human induced pluripotent stem cells: identification of critical pathways governing their adipogenic capacity. *Scientific reports*. 6:3249.
- Hafner A-L, Mohsen-Kanson T and C. Dani. 2016b. A protocol for the differentiation of brown adipose progenitors derived from human induced pluripotent stem cells at a high efficiency with no gene transfer. *Nat Protocol Exchange*. Doi: <https://doi.org/10.1038/protex.2016.067>
- Hafner, A.-L., and C. Dani. 2014. Human induced pluripotent stem cells: a new source for brown and white adipocytes. *World journal of stem cells*. 6:467.
- Hafner, A.-L., T. Mohsen-Kanson, and C. Dani. 2018. Differentiation of Brown Adipocyte Progenitors Derived from Human Induced Pluripotent Stem Cells. In *Adipose-Derived Stem Cells*. Springer. 31-39.
- Hajri, T., and N.A. Abumrad. 2002. Fatty acid transport across membranes: relevance to nutrition and metabolic pathology. *Annual review of nutrition*. 22:383-415.
- Hamilton, J.A., F. Kamp, and W. Guo. 2002. Mechanism of cellular uptake of long-chain fatty acids: Do we need cellular proteins? *Molecular and cellular biochemistry*. 239:17-23.
- Han, J., J.-E. Lee, J. Jin, J.S. Lim, N. Oh, K. Kim, S.-I. Chang, M. Shibuya, H. Kim, and G.Y. Koh. 2011. The spatiotemporal development of adipose tissue. *Development*. 138:5027-5037.
- Hardwick, A., E. Linton, and N. Rothwell. 1989. Thermogenic effects of the antigluocorticoid RU-486 in the rat: involvement of corticotropin-releasing factor and sympathetic activation of brown adipose tissue. *Endocrinology*. 124:1684-1688.
- Harms, M., and P. Seale. 2013. Brown and beige fat: development, function and therapeutic potential. *Nature medicine*. 19:1252.
- Haslam, D., and W. James. 2005. Obesity *Lancet*. 366: 1197–1209. Google Scholar, Crossref, Medline.
- Hauer, H., G. Entenmann, M. Wabitsch, D. Gaillard, G. Ailhaud, R. Negrel, and E.-F. Pfeiffer. 1989. Promoting effect of glucocorticoids on the differentiation of human adipocyte precursor cells cultured in a chemically defined medium. *The Journal of clinical investigation*. 84:1663-1670.
- Hauer, H., K. Rohrig, and T. Petruschke. 1995. Effects of epidermal growth factor (EGF), platelet-derived growth factor (PDGF) and fibroblast growth factor (FGF) on human adipocyte development and function. *European journal of clinical investigation*. 25:90-96.
- Hayward, A.S., N. Sano, S.A. Przyborski, and N.R. Cameron. 2013. Acrylic-acid-functionalized PolyHIPE scaffolds for use in 3D cell culture. *Macromolecular rapid communications*. 34:1844-1849.
- Hegele, R.A., H. Cao, C. Frankowski, S.T. Mathews, and T. Leff. 2002. PPAR γ F388L, a transactivation-deficient mutant, in familial partial lipodystrophy. *Diabetes*. 51:3586-3590.
- Heywood, H.K., P.K. Sembi, D.A. Lee, and D.L. Bader. 2004. Cellular utilization determines viability and matrix distribution profiles in chondrocyte-seeded alginate constructs. *Tissue engineering*. 10:1467-1479.
- Hondares, E., R. Iglesias, A. Giralt, F.J. Gonzalez, M. Giralt, T. Mampel, and F. Villarroya. 2011. Thermogenic activation induces FGF21 expression and release in brown adipose tissue. *Journal of Biological Chemistry*. 286:12983-12990.

- Horton, J.D. 2002. Sterol regulatory element-binding proteins: transcriptional activators of lipid synthesis. Portland Press Limited.
- Horvath, P., N. Aulner, M. Bickle, A.M. Davies, E. Del Nery, D. Ebner, M.C. Montoya, P. Östling, V. Pietiäinen, and L.S. Price. 2016. Screening out irrelevant cell-based models of disease. *Nature reviews Drug discovery*. 15:751.
- Hosokawa, A., T. Takaoka, and H. Katsuta. 1971. Non-essential amino acid requirements of mammalian cells in tissue culture. *The Japanese journal of experimental medicine*. 41:273.
- Hou, P., Y. Li, X. Zhang, C. Liu, J. Guan, H. Li, T. Zhao, J. Ye, W. Yang, and K. Liu. 2013. Pluripotent stem cells induced from mouse somatic cells by small-molecule compounds. *Science*. 341:651-654.
- Hu, E., P. Tontonoz, and B.M. Spiegelman. 1995. Transdifferentiation of myoblasts by the adipogenic transcription factors PPAR gamma and C/EBP alpha. *Proceedings of the national academy of sciences*. 92:9856-9860.
- Hudak, C.S., O. Gulyaeva, Y. Wang, S.-m. Park, L. Lee, C. Kang, and H.S. Sul. 2014. Pref-1 marks very early mesenchymal precursors required for adipose tissue development and expansion. *Cell reports*. 8:678-687.
- Ikeda, S.-i., Y. Tamura, S. Kakehi, H. Sanada, R. Kawamori, and H. Watada. 2016. Exercise-induced increase in IL-6 level enhances GLUT4 expression and insulin sensitivity in mouse skeletal muscle. *Biochemical and biophysical research communications*. 473:947-952.
- Inman, G.J., F.J. Nicolás, J.F. Callahan, J.D. Harling, L.M. Gaster, A.D. Reith, N.J. Laping, and C.S. Hill. 2002. SB-431542 is a potent and specific inhibitor of transforming growth factor- β superfamily type I activin receptor-like kinase (ALK) receptors ALK4, ALK5, and ALK7. *Molecular pharmacology*. 62:65-74.
- Item, F., and D. Konrad. 2012. Visceral fat and metabolic inflammation: the portal theory revisited. *Obesity Reviews*. 13:30-39.
- Iyengar, P., V. Espina, T.W. Williams, Y. Lin, D. Berry, L.A. Jelicks, H. Lee, K. Temple, R. Graves, and J. Pollard. 2005. Adipocyte-derived collagen VI affects early mammary tumor progression in vivo, demonstrating a critical interaction in the tumor/stroma microenvironment. *The Journal of clinical investigation*. 115:1163-1176.
- Jespersen, N.Z., T.J. Larsen, L. Peijs, S. Daugaard, P. Homøe, A. Loft, J. de Jong, N. Mathur, B. Cannon, and J. Nedergaard. 2013. A classical brown adipose tissue mRNA signature partly overlaps with brite in the supraclavicular region of adult humans. *Cell metabolism*. 17:798-805.
- Jo, S.J., W.W. Choi, E.S. Lee, J.Y. Lee, H.S. Park, D.W. Moon, H.C. Eun, and J.H. Chung. 2011. Temporary Increase of PPAR- γ and Transient Expression of UCP-1 in Stromal Vascular Fraction Isolated Human Adipocyte Derived Stem Cells During Adipogenesis. *Lipids*. 46:487-494.
- Jongpaiboonkit, L., W.J. King, G.E. Lyons, A.L. Paguirigan, J.W. Warrick, D.J. Beebe, and W.L. Murphy. 2008. An adaptable hydrogel array format for 3-dimensional cell culture and analysis. *Biomaterials*. 29:3346-3356.
- Kaestner, K.H., R.J. Christy, and M.D. Lane. 1990. Mouse insulin-responsive glucose transporter gene: characterization of the gene and trans-activation by the CCAAT/enhancer binding protein. *Proceedings of the National Academy of Sciences*. 87:251-255.
- Kajimura, S., and M. Saito. 2014. A new era in brown adipose tissue biology: molecular control of brown fat development and energy homeostasis. *Annual review of physiology*. 76:225-249.
- Kajimura, S., P. Seale, K. Kubota, E. Lunsford, J.V. Frangioni, S.P. Gygi, and B.M. Spiegelman. 2009. Initiation of myoblast to brown fat switch by a PRDM16-C/EBP- β transcriptional complex. *Nature*. 460:1154.
- Kamp, F., and J.A. Hamilton. 2006. How fatty acids of different chain length enter and leave cells by free diffusion. *Prostaglandins, leukotrienes and essential fatty acids*. 75:149-159.
- Kanazawa, A., Y. Kawamura, A. Sekine, A. Iida, T. Tsunoda, A. Kashiwagi, Y. Tanaka, T. Babazono, M. Matsuda, and K. Kawai. 2005. Single nucleotide polymorphisms in the gene encoding Krüppel-like factor 7 are associated with type 2 diabetes. *Diabetologia*. 48:1315-1322.

- Kanda, T., J.D. Brown, G. Orasanu, S. Vogel, F.J. Gonzalez, J. Sartoretto, T. Michel, and J. Plutzky. 2008. PPAR γ in the endothelium regulates metabolic responses to high-fat diet in mice. *The Journal of clinical investigation*. 119.
- Karamanlidis, G., A. Karamitri, K. Docherty, D.G. Hazlerigg, and M.A. Lomax. 2007. C/EBP β reprograms white 3T3-L1 preadipocytes to a brown adipocyte pattern of gene expression. *Journal of Biological Chemistry*. 282:24660-24669.
- Katz, A.J., A. Tholpady, S.S. Tholpady, H. Shang, and R.C. Ogle. 2005. Cell surface and transcriptional characterization of human adipose-derived adherent stromal (hADAS) cells. *Stem cells*. 23:412-423.
- Kaupmann, K., K. Huggel, J. Heid, P.J. Flor, S. Bischoff, S.J. Mickel, G. McMaster, C. Angst, H. Bittiger, and W. Froestl. 1997. Expression cloning of GABAB receptors uncovers similarity to metabotropic glutamate receptors. *Nature*. 386:239.
- Kazantzis, M., V. Takahashi, J. Hinkle, S. Kota, V. Zilberfarb, T. Issad, M. Abdelkarim, L. Chouchane, and A.D. Strosberg. 2012. PAZ6 cells constitute a representative model for human brown pre-adipocytes. *Frontiers in endocrinology*. 3:13.
- Keipert, S., M. Kutschke, D. Lamp, L. Brachthäuser, F. Neff, C.W. Meyer, R. Oelkrug, A. Kharitonov, and M. Jastroch. 2015. Genetic disruption of uncoupling protein 1 in mice renders brown adipose tissue a significant source of FGF21 secretion. *Molecular metabolism*. 4:537-542.
- Keipert, S., M. Ost, K. Johann, F. Imber, M. Jastroch, E.M. Van Schothorst, J. Keijer, and S. Klaus. 2013. Skeletal muscle mitochondrial uncoupling drives endocrine cross-talk through the induction of FGF21 as a myokine. *American Journal of Physiology-Endocrinology and Metabolism*. 306:E469-E482.
- Keller, G.M. 1995. In vitro differentiation of embryonic stem cells. *Current opinion in cell biology*. 7:862-869.
- Kern, P.A. 1988. Recombinant human tumor necrosis factor does not inhibit lipoprotein lipase in primary cultures of isolated human adipocytes. *Journal of lipid research*. 29:909-914.
- Kersten, S. 2001. Mechanisms of nutritional and hormonal regulation of lipogenesis. *EMBO reports*. 2:282-286.
- Khan, T., E.S. Muise, P. Iyengar, Z.V. Wang, M. Chandalia, N. Abate, B.B. Zhang, P. Bonaldo, S. Chua, and P.E. Scherer. 2009. Metabolic dysregulation and adipose tissue fibrosis: role of collagen VI. *Molecular and cellular biology*. 29:1575-1591.
- Kilroy, G.E., S.J. Foster, X. Wu, J. Ruiz, S. Sherwood, A. Heifetz, J.W. Ludlow, D.M. Stricker, S. Potiny, and P. Green. 2007. Cytokine profile of human adipose-derived stem cells: Expression of angiogenic, hematopoietic, and pro-inflammatory factors. *Journal of cellular physiology*. 212:702-709.
- Kim, J.B., and B.M. Spiegelman. 1996. ADD1/SREBP1 promotes adipocyte differentiation and gene expression linked to fatty acid metabolism. *Genes & development*. 10:1096-1107.
- Kiwaki, K., and J.A. Levine. 2003. Differential effects of adrenocorticotrophic hormone on human and mouse adipose tissue. *Journal of Comparative Physiology B*. 173:675-678.
- Kleiner, S., N. Douris, E.C. Fox, R.J. Mepani, F. Verdeguer, J. Wu, A. Kharitonov, J.S. Flier, E. Maratos-Flier, and B.M. Spiegelman. 2012. FGF21 regulates PGC-1 α and browning of white adipose tissues in adaptive thermogenesis. *Genes & development*. 26:271-281.
- Kleinfeld, A.M., P. Chu, and C. Romero. 1997. Transport of long-chain native fatty acids across lipid bilayer membranes indicates that transbilayer flip-flop is rate limiting. *Biochemistry*. 36:14146-14158.
- Klingelutz, A.J., F.A. Gourronc, A. Chaly, D.A. Wadkins, A.J. Burand, K.R. Markan, S.O. Idiga, M. Wu, M.J. Potthoff, and J.A. Ankrum. 2018. Scaffold-free generation of uniform adipose spheroids for metabolism research and drug discovery. *Scientific reports*. 8:523.
- Knight, E., and S. Przyborski. 2015. Advances in 3D cell culture technologies enabling tissue-like structures to be created in vitro. *Journal of anatomy*. 227:746-756.

- Knittle, J., K. Timmers, F. Ginsberg-Fellner, R. Brown, and D. Katz. 1979. The growth of adipose tissue in children and adolescents. Cross-sectional and longitudinal studies of adipose cell number and size. *The Journal of clinical investigation*. 63:239-246.
- Kouidhi, M., P. Villageois, C.M. Mounier, C. Ménigot, Y. Rival, D. Piwnica, J. Aubert, B. Chignon-Sicard, and C. Dani. 2015. Characterization of human knee and chin adipose-derived stromal cells. *Stem cells international*. 2015.
- Kuhn, E., N. Binart, and M. Lombes. 2012. Brown, white, beige: the color of fat and new therapeutic perspectives for obesity. In *Annales d'endocrinologie*. Vol. 73. S2-8.
- Kurachi, H., H. Adachi, S. Ohtsuka, K. Morishige, K. Amemiya, Y. Keno, I. Shimomura, K. Tokunaga, A. Miyake, and Y. Matsuzawa. 1993. Involvement of epidermal growth factor in inducing obesity in ovariectomized mice. *American Journal of Physiology-Endocrinology and Metabolism*. 265:E323-E331.
- Kwok, K.H., K.S. Lam, and A. Xu. 2016. Heterogeneity of white adipose tissue: molecular basis and clinical implications. *Experimental & molecular medicine*. 48:e215.
- Lang, D., M.M. Lu, L. Huang, K.A. Engleka, M. Zhang, E.Y. Chu, S. Lipner, A. Skoultchi, S.E. Millar, and J.A. Epstein. 2005. Pax3 functions at a nodal point in melanocyte stem cell differentiation. *Nature*. 433:884.
- Langin, D. 2006. Control of fatty acid and glycerol release in adipose tissue lipolysis. *Comptes rendus biologies*. 329:598-607.
- Lau, D., G. Shillabeer, K. Wong, S. Tough, and J. Russell. 1990. Influence of paracrine factors on preadipocyte replication and differentiation. *International journal of obesity*. 14:193-201.
- Lee, G., H. Kim, Y. Elkabetz, G. Al Shamy, G. Panagiotakos, T. Barberi, V. Tabar, and L. Studer. 2007. Isolation and directed differentiation of neural crest stem cells derived from human embryonic stem cells. *Nature biotechnology*. 25:1468.
- Lee, M.-J., Y. Wu, and S.K. Fried. 2013. Adipose tissue heterogeneity: implication of depot differences in adipose tissue for obesity complications. *Molecular aspects of medicine*. 34:1-11.
- Lee, P., M.M. Swarbrick, J.T. Zhao, and K.K. Ho. 2011. Inducible brown adipogenesis of supraclavicular fat in adult humans. *Endocrinology*. 152:3597-3602.
- Lee, Y.-H., A.P. Petkova, E.P. Mottillo, and J.G. Granneman. 2012. In vivo identification of bipotential adipocyte progenitors recruited by β 3-adrenoceptor activation and high-fat feeding. *Cell metabolism*. 15:480-491.
- Lepper, C., S.J. Conway, and C.-M. Fan. 2009. Adult satellite cells and embryonic muscle progenitors have distinct genetic requirements. *Nature*. 460:627.
- Lepper, C., and C.M. Fan. 2010. Inducible lineage tracing of Pax7-descendant cells reveals embryonic origin of adult satellite cells. *genesis*. 48:424-436.
- Li, D., S. Yea, S. Li, Z. Chen, G. Narla, M. Banck, J. Laborda, S. Tan, J.M. Friedman, and S.L. Friedman. 2005. Krüppel-like factor-6 promotes preadipocyte differentiation through histone deacetylase 3-dependent repression of DLK1. *Journal of Biological Chemistry*. 280:26941-26952.
- Li, Z., M. Leung, R. Hopper, R. Ellenbogen, and M. Zhang. 2010. Feeder-free self-renewal of human embryonic stem cells in 3D porous natural polymer scaffolds. *biomaterials*. 31:404-412.
- Lidell, M.E., M.J. Betz, O.D. Leinhard, M. Heglind, L. Elander, M. Slawik, T. Mussack, D. Nilsson, T. Romu, and P. Nuutila. 2013. Evidence for two types of brown adipose tissue in humans. *Nature medicine*. 19:631.
- Lihn, A., S.B. Pedersen, and B. Richelsen. 2005. Adiponectin: action, regulation and association to insulin sensitivity. *Obesity reviews*. 6:13-21.
- Lin, F.-T., and M.D. Lane. 1992. Antisense CCAAT/enhancer-binding protein RNA suppresses coordinate gene expression and triglyceride accumulation during differentiation of 3T3-L1 preadipocytes. *Genes & development*. 6:533-544.
- Lin, F.-T., and M.D. Lane. 1994. CCAAT/enhancer binding protein alpha is sufficient to initiate the 3T3-L1 adipocyte differentiation program. *Proceedings of the National Academy of Sciences*. 91:8757-8761.

- Lindroos, J., J. Husa, G. Mitterer, A. Haschemi, S. Rauscher, R. Haas, M. Gröger, R. Loewe, N. Kohrgruber, and K.F. Schrögenderfer. 2013. Human but not mouse adipogenesis is critically dependent on LMO3. *Cell metabolism*. 18:62-74.
- Linhart, H.G., K. Ishimura-Oka, F. DeMayo, T. Kibe, D. Repka, B. Poindexter, R.J. Bick, and G.J. Darlington. 2001. C/EBP α is required for differentiation of white, but not brown, adipose tissue. *Proceedings of the National Academy of Sciences*. 98:12532-12537.
- Lobo, S., B.M. Wiczer, A.J. Smith, A.M. Hall, and D.A. Bernlohr. 2007. Fatty acid metabolism in adipocytes: functional analysis of fatty acid transport proteins 1 and 4. *Journal of lipid research*. 48:609-620.
- Logan, C.Y., and R. Nusse. 2004. The Wnt signaling pathway in development and disease. *Annu. Rev. Cell Dev. Biol.* 20:781-810.
- Lolmède, K., C. Duffaut, A. Zakaroff-Girard, and A. Bouloumié. 2011. Immune cells in adipose tissue: key players in metabolic disorders. *Diabetes & metabolism*. 37:283-290.
- Long, J.Z., K.J. Svensson, L. Tsai, X. Zeng, H.C. Roh, X. Kong, R.R. Rao, J. Lou, I. Lokurkar, and W. Baur. 2014. A smooth muscle-like origin for beige adipocytes. *Cell metabolism*. 19:810-820.
- Longo, K.A., W.S. Wright, S. Kang, I. Gerin, S.-H. Chiang, P.C. Lucas, M.R. Opp, and O.A. MacDougald. 2004. Wnt10b inhibits development of white and brown adipose tissues. *Journal of Biological Chemistry*. 279:35503-35509.
- Lowell, B.B., S. Vetrana, A. Hamann, J.A. Lawitts, J. Himms-Hagen, B.B. Boyer, L.P. Kozak, and J.S. Flier. 1993. Development of obesity in transgenic mice after genetic ablation of brown adipose tissue. *Nature*. 366:740.
- Lu, H.H., S.F. El-Amin, K.D. Scott, and C.T. Laurencin. 2003. Three-dimensional, bioactive, biodegradable, polymer–bioactive glass composite scaffolds with improved mechanical properties support collagen synthesis and mineralization of human osteoblast-like cells in vitro. *Journal of Biomedical Materials Research Part A: An Official Journal of The Society for Biomaterials, The Japanese Society for Biomaterials, and The Australian Society for Biomaterials and the Korean Society for Biomaterials*. 64:465-474.
- Lyon, C.J., R.E. Law, and W.A. Hsueh. 2003. Minireview: adiposity, inflammation, and atherogenesis. *Endocrinology*. 144:2195-2200.
- MacDougald, O.A., and C.F. Burant. 2007. The rapidly expanding family of adipokines. *Cell metabolism*. 6:159-161.
- Macfarlane, D.P., S. Forbes, and B.R. Walker. 2008. Glucocorticoids and fatty acid metabolism in humans: fuelling fat redistribution in the metabolic syndrome. *Journal of Endocrinology*. 197:189-204.
- Magré, J., M. Delépine, E. Khallouf, T. Gedde-Dahl Jr, L. Van Maldergem, E. Sobel, J. Papp, M. Meier, A. Mégarbané, and M. Lathrop. 2001. Identification of the gene altered in Berardinelli–Seip congenital lipodystrophy on chromosome 11q13. *Nature genetics*. 28:365.
- Majka, S.M., H.L. Miller, K.M. Helm, A.S. Acosta, C.R. Childs, R. Kong, and D.J. Klemm. 2014. Analysis and isolation of adipocytes by flow cytometry. In *Methods in enzymology*. Vol. 537. Elsevier. 281-296.
- Mariman, E.C., and P. Wang. 2010. Adipocyte extracellular matrix composition, dynamics and role in obesity. *Cellular and molecular life sciences*. 67:1277-1292.
- Markan, K.R., M.C. Naber, M.K. Ameka, M.D. Anderegg, D.J. Mangelsdorf, S.A. Kliewer, M. Mohammadi, and M.J. Potthoff. 2014. Circulating FGF21 is liver derived and enhances glucose uptake during refeeding and overfeeding. *Diabetes*. 63:4057-4063.
- Markussen, L.K., M.S. Isidor, P. Breining, E.S. Andersen, N.E. Rasmussen, L.I. Petersen, S.B. Pedersen, B. Richelsen, and J.B. Hansen. 2017. Characterization of immortalized human brown and white pre-adipocyte cell models from a single donor. *PloS one*. 12:e0185624.
- Marques, B.G., D.B. Hausman, and R.J. Martin. 1998. Association of fat cell size and paracrine growth factors in development of hyperplastic obesity. *American Journal of Physiology-Regulatory, Integrative and Comparative Physiology*. 275:R1898-R1908.

- Martinez, F.O., and S. Gordon. 2014. The M1 and M2 paradigm of macrophage activation: time for reassessment. *F1000prime reports*. 6.
- Mauney, J.R., T. Nguyen, K. Gillen, C. Kirker-Head, J.M. Gimble, and D.L. Kaplan. 2007. Engineering adipose-like tissue in vitro and in vivo utilizing human bone marrow and adipose-derived mesenchymal stem cells with silk fibroin 3D scaffolds. *Biomaterials*. 28:5280-5290.
- Maurizi, G., L. Della Guardia, A. Maurizi, and A. Poloni. 2018. Adipocytes properties and crosstalk with immune system in obesity-related inflammation. *Journal of cellular physiology*. 233:88-97.
- Mazzucotelli, A., N. Viguerie, C. Tiraby, J.-S. Annicotte, A. Mairal, E. Klimcakova, E. Lepin, P. Delmar, S. Dejean, and G. Tavernier. 2007. The transcriptional coactivator peroxisome proliferator-activated receptor (PPAR) γ coactivator-1 α and the nuclear receptor PPAR α control the expression of glycerol kinase and metabolism genes independently of PPAR γ activation in human white adipocytes. *Diabetes*. 56:2467-2475.
- McCauley, H.A., and J.M. Wells. 2017. Pluripotent stem cell-derived organoids: using principles of developmental biology to grow human tissues in a dish. *Development*. 144:958-962.
- McConnell, B.B., and V.W. Yang. 2010. Mammalian Krüppel-like factors in health and diseases. *Physiological reviews*. 90:1337-1381.
- McKeon, C., and T. Pham. 1991. Transactivation of the human insulin receptor gene by the CAAT/enhancer binding protein. *Biochemical and biophysical research communications*. 174:721-728.
- McLaughlin, T., S.E. Ackerman, L. Shen, and E. Engleman. 2017. Role of innate and adaptive immunity in obesity-associated metabolic disease. *The Journal of clinical investigation*. 127:5-13.
- Mehta, G., A.Y. Hsiao, M. Ingram, G.D. Luker, and S. Takayama. 2012. Opportunities and challenges for use of tumor spheroids as models to test drug delivery and efficacy. *Journal of Controlled Release*. 164:192-204.
- Messana, J.M., N.S. Hwang, J. Coburn, J.H. Elisseeff, and Z. Zhang. 2008. Size of the embryoid body influences chondrogenesis of mouse embryonic stem cells. *Journal of tissue engineering and regenerative medicine*. 2:499-506.
- Milet, C., M. Bleher, K. Allbright, M. Orgeur, F. Coulpier, D. Duprez, and E. Havis. 2017. *Egr1* deficiency induces browning of inguinal subcutaneous white adipose tissue in mice. *Scientific reports*. 7:16153.
- Min, S.Y., J. Kady, M. Nam, R. Rojas-Rodriguez, A. Berkenwald, J.H. Kim, H.-L. Noh, J.K. Kim, M.P. Cooper, and T. Fitzgibbons. 2016. Human 'brite/beige' adipocytes develop from capillary networks, and their implantation improves metabolic homeostasis in mice. *Nature medicine*. 22:312.
- Miranville, A., C. Heeschen, C. Sengenès, C. Curat, R. Busse, and A. Bouloumie. 2004. Improvement of postnatal neovascularization by human adipose tissue-derived stem cells. *Circulation*. 110:349-355.
- Mitterberger, M.C., S. Lechner, M. Mattesich, A. Kaiser, D. Probst, N. Wenger, G. Pierer, and W. Zwerschke. 2012. DLK1 (PREF1) is a negative regulator of adipogenesis in CD105+/CD90+/CD34+/CD31-/FABP4- adipose-derived stromal cells from subcutaneous abdominal fat pads of adult women. *Stem Cell Research*. 9:35-48.
- Miura, K., Y. Okada, T. Aoi, A. Okada, K. Takahashi, K. Okita, M. Nakagawa, M. Koyanagi, K. Tanabe, and M. Ohnuki. 2009. Variation in the safety of induced pluripotent stem cell lines. *Nature biotechnology*. 27:743.
- Mohsen-Kanson, T., A.L. Hafner, B. Wdziekonski, Y. Takashima, P. Villageois, A. Carrière, M. Svensson, C. Bagnis, B. Chignon-Sicard, and P.A. Svensson. 2014. Differentiation of human induced pluripotent stem cells into brown and white adipocytes: role of Pax3. *Stem Cells*. 32:1459-1467.
- Moretti, A., M. Bellin, A. Welling, C.B. Jung, J.T. Lam, L. Bott-Flügel, T. Dorn, A. Goedel, C. Höhnke, and F. Hofmann. 2010. Patient-specific induced pluripotent stem-cell models for long-QT syndrome. *New England Journal of Medicine*. 363:1397-1409.

- Mori, T., H. Sakaue, H. Iguchi, H. Gomi, Y. Okada, Y. Takashima, K. Nakamura, T. Nakamura, T. Yamauchi, and N. Kubota. 2005. Role of Krüppel-like factor 15 (KLF15) in transcriptional regulation of adipogenesis. *Journal of Biological Chemistry*. 280:12867-12875.
- Moro, C., J. Galitzky, C. Sengenès, F. Crampes, M. Lafontan, and M. Berlan. 2004. Functional and pharmacological characterization of the natriuretic peptide-dependent lipolytic pathway in human fat cells. *Journal of Pharmacology and Experimental Therapeutics*. 308:984-992.
- Morrison, R.F., and S.R. Farmer. 1999. Role of PPAR γ in regulating a cascade expression of cyclin-dependent kinase inhibitors, p18 (INK4c) and p21 (Waf1/Cip1), during adipogenesis. *Journal of Biological Chemistry*. 274:17088-17097.
- Muller, S., I. Ader, J. Creff, H. Leménager, P. Achard, L. Casteilla, L. Sensebe, A. Carrière, and F. Deschaseaux. 2019. Human adipose stromal-vascular fraction self-organizes to form vascularized adipose tissue in 3D cultures. *Scientific reports*. 9:7250.
- Murholm, M., M.S. Isidor, A.L. Basse, S. Winther, C. Sørensen, J. Skovgaard-Petersen, M.M. Nielsen, A.S. Hansen, B. Quistorff, and J.B. Hansen. 2013. Retinoic acid has different effects on UCP1 expression in mouse and human adipocytes. *BMC cell biology*. 14:41.
- Nakamura, Y., E. Hinoi, T. Takarada, Y. Takahata, T. Yamamoto, H. Fujita, S. Takada, S. Hashizume, and Y. Yoneda. 2011. Positive regulation by GABABR1 subunit of leptin expression through gene transactivation in adipocytes. *PloS one*. 6:e20167.
- Nakatsuji, N., F. Nakajima, and K. Tokunaga. 2008. HLA-haplotype banking and iPS cells. *Nature biotechnology*. 26:739.
- Naylor, C., and W.A. Petri Jr. 2016. Leptin regulation of immune responses. *Trends in Molecular medicine*. 22:88-98.
- Nedergaard, J., T. Bengtsson, and B. Cannon. 2007. Unexpected evidence for active brown adipose tissue in adult humans. *American Journal of Physiology-Endocrinology and Metabolism*. 293:E444-E452.
- Nedergaard, J., N. Petrovic, E.M. Lindgren, A. Jacobsson, and B. Cannon. 2005. PPAR γ in the control of brown adipocyte differentiation. *Biochimica et Biophysica Acta (BBA)-Molecular Basis of Disease*. 1740:293-304.
- Neumann, K., M. Endres, J. Ringe, B. Flath, R. Manz, T. Häupl, M. Sittinger, and C. Kaps. 2007. BMP7 promotes adipogenic but not osteo-/chondrogenic differentiation of adult human bone marrow-derived stem cells in high-density micro-mass culture. *Journal of cellular biochemistry*. 102:626-637.
- Nguyen, H.N., B. Byers, B. Cord, A. Shcheglovitov, J. Byrne, P. Gujar, K. Kee, B. Schüle, R.E. Dolmetsch, and W. Langston. 2011. LRRK2 mutant iPSC-derived DA neurons demonstrate increased susceptibility to oxidative stress. *Cell stem cell*. 8:267-280.
- Nishimura, T., Y. Nakatake, M. Konishi, and N. Itoh. 2000. Identification of a novel FGF, FGF-21, preferentially expressed in the liver. *Biochimica et Biophysica Acta (BBA)-Gene Structure and Expression*. 1492:203-206.
- Nishio, M., T. Yoneshiro, M. Nakahara, S. Suzuki, K. Saeki, M. Hasegawa, Y. Kawai, H. Akutsu, A. Umezawa, and K. Yasuda. 2012. Production of functional classical brown adipocytes from human pluripotent stem cells using specific hemopoietin cocktail without gene transfer. *Cell metabolism*. 16:394-406.
- Nishizawa, M., K. Chonabayashi, M. Nomura, A. Tanaka, M. Nakamura, A. Inagaki, M. Nishikawa, I. Takei, A. Oishi, and K. Tanabe. 2016. Epigenetic variation between human induced pluripotent stem cell lines is an indicator of differentiation capacity. *Cell stem cell*. 19:341-354.
- Oishi, Y., I. Manabe, K. Tobe, K. Tsushima, T. Shindo, K. Fujiu, G. Nishimura, K. Maemura, T. Yamauchi, and N. Kubota. 2005. Krüppel-like transcription factor KLF5 is a key regulator of adipocyte differentiation. *Cell metabolism*. 1:27-39.
- Okita, K., T. Ichisaka, and S. Yamanaka. 2007. Generation of germline-competent induced pluripotent stem cells. *nature*. 448:313.

- OLSSON, H., and P. BELFRAGE. 1987. The regulatory and basal phosphorylation sites of hormone-sensitive lipase are dephosphorylated by protein phosphatase-1, 2A and 2C but not by protein phosphatase-2B. *European journal of biochemistry*. 168:399-405.
- Ortmann, D., and L. Vallier. 2017. Variability of human pluripotent stem cell lines. *Current opinion in genetics & development*. 46:179-185.
- Osafune, K., L. Caron, M. Borowiak, R.J. Martinez, C.S. Fitz-Gerald, Y. Sato, C.A. Cowan, K.R. Chien, and D.A. Melton. 2008. Marked differences in differentiation propensity among human embryonic stem cell lines. *Nature biotechnology*. 26:313.
- Ouchi, N., S. Kihara, T. Funahashi, Y. Matsuzawa, and K. Walsh. 2003. Obesity, adiponectin and vascular inflammatory disease. *Current opinion in lipidology*. 14:561-566.
- Ouchi, N., S. Kihara, T. Funahashi, T. Nakamura, M. Nishida, M. Kumada, Y. Okamoto, K. Ohashi, H. Nagaretani, and K. Kishida. 2003. Reciprocal association of C-reactive protein with adiponectin in blood stream and adipose tissue. *Circulation*. 107:671-674.
- Park, B.O., R. Ahrends, and M.N. Teruel. 2012. Consecutive positive feedback loops create a bistable switch that controls preadipocyte-to-adipocyte conversion. *Cell reports*. 2:976-990.
- Peckett, A.J., D.C. Wright, and M.C. Riddell. 2011. The effects of glucocorticoids on adipose tissue lipid metabolism. *Metabolism*. 60:1500-1510.
- Pei, H., Y. Yao, Y. Yang, K. Liao, and J. Wu. 2011. Krüppel-like factor KLF9 regulates PPAR γ transactivation at the middle stage of adipogenesis. *Cell death and differentiation*. 18:315.
- Pellegrinelli, V., J. Heuvingh, O. Du Roure, C. Rouault, A. Devulder, C. Klein, M. Lacasa, E. Clément, D. Lacasa, and K. Clément. 2014. Human adipocyte function is impacted by mechanical cues. *The Journal of pathology*. 233:183-195.
- Pellegrinelli, V., C. Rouault, N. Veyrie, K. Clément, and D. Lacasa. 2014. Endothelial cells from visceral adipose tissue disrupt adipocyte functions in a three-dimensional setting: partial rescue by angiopoietin-1. *Diabetes*. 63:535-549.
- Petrenko, Y., E. Syková, and Š. Kubinová. 2017. The therapeutic potential of three-dimensional multipotent mesenchymal stromal cell spheroids. *Stem cell research & therapy*. 8:1-9.
- Phillips, D.J. 2005. Activins, inhibins and follistatins in the large domestic species. *Domestic animal endocrinology*. 28:1-16.
- Pierleoni, C., F. Verdenelli, M. Castellucci, and S. Cinti. 1998. Fibronectins and basal lamina molecules expression in human subcutaneous white adipose tissue. *European journal of histochemistry: EJH*. 42:183-188.
- Pisani, D.F., M. Djedaini, G.E. Beranger, C. Elabd, M. Scheideler, G.P. Ailhaud, and E.-Z. Amri. 2011. Differentiation of human adipose-derived stem cells into "brite"(brown-in-white) adipocytes. *Frontiers in endocrinology*. 2:87.
- Poissonnet, C.M., A.R. Burdi, and S.M. Garn. 1984. The chronology of adipose tissue appearance and distribution in the human fetus. *Early human development*. 10:1-11.
- Poitout, V., and R.P. Robertson. 2007. Glucolipototoxicity: fuel excess and β -cell dysfunction. *Endocrine reviews*. 29:351-366.
- Porter, C., D.N. Herndon, M. Chondronikola, T. Chao, P. Annamalai, N. Bhattarai, M.K. Saraf, K.D. Capek, P.T. Reidy, and A.C. Daquinag. 2016. Human and mouse brown adipose tissue mitochondria have comparable UCP1 function. *Cell metabolism*. 24:246-255.
- Pradhan, A.D., J.E. Manson, N. Rifai, J.E. Buring, and P.M. Ridker. 2001. C-reactive protein, interleukin 6, and risk of developing type 2 diabetes mellitus. *Jama*. 286:327-334.
- Puigserver, P., Z. Wu, C.W. Park, R. Graves, M. Wright, and B.M. Spiegelman. 1998. A cold-inducible coactivator of nuclear receptors linked to adaptive thermogenesis. *Cell*. 92:829-839.

- Ragolia, L., and N. Begum. 1998. Protein phosphatase-1 and insulin action. In *Insulin Action*. Springer. 49-58.
- Rajala, M.W., and P.E. Scherer. 2003. Minireview: the adipocyte—at the crossroads of energy homeostasis, inflammation, and atherosclerosis. *Endocrinology*. 144:3765-3773.
- Ramage, L.E., M. Akyol, A.M. Fletcher, J. Forsythe, M. Nixon, R.N. Carter, E.J. van Beek, N.M. Morton, B.R. Walker, and R.H. Stimson. 2016. Glucocorticoids acutely increase brown adipose tissue activity in humans, revealing species-specific differences in UCP-1 regulation. *Cell metabolism*. 24:130-141.
- Rauscher, F.M., P.J. Goldschmidt-Clermont, B.H. Davis, T. Wang, D. Gregg, P. Ramaswami, A.M. Pippen, B.H. Annex, C. Dong, and D.A. Taylor. 2003. Aging, progenitor cell exhaustion, and atherosclerosis. *Circulation*. 108:457-463.
- Ravi, M., V. Paramesh, S. Kaviya, E. Anuradha, and F.P. Solomon. 2015. 3D cell culture systems: advantages and applications. *Journal of cellular physiology*. 230:16-26.
- Reaven, G.M. 1988. Role of insulin resistance in human disease. *Diabetes*. 37:1595-1607.
- Ribet, C., E. Montastier, C. Valle, V. Bezaire, A. Mazzucotelli, A. Mairal, N. Viguerie, and D. Langin. 2010. Peroxisome proliferator-activated receptor- α control of lipid and glucose metabolism in human white adipocytes. *Endocrinology*. 151:123-133.
- Rim, J.S., and L.P. Kozak. 2002. Regulatory motifs for CREB-binding protein and Nfe2l2 transcription factors in the upstream enhancer of the mitochondrial uncoupling protein 1 gene. *Journal of Biological Chemistry*. 277:34589-34600.
- Roberts, L.D., P. Boström, J.F. O’Sullivan, R.T. Schinzel, G.D. Lewis, A. Dejam, Y.-K. Lee, M.J. Palma, S. Calhoun, and A. Georgiadi. 2014. β -Aminoisobutyric acid induces browning of white fat and hepatic β -oxidation and is inversely correlated with cardiometabolic risk factors. *Cell metabolism*. 19:96-108.
- Robinson, L.J., J.M. Law, M.E. Symonds, and H. Budge. 2016. Brown adipose tissue activation as measured by infrared thermography by mild anticipatory psychological stress in lean healthy females. *Experimental physiology*. 101:549-557.
- Rodriguez, A.-M., C. Elabd, F. Delteil, J. Astier, C. Vernochet, P. Saint-Marc, J. Guesnet, A. Guezennec, E.-Z. Amri, and C. Dani. 2004. Adipocyte differentiation of multipotent cells established from human adipose tissue. *Biochemical and biophysical research communications*. 315:255-263.
- Rony, I., A. Baten, J.A. Bloomfield, M. Islam, M. Billah, and K. Islam. 2015. Inducing pluripotency in vitro: recent advances and highlights in induced pluripotent stem cells generation and pluripotency reprogramming. *Cell proliferation*. 48:140-156.
- Rosell, M., M. Kaforou, A. Frontini, A. Okolo, Y.-W. Chan, E. Nikolopoulou, S. Millership, M.E. Fenech, D. MacIntyre, and J.O. Turner. 2014. Brown and white adipose tissues: intrinsic differences in gene expression and response to cold exposure in mice. *American Journal of Physiology-Endocrinology and Metabolism*. 306:E945-E964.
- Rosen, E.D., C.-H. Hsu, X. Wang, S. Sakai, M.W. Freeman, F.J. Gonzalez, and B.M. Spiegelman. 2002. C/EBP α induces adipogenesis through PPAR γ : a unified pathway. *Genes & development*. 16:22-26.
- Rosen, E.D., and B.M. Spiegelman. 2000. Molecular regulation of adipogenesis. *Annual review of cell and developmental biology*. 16:145-171.
- Rosen, E.D., and B.M. Spiegelman. 2014. What we talk about when we talk about fat. *Cell*. 156:20-44.
- Rosenwald, M., A. Perdikari, T. Rülcke, and C. Wolfrum. 2013. Bi-directional interconversion of brite and white adipocytes. *Nature cell biology*. 15:659.
- Rosenwald, M., and C. Wolfrum. 2014. The origin and definition of brite versus white and classical brown adipocytes. *Adipocyte*. 3:4-9.
- Ross, S.E., N. Hemati, K.A. Longo, C.N. Bennett, P.C. Lucas, R.L. Erickson, and O.A. MacDougald. 2000. Inhibition of adipogenesis by Wnt signaling. *Science*. 289:950-953.

- Rotter, V., I. Nagaev, and U. Smith. 2003. Interleukin-6 (IL-6) induces insulin resistance in 3T3-L1 adipocytes and is, like IL-8 and tumor necrosis factor- α , overexpressed in human fat cells from insulin-resistant subjects. *Journal of Biological Chemistry*. 278:45777-45784.
- Roux, C., D.F. Pisani, H.B. Yahia, M. Djedaini, G.E. Beranger, J.-C. Chambard, D. Ambrosetti, J.-F. Michiels, V. Breuil, and G. Ailhaud. 2013. Chondrogenic potential of stem cells derived from adipose tissue: a powerful pharmacological tool. *Biochemical and biophysical research communications*. 440:786-791.
- Ryall, R.L., and R. Goldrick. 1977. Glycerokinase in human adipose tissue. *Lipids*. 12:272-277.
- Ryo, M., T. Nakamura, S. Kihara, M. Kumada, S. Shibazaki, M. Takahashi, M. Nagai, Y. Matsuzawa, and T. Funahashi. 2004. Adiponectin as a biomarker of the metabolic syndrome. *Circulation journal*. 68:975-981.
- Sadur, C., and R. Eckel. 1982. Insulin stimulation of adipose tissue lipoprotein lipase. Use of the euglycemic clamp technique. *The Journal of clinical investigation*. 69:1119-1125.
- Saito, M., Y. Okamatsu-Ogura, M. Matsushita, K. Watanabe, T. Yoneshiro, J. Nio-Kobayashi, T. Iwanaga, M. Miyagawa, T. Kameya, and K. Nakada. 2009. High incidence of metabolically active brown adipose tissue in healthy adult humans: effects of cold exposure and adiposity. *Diabetes*. 58:1526-1531.
- Samuelsson, L., K. Strömberg, K. Vikman, G. Bjursell, and S. Enerbäck. 1991. The CCAAT/enhancer binding protein and its role in adipocyte differentiation: evidence for direct involvement in terminal adipocyte development. *The EMBO journal*. 10:3787-3793.
- Sanchez-Gurmaches, J., C.-M. Hung, C.A. Sparks, Y. Tang, H. Li, and D.A. Guertin. 2012. PTEN loss in the Myf5 lineage redistributes body fat and reveals subsets of white adipocytes that arise from Myf5 precursors. *Cell metabolism*. 16:348-362.
- Santos, O.F., and S.K. Nigam. 1993. HGF-induced tubulogenesis and branching of epithelial cells is modulated by extracellular matrix and TGF- β . *Developmental biology*. 160:293-302.
- Sata, M., D. Fukuda, K. Tanaka, Y. Kaneda, H. Yashiro, and I. Shirakawa. 2005. The role of circulating precursors in vascular repair and lesion formation. *Journal of cellular and molecular medicine*. 9:557-568.
- Sato, H., M. Takahashi, H. Ise, A. Yamada, S.-i. Hirose, Y.-i. Tagawa, H. Morimoto, A. Izawa, and U. Ikeda. 2006. Collagen synthesis is required for ascorbic acid-enhanced differentiation of mouse embryonic stem cells into cardiomyocytes. *Biochemical and biophysical research communications*. 342:107-112.
- Schulz, T.J., T.L. Huang, T.T. Tran, H. Zhang, K.L. Townsend, J.L. Shadrach, M. Cerletti, L.E. McDougall, N. Giorgadze, and T. Tchekonia. 2011. Identification of inducible brown adipocyte progenitors residing in skeletal muscle and white fat. *Proceedings of the National Academy of Sciences*. 108:143-148.
- Scotney, H., M.E. Symonds, J. Law, H. Budge, D. Sharkey, and K.N. Manolopoulos. 2017. Glucocorticoids modulate human brown adipose tissue thermogenesis in vivo. *Metabolism*. 70:125-132.
- Seale, P., B. Bjork, W. Yang, S. Kajimura, S. Chin, S. Kuang, A. Scime, S. Devarakonda, H.M. Conroe, and H. Erdjument-Bromage. 2008. PRDM16 controls a brown fat/skeletal muscle switch. *Nature*. 454:961.
- SENGENÈS, C., M. BERLAN, I. DE GLISEZINSKI, M. Lafontan, and J. GALITZKY. 2000. Natriuretic peptides: a new lipolytic pathway in human adipocytes. *The FASEB Journal*. 14:1345-1351.
- Sengenès, C., A. Bouloumié, H. Hauner, M. Berlan, R. Busse, M. Lafontan, and J. Galitzky. 2003. Involvement of a cGMP-dependent pathway in the natriuretic peptide-mediated hormone-sensitive lipase phosphorylation in human adipocytes. *Journal of Biological Chemistry*. 278:48617-48626.
- Seo, T., M. Al-Haideri, E. Treskova, T.S. Worgall, Y. Kako, I.J. Goldberg, and R.J. Deckelbaum. 2000. Lipoprotein lipase-mediated selective uptake from low density lipoprotein requires cell surface proteoglycans and is independent of scavenger receptor class B type 1. *Journal of Biological Chemistry*. 275:30355-30362.
- Shabalina, I.G., N. Petrovic, J.M. de Jong, A.V. Kalinovich, B. Cannon, and J. Nedergaard. 2013. UCP1 in brite/beige adipose tissue mitochondria is functionally thermogenic. *Cell reports*. 5:1196-1203.
- Shackleton, S., D.J. Lloyd, S.N. Jackson, R. Evans, M.F. Niermeijer, B.M. Singh, H. Schmidt, G. Brabant, S. Kumar, and P.N. Durrington. 2000. LMNA, encoding lamin A/C, is mutated in partial lipodystrophy. *Nature genetics*. 24:153.

- Shan, T., X. Liang, P. Bi, P. Zhang, W. Liu, and S. Kuang. 2013. Distinct populations of adipogenic and myogenic Myf5-lineage progenitors in white adipose tissues. *Journal of lipid research*. 54:2214-2224.
- Sharma, R., S.Z. Barakzai, S.E. Taylor, and F.X. Donadeu. 2016. Epidermal-like architecture obtained from equine keratinocytes in three-dimensional cultures. *Journal of tissue engineering and regenerative medicine*. 10:627-636.
- Sharp, L.Z., K. Shinoda, H. Ohno, D.W. Scheel, E. Tomoda, L. Ruiz, H. Hu, L. Wang, Z. Pavlova, and V. Gilsanz. 2012. Human BAT possesses molecular signatures that resemble beige/brite cells. *PLoS one*. 7:e49452.
- Shi, Y., H. Inoue, J.C. Wu, and S. Yamanaka. 2017. Induced pluripotent stem cell technology: a decade of progress. *Nature reviews Drug discovery*. 16:115.
- Shiba, Y., T. Gomibuchi, T. Seto, Y. Wada, H. Ichimura, Y. Tanaka, T. Ogasawara, K. Okada, N. Shiba, and K. Sakamoto. 2016. Allogeneic transplantation of iPS cell-derived cardiomyocytes regenerates primate hearts. *Nature*. 538:388.
- Shinoda, K., I.H. Luijten, Y. Hasegawa, H. Hong, S.B. Sonne, M. Kim, R. Xue, M. Chondronikola, A.M. Cypess, and Y.-H. Tseng. 2015. Genetic and functional characterization of clonally derived adult human brown adipocytes. *Nature medicine*. 21:389.
- Shulman, G.I. 2000. Cellular mechanisms of insulin resistance. *The Journal of clinical investigation*. 106:171-176.
- Simunovic, M., and A.H. Brivanlou. 2017. Embryoids, organoids and gastruloids: new approaches to understanding embryogenesis. *Development*. 144:976-985.
- Sjöström, L., P. Björntorp, and J. Månsson. 1973. An optimal assay system for subcellular determination of de novo fatty acid synthesis in human adipose tissue. *Scandinavian journal of clinical and laboratory investigation*. 31:191-204.
- Spalding, K.L., E. Arner, P.O. Westermark, S. Bernard, B.A. Buchholz, O. Bergmann, L. Blomqvist, J. Hoffstedt, E. Näslund, and T. Britton. 2008. Dynamics of fat cell turnover in humans. *Nature*. 453:783.
- Stadtfeld, M., and K. Hochedlinger. 2010. Induced pluripotency: history, mechanisms, and applications. *Genes & development*. 24:2239-2263.
- Stahl, A., J.G. Evans, S. Pattel, D. Hirsch, and H.F. Lodish. 2002. Insulin causes fatty acid transport protein translocation and enhanced fatty acid uptake in adipocytes. *Developmental cell*. 2:477-488.
- Stanford, K.I., R.J. Middelbeek, K.L. Townsend, D. An, E.B. Nygaard, K.M. Hitchcox, K.R. Markan, K. Nakano, M.F. Hirshman, and Y.-H. Tseng. 2012. Brown adipose tissue regulates glucose homeostasis and insulin sensitivity. *The Journal of clinical investigation*. 123.
- Stokes, A., and S.H. Preston. 2017. Deaths attributable to diabetes in the United States: comparison of data sources and estimation approaches. *PLoS One*. 12:e0170219.
- Strack, A.M., M. Bradbury, and M.F. Dallman. 1995. Corticosterone decreases nonshivering thermogenesis and increases lipid storage in brown adipose tissue. *American Journal of Physiology-Regulatory, Integrative and Comparative Physiology*. 268:R183-R191.
- STRÅLFORS, P., and R.C. Honnor. 1989. Insulin-induced dephosphorylation of hormone-sensitive lipase: Correlation with lipolysis and cAMP-dependent protein kinase activity. *European journal of biochemistry*. 182:379-385.
- Su, S., A.R. Guntur, D.C. Nguyen, S.S. Fakory, C.C. Doucette, C. Leech, H. Lotana, M. Kelley, J. Kohli, and J. Martino. 2018. A renewable source of human beige adipocytes for development of therapies to treat metabolic syndrome. *Cell reports*. 25:3215-3228. e3219.
- Symonds, M.E. 2013. Brown adipose tissue growth and development. *Scientifica*. 2013.
- Szczepny, A., C.A. Hogarth, J. Young, and K.L. Loveland. 2009. Identification of Hedgehog signaling outcomes in mouse testis development using a hanging drop-culture system. *Biology of reproduction*. 80:258-263.

- Takahashi, K., K. Tanabe, M. Ohnuki, M. Narita, T. Ichisaka, K. Tomoda, and S. Yamanaka. 2007. Induction of pluripotent stem cells from adult human fibroblasts by defined factors. *cell*. 131:861-872.
- Takahashi, K., and S. Yamanaka. 2006. Induction of pluripotent stem cells from mouse embryonic and adult fibroblast cultures by defined factors. *cell*. 126:663-676.
- Takebe, T., K. Sekine, M. Enomura, H. Koike, M. Kimura, T. Ogaeri, R.-R. Zhang, Y. Ueno, Y.-W. Zheng, and N. Koike. 2013. Vascularized and functional human liver from an iPSC-derived organ bud transplant. *Nature*. 499:481.
- Tallquist, M.D., K.E. Weismann, M. Hellstrom, and P. Soriano. 2000. Early myotome specification regulates PDGFA expression and axial skeleton development. *Development*. 127:5059-5070.
- Tamama, K., V.H. Fan, L.G. Griffith, H.C. Blair, and A. Wells. 2006. Epidermal growth factor as a candidate for ex vivo expansion of bone marrow-derived mesenchymal stem cells. *Stem cells*. 24:686-695.
- Tamori, Y., J. Masugi, N. Nishino, and M. Kasuga. 2002. Role of peroxisome proliferator-activated receptor- γ in maintenance of the characteristics of mature 3T3-L1 adipocytes. *Diabetes*. 51:2045-2055.
- Tanaka, T., N. Yoshida, T. Kishimoto, and S. Akira. 1997. Defective adipocyte differentiation in mice lacking the C/EBP β and/or C/EBP δ gene. *The EMBO journal*. 16:7432-7443.
- Tang, Q.-Q., M. Grønberg, H. Huang, J.-W. Kim, T.C. Otto, A. Pandey, and M.D. Lane. 2005. Sequential phosphorylation of CCAAT enhancer-binding protein β by MAPK and glycogen synthase kinase 3 β is required for adipogenesis. *Proceedings of the National Academy of Sciences*. 102:9766-9771.
- Tang, Q.-Q., T.C. Otto, and M.D. Lane. 2004. Commitment of C3H10T1/2 pluripotent stem cells to the adipocyte lineage. *Proceedings of the National Academy of Sciences*. 101:9607-9611.
- Tang, W., D. Zeve, J.M. Suh, D. Bosnakovski, M. Kyba, R.E. Hammer, M.D. Tallquist, and J.M. Graff. 2008. White fat progenitor cells reside in the adipose vasculature. *Science*. 322:583-586.
- Taura, D., M. Noguchi, M. Sone, K. Hosoda, E. Mori, Y. Okada, K. Takahashi, K. Homma, N. Oyamada, and M. Inuzuka. 2009. Adipogenic differentiation of human induced pluripotent stem cells: comparison with that of human embryonic stem cells. *FEBS letters*. 583:1029-1033.
- Tchkonia, T., M. Lenburg, T. Thomou, N. Giorgadze, G. Frampton, T. Pirtskhalava, A. Cartwright, M. Cartwright, J. Flanagan, and I. Karagiannides. 2007. Identification of depot-specific human fat cell progenitors through distinct expression profiles and developmental gene patterns. *American Journal of Physiology-Endocrinology and Metabolism*. 292:E298-E307.
- Thomson, J.A., J. Itskovitz-Eldor, S.S. Shapiro, M.A. Waknitz, J.J. Swiergiel, V.S. Marshall, and J.M. Jones. 1998. Embryonic stem cell lines derived from human blastocysts. *science*. 282:1145-1147.
- Tibbitt, M.W., and K.S. Anseth. 2009. Hydrogels as extracellular matrix mimics for 3D cell culture. *Biotechnology and bioengineering*. 103:655-663.
- Timmons, J.A., K. Wennmalm, O. Larsson, T.B. Walden, T. Lassmann, N. Petrovic, D.L. Hamilton, R.E. Gimeno, C. Wahlestedt, and K. Baar. 2007. Myogenic gene expression signature establishes that brown and white adipocytes originate from distinct cell lineages. *Proceedings of the National Academy of Sciences*. 104:4401-4406.
- Tiraby, C., G. Tavernier, C. Lefort, D. Larrouy, F. Bouillaud, D. Ricquier, and D. Langin. 2003. Acquisition of brown fat cell features by human white adipocytes. *Journal of Biological Chemistry*. 278:33370-33376.
- Tontonoz, P., E. Hu, R.A. Graves, A.I. Budavari, and B.M. Spiegelman. 1994. mPPAR gamma 2: tissue-specific regulator of an adipocyte enhancer. *Genes & development*. 8:1224-1234.
- Tontonoz, P., E. Hu, and B.M. Spiegelman. 1994. Stimulation of adipogenesis in fibroblasts by PPAR γ 2, a lipid-activated transcription factor. *Cell*. 79:1147-1156.
- Toole, B. 2009. Hyaluronan: from extracellular glue to cell signaling cue. *International Journal of Experimental Pathology*. 90.

- Topman, G., N. Shoham, O. Sharabani-Yosef, F.-H. Lin, and A. Gefen. 2013. A new technique for studying directional cell migration in a hydrogel-based three-dimensional matrix for tissue engineering model systems. *Micron*. 51:9-12.
- Tran, K.-V., O. Gealekman, A. Frontini, M.C. Zingaretti, M. Morroni, A. Giordano, A. Smorlesi, J. Perugini, R. De Matteis, and A. Sbarbati. 2012. The vascular endothelium of the adipose tissue gives rise to both white and brown fat cells. *Cell metabolism*. 15:222-229.
- Tran, T.T., and C.R. Kahn. 2010. Transplantation of adipose tissue and stem cells: role in metabolism and disease. *Nature Reviews Endocrinology*. 6:195.
- Tseng, Y.-H., A.M. Cypess, and C.R. Kahn. 2010. Cellular bioenergetics as a target for obesity therapy. *Nature reviews Drug discovery*. 9:465.
- Tseng, Y.-H., E. Kokkotou, T.J. Schulz, T.L. Huang, J.N. Winnay, C.M. Taniguchi, T.T. Tran, R. Suzuki, D.O. Espinoza, and Y. Yamamoto. 2008. New role of bone morphogenetic protein 7 in brown adipogenesis and energy expenditure. *Nature*. 454:1000.
- Unser, A.M., Y. Tian, and Y. Xie. 2015. Opportunities and challenges in three-dimensional brown adipogenesis of stem cells. *Biotechnology advances*. 33:962-979.
- Urbich, C., and S. Dimmeler. 2005. Risk factors for coronary artery disease, circulating endothelial progenitor cells, and the role of HMG-CoA reductase inhibitors. *Kidney international*. 67:1672-1676.
- van den Dolder, J., P.H. Spauwen, and J.A. Jansen. 2003. Evaluation of various seeding techniques for culturing osteogenic cells on titanium fiber mesh. *Tissue engineering*. 9:315-325.
- van Marken Lichtenbelt, W.D., J.W. Vanhommerig, N.M. Smulders, J.M. Drossaerts, G.J. Kemerink, N.D. Bouvy, P. Schrauwen, and G.J. Teule. 2009. Cold-activated brown adipose tissue in healthy men. *New England Journal of Medicine*. 360:1500-1508.
- Vázquez-Vela, M.E.F., N. Torres, and A.R. Tovar. 2008. White adipose tissue as endocrine organ and its role in obesity. *Archives of medical research*. 39:715-728.
- Villarroya, F., R. Cereijo, J. Villarroya, and M. Giralt. 2017. Brown adipose tissue as a secretory organ. *Nature Reviews Endocrinology*. 13:26.
- Villena, J., K. Kim, and H. Sul. 2002. Pref-1 and ADSF/resistin: two secreted factors inhibiting adipose tissue development. *Hormone and Metabolic Research*. 34:664-670.
- Virtanen, K.A., M.E. Lidell, J. Orava, M. Heglund, R. Westergren, T. Niemi, M. Taittonen, J. Laine, N.-J. Savisto, and S. Enerbäck. 2009. Functional brown adipose tissue in healthy adults. *New England Journal of Medicine*. 360:1518-1525.
- Vodyanik, M.A., J. Yu, X. Zhang, S. Tian, R. Stewart, J.A. Thomson, and I.I. Slukvin. 2010. A mesoderm-derived precursor for mesenchymal stem and endothelial cells. *Cell stem cell*. 7:718-729.
- Volz, A.-C., B. Huber, and P.J. Kluger. 2016. Adipose-derived stem cell differentiation as a basic tool for vascularized adipose tissue engineering. *Differentiation*. 92:52-64.
- Waldén, T.B., I.R. Hansen, J.A. Timmons, B. Cannon, and J. Nedergaard. 2011. Recruited vs. nonrecruited molecular signatures of brown, "brite," and white adipose tissues. *American journal of physiology-endocrinology and metabolism*. 302:E19-E31.
- Walden, T.B., J.A. Timmons, P. Keller, J. Nedergaard, and B. Cannon. 2009. Distinct expression of muscle-specific microRNAs (myomirs) in brown adipocytes. *Journal of cellular physiology*. 218:444-449.
- Wang, G.-X., X.-Y. Zhao, Z.-X. Meng, M. Kern, A. Dietrich, Z. Chen, Z. Cozakov, D. Zhou, A.L. Okunade, and X. Su. 2014. The brown fat-enriched secreted factor Nrg4 preserves metabolic homeostasis through attenuation of hepatic lipogenesis. *Nature medicine*. 20:1436.
- Wang, Q.A., C. Tao, R.K. Gupta, and P.E. Scherer. 2013. Tracking adipogenesis during white adipose tissue development, expansion and regeneration. *Nature medicine*. 19:1338.
- Wang, Y., A. Singh, P. Xu, M.A. Pindrus, D.J. Blasioli, and D.L. Kaplan. 2006. Expansion and osteogenic differentiation of bone marrow-derived mesenchymal stem cells on a vitamin C functionalized polymer. *Biomaterials*. 27:3265-3273.

- Wankhade, U.D., J.-H. Lee, P.K. Dagur, H. Yadav, M. Shen, W. Chen, A.B. Kulkarni, J.P. McCoy, T. Finkel, and A.M. Cypess. 2018. TGF- β receptor 1 regulates progenitors that promote browning of white fat. *Molecular metabolism*. 16:160-171.
- Wellen, K.E., and G.S. Hotamisligil. 2005. Inflammation, stress, and diabetes. *The Journal of clinical investigation*. 115:1111-1119.
- Wells, E.K., O. Yarborough III, R.P. Lifton, L.G. Cantley, and M.J. Caplan. 2013. Epithelial morphogenesis of MDCK cells in three-dimensional collagen culture is modulated by interleukin-8. *American Journal of Physiology-Cell Physiology*. 304:C966-C975.
- Whittle, A.J., S. Carobbio, L. Martins, M. Slawik, E. Hondares, M.J. Vázquez, D. Morgan, R.I. Csikasz, R. Gallego, and S. Rodriguez-Cuenca. 2012. BMP8B increases brown adipose tissue thermogenesis through both central and peripheral actions. *Cell*. 149:871-885.
- Willerth, S.M., K.J. Arendas, D.I. Gottlieb, and S.E. Sakiyama-Elbert. 2006. Optimization of fibrin scaffolds for differentiation of murine embryonic stem cells into neural lineage cells. *Biomaterials*. 27:5990-6003.
- Wong, H., and M.C. Schotz. 2002. The lipase gene family. *Journal of lipid research*. 43:993-999.
- Wong, H., D. Yang, J.S. Hill, R.C. Davis, J. Nikazy, and M.C. Schotz. 1997. A molecular biology-based approach to resolve the subunit orientation of lipoprotein lipase. *Proceedings of the National Academy of Sciences*. 94:5594-5598.
- Wu, D., A.B. Molofsky, H.-E. Liang, R.R. Ricardo-Gonzalez, H.A. Jouihan, J.K. Bando, A. Chawla, and R.M. Locksley. 2011. Eosinophils sustain adipose alternatively activated macrophages associated with glucose homeostasis. *Science*. 332:243-247.
- Wu, J., P. Boström, L.M. Sparks, L. Ye, J.H. Choi, A.-H. Giang, M. Khandekar, K.A. Virtanen, P. Nuutila, and G. Schaart. 2012. Beige adipocytes are a distinct type of thermogenic fat cell in mouse and human. *Cell*. 150:366-376.
- Wu, J., P. Cohen, and B.M. Spiegelman. 2013. Adaptive thermogenesis in adipocytes: is beige the new brown? *Genes & development*. 27:234-250.
- Wu, J., S.V. Srinivasan, J.C. Neumann, and J.B. Lingrel. 2005. The KLF2 transcription factor does not affect the formation of preadipocytes but inhibits their differentiation into adipocytes. *Biochemistry*. 44:11098-11105.
- Wu, Z., E.D. Rosen, R. Brun, S. Hauser, G. Adelmant, A.E. Troy, C. McKeon, G.J. Darlington, and B.M. Spiegelman. 1999. Cross-regulation of C/EBP α and PPAR γ controls the transcriptional pathway of adipogenesis and insulin sensitivity. *Molecular cell*. 3:151-158.
- Wueest, S., F.C. Lucchini, T.D. Challa, W. Müller, M. Blüher, and D. Konrad. 2016. Mesenteric fat lipolysis mediates obesity-associated hepatic steatosis and insulin resistance. *Diabetes*. 65:140-148.
- Xue, R., M.D. Lynes, J.M. Dreyfuss, F. Shamsi, T.J. Schulz, H. Zhang, T.L. Huang, K.L. Townsend, Y. Li, and H. Takahashi. 2015. Clonal analyses and gene profiling identify genetic biomarkers of the thermogenic potential of human brown and white preadipocytes. *Nature medicine*. 21:760.
- Yamanaka, S. 2012. Induced pluripotent stem cells: past, present, and future. *Cell stem cell*. 10:678-684.
- Yao, X., B. Salingova, and C. Dani. 2018. Brown-Like Adipocyte Progenitors Derived from Human iPS Cells: A New Tool for Anti-obesity Drug Discovery and Cell-Based Therapy? In *Brown Adipose Tissue*. Springer. 97-105.
- Yellaturu, C.R., X. Deng, E.A. Park, R. Raghov, and M.B. Elam. 2009. Insulin enhances the biogenesis of nuclear sterol regulatory element-binding protein (SREBP)-1c by posttranscriptional down-regulation of Insig-2A and its dissociation from SREBP cleavage-activating protein (SCAP)· SREBP-1c complex. *Journal of biological chemistry*. 284:31726-31734.
- Yin, H., A. Pasut, V.D. Soleimani, C.F. Bentzinger, G. Antoun, S. Thorn, P. Seale, P. Fernando, W. van IJcken, and F. Grosveld. 2013. MicroRNA-133 controls brown adipose determination in skeletal muscle satellite cells by targeting Prdm16. *Cell metabolism*. 17:210-224.

- Yudkin, J.S., C. Stehouwer, J. Emeis, and S. Coppack. 1999. C-reactive protein in healthy subjects: associations with obesity, insulin resistance, and endothelial dysfunction: a potential role for cytokines originating from adipose tissue? *Arteriosclerosis, thrombosis, and vascular biology*. 19:972-978.
- Zamani, N., and C.W. Brown. 2010. Emerging roles for the transforming growth factor- β superfamily in regulating adiposity and energy expenditure. *Endocrine reviews*. 32:387-403.
- Zaragosi, L.-E., B. Wdziekonski, P. Villageois, M. Keophiphath, M. Maumus, T. Tchkonja, V. Bourlier, T. Mohsen-Kanson, A. Ladoux, and C. Elabd. 2010. Activin a plays a critical role in proliferation and differentiation of human adipose progenitors. *Diabetes*. 59:2513-2521.
- Zaragosi, L.E., G. Ailhaud, and C. Dani. 2006. Autocrine fibroblast growth factor 2 signaling is critical for self-renewal of human multipotent adipose-derived stem cells. *Stem cells*. 24:2412-2419.
- Zegers, M.M. 2014. 3D in vitro cell culture models of tube formation. In *Seminars in cell & developmental biology*. Vol. 31. Elsevier. 132-140.
- Zhang, J., Y. Zhang, T. Sun, F. Guo, S. Huang, M. Chandalia, N. Abate, D. Fan, H.-B. Xin, and Y.E. Chen. 2013. Dietary obesity-induced Egr-1 in adipocytes facilitates energy storage via suppression of FOXC2. *Scientific reports*. 3:1476.
- Zhang, Y., R. Proenca, M. Maffei, M. Barone, L. Leopold, and J.M. Friedman. 1994. Positional cloning of the mouse obese gene and its human homologue. *Nature*. 372:425.
- Zhao, T., Z.-N. Zhang, Z. Rong, and Y. Xu. 2011. Immunogenicity of induced pluripotent stem cells. *Nature*. 474:212.
- Zhu, S., G. Cheng, H. Zhu, and G. Guan. 2015. A study of genes involved in adipocyte differentiation. *Journal of Pediatric Endocrinology and Metabolism*. 28:93-99.
- Zhu, Y., C. Qi, J.R. Korenberg, X.-N. Chen, D. Noya, M.S. Rao, and J.K. Reddy. 1995. Structural organization of mouse peroxisome proliferator-activated receptor gamma (mPPAR gamma) gene: alternative promoter use and different splicing yield two mPPAR gamma isoforms. *Proceedings of the National Academy of Sciences*. 92:7921-7925.
- Ziccardi, P., F. Nappo, G. Giugliano, K. Esposito, R. Marfella, M. Cioffi, F. D'Andrea, A.M. Molinari, and D. Giugliano. 2002. Reduction of inflammatory cytokine concentrations and improvement of endothelial functions in obese women after weight loss over one year. *Circulation*. 105:804-809.
- Zilberfarb, V., F. Piétri-Rouxel, R. Jockers, S. Krief, C. Delouis, T. Issad, and A.D. Strosberg. 1997. Human immortalized brown adipocytes express functional beta3-adrenoceptor coupled to lipolysis. *Journal of Cell Science*. 110:801-807.
- Zingaretti, M.C., F. Crosta, A. Vitali, M. Guerrieri, A. Frontini, B. Cannon, J. Nedergaard, and S. Cinti. 2009. The presence of UCP1 demonstrates that metabolically active adipose tissue in the neck of adult humans truly represents brown adipose tissue. *The FASEB Journal*. 23:3113-3120.
- Zuk, P.A., M. Zhu, P. Ashjian, D.A. De Ugarte, J.I. Huang, H. Mizuno, Z.C. Alfonso, J.K. Fraser, P. Benhaim, and M.H. Hedrick. 2002. Human adipose tissue is a source of multipotent stem cells. *Molecular biology of the cell*. 13:4279-4295.
- Zuk, P.A., M. Zhu, H. Mizuno, J. Huang, J.W. Futrell, A.J. Katz, P. Benhaim, H.P. Lorenz, and M.H. Hedrick. 2001. Multilineage cells from human adipose tissue: implications for cell-based therapies. *Tissue engineering*. 7:211-228.
- Zwierzina, M.E., A. Ejaz, M. Bitsche, M.J. Blumer, M.C. Mitterberger, M. Mattesich, A. Amann, A. Kaiser, E.J. Pechriggl, and S. Hörl. 2015. Characterization of DLK1 (PREF1)+/CD34+ cells in vascular stroma of human white adipose tissue. *Stem cell research*. 15:403-418.